AN ABSTRACT OF THE THESIS OF

Richard Turton for the degree of Master of Science

in Chemical Engineering presented on June 8, 1979

Title: COMBUSTION OF WOOD CHAR IN A TRANSPORT REACTOR

Abstract approved: Redacted for Privacy

Ferhan Kayihan

Experiments were carried out to find certain physical properties of the wood char used as feed stock to the reactor. The bulk density of the fuel was found to be in the range 300-850 kg/M^3 while the internal surface area, found by the physi-adsorption of nitrogen at 78 K, was estimated to be in the range 2-5.5 x 10^5 M^2/kg. The combustible content of the fuel was also evaluated and was found to vary from 50% by weight to 95% by weight. The particle size distributions of fuel before and after combustion was also evaluated.

Experimental test runs were carried out on the reactor, after the solids and air feed systems had been calibrated. Thermocouples and gas sampling ports were situated along the length of the reactor and hence temperature and gas concentration profiles were experimentally determined.

A computer simulated model for the combustion process occurring in the reactor was developed. This model was tested against the experimental results obtained from the test runs on the reactor. The model was found to be sensitive to changes in the

terminal velocity of the particles, the particle size distribution, and the amount of gas bypassing the reaction zone.

The comparison between the predicted and experimental results showed that the model tended to overpredict the amount of combustion taking place in the reactor, although the predicted temperature profiles compared favorably with the experimental observations.

Combustion of Wood Char in a Transport Reactor

by

Richard Turton

A THESIS

submitted to

Oregon State University

in partial fulfillment of
the requirements for the
degree of

Master of Science

Completed June 1979

Commencement June 1980

APPROVED:

Redacted for Privacy

Assistant Professor of Chemical Engineering
in charge of major

Redacted for Privacy

Head of Department of Chemical Engineering

Redacted for Privacy

Dean of Graduate School

Date thesis is presented June 8, 1979

Typed by Opal Grossnicklaus for Richard Turton

DEDICATION

To Don and Joyce

For all their years of patience and love

ACKNOWLEDGEMENT

I would first like to thank my major professor and friend Dr. Ferhan Kayihan, whose guidance and wisdom have inspired me throughout my stay at Oregon State University. I think it is fair to say that without his continual encouragement and suggestions the completion of this thesis might still be just a figment of my imagination.

It is difficult to single out members of the staff who have not helped me throughout my stay in the United States. However, I would especially like to thank Dr.'s Wicks, Mrazek, Levenspiel and Fitzgerald, all of whom have shown me great kindness and whose classes have always been so stimulating. I would also like to express my thanks to Dr. D. Junge for the continued financial support throughout my stay at Oregon State.

When one comes to a country for the first time a sense of loneliness and isolation from one's family, is inevitable. However, in my case these feelings lasted only until I met the Bacon family. Their warmth and friendship were so genuine that I was compelled to forget my troubles. My special thanks go to Meric and Marion whose food bills have probably doubled since they met me (not to mention the beer). Thanks also go to Kenny and Judy Brown for many happy nights of interesting conversation and pinball playing.

Finally, I come to my future wife, Meredith. What can you say about someone you adore!? I could expound on how she has helped me or how she has lifted my spirits when they began to droop. However, I think that all this may be summarized by saying that her total faith in me has been my greatest inspiration. To Meredith, goes my deepest love and thanks.

NOTATION

A	Area (M^2)
C	Specific Heat Capacity (J/Kg K)
C_1	The Component of Drag Coefficient Associated with the Non-Sphericity of a Particle
Cd	The Drag Coefficient of a Particle Falling in a Medium
d	Diameter (M)
D	Diffusivity (M^2/s)
E	Emissivity
F	Flowrate (Kg/s)
$\triangle F$	Change of Flowrate of Solids Due to Combustion in the Initial Heat Balance (Kg)
h	Heat Transfer Coefficient (W/M^2K)
$\triangle H$	Heat of Reaction for the Combustion of Carbon with Air Yielding Carbon Dioxide only: $C + O_2 = CO_2$ (J/Mole)
$\bar{k}$	Thermal Conductivity (W/M k)
$k_{chem}, k_{diff}, k_{ov}$	Reaction Rate Coefficients for the Chemical, Mass Transfer and Overall Process Steps ($Mole/M^2/s$)
Kd	$CdRe_s^2$
L	The Length Travelled in the Reaction Section of the Model (M)
M	Mass (Kg)
N	Number of Particles
Pr	Prandl Number
Q_{rad}, Q_{conv}	The Rate of Heat Transfer by Radiation and Convection from the Walls of Reactor (W/M)
r	The Radius of a Particle (M)
R	The Universal Gas Constant (J/Mole K)
$\bar{R}$	Resistance to Reaction (s M^2/Mole)
Re	Reynolds Number
Sc	Schmidt Number
SC	Stoichiometric Coefficients in a Chemical Equation
T	Temperature (k)
V	Velocity (M/s)
W	Weight Fraction in Size Distribution
X_A	Overall Conversion of Carbon
$Y_{O_2}, Y_{CO_2}, Y_{N_2}$	Mole Fractions of Oxygen, Carbon Dioxide, and Nitrogen in the Combustion Gas

<u>Greek Symbols</u>

α'	Inorganic Weight Fraction in the Product Ash
β	Combustible Weight Fraction in the Wood Char Feed
β	Volume Fraction for Gas Split

ψ	The Surface Sphericity
ε	The Effectiveness Factor for the Reaction of Porous Carbon
ρ	Density (Kg/M^3)
ϕ	The Form Sphericity
σ	The Steffan-Boltzman Constant (W/M^2K^4)
γ	Volume Fraction of Reactor Split

Subscripts

p	Particle
g	Gas
c	Carbon
w	Wall
R	Reactor
s	Particle Surface

TABLE OF CONTENTS

LIST OF FIGURES

LIST OF TABLES

COMBUSTION STUDIES IN THE TRANSPORT REACTOR

I INTRODUCTION

The problem of excessive particulate emissions from Wood-fired Boilers has plagued this type of equipment throughout its history. A common practice for the operation of these boilers is the reinjection of particles, collected in the multiclone separators, back into the boiler system. Although this reinjection eliminates the problem of what to do with the fines. It, however, causes another problem.

By reintroducing small particles into the system the particle size distribution within the boiler is changed from what it would be if reinjection were not permitted. Thus, the number of small particles in the system is increased and this increases the loading on the cyclones which in turn leads to higher particulate emissions.

An alternative to reinjection is the removal of the particles from the main boiler to a small burner unit, where more efficient combustion can take place.

The combustion of small wood char particles in a burner, auxiliary to the main boiler has been studied. Some of the problems arising from the design and operation of such a burner have been identified and analyzed in this research work.

1.1 Need for Research

There are many problems involved in the accurate design of a Wood Char Burner. The mode of operation of the burner (e.g. Fluidized Bed, Plug Flow, Backmix etc.) is not obvious.

The vast majority of previous research work on carbon combustion was carried out using coal as the source of carbon. Owing to this lack of information on wood char combustion, accurate predictions of particle burning times are impossible. Further complications arise due to the lack of experimental data on the physical properties of wood char.

Due to the above factors and the growing need to reduce particulate emissions from wood fired boilers a program dealing with basic research on wood char burners was started at Oregon State University.

1.2 The Goals of the Research

An experimental wood char burner has been constructed at Oregon State University for basic research into the combustion of wood char, obtained from various types of wood fired boilers. Figure 1 is a photograph of the installation which is situated at the Experimental Station, Fairplay, Corvallis, Oregon.

The goals of the author's research were threefold.

First, a computer simulated model of the reactor was to be developed. This would allow certain unknown parameters, relevant to the combustion of wood char, to be evaluated. The computer model would also aid the design of possible future burners of this type.

Second, experiments on the burner were to be carried out in order to check the assumptions and accuracy of the combustion model.

Third, experiments were to be performed on the wood char in order that certain physical properties, required in the model, could be obtained.

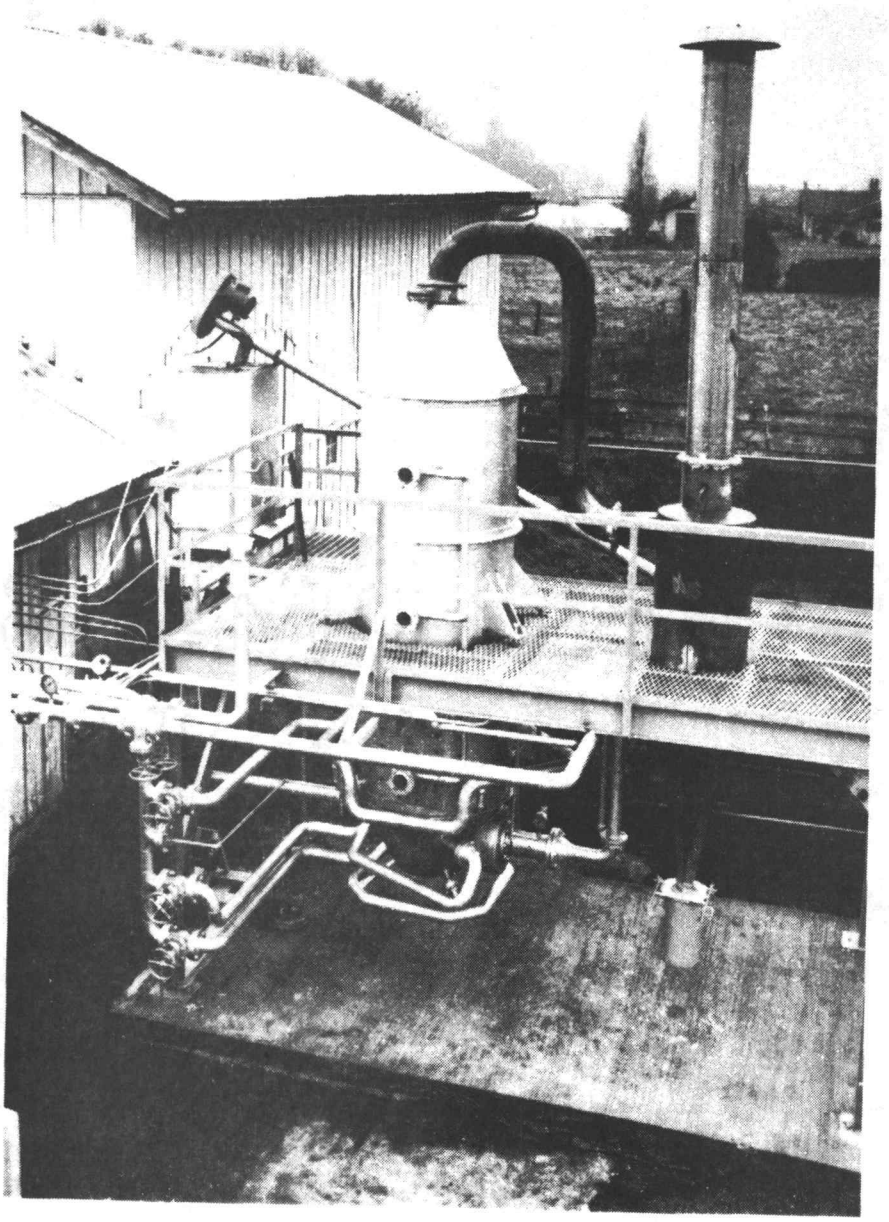

Figure 1. The experimental facility at Fairplay.

2. THE LITERATURE SEARCH

A literature search was carried out at the beginning of this work. Information obtained from this search and subsequent searches was used to evaluate the merits of different approaches to the combustion problem. A summary of this information is given below.

2.1. Combustion

Considerable work has been carried out on the combustion of carbon in the last fifty years. Most of this research has used coal as its primary source of carbon.

The kinetics of combustion reactions has been dealt with, in some detail by Nusselt (1), Spalding (2), Essenhigh (3), and Frank-Kameneski (4). A review of such work along with a summary of their findings is given by Field et al. (5).

The particles sizes considered in the above works, range from 25 to 4000 microns and hence the correlations presented may be used in this study.

There are many physical and phenomenological models of combustion in use today. Many of these models assume that the carbon particles may be well represented by some simple geometric shape (e.g. spheres, flat plates). This assumption simplifies the mathematics and allows the simple formulation of the conversion and

burning time.

Possibly the most well known models are the Shrinking Sphere, Shrinking Core and uniform conversion models. The first two models were originally developed by Yagi and Kunii (6 & 7). The third model along with a comprehensive description of the first two is given by Levenspiel (8).

For any combustion model it is necessary to evaluate a chemical reaction rate. The process which occurs at the temperatures considered here (i.e. less than 1400 K) is thought to be an adsorption-desorption process. The net rate at which reaction takes place for this process has been studied by various researchers. Parker and Hottel (9), Tu, Davis and Hottel (10). Golovina and Khaustovich (11) and Gray and Kimber (12). The value used in this work was that obtained by Parker and Hottel (9). They studied the burning rate of small carbon spheres in air at temperatures between 900 and 1400 K.

The primary combustion product was found to be carbon dioxide, this may in fact be false and Field et al. (5) give a comprehensive review of the surface carbon-oxygen reaction.

It is also necessary to evaluate the mass transfer coefficient for the transport of atmospheric oxygen from the bulk air stream to the surface of the particle. The value used here was that predicted by the well known Froessling equation (13).

It becomes apparent that the reaction rates predicted by the

shrinking sphere and core models, using the above correlation, are a gross underestimate. This underestimation is believed to be due to the fact that the carbon used here has a very large internal surface area. The effect of porosity and internal surface area on the reaction rate is considered by Walker et al. (14). The approach used by Walker is similar to the one often adopted for solid catalyst reactions. The internal surface area is combined with the surface reaction coefficient and modified by an effectiveness factor which accounts for the resistance to pore diffusion. This approach is, in essence, the same as that proposed by Thiele (15) and Weiss (16).

2.2. Particle Transport Processes

The entrainment of particles of different shapes and sizes has been studied by Zenz and Othmer (17), Knudsen and Katz (18) and Brown (19). These studies give several correlations for the drag coefficient. However, the bulk of the above work is applicable to either small particles in the stokes Regime ($Re_p < 0.1$) or the larger particles in the Newton's Law regime ($Re_p > 1000$). Unfortunately, the bulk of the solids used here have particle Reynolds numbers in the intermediate region (0-200) and hence the above correlations are of only limited value.

Becker (20), however, studies the effects of shape on the particles terminal velocity in this intermediate range. It is from this

work, that the correlations used here, were taken.

Finally, the evaluation of heat transfer coefficients used in the prediction of convective and radiant heat transfer were taken from Welty, Wicks and Wilson (21) and Rohsenow and Hartnett (22). The convective heat transfer coefficient for gas to particles was taken from the Ranz and Marshall equation (23), while for the situation of heat transfer from the hot walls of the reactor to the gas, the Colburn analogy (24) was used.

3. THE COMPUTER SIMULATED MODEL OF COMBUSTION

3.1. Description of the Processes Occurring within the Reactor

The reactor used in the experimental test runs is shown in Figure 1.1 and a schematic diagram illustrating the flows to and from the reactor is given in Figure 3.1 and a full description of how the reactor was operated is given in Appendix (I). It is sufficient to note that these are basically two modes of operation for the reactor.

First, the combustion air can be introduced tangentially. This produces a swirling mass of hot gas and entrained particles. Figure 3.2 is a photograph from the top view port, which was taken whilst the reactor was being operated in this mode. Due to the swirling action of the gas, the reactor looks very much like a cyclone. The particles are thrown outward by the centrifugal force and tend to move in an anulus near the wall of the reactor. Some scraping action occurs as particles are thrown against the refractory lined walls of the reactor. This scraping action tends to slow the movement of the particles and hence increases their mean residence time within the reactor.

Second, the mode of operation is achieved by directing the main combustion air into the very bottom of the reactor. This air is fed via the radial ports situated at the base of the combustion chamber. Some turbulence and mixing occurs at the lower portions of the

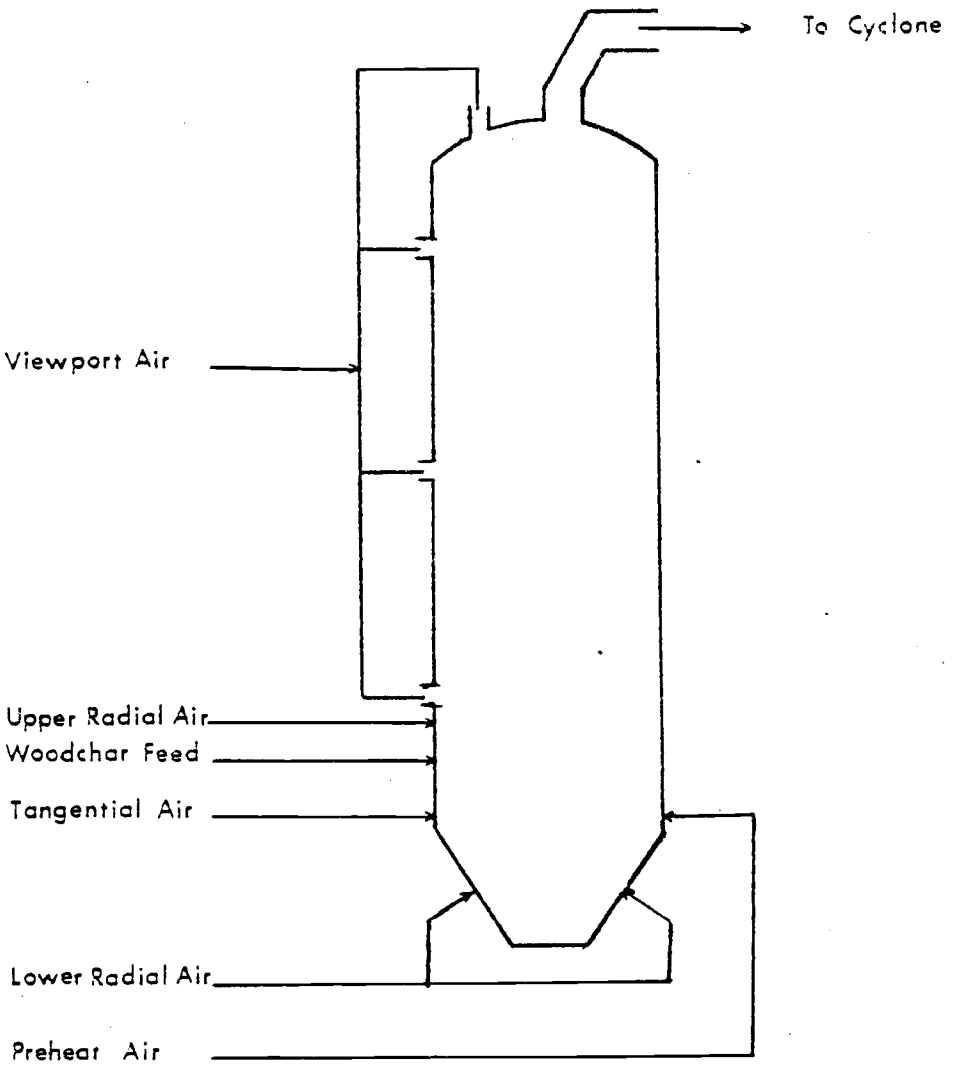

Figure 3.1 : Schematic Diagram of Flows to and from the Charburner

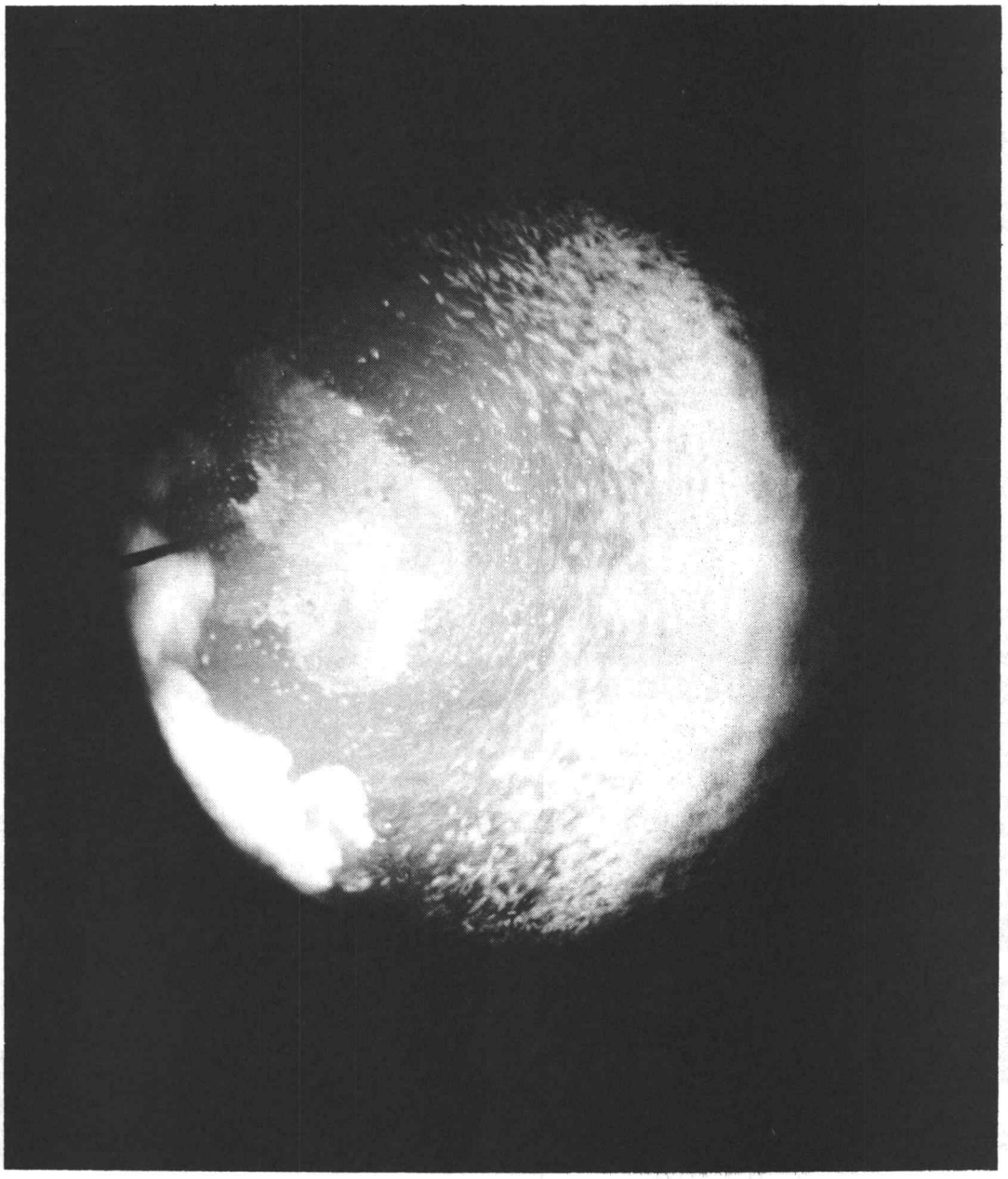

Figure 3.2. Photograph showing the reaction chamber whilst operating in the tangential mode. The photograph was taken from the top viewport and looks down into the reactor.

reactor and this is illustrated in Figure 3.3. This turbulence dies out however as the gas and entrained particle move upward, and the scraping action of the particles against the walls is much less than in the previous mode.

As cold air and char particles are fed into the hot combustion zone of the reactor, several processes occur simultaneously. In order to be able to mathematically describe these processes it is necessary to recognize and understand what happens.

As a cold char particle enters the reactor it is immediately exposed to the hot inside walls of the reactor. Thus heat is transferred by radiation to the particle from the refractory walls. The particle will also come in contact with the hot combustion gases present within the reactor. Thus the particle will also receive heat by convection from the hot gases in the reactor. If the particle is very small then the convective heat transfer coefficient will be large and the time required to raise the particle's temperature to near that of the gas may be only a few milliseconds. Thus, the small particles will begin to react only a very short time after entering, while the larger particles may take considerably longer to reach a temperature at which significant combustion may take place. Another process which effects the particles is that of entrainment. The terminal velocity of a small particle will be small and hence entrainment into the gas stream will occur immediately on entering the reactor. This is not so for larger particles. If a particle has a terminal velocity

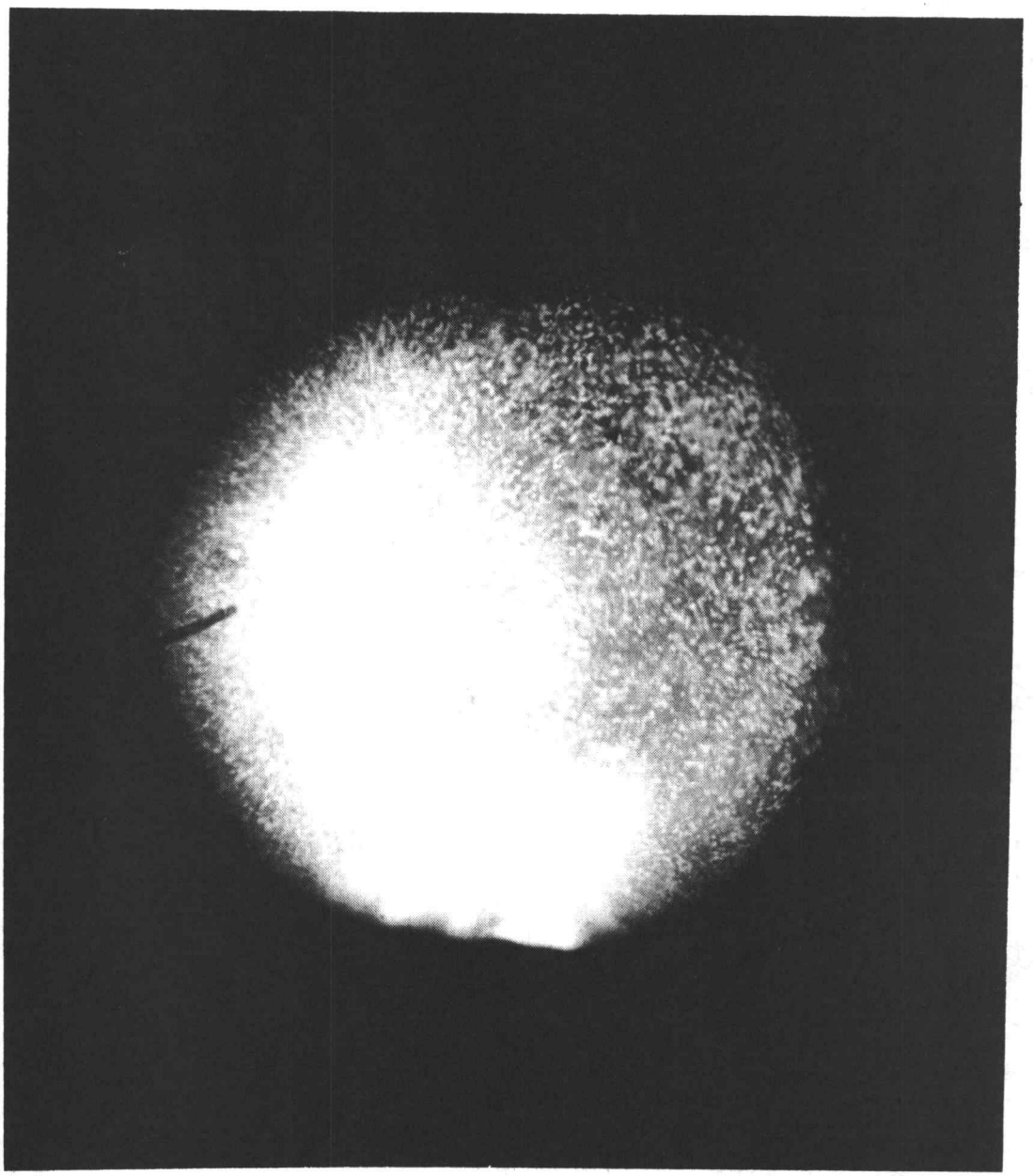

Figure 3.3. Photograph showing the reaction chamber whilst operating in the radial mode. The photograph was taken from the top viewport and looks down into the reactor.

less than the gas velocity within the reactor then entrainment is not likely to take place. These large particles will start to fall when they enter the reactor. However since the gas flow is swirling and fairly turbulent these particles are bumped and blown around and are exposed to the hot gases and reactor walls. This allows a certain amount of reaction to take place even for these large particles. Heat transfer by conduction from the hot reactor walls and inter particle collisions are also possible. However, its prediction may well be of a stochastic nature and is far more complicated than the other processes described.

For the case of cold inlet air entering the reactor the transport processes involved are slightly different.

The heat transferred to the air by radiation from the reactor walls is small. This is because diatomic gases of symmetrical composition such as O_2, N_2 and H_2 may be considered transparent to thermal radiation. There will, however, be some radiation to the CO_2 formed by combustion but for the temperature range considered here the effective emmisivity will be low (less than 0.08). The inlet air will also receive heat by convection, both from the reactor walls and the burning particles. Finally, there will also be an amount of mixing between the inlet air and the hot combustion gas present in the reactor.

The above description outlines the processes of heat and mass

transfer occurring within the reactor. In the following section the assumptions used in the combustion model are reviewed and discussed.

3.2. Assumptions Made in the Combustion Model

Whenever a real process is mathematically modelled it becomes necessary to make certain simplifying assumptions. Without these assumptions the mathematics describing the process may become unbearably complicated or even worse - non-solvable.

So the key question is what assumptions can be made to simplify the mathematics yet still be justified from a physical standpoint.

The following section outlines the assumptions made in the model and gives a brief explanation of why the assumptions were made.

3.2.1

All the combustion is assumed to take place within the reactor. Thus, combustion in the cyclone and the associated piping is ignored.

Since neither the pipework nor the cyclone is insulated considerable cooling of the combustion products occurs on leaving the reactor. This cooling will tend to slow the reaction. It was also observed that little carryover from the reaction chamber occurred. Therefore, the fact that at most only 10% of the feed is carried out of the reactor and that as soon as it leaves the reactor, considerable cooling takes place,

it is justified to make this assumption.

3.2.2

The wood char particles are assumed to be isothermal.

For small particles this assumption will be accurate, since the mass of the particle is small and the thermal conductivity reasonably high. For larger particle at high rates of combustion it is quite likely that some temperature profile will exist within the particle. However, it has been shown for the similar process of heterogeneous catalyst that the temperature profile in the particle will only be significant when a temperature difference exists across the gas boundary layer (Levenspiel, 8). Since the effect of the boundary layer temperature gradient will be more significant than the gradient within the particle, it is reasonable to ignore the latter.

3.2.3

The temperature of a wood char particle is assumed never to exceed that of the surrounding gas.

This assumption allows for a particle to warm up to the gas temperature but once it has reached it the particle temperature moves with that of the gas. Thus in effect, the convective heat transfer coefficient is assumed to be very large at high temperatures. The convective heat transfer coefficient for a spherical particle in a fluid

medium is given by the Ranz and Marshall Equation.

$$h = \frac{k}{d_p} (2 + 0.6\ Re_p^{1/2} Pr^{1/3})$$

The value of this coefficient is rather insensitive to temperature variation. However, it is inversely proportional to the particle diameter to some positive power i.e.

$$h \propto \frac{1}{d_p^n} \qquad \text{where} \qquad 1/2 \leq n \leq 1$$

For small particles (low Re_p) the heat transfer coefficient is very large, but for larger particles the value is greatly reduced.

It would seem that the assumption that all particles have a temperature less than or equal to the gas temperature is erroneous for large particle. However, it was found that the computation of an individual heat balance for a particle at high temperatures caused the system of ordinary differential equations to become exceedingly stiff. Therefore, since this assumption allows the systems of equations describing the reaction process to be solved fairly easily and further, since this is a conservative estimate of particle combustion, it was adopted.

3.2.4

The only combustion reaction which was considered to take place was the direct oxidation of fuel to carbon dioxide i.e.

$$C_{(s)} + O_{2\,(g)} \rightarrow CO_{2\,(g)}$$

At the temperatures at which the test runs were carried out the gas phase oxidation of carbon monoxide to carbon dioxide is very rapid. Thus it would seem reasonable to assume that any carbon monoxide formed by combustion would be very quickly converted to carbon dioxide.

It is, however, worth noting that at the operating temperatures used here, it has been found (Field et al., 5) that the primary combustion product is, in fact, carbon monoxide.

For large particles the gas phase oxidation of carbon monoxide will occur very close to the particle surface. This situation is well represented by the above reaction scheme.

For small particles, the boundary layer of gas around the particle is very thin. Hence, the possibility of carbon monoxide escaping into the bulk gas stream and reacting there, is much higher. This two step reaction process is not the same as the one step, heterogeneous reaction described above. Thus for small particles we may have

$$\underset{\text{heterogeneous}}{C_{(s)} + 1/2\ O_{2(g)} \rightarrow CO_{(g)}} \underset{\text{homogeneous}}{+ 1/2\ O_2 \rightarrow CO_{2(g)}}$$

The situation described above has been modelled in essence by various workers (e.g. Spalding, 2). The solution however may be very

involved. Thus the one step reaction scheme has been used due to its simplicity.

3.2.5

Due to lack of experimental research the variation of the shape and inorganic and water content, with particle size has been ignored. The first property was known to vary with the size of the particle, since various samples were studied under an optical microscope. It was however felt that these variations could be adequately accounted for by assigning mean values for each feed sample.

3.2.6

All the char particles are assumed to have a form sphericity of 0.63 and a surface sphericity of 0.40. These values were estimated with the aid of a microscope and compared reasonably well with values from the literature (25). An effective spherical diameter of 0.6 is also assumed and again this is estimated by observation. It is recognized that the assumptions in 3.2.5 and 3.2.6 are rather crude--however, the combustion model can be adapted quite easily, to account for such variations.

The above discussion outlines the main assumptions of the model. The following section covers the derivation of equations and the general approach used to describe the combustion process.

3.3. The Combustion Model

The combustion model developed in this work is presented here by giving a general descritpion of what the model is capable of doing. It should be pointed out that in using the model, the degree of sophistication may be arbitrarily specified by choosing what sections of the model are to be included. This allows a comparison between a complicated system description and a simple one, to be made. As an example the fourth section of the model, described below, evaluates the surface average particle diameter. It was originally thought that this typical particle size could be used to predict the behavior of the whole particle size distribution. Unfortunately, this typical particle size may underpredict the burning time for larger particles and by using this unisize distribution the combustion process is not accurately described. Although by including the option for a mean size evaluation, the prediction of a unisize distribution may be computed and in some cases may be used.

The following discussion considers the six main sub-sections of the model and describes each section. These sub-sections can be combined in series to give the overall process description.

3.3.1. The Initial Heat Balance (Sub-section 1)

The processes which occur when char particles and cold air enter the reaction chamber were discussed in 3.1.

The purpose of this section in the model is to take account of the processes which occur immediately on entering the reactor. These are namely, the combustion of very small particles and the reduction of the large particles to a size at which entrainment may take place.

For very small particles the convective heat transfer coefficient is extremely large. It can be shown that the time required (t_f) for a particle originally at a temperature T_1 to rise to a temperature T_2 whilst surrounded by a gas at a temperature of T_g is given by:

$$t_f = \frac{\rho C_p d_p^2}{12 \bar{k}} \log_e \frac{(T_g - T_1)}{(T_g - T_2)} \qquad 3.1$$

From equation 3.1 it is obvious that the time required for a very small particle to warm up to near gas temperature is very small (a few milliseconds for particles less than 100 micron). It can also be shown that the burning times for a small particle is also low. Thus the combined heating and reaction time for, say, a 10 micron particle in a gas stream at 1000K is less than 150 milliseconds. It would thus seem reasonable to assume that small particles less than a certain maximum size, react immediately upon entering the reactor (assuming of course that they immediately come in contact with hot combustion gas). The value of the maximum size particle to

completely react may be changed. By assigning a value less than the smallest size in the particle distribution this effect is eliminated.

As mentioned previously the gas velocity within the reaction chamber will, in general, not be sufficient to entrain all the particles. It is thus necessary to estimate the size of a particle which may just be entrained by the gas. The effect of the shape and size of a particle on its terminal velocity was considered in Appendix E. From this section the particle size which is just entrained by a gas velocity V_g is given by:

$$d_p = \frac{3\, C_d\, V_g^{\,2}}{4\, (\rho_p - \rho)\, g\, \psi} \qquad 3.2$$

where the value of C_d is a function of particle Reynolds number and various shape factors (see Appendix E).

The value of particle diameter given in equation 3.2 refers to the equivalent diameter of an equal volume sphere and must be used accordingly.

It is assumed that particles with size greater than that predicted by equation 3.2 will not be entrained. This does not mean that these particles will fall to the bottom of the reaction chamber and stay there. On the contrary, these particles will be swept and blown around sampling the hot gas and hot reactor walls. A certain amount of combustion will take place. When enough reaction has occurred, so that the particle size has been reduced to that given by 3.2,

entrainment can then take place. The particle will then leave the bottom of the reactor and travel upward through the reactor.

Thus two combustion processes occur in the initial heat balance. The very small particles are seen to react almost as soon as they enter the reactor. The large particles do not get entrained immediately. However, they move about and react until their size is small enough for entrainment to take place. At steady state the number of large particles in the bottom of the reactor is constant. Hence in the heat and mass balance for the bottom part of the reaction chamber the large particles may be assumed to shrink to the size of the entrainable particles.

The initial heat balance finds the temperature which is the root of the non-linear equations describing the above process.

The equations describing this process are written in the function subprogram Heat B1 (see listing of program in Appendix G). This function evaluates the error in the heat balance when an input temperature is specified. By using this evaluation in conjunction with an interval halving root finding technique the correct exit temperature for particles and gas is found.

Perhaps the easiest way to follow the logic of the above procedure is to study the effect of particle size distribution before and after the heat balance. This is illustrated in Figure 3.4.

It should also be noted that there is provision for the inclusion

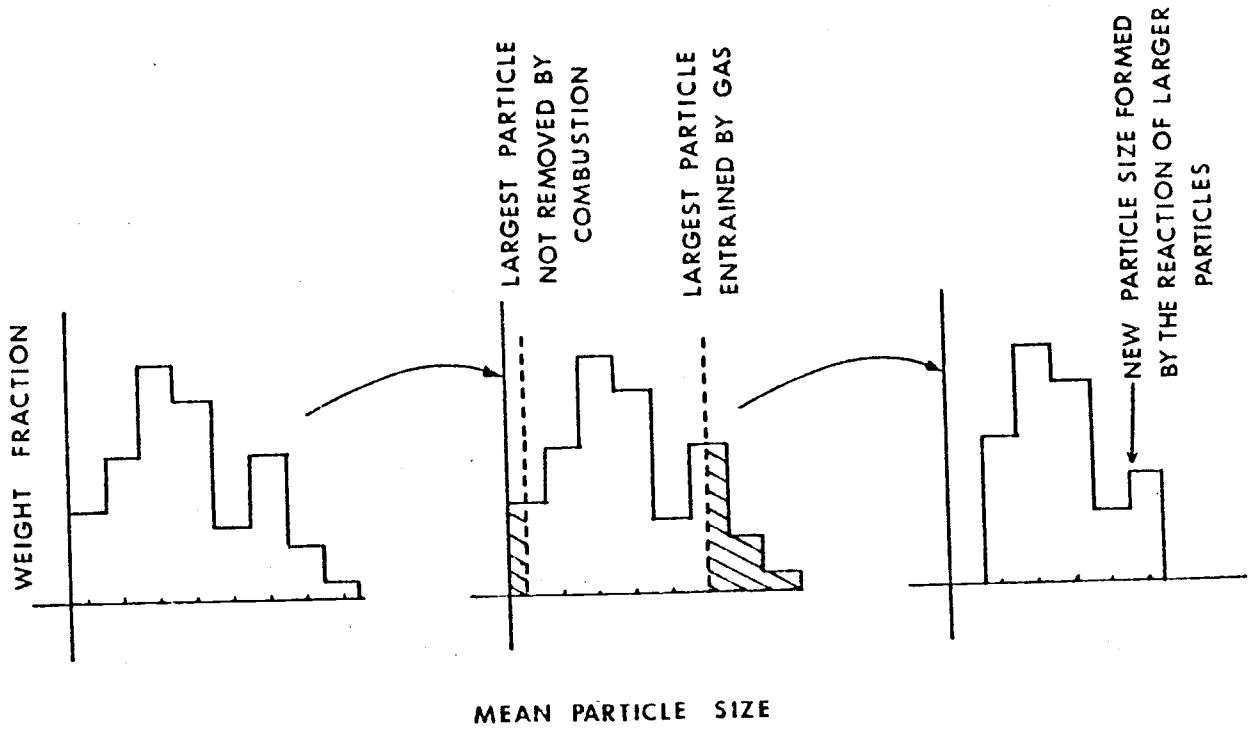

Initial Size Distribution

The Effect, on the Distribution, of Processes Occuring in the Initial Heat Balance

Size Distribution Entering the Reaction Section of the Model

Fig 3.4 The Processes Occuring in the Initial Heat Balance

of a zero terminal velocity. Thus the situation where all the particles are entrained can be simulated.

3.3.2 The Gas Stream and Reactor Split (Sub-Section 2)

After the initial heat balance has been calculated, the gas and solids begin to move upward through the reactor.

When all the main combustion air is introduced via the bottom radial ports then the solids and gas move upward and can be physically described by a plug-flow model.

However, when the main air is introduced tangentially, the solids are pushed toward the outside of the reactor and move in a swirling annulus up through the reactor (see Figure 3.2). To describe what happens in this mode of operation is not straightforward. It was however decided to simulate this tangential mode by splitting both the gas stream and reaction zone. This is illustrated in Figure 3.5.

The reactor volume is split into a reaction section and a bypass section. All the solids are assumed to move in the reaction section. However, only a portion of the gas will move with the solids, the remaining gas will move through the bypass section. Both the amount of gas flowing in a section and the volume of the section may be chosen. Hence, the gas velocity in the reaction section may be adjusted and this in turn will effect the residence time of the solids in the reaction

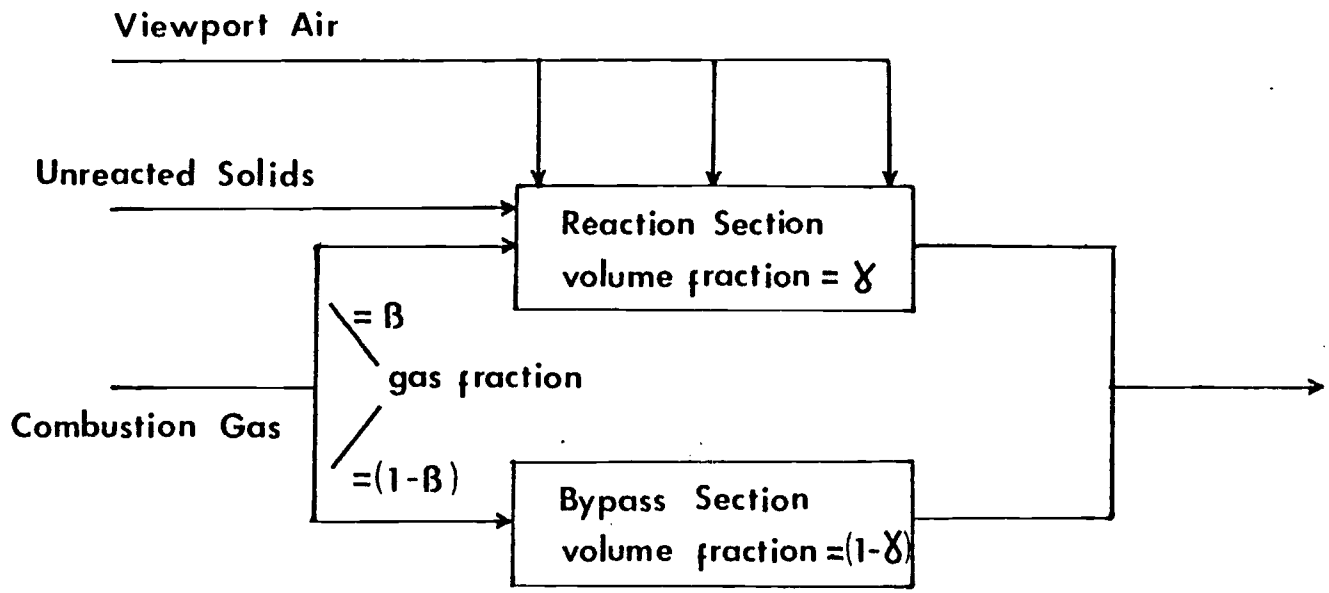

Fig 3.5 The Gas Stream and Reactor Split

zone.

It is assumed that there will be no heat or mass transfer between the two reactor zones until mixing occurs at the top of the reactor.

The split of gas flows and reactor volume is carried out by the subroutine Gasplit (see Appendix G). It should be noted that by choosing both the split parameters as unity, the situation where all the gas and solids move together through the reactor is simulated.

3.3.3. Calculation of the New Particle Size Distribution (Sub-Section 3)

The amount of solids leaving the bottom of the reactor with the gas will, in general, not be the same as the amount fed to the reactor. This is because certain size reduction of the larger particles must take place to allow for entrainment. The weight fractions of the various particles must be recalculated with respect to the amount of char remaining.

For the small particles which totally reacted the new weight fractions are obviously zero. For the remaining particles, excluding the size just entrained, the new weight fractions are given by:

$$w_i' = w_i \ (F_c^{\,o}/F_c) \qquad 3.3$$

while for the particle size just entrained we have

$$w_j' = \left(\sum_{i>j} w_i \quad F_c^{\,o} - \triangle F_c\right)/F_c \qquad 3.4$$

Where $\triangle F_c$ is the carbon lost in the initial heat balance due to reduction of the large solids to size j.

3.3.4. Surface Average - Mean Particle Size (Sub-Section 4)

Later in the description of the model it becomes necessary to integrate a certain system of ordinary differential equations. Each particle size will possess different kinetic and transport rates - and should thus have a system of equations to describe these processes. However, if a suitable mean particle size can be calculated then the description of the processes may be summarized by this typical particle. This, of course, will greatly simplify the mathematics and will present a smaller system of differential equations to solve.

In heterogeneous processes one of the most important parameters of the transport pehnomena is the surface area of the solid phase. It would thus seem logical to adopt a surface average mean particle size.

The procedure for calculating this mean particle size is based on that given by Kunii and Levenspiel (26) and is modified for the case of changing density with particle size. The surface average particle size $\overline{d}_p$ is given by

$$\bar{d}_p = \frac{\Sigma\, w_i/\rho_{p_i}}{\Sigma\, w_i/d_{p_i}\rho_{p_i}} \qquad 3.5$$

The evaluation of $\bar{d}_p$ is carried out by the sub-program SAVEDP (see Appendix G). Equation 3.5 gives the mean surface average particle size when spherical particles are considered. Thus, equivalent spherical diameters should be used in this evaluation.

3.3.5. The Reaction Section

The amount of gas, the particle size distribution and the volume of the reaction section have all been evaluated. All that remains is to correctly evaluate the kinetic, heat and mass transfer processes which occur as the particles and gas move upward toward the exit.

Since the particle size, gas composition and temperature all change through the reactor it is necessary to evaluate the correct differential equations which accurately describe this situation. These equations must then be integrated along the length of the reactor.

A slip velocity between the particles and the gas will exist, due to the non-zero terminal velocity of a particle. It is, therefore, more convenient to consider a differential length increment rather than a time increment. The processes occurring within this differential increment are illustrated in Figure 3.6.

The following section develops the equations used in the reaction

section and illustrates the technique used for the integration.

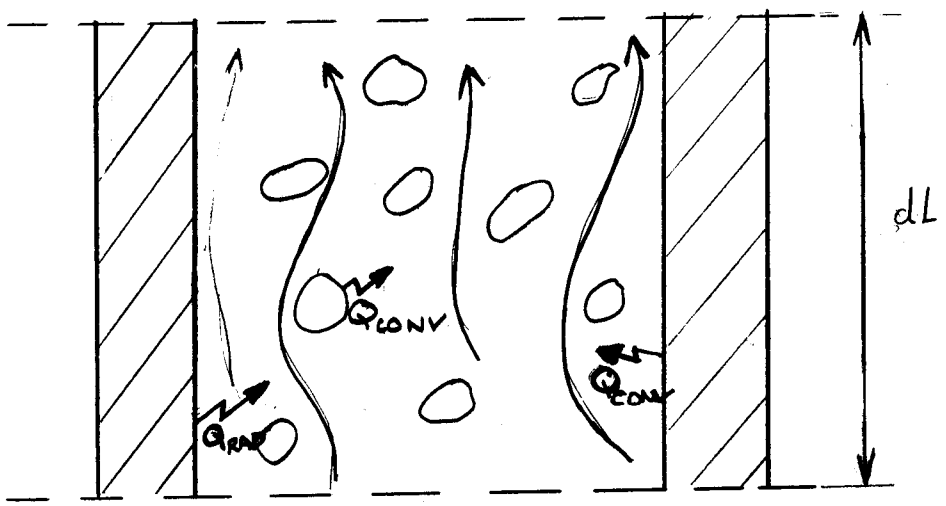

Figure 3.6. The processes occurring within a differential length increment of the reaction section.

Material Balance on a Char Particle. For a char particle of size d_p the rate of reaction may be expressed as (see Appendix F)

$$\frac{dM_p}{dt} = -k_{ov} y_{O_2} \frac{\pi d_p^2}{\phi} \qquad 3.6$$

Since we are interested in a length dependence equation 3.6 may be written as

$$\frac{dM_p}{dt} = -k_{ov} y_{O_2} \frac{\pi d_p^2}{\phi} \frac{1}{V_p} \qquad 3.7$$

Where V_p is the net upward particle velocity Equation 3.7 may be equivalently expressed in terms of conversion.

Since $1 - X_A = M_p/M_p^o$

we have

$$M_p^o \frac{dX_A}{dL} = \frac{dM_p}{dL} = k_{ov} y_{O_2} \frac{\pi d_p^2}{\phi} \frac{1}{V_p}$$

or

$$\frac{dX_A}{dL} = \frac{k_{ov} y_{O_2} \pi d_p^2}{M_p^c} \frac{1}{V_p}$$

$$\frac{dX_A}{dL} = \frac{k_{ov} y_{O_2}}{V_p \phi \rho_p d_p} (1 - X_A) \qquad 3.8$$

The heat balance on a single particle is considered next.

<u>Heat Balance on a Char Particle</u>. One of the assumptions in this model is that a particle may never exceed the gas temperature. The following equations, therefore, will only apply at particle temperatures less than the gas temperature.

The enthalpy balance for a particle of diameter d_p and temperature T_p is given by

$$\frac{d}{dL} (M_p C_p T_p) = \frac{dM_p}{dL} \Delta H + Q_{RAD} + Q_{CONV} \qquad 3.9$$

where

$$Q_{RAD} = \sigma E A_p (T_w^4 - T_p^4)/V_p$$

$$Q_{CONV} = h_p A_p (T_g - T_p)/V_p$$

The term $(M_p C_p T_p)$ on the L.H.S. of equation 3.9 contains

3 length dependent quantities. However for the sake of simplicity we may assume that the specific heat of the carbon (C_p) is effectively constant over the incremental length. Thus the L. H. S. of equation 3.9 may be written as

$$\frac{d}{dL}(M_p C_p T_p) = M_p C_p \frac{d}{dL}(T_p) + T_p C_p \frac{dM_p}{dL}$$

Using the above relationship in equation 3.9 and rearranging terms we may write

$$\frac{\phi V_p d_p \rho_p C_p}{6} \frac{dT_p}{dL} = \sigma E(T_w^4 - T_p^4) + h_p(T_g - T_p) + k_{ov} y_{O_2} (C_p T_p - \Delta H) \qquad 3.10$$

From equations 3.8 and 3.10 it can be seen that we must have a relationship between the particle diameter d_p and the distance travelled in the reactor L. A differential equation may, of course, be written to describe the particle shrinkage. However it is more convenient to use the algebraic relationship between diameter and conversion i.e.

$$d_p = d_p^o \left(\frac{\rho_p^o (1 - X_A)}{\rho_p} \right)^{1/3} \qquad 3.11$$

Equation 3.11 assumes that the particle may be represented by a shrinking sphere and this is further considered in Appendix F.

The equations presented above describe what happens to a

particle of a particular size as it moves through the reaction zone. The particles of char entering the reactor will not be of the same initial size. It is thus necessary to choose a typical particle size and represent the initial size distribution by this typical particle. Alternatively, if it is not justified to use a mean particles size then the distribution may be represented by a number of discrete size cuts.

The second method is the more general and is used here, it should be noted that a mean particle size may easily be handled by the general size cut approach, by assigning each size cut the mean particle size.

Before the gas balances are considered, it should be restated that both particles and gas are assumed to move in plug flow through the reactor. There will, of course be a slip velocity between particles and gas however the possibility of backmixing is not considered here.

<u>Overall Mass Balance for the Gas</u>. The overall mass balance for the gas can be written as:

$$\frac{dF_g}{dL} = F_c^{\,o} \frac{d\overline{X}_A}{dL} \left(\sum_{i = \text{products}} SC_i - \sum_{j = \text{reactants}} SC_j \right) \qquad 3.12$$

where SC_i is the stoichiometric coefficient of species i.

It was previously stated that the only reaction considered to be taking place was

$$C_{(s)} + O_{2\,(g)} \rightarrow CO_{2\,(g)}$$

Thus the stoichiometric coefficients for reactants and products are equal (the carbon is not included since it is in the solid phase). This means that the R.H.S. of equation 3.12 is zero, thus we may write

$$\frac{dF_g}{dL} = 0. \qquad 3.13$$

<u>Material Balance on Oxygen and Carbon Dioxide</u>. Again it is more convenient to express this relationship algebraically rather than differentially. Thus we may write

$$y_{O_2} = 0.21 - \overline{X}_A F_c^{\,o}/F_g$$

and

$$y_{CO_2} = \overline{X}_A F_c^{\,o}/F_g$$

<u>Heat Balance on the Gas</u>. The heat balance on the gas may be written in the following form

$$\frac{d}{dL}\left(\sum_i M_i C_i T_g\right) = \sigma E\,(T_w^{\,4} - T_g^{\,4}) \sum_i \frac{N_i \pi d_{p_i}^{\,2}}{V_{p_i}} + \pi\, d_R\, h_g (T_w - T_g)$$

$$+ h_p \sum_j \frac{N_j \pi d_{p_j}^{\,2}}{V_{p_j}} (T_g - T_{p_j}) - \frac{d\overline{X}_A}{dL} \Delta H F_c^{\,o} \qquad 3.14$$

where i - are all the components at the gas temperature

j - are all the components not at the gas temperature

It should be noted that the reaction term uses the overall conversion and does not specify that the particle must be at the gas temperature. However it may be reasoned that as soon as appreciable reaction takes place particle temperature will rapidly rise and very quickly reach the gas temperature. Thus, by including the overall conversion negligible error will be introduced.

The term or the L.H.S. of equation 3.14 inclues all species at the gas temperature. As in the case of a single particle we may assume that the specific heats are constant over the incremental length element and we may write

$$\frac{d}{dL}\sum_i M_i C_i T_g = \sum_i M_i C_i \frac{dT_g}{dL} + T_g \frac{d}{dL}\sum_i C_i M_i \qquad 3.15$$

Since the bulk of the enthalpy is carried by the gas we can effectively consider the total heat capacity of the stream to be a constant. Thus we can write

$$\sum_i M_i C_i \frac{dT_g}{dL} = \sigma E (T_w^4 - T_g^4) \sum_i \frac{N_i \pi d_{p_i}^2}{V_{p_i}} + \pi d_R h_g (T_w - T_g)$$

$$+ hp \sum_j \frac{N_j \pi d_{p_j}^2}{V_{p_j}} (T_{p_j} - T_g) - \frac{d\overline{X}_A}{dL} \triangle H F_c^o \qquad 3.16$$

The above equations describe the situation occurring within the

reaction part of the model. All that is required is the integration of these differential equations to yield the temperature and conversion profiles within the reactor.

The Method of Integrating the System of Equations. It was mentioned previously that the system of differential equations used to describe the combustion of a single particle may be "stiff." The term stiff means that one of the variables (i. e. temperature in this case) changes by a large amount very quickly, as compared with the other variables (conversion and mole fractions, etc.). Although this does not sound like a problem, it is. Since the integration must be carried out numerically, the step size used must be capable of handling this large change in the stiff variable. Thus the step size may have to be extremely small at the point where the stiffness arises.

By not allowing a particle's temperature to rise above the gas temperature the problem of stiffness is somewhat reduced. This is because as soon as the particle reacts appreciably, this is where the stiffness occurs, it is assumed to move to the gas temperature and stay there. The gas and hot particles provide a large thermal mass which slows down the large temperature changes, to a certain extent. However the stiffness is still present in the system and caution must be used when solution techniques are considered. Field et al. (5) consider the solution of the heat balance on a particle using

a graphical approach--this allows the equilibrium burning temperature to be calculated.

Several approaches were tried in order to reduce the computation time for solving the equations.

First, a variable step method due to Gears (26) was used. This algorithm was available from the International Mathematics and Statistics Library and this sophisticated technique provided good accuracy. However, since the model could only be used if this particular program were available it was decided to search for an alternative technique.

The second approach used an explicit Euler technique (27) and as might be expected could not handle the stiffness of the problem without a huge number of steps.

Finally a technique was adopted which was previously used by Kayihan (28) for a similar problem. This method uses the analytical solution of a 1st order differential equation as an approximation to the solution for a small step length. Then, the variables are updated for this step of the integration and these updated variables are used in the calculation of the next integration step. This method is illustrated below:

For a 1st order differential equation of the form:

$$\tau \frac{dx}{dt} + x = F \qquad \text{where F is a constant}$$

we may write $x = x_o + (F - x_o)(1-e^{-t/\tau})$

If an incremental stepwise integration is used with step size dt then we have the following recursive relationship.

$$X_{N+1} = X_N + (F-X_N)(1-e^{-dt/\tau}) \qquad 3.17$$

For the case when F is a constant, equation 3.17 gives the exact analytical solution. However if F is a function of x say, then we have only an approximate relationship. The error in the approximation depends upon how much F changes in dt. This approach, however, allows for the most dominant term in the equation to be accounted for analytically. Thus, this type of solution is implicit in form and the step length needed for a given accuracy will depend upon the non-linearity of the problem.

It was found that 3 figure accuracy could be obtained with this method, for the system of equations describing the reactor, using between 200 and 300 step lengths. This represents a reasonable compromise between precision and computation time and was, therefore, adopted. The actual value of the step length used depends upon the value of the temperature gradient for the previous step. If the gradient is high--then a very small step is taken. Conversely if the temperature gradient was small for the previous step then a larger step is chosen. This approach allows the stiff part of the solution to be evaluated economically without using unnecessarily small steps

for the non-stiff part of the solution.

3.3.6. The Intermediate Heat Balances (Sub-Section 6)

Since view port air is introduced at various points along the length of the reaction zone, it is necessary to account for the changing temperature and oxygen concentration.

The approach adopted here is to assume that the hot combustion gas and the cold view port air mix instantaneously.

This means that when the particles and gas reach a view port, the heat and mass balances must be solved.

Thus the cold view port air is instantaneously mixed with the mass of hot gas and reacting particles. The resulting gas conditions and temperature are found and the reaction is allowed to continue up through the reactor, until the next view port is encountered. This process is continued until the top of the reactor is reached. At this point the 'Bypass Gas' is mixed with the combination products and the final heat and mass balance is solved.

The evaluation of the above heat and mass balances is carried out by the subroutine "HEATB2" in the model (Appendix G). The resulting temperature and conversion profiles etc. will have discontinuities at these mixing points as can be seen in the following chapter.

This chapter has outlined the processes modeled and described

the working equations of the combustion model.

The next chapter presents the results for the experimental runs and compares them with the results predicted by the model.

4. COMPARISON OF THE EXPERIMENTAL RESULTS WITH THE RESULTS PREDICTED BY THE MODEL

In chapter 3 the model of combustion was developed. The purpose of this chapter is to compare the results predicted by the model with those obtained by experiment.

The results predicted by the model may be presented in several ways. However, it was decided to concentrate on the temperature profile within the reactor. The reasons for doing this are twofold. First, the temperatures within the reactor were known reasonably accurately and second the temperature profile is more sensitive than the oxygen concentration profile. The other parameters, however, are also considered, but with slightly less emphasis.

In the following comparison only ten of the eighteen test runs are considered. The results for all eighteen runs are given in Appendix D. For the first eight runs there was no flow meter installed on the view port airline and since estimating the view port air would be difficult the analysis of these results was not undertaken.

4.1. The Effect of the Overall Mass Balance on the Predictions of the Model

It becomes apparent when the results are analyzed that the effect of the mass balance on the temperature, or oxygen, profile is considerable.

The adiabatic flame temperatures for various excess air to carbon ratios are presented in Table 4.1. The effect of conversion of carbon and the fraction of inorganic ash (assumed to have the same specific heat capacity as carbon) is also considered. If the results in Table 4.1 are studied it becomes obvious that the percentage of excess air used has a great effect on the adiabatic plant temperature. For example, the temperature difference between using 80% and 100% excess air, is approximately 100 K. This change represents only a 10% difference in the overall mass balance. Thus the ratio of air to solids feed is very critical.

During the analysis of the experimental data the evaluation of the solids feed rate was carried out by two different methods (see Appendix D). The first method made use of the bulk density of the fuel coupled with the calibration curve for the solids feed system. This method provided a "direct" evaluation of the mass flow of solids into the reactor. The second method utilized an "indirect" approach. This consisted of back calculating the material balance using the molar flow rate of air, the conversion of carbon and the mole fraction of oxygen in the cyclone.

These two approaches should, ideally, give the same results. This was not the case however and the results for both methods of calculation are given in Appendix D. The results for the two methods differed by an average of 30% with the in-direct method predicting

Table 4.1. Adiabatic flame temperature for carbon combustion.

THE ADIABATIC FLAME TEMPERATURE FOR THE COMBUSTION OF CARBON

CONVERSION OF CARBON =100.00 %

% XS AIR	80.0000	85.0000	90.0000	95.0000	100.0000	105.0000	110.0000	115.0000	120.0000	125.0000	130.0000	135.0000
ASH FR												
0.0000	1632.46	1601.28	1571.60	1543.17	1516.04	1490.05	1465.20	1441.33	1418.40	1396.40	1375.29	1354.95
.0500	1628.15	1597.23	1567.71	1539.49	1512.56	1486.73	1461.98	1438.27	1415.50	1393.60	1372.59	1352.36
.1000	1623.48	1592.77	1563.46	1535.44	1508.67	1483.04	1458.45	1434.90	1412.28	1390.49	1369.63	1349.50
.1500	1618.24	1587.79	1558.74	1530.98	1504.37	1478.94	1454.51	1431.11	1408.65	1387.07	1366.31	1346.34
.2000	1612.43	1582.29	1553.44	1525.95	1499.59	1474.38	1450.15	1426.96	1404.65	1383.23	1362.63	1342.81
.2500	1605.89	1576.06	1547.58	1520.29	1494.20	1469.24	1445.27	1422.24	1400.14	1378.92	1358.48	1338.82
.3000	1598.58	1569.06	1540.89	1513.96	1488.13	1463.43	1439.72	1416.95	1395.05	1374.04	1353.81	1334.30
.3500	1590.17	1561.07	1533.31	1506.70	1481.23	1456.79	1433.39	1410.88	1389.24	1368.49	1348.47	1329.17
.4000	1580.58	1551.94	1524.55	1498.35	1473.29	1449.22	1426.08	1403.93	1382.55	1362.06	1342.29	1323.25
.4500	1569.42	1541.30	1514.43	1488.70	1464.00	1440.35	1417.62	1395.78	1374.82	1354.59	1335.13	1316.35

CONVERSION OF CARBON = 95.00 %

% XS AIR	80.0000	85.0000	90.0000	95.0000	100.0000	105.0000	110.0000	115.0000	120.0000	125.0000	130.0000	135.0000
ASH FR												
0.0000	1570.77	1540.94	1512.56	1485.38	1459.44	1434.59	1410.83	1388.00	1366.11	1345.09	1324.86	1305.46
.0500	1566.73	1537.10	1508.88	1481.90	1456.12	1431.42	1407.77	1385.09	1363.30	1342.40	1322.32	1302.97
.1000	1562.21	1532.85	1504.63	1478.06	1452.43	1427.89	1404.44	1381.88	1360.24	1339.49	1319.52	1300.27
.1500	1557.28	1528.13	1500.32	1473.76	1448.34	1424.00	1400.71	1378.35	1356.87	1336.22	1316.35	1297.26
.2000	1551.73	1522.89	1495.34	1469.04	1443.82	1419.70	1396.56	1374.35	1353.03	1332.59	1312.88	1293.94
.2500	1545.56	1517.02	1489.74	1463.64	1438.74	1414.82	1391.89	1369.89	1348.78	1328.49	1308.93	1290.15
.3000	1538.55	1510.33	1483.41	1457.62	1432.93	1409.32	1386.65	1364.86	1343.95	1323.88	1304.52	1285.90
.3500	1530.62	1502.76	1476.19	1450.72	1426.39	1403.04	1380.63	1359.10	1338.45	1318.58	1299.44	1281.02
.4000	1521.49	1494.09	1467.89	1442.84	1418.82	1395.78	1373.73	1352.51	1332.12	1312.46	1293.58	1275.42
.4500	1510.90	1483.98	1458.24	1433.65	1410.05	1387.43	1365.69	1344.78	1324.71	1305.41	1286.78	1268.88

CONVERSION OF CARBON = 90.00 %

% XS AIR	80.0000	85.0000	90.0000	95.0000	100.0000	105.0000	110.0000	115.0000	120.0000	125.0000	130.0000	135.0000
ASH FR												
0.0000	1508.67	1480.24	1453.11	1427.22	1407.47	1378.82	1356.09	1334.36	1313.50	1293.47	1274.23	1255.65
.0500	1504.83	1476.61	1449.63	1423.95	1399.31	1375.81	1353.24	1331.61	1310.85	1290.93	1271.79	1253.37
.1000	1500.58	1472.56	1445.85	1420.27	1395.83	1372.49	1350.07	1328.60	1307.95	1288.18	1269.14	1250.83
.1500	1495.91	1468.10	1441.59	1416.22	1391.99	1368.80	1346.55	1325.22	1304.73	1285.07	1266.18	1247.98
.2000	1490.67	1463.12	1436.87	1411.71	1387.69	1364.70	1342.60	1321.49	1301.15	1281.65	1262.86	1244.81
.2500	1484.81	1457.57	1431.53	1406.68	1382.86	1360.09	1338.19	1317.23	1297.11	1277.75	1259.13	1241.23
.3000	1478.17	1451.24	1425.56	1400.97	1377.42	1354.85	1333.21	1312.46	1292.54	1273.40	1254.93	1237.10
.3500	1470.64	1444.08	1418.71	1394.43	1371.19	1348.93	1327.56	1307.01	1287.35	1268.36	1250.15	1232.57
.4000	1461.98	1435.83	1410.88	1386.96	1364.03	1342.09	1321.02	1300.79	1281.33	1262.61	1244.60	1227.28
.4500	1451.97	1426.29	1401.75	1378.25	1355.73	1334.15	1313.40	1293.47	1274.33	1255.71	1238.17	1221.10

Table 4.2. Gas composition for adiabatic flame calculations.

THE MOLE/VOLUME FRACTIONS OF OXYGEN AND CARBON DIOXIDE FOR THE COMBUSTION OF CARBON
THE REACTION CARBON(S) + OXYGEN(G) =CARBON DIOXIDE(G) IS ASSUMED TO TAKE PLACE.

% XS AIR	80.00	90.00	100.00	110.00	120.00	130.00	140.00	150.00
CONVERSION =	100.00							
M F OXYGEN=	.0933	.0995	.1050	.1100	.1145	.1187	.1225	.1260
M F CO2 =	.1167	.1105	.1050	.1000	.0955	.0913	.0875	.0840
CONVERSION =	98.00							
M F OXYGEN=	.0957	.1017	.1071	.1120	.1165	.1205	.1242	.1277
M F CO2 =	.1143	.1083	.1029	.0980	.0935	.0895	.0857	.0823
CONVERSION =	96.00							
M F OXYGEN=	.0980	.1039	.1092	.1140	.1184	.1223	.1260	.1294
M F CO2 =	.1120	.1061	.1008	.0960	.0916	.0877	.0840	.0806
CONVERSION =	94.00							
M F OXYGEN=	.1003	.1061	.1113	.1160	.1203	.1242	.1277	.1310
M F CO2 =	.1097	.1039	.0987	.0940	.0897	.0858	.0823	.0790
CONVERSION =	92.00							
M F OXYGEN=	.1027	.1083	.1134	.1180	.1222	.1260	.1295	.1327
M F CO2 =	.1073	.1017	.0966	.0920	.0878	.0840	.0805	.0773
CONVERSION =	90.00							
M F OXYGEN=	.1050	.1105	.1155	.1200	.1241	.1278	.1312	.1344
M F CO2 =	.1050	.0995	.0945	.0900	.0859	.0822	.0788	.0756
CONVERSION =	88.00							
M F OXYGEN=	.1073	.1127	.1176	.1220	.1260	.1297	.1330	.1361
M F CO2 =	.1027	.0973	.0924	.0880	.0840	.0803	.0770	.0739
CONVERSION =	86.00							
M F OXYGEN=	.1097	.1149	.1197	.1240	.1279	.1315	.1347	.1378
M F CO2 =	.1003	.0951	.0903	.0860	.0821	.0785	.0753	.0722
CONVERSION =	84.00							
M F OXYGEN=	.1120	.1172	.1218	.1260	.1298	.1333	.1365	.1394
M F CO2 =	.0980	.0928	.0882	.0840	.0802	.0767	.0735	.0706
CONVERSION =	82.00							
M F OXYGEN=	.1143	.1194	.1239	.1280	.1317	.1351	.1383	.1411
M F CO2 =	.0957	.0906	.0861	.0820	.0783	.0749	.0717	.0689
CONVERSION =	80.00							
M F OXYGEN=	.1167	.1216	.1260	.1300	.1336	.1370	.1400	.1428
M F CO2 =	.0933	.0884	.0840	.0800	.0764	.0730	.0700	.0672

higher flow rates than the direct method, for all cases. This difference will obviously have a considerable effect on the temperature profile within the reactor.

Due to the importance of the overall mass balance, the model was tested with both the direct and indirect methods of calculating the solids feed rate. These results are given in Figures 4.7-4.10 and also in Tables J.1-J.20 at the end of this thesis. In all of the computer runs made here, the size of particle which would completely react in the initial heat balance was set to zero. Thus the only combustion which takes place in the initial heat balance (see 3.3.1) is that due to the reduction of large particles to an entrainable size.

The profiles presented in Figures 4.1-4.10 do not compare particularly well with the experimental observations. However two generalizations may be made about the results. Firstly the profiles predicted by the model for the two different solids flow rates seem to lie in the general vicinity of the experimental observations. This is nothing startling, however since, the spread between the two predicted profiles may be as much as 250 K for any given position in the reactor. The second point is more informative. It would seem that the final experimental point (at 2.5 m along the reactor) lies fairly close to the profile predicted for the "direct" calculation method. Since the conversions predicted by the model and the

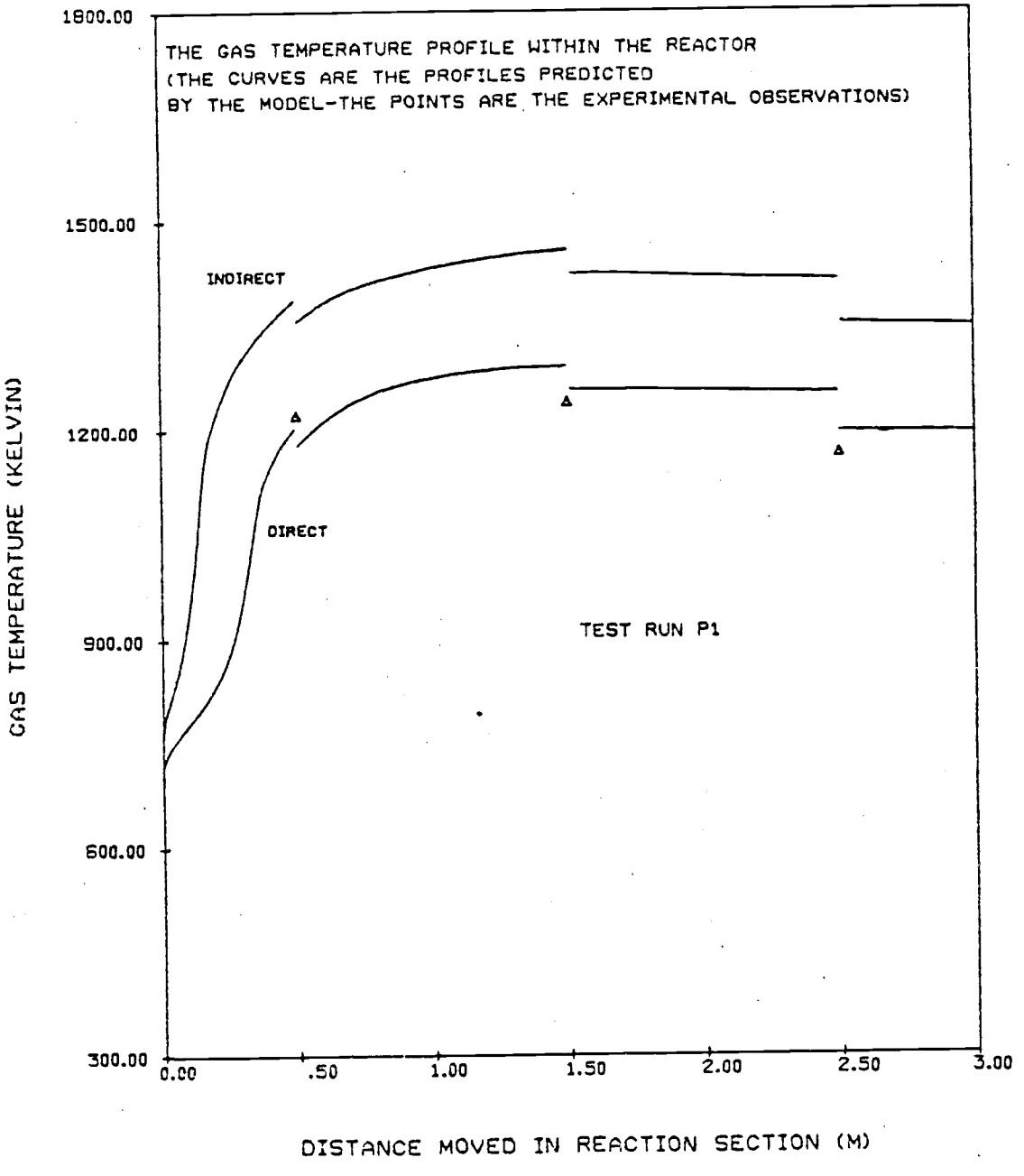

Figure 4.1 A comparison between the experimental and predicted results for both indirect and direct calculation of solids flow rate, for Run P1.

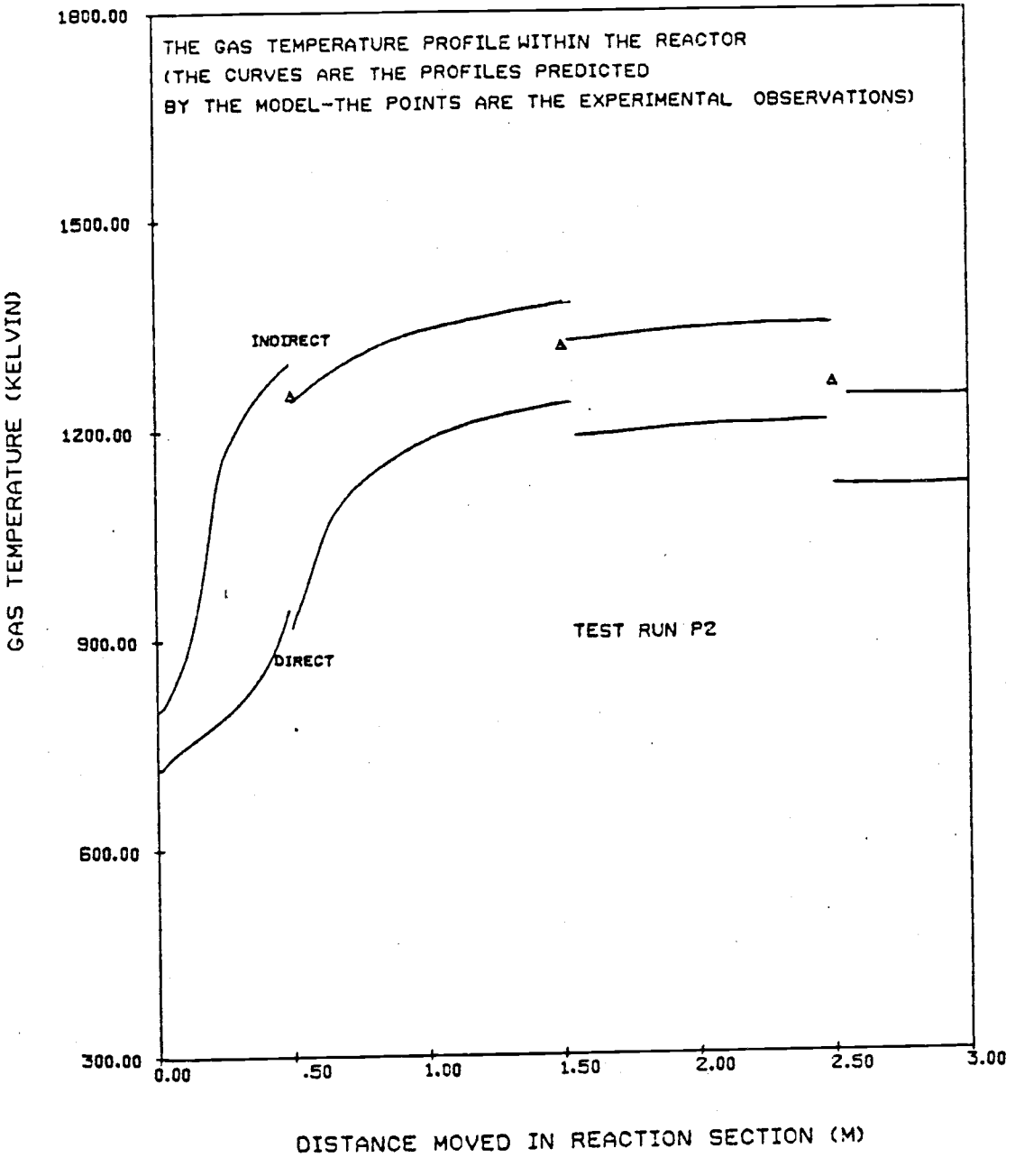

Figure 4.2. A comparison between the experimental and predicted results for both indirect and direct calculation of solids flow rate, for Run P2.

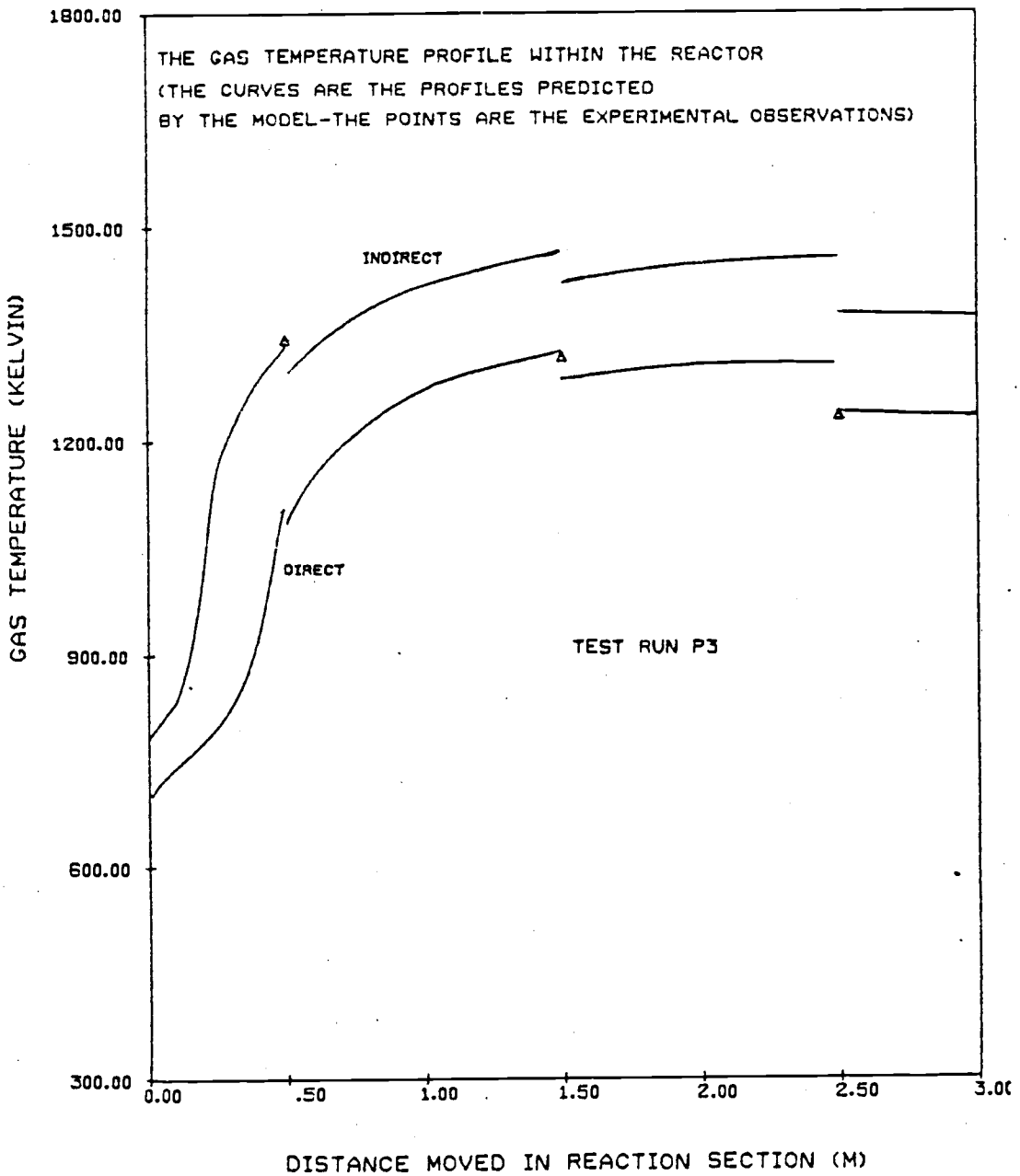

Figure 4.3. A comparison between the experimental and predicted results for both indirect and direct calculation of solids flow rate, for Run P3.

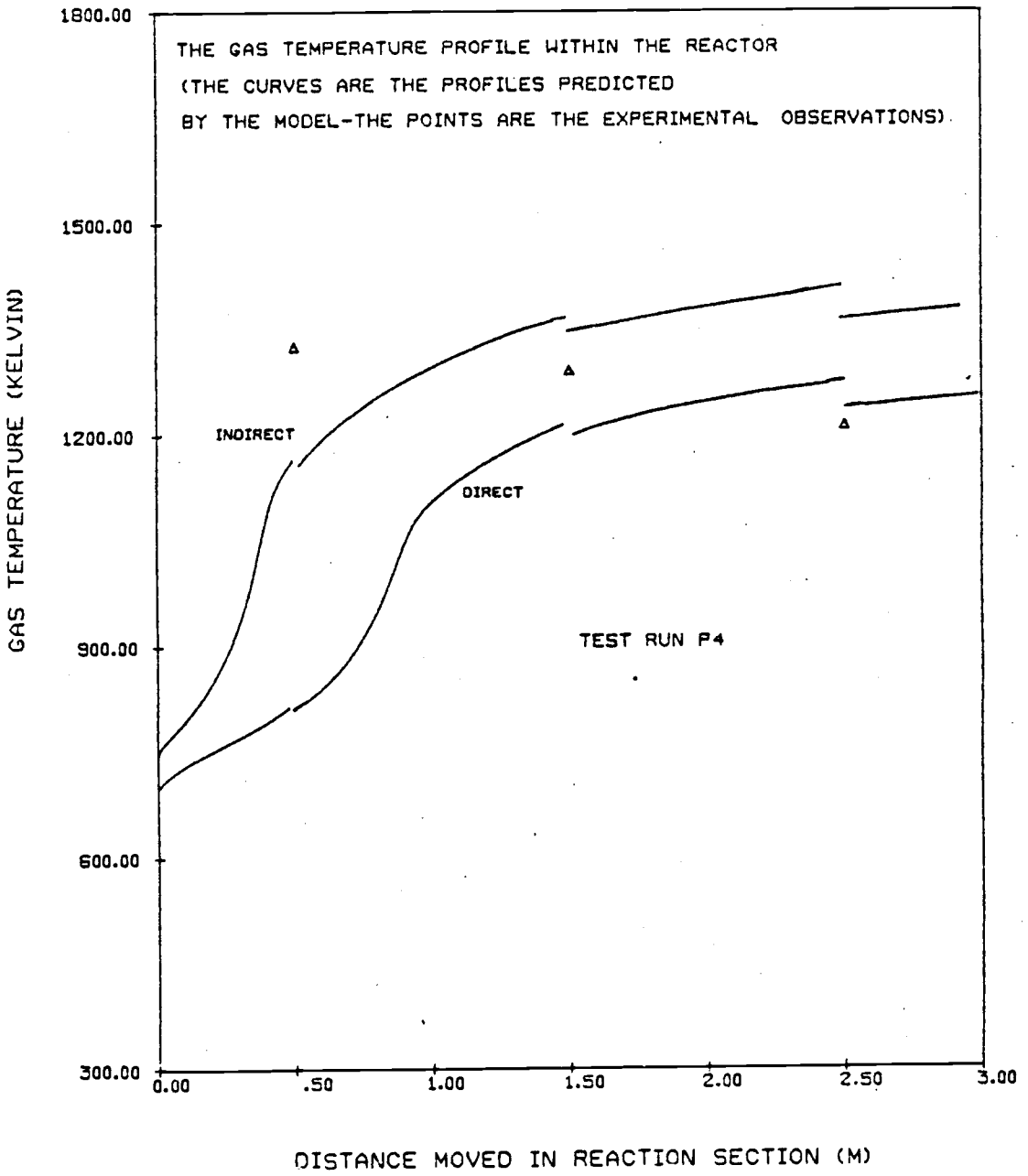

Figure 4.4. A comparison between the experimental and predicted results for both indirect and direct calculation of solids flow rate, for Run P4.

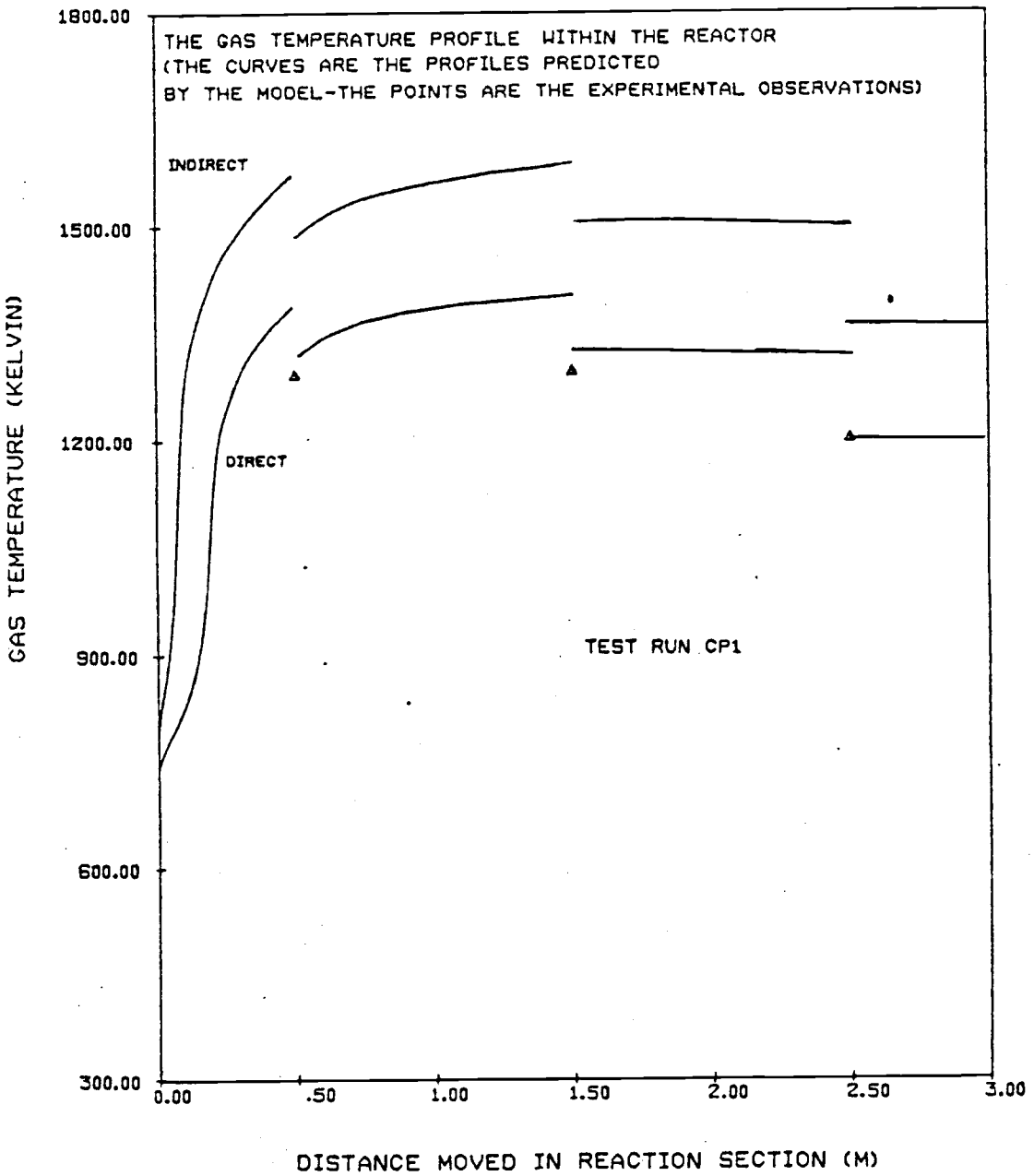

Figure 4.5. A comparison between the experimental and predicted results for both indirect and direct calculation of solids flow rate, for Run CP1.

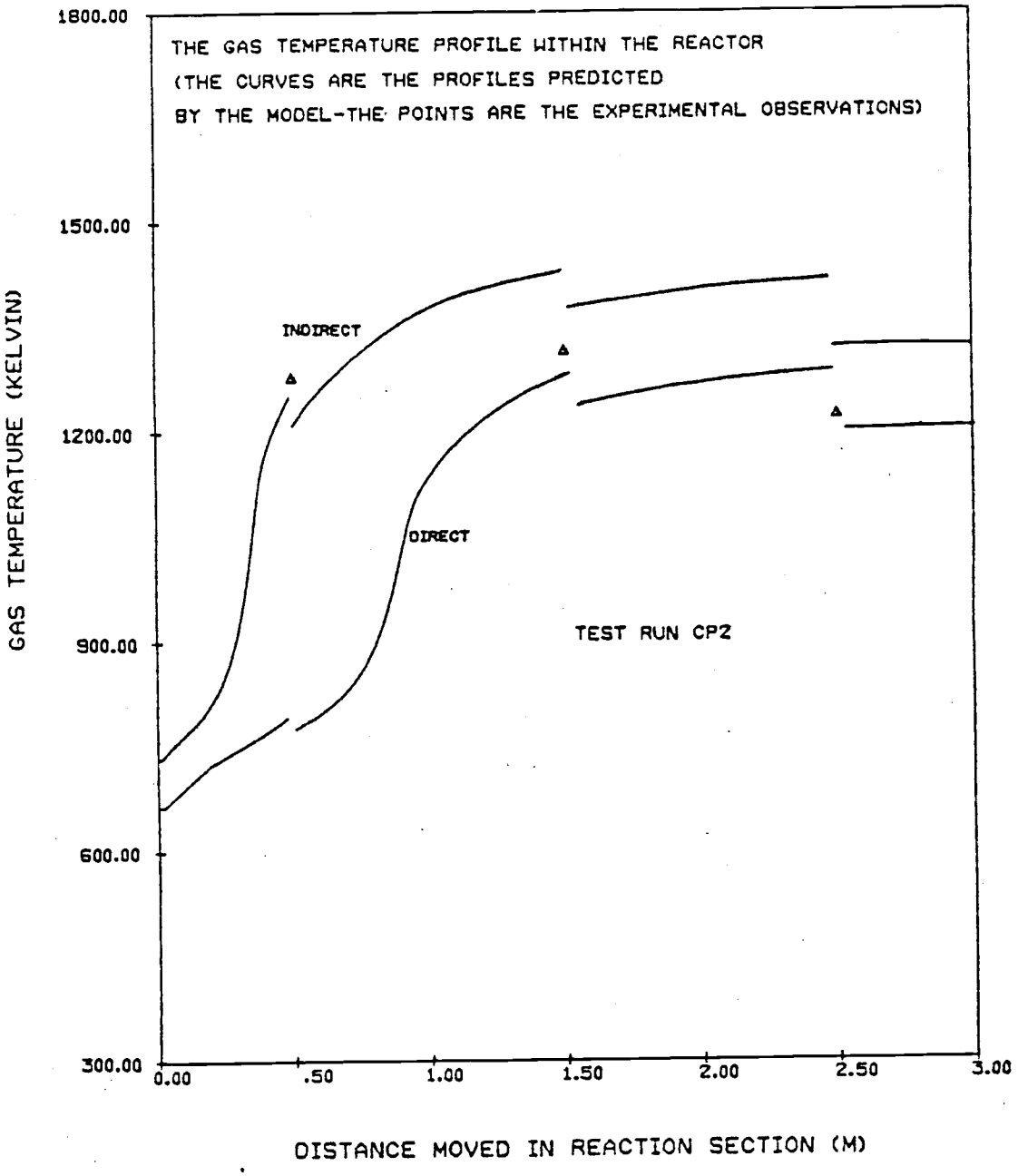

Figure 4.6. A comparison between the experimental and predicted results for both indirect and direct calculation of solids flow rate, for Run CP2.

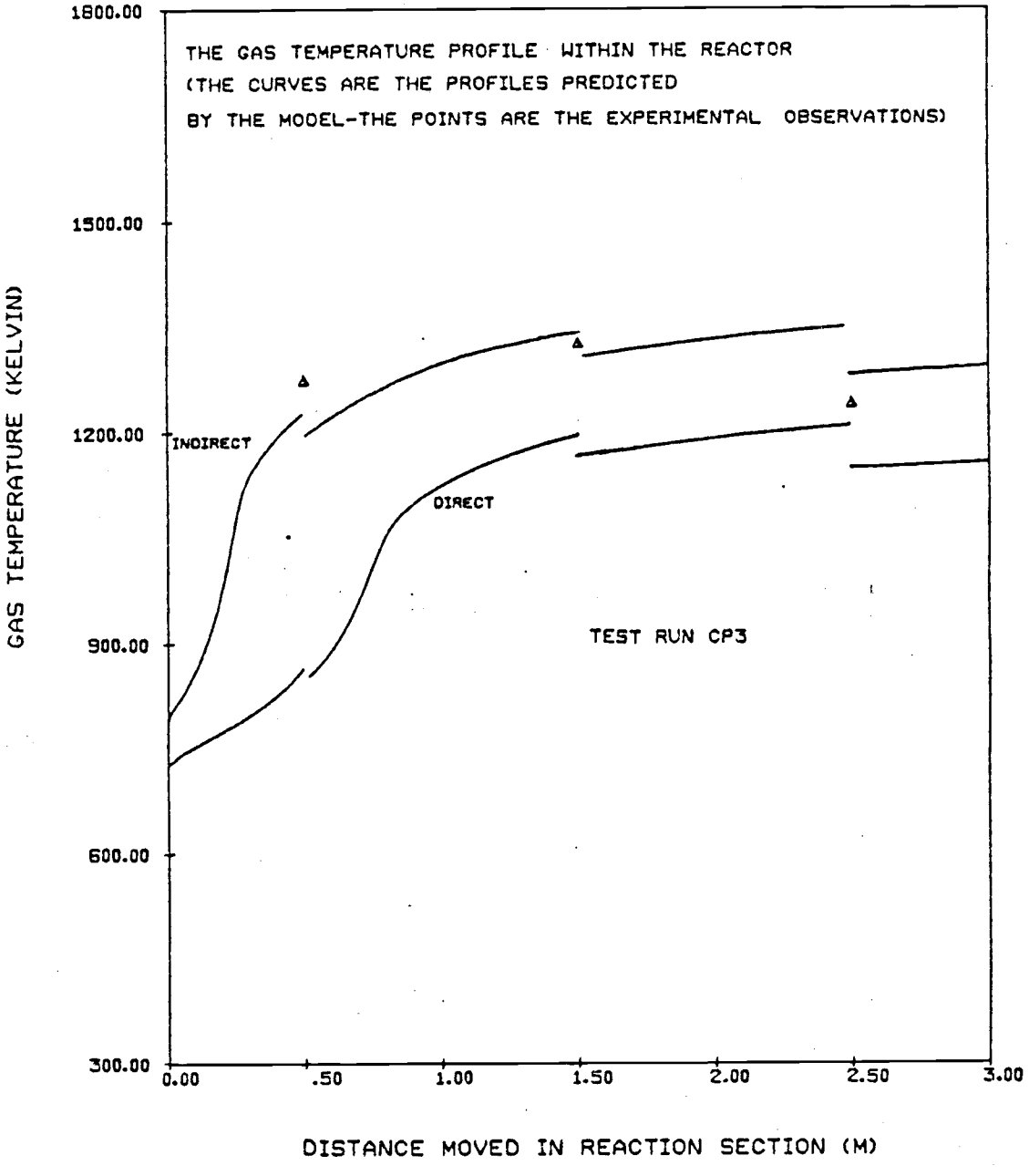

Figure 4.7. A comparison between the experimental and predicted results for both indirect and direct calculation of solids flow rate, for Run CP3.

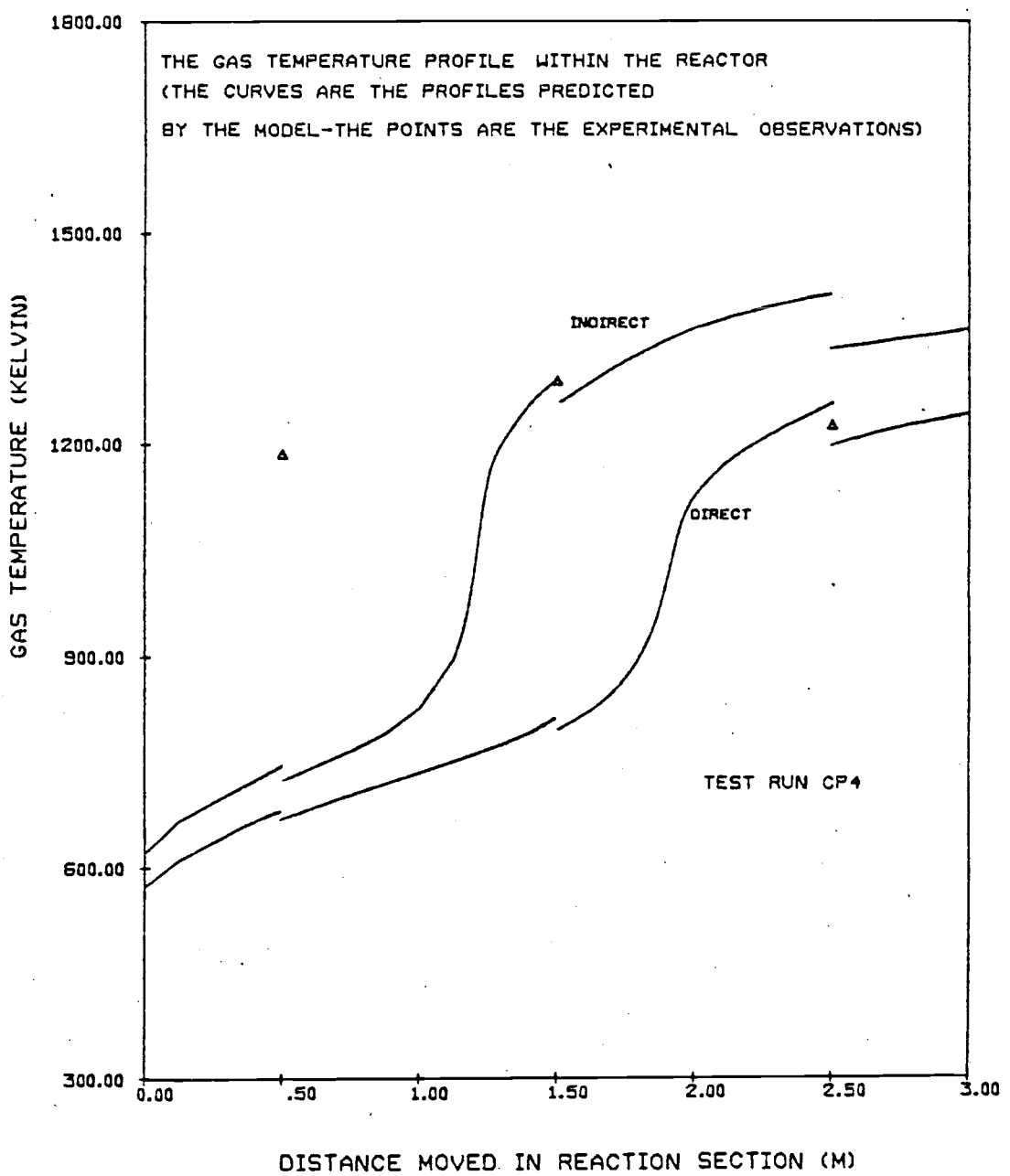

Figure 4.8. A comparison between the experimental and predicted results for both indirect and direct calculation of solids flow rate, for Run CP4.

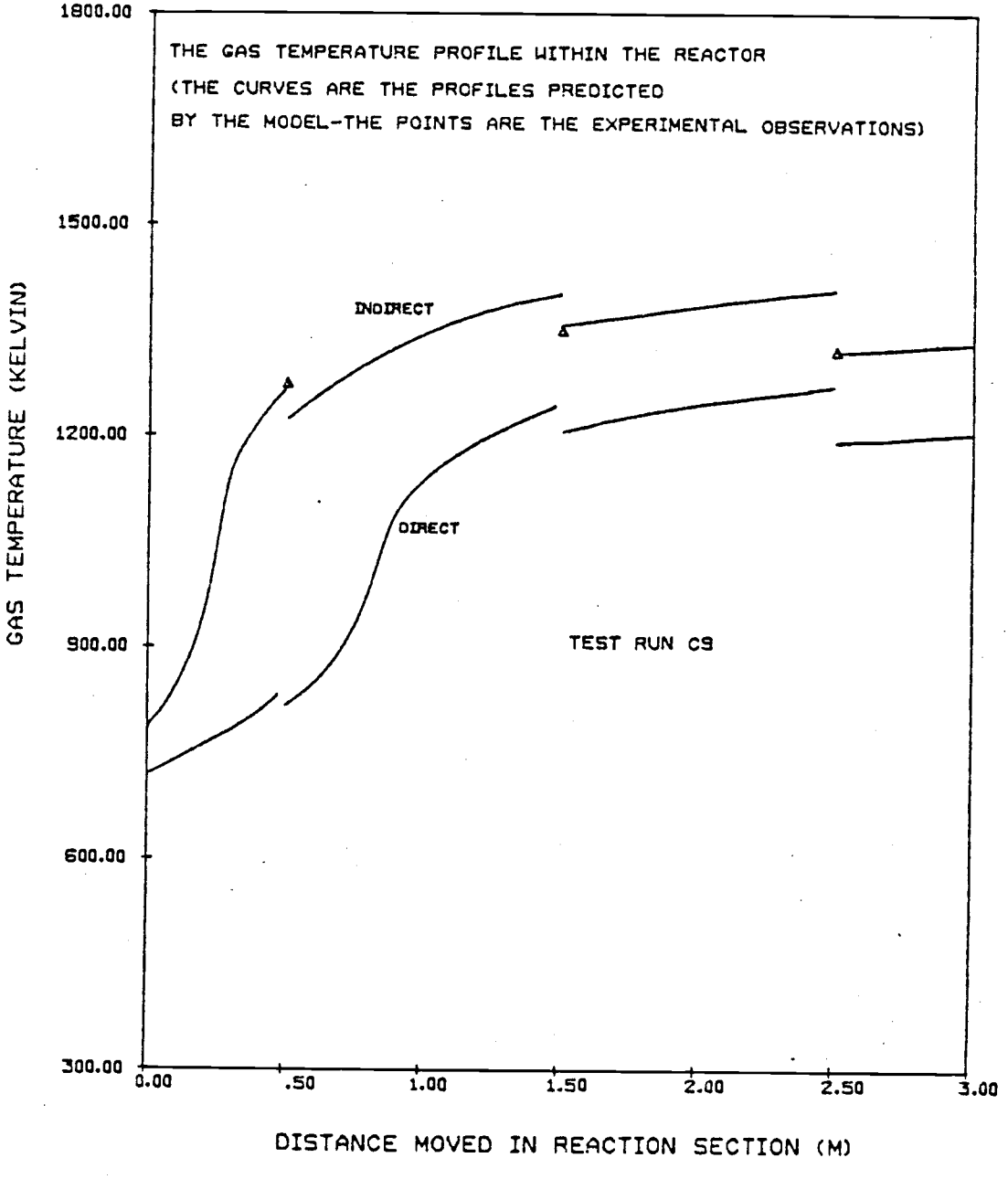

Figure 4.9. A comparison between the experimental and predicted results for both indirect and direct calculation of solids flow rate, for Run CP9.

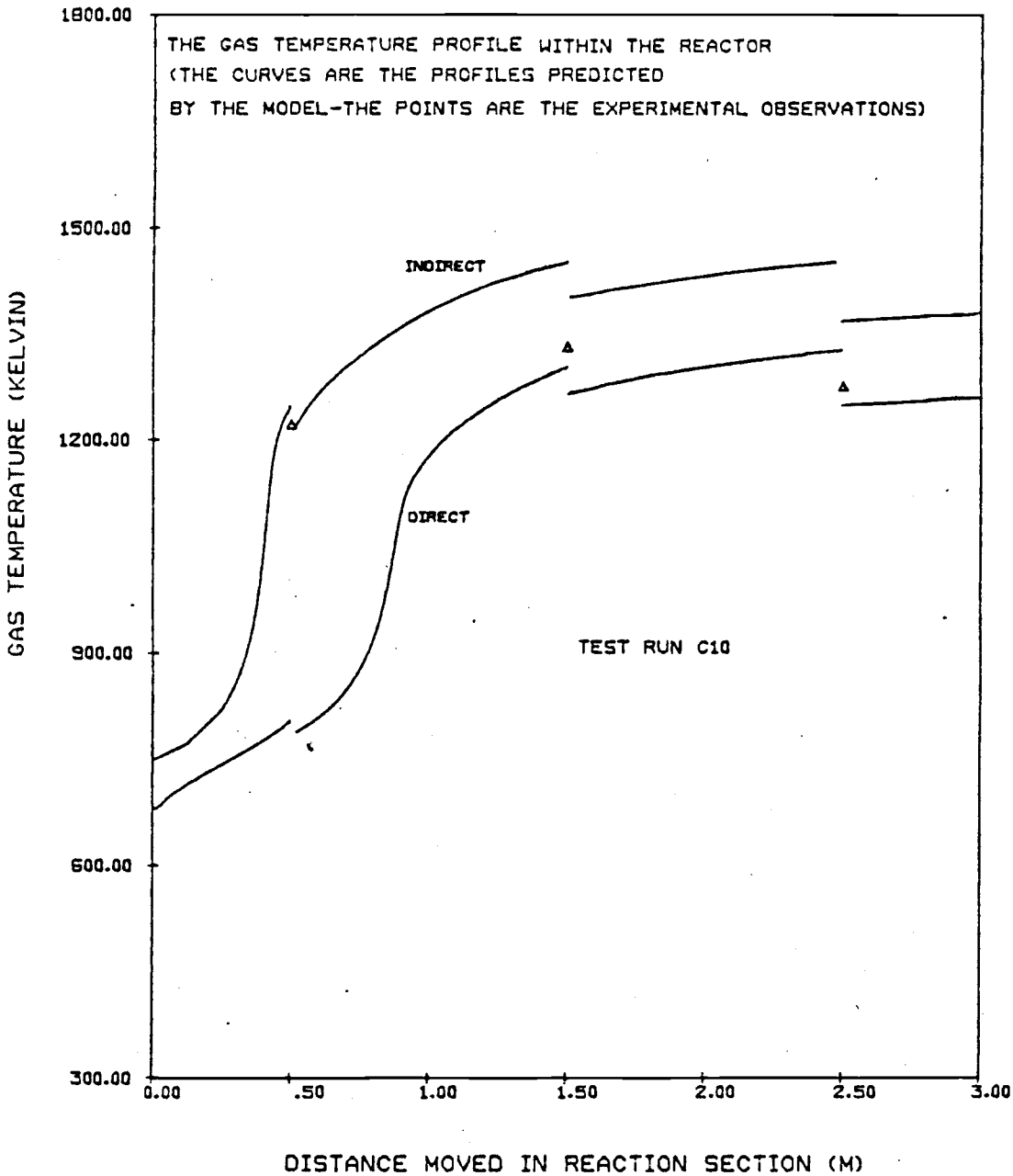

Figure 4.10. A comparison between the experimental and predicted results for both indirect and direct calculation of solids flow rate, for Run C10.

experimentally found values are both high (between 90-100%). The overall heat and mass balance favors the "direct" calculation method. Thus most of the remaining comparisons are made using the solids feed rate calculated by the "direct" method.

4.2. The Effect of the Particle Terminal Velocity on the Predicted Profile

The terminal velocity of a particle will have an important effect upon the time that the particle spends in the reactor. For small particles the terminal velocity will be small and these particles will move with a velocity very close to that of the gas. For larger particles this is not the case. The terminal velocity of such particles will be correspondingly greater and thus the average time spent in the reactor will be considerably greater than the residence time of the gas.

The terminal velocity of a particle will depend upon many factors and a discussion of the free fall velocity for non-spherical particles is given in Appendix E. The method used to calculate the terminal velocity of a particle is taken from Becker (20) and the results for a variety of particle densities are again presented in Appendix E.

The results presented in Figures 4.1-4.10 were obtained by using the above correlation for terminal velocity. However in using this approach it was necessary to estimate two surface parameters

i.e. form and surface sphericity. This estimation relied heavily on observation and it is possible that the values used could be as much as 20% in error. For this reason the effect of the temperature profiles of a change in terminal velocity has been studied.

In Figures 4.11-4.13 (Tables J.21-J 26) the effect of multiplying the terminal velocity found by the Becker correlation by a constant, is shown. The value of this constant multiplier was chosen arbitrarily and ranges from 0.8 to 2.0.

The overall result of changing the particle terminal velocity is to change the temperature at which the products leave the initial heat balance and enter the reaction zone. By making the terminal velocity greater (i.e. by multiplying by a factor greater than unity) the amount of solids which will not get entrained by the gas stream is increased. This in turn increases the amount of combustion which must occur in the initial heat balance. Hence the temperature of solids and gas entering the reaction zone of the model will be higher. The converse is true, and by multiplying by a factor less than one the temperature of gas and solids leaving the initial heat balance will be lower.

By changing the inlet temperature to the reaction zone, the position of the knee of the curve--which is effectively the ignition point--will change. Thus if the temperature of the inlet gas is hotter, the knee of the curve moves to the left while if it is cooler then the

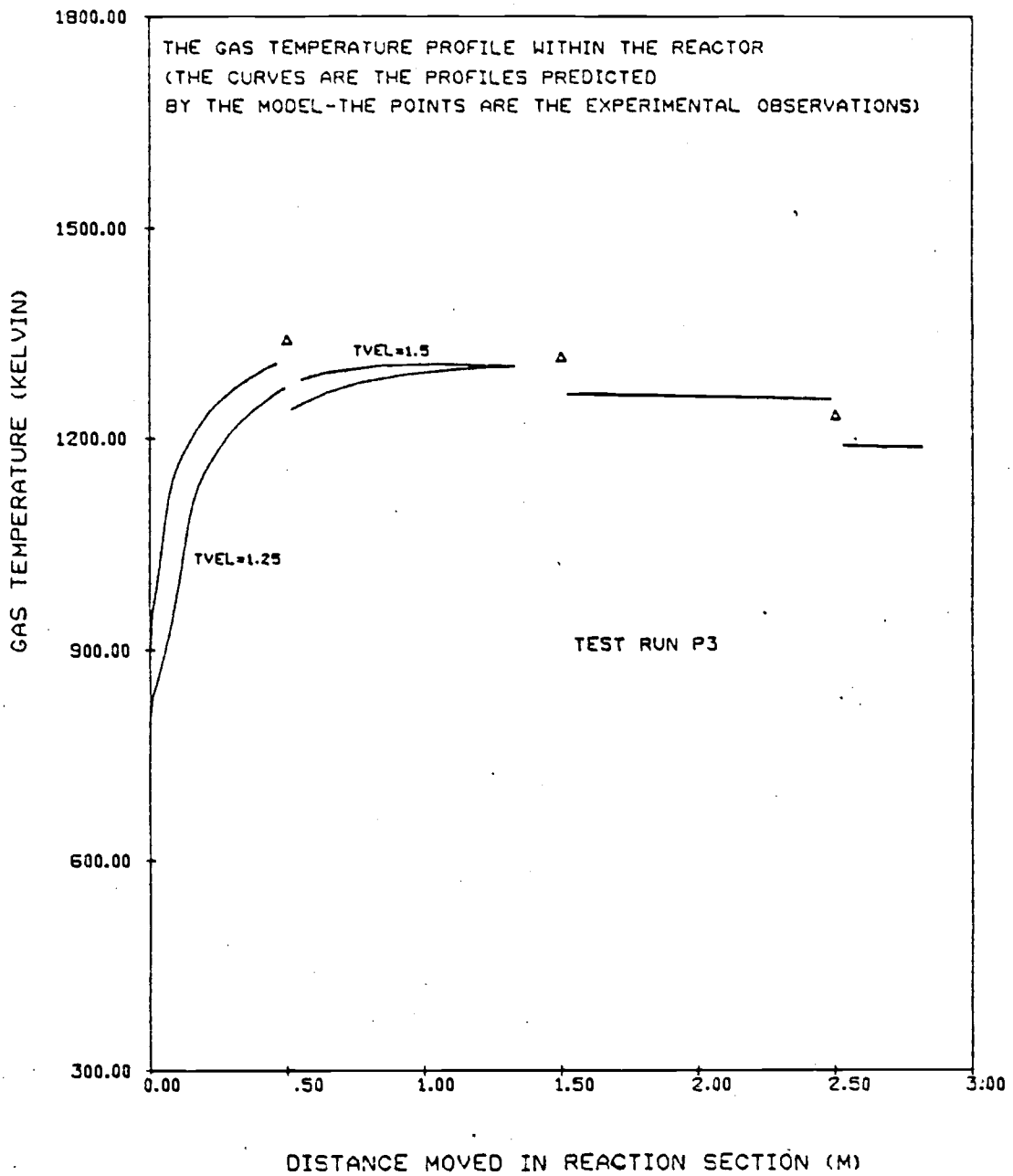

Figure 4.11. A comparison between predictions using different terminal velocity correlations. The results are for the direct calculation of solids flow rate for run P3 (the results are for 1.5 and 1.2 times the correlation used for terminal velocity).

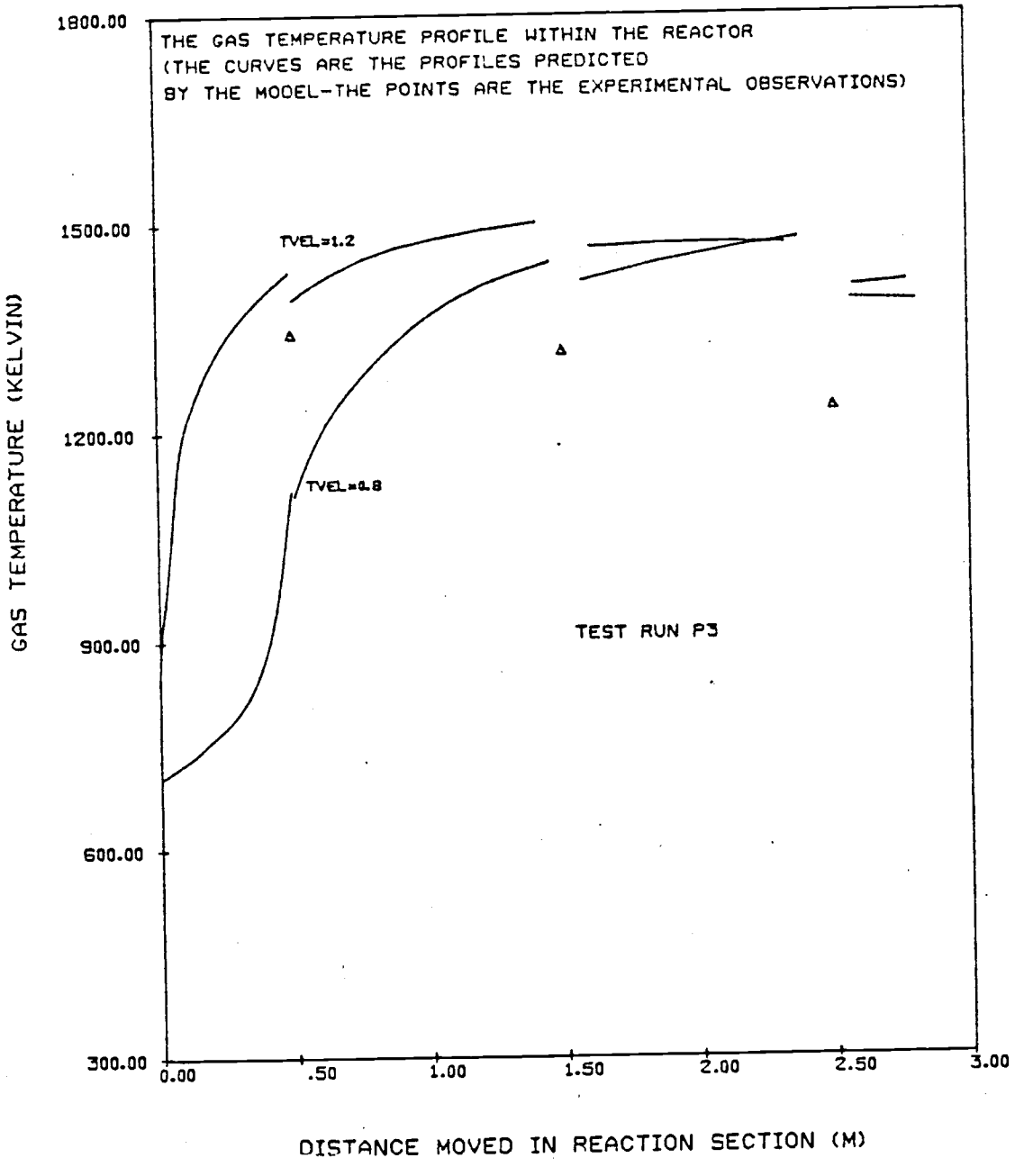

Figure 4.12. A comparison between predictions using different terminal velocity correlations. The results are for the indirect calculation of solids flow rate for run P2 (the results are for 1.2 and 0.8 times the correlation used for terminal velocity).

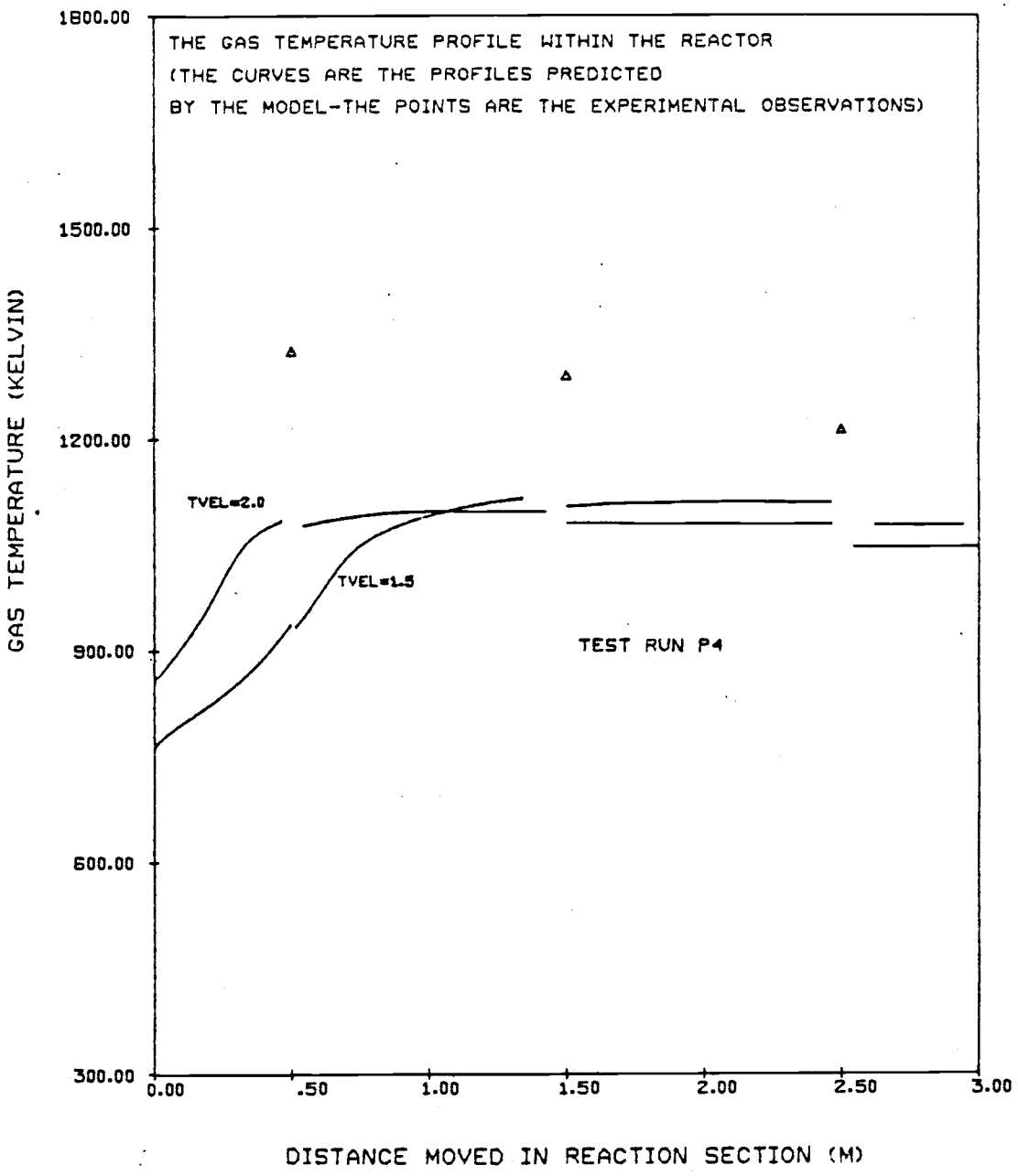

Figure 4.13. A comparison between predictions using different terminal velocity correlations. The results are for the direct calculation of solids flow rate for Run P4 (the results are for 2.0 and 4.5 times the correlation used for terminal velocity).

knee moves to the right. This effectively controls the point at which ignition occurs in the reactor. The term ignition may be a little confusing--however it refers here, to a point where considerable reaction takes place in the bulk of the solids--thus a large temperature rise is observed.

Since this parameter is again an important one it was decided to compute the results of all the test runs with a change in the particle terminal velocity. The value chosen for the multiplier was found by trial and error and was taken to be 1.5 for all the test runs considered. These results are shown in Figures 4.14-14.21.and also in Tables J.27-J.36.

From studying Figures 4.14-4.23 it becomes apparent that the predicted profiles compare well with the experimental observations, for the majority of the cases. Only for test run P4 and CP3 do the predicted profiles show any appreciable discrepancy. This improvement in the fit of the model to the data is explained by the fact that using the original terminal velocity correlation the model tended to underpredict the temperature at the first thermocouple (i.e. at 0.5 M along the reactor). Thus by increasing the particle terminal velocity the inlet temperature to the reaction zone will increase. This will push the knee of the profile toward the reactor entrance and thus predict a higher temperature at the first thermocouple.

It would thus appear that by using this modified terminal velocity

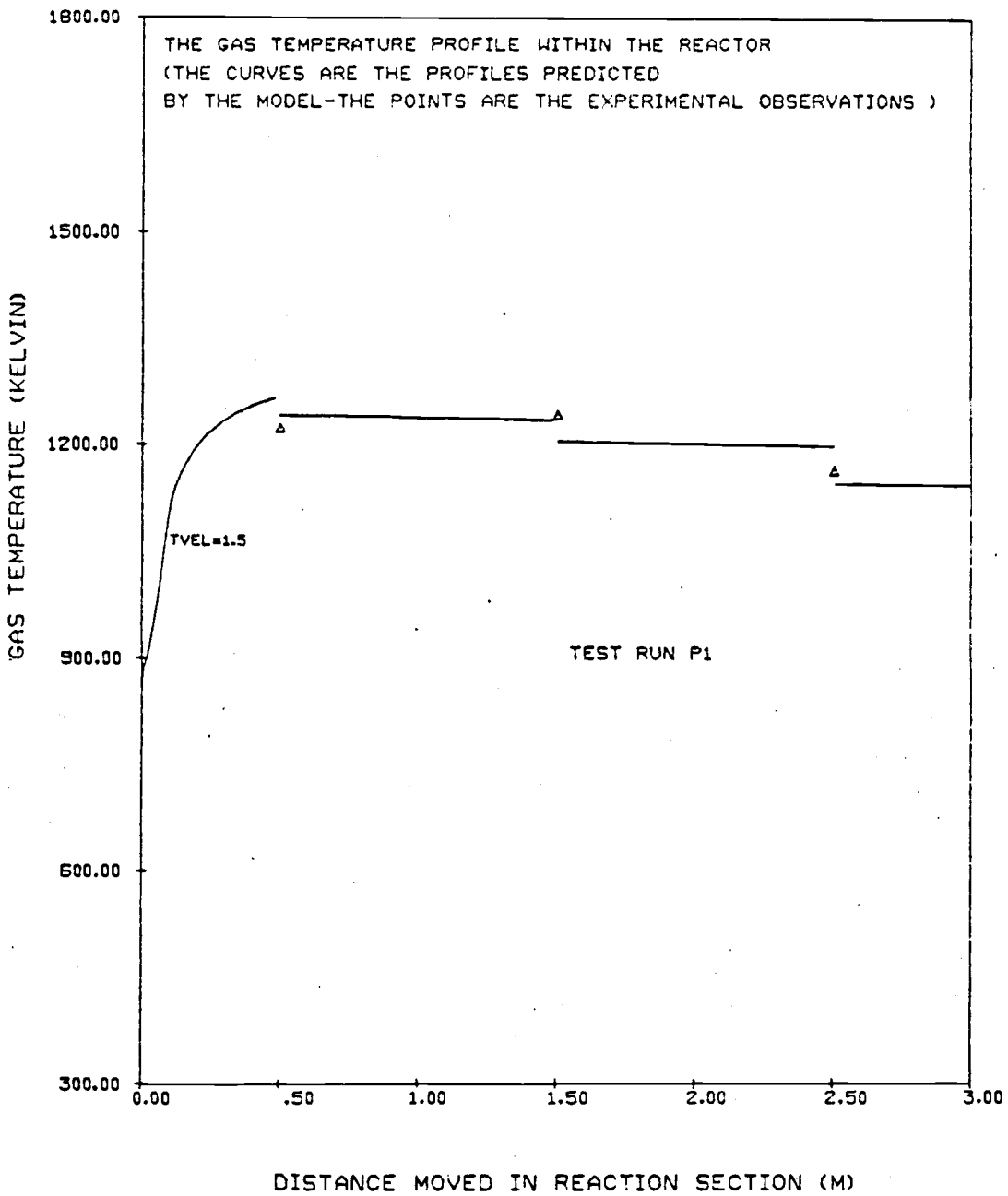

Figure 4.14. Comparison of experimental and predicted profiles, using a terminal velocity 1.5 times greater than the original correlation, for run P1 (direct calculation of solids flow rate).

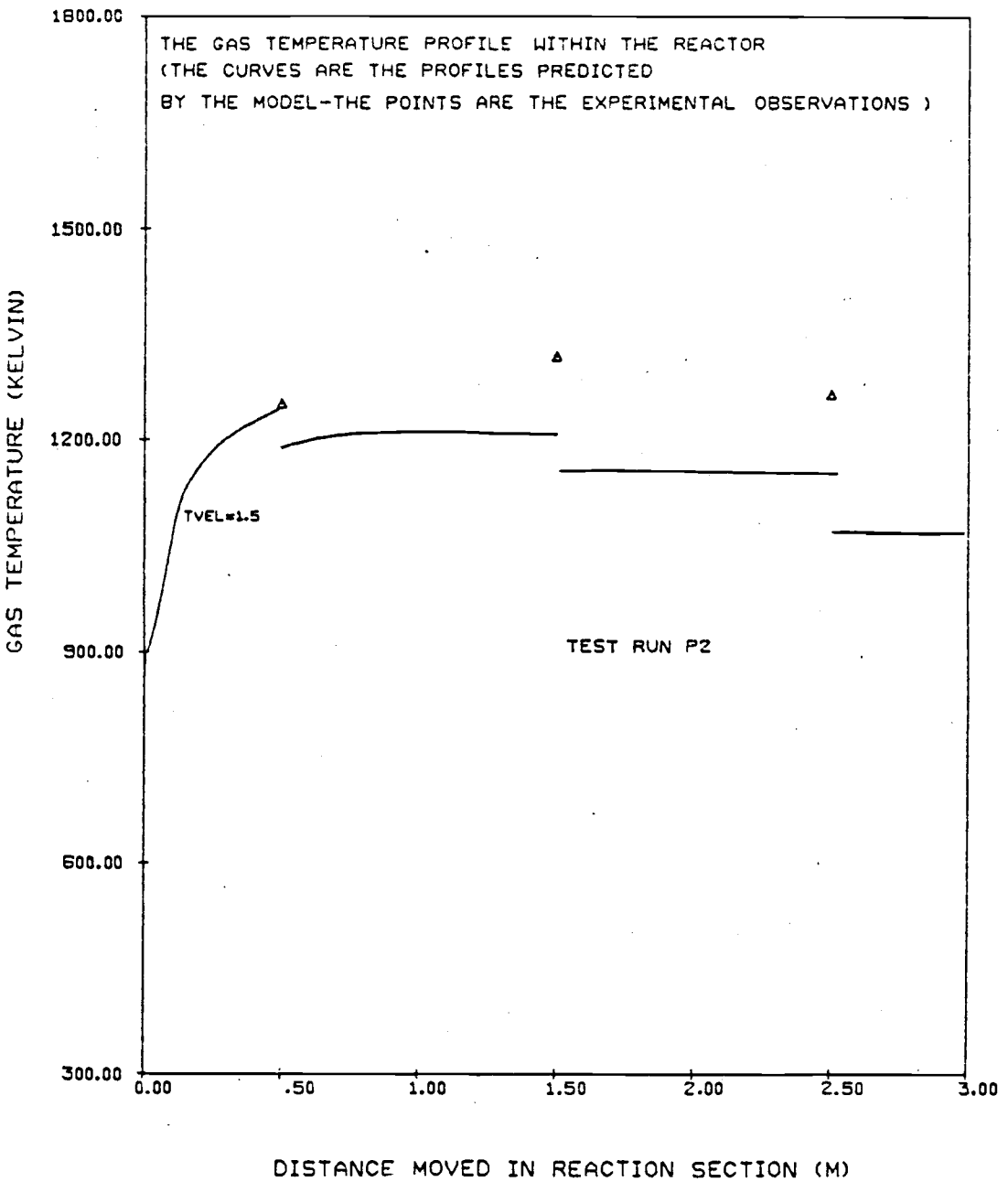

Figure 4.15. Comparison of experimental and predicted profiles, using a terminal velocity 1.5 times greater than the original correlation, for run P2 (direct calculation of solids flow rate).

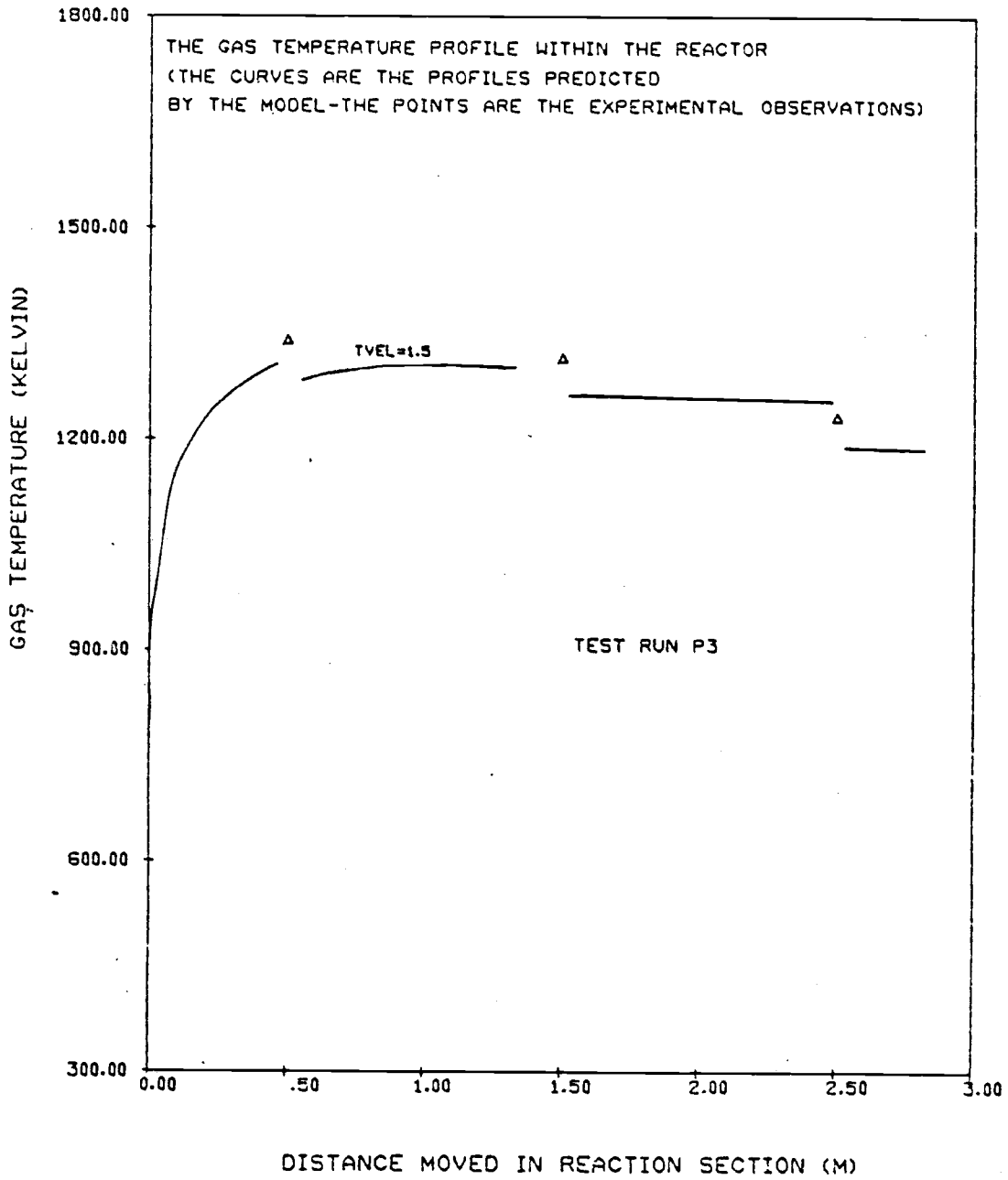

Figure 4.16. Comparison of experimental and predicted profiles using a terminal velocity 1.5 times greater than the original correlation, for run P3 (direct calculation of solids flow rate).

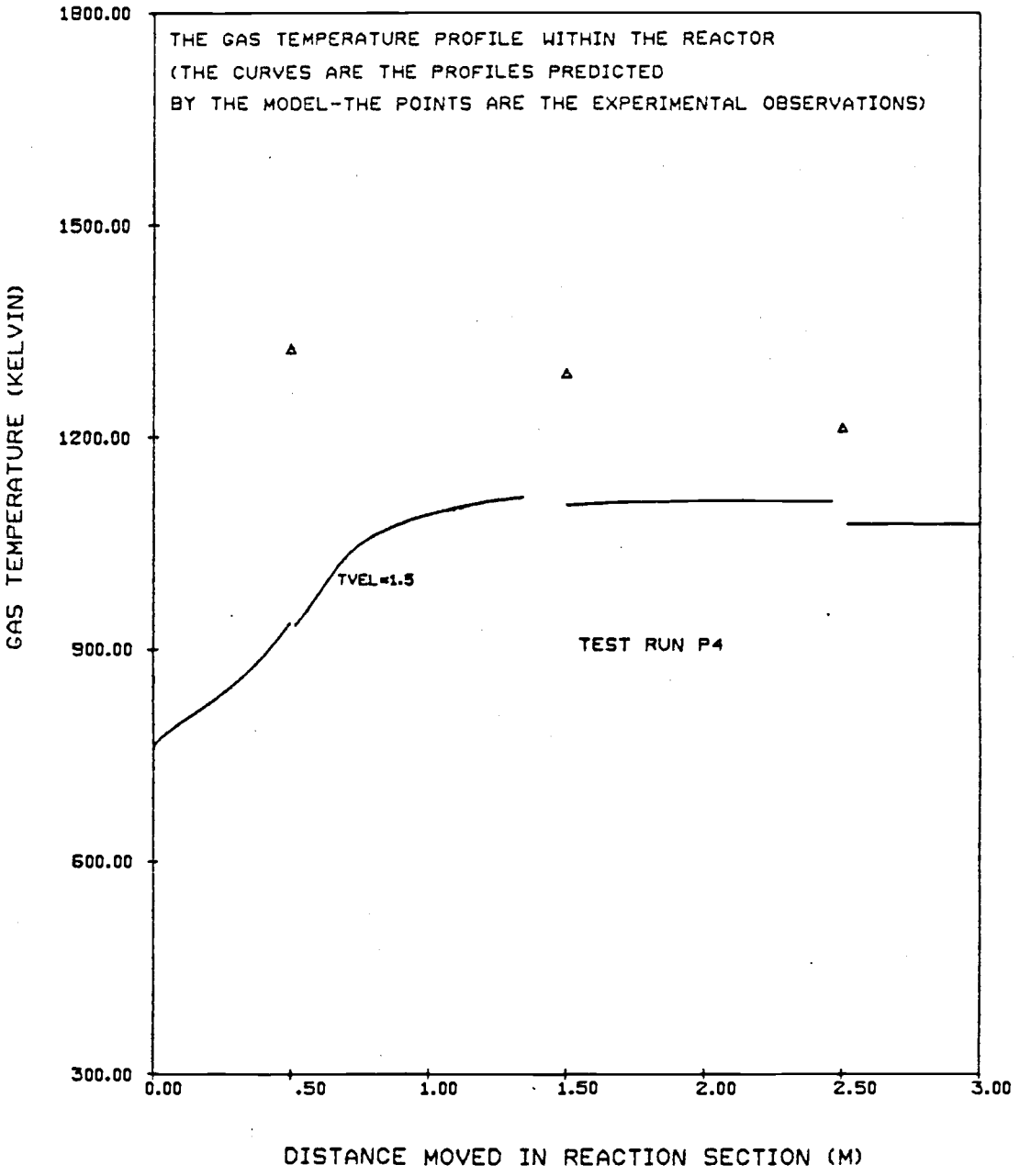

Figure 4.17. Comparison of experimental and predicted profiles, using a terminal velocity 1.5 times greater than the original correlation, for run P4 (direct calculation of solids flow rate).

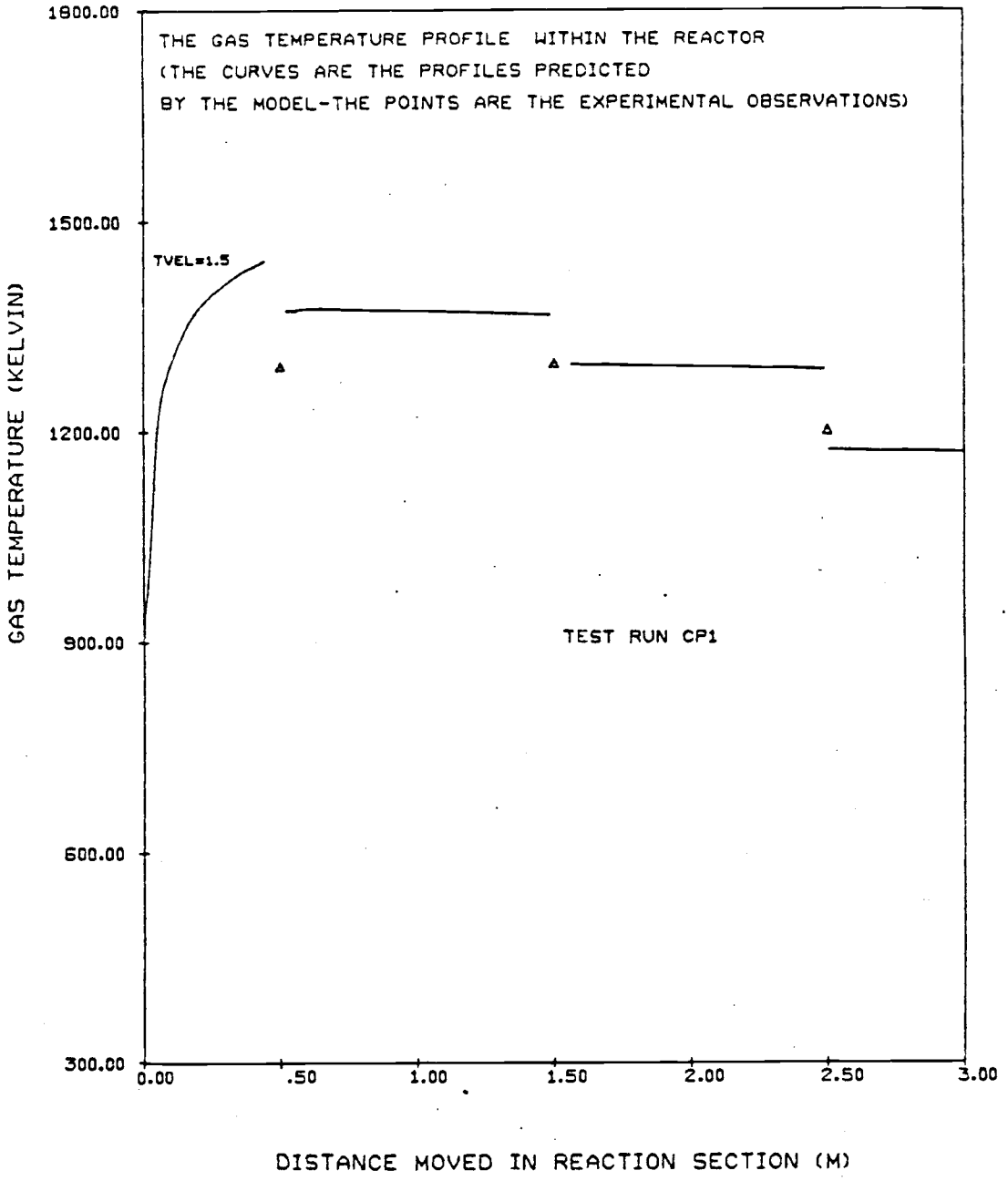

Figure 4.18. Comparison of experimental and predicted profiles, using a terminal velocity 1.5 times greater than the original correlation, for run CP1 (direct calculation of solids flow rate).

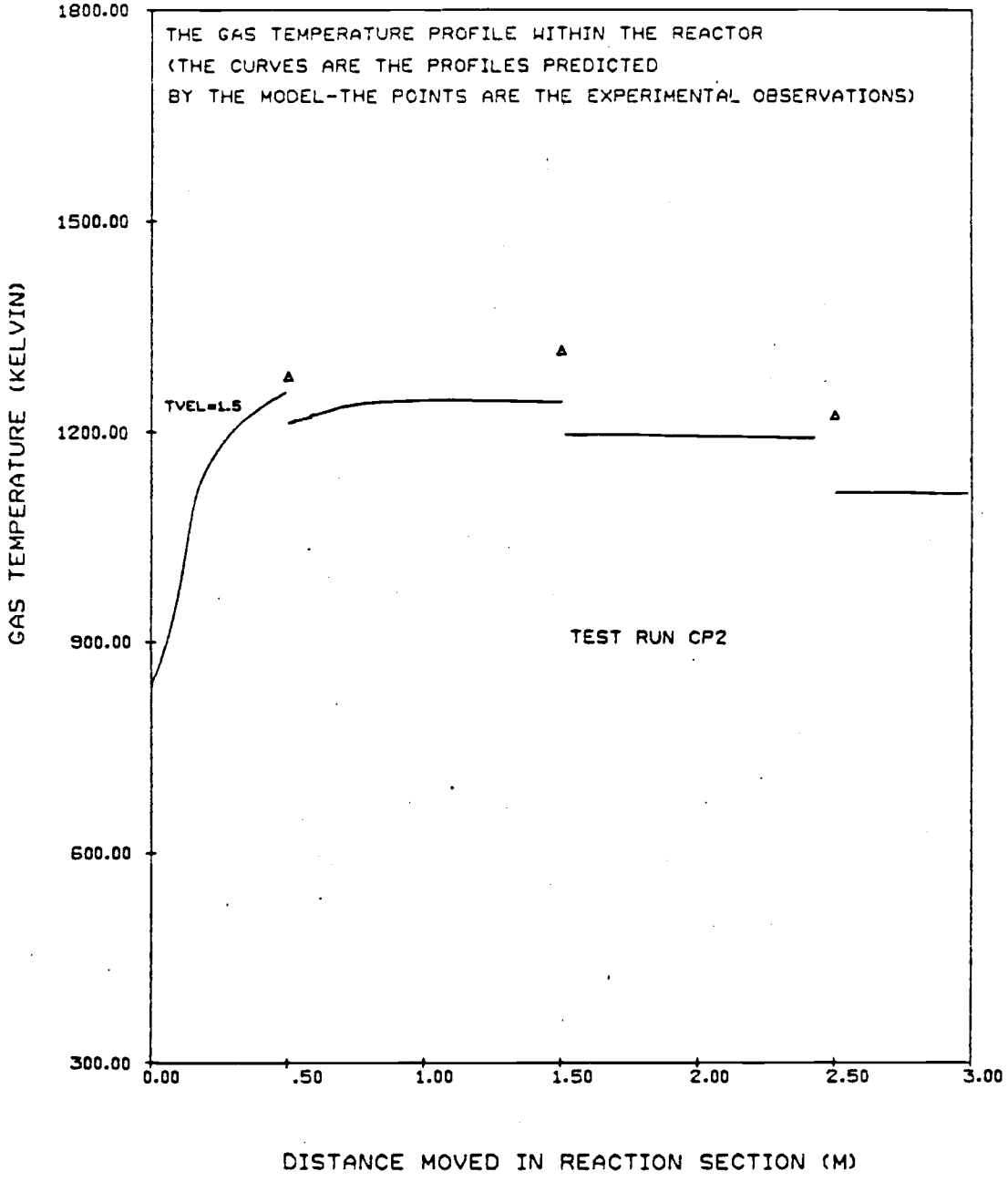

Figure 4.19. Comparison of experimental and predicted profiles, using a terminal velocity 1.5 times greater than the original correlation, for run CP2 (direct calculation of solids flow rate).

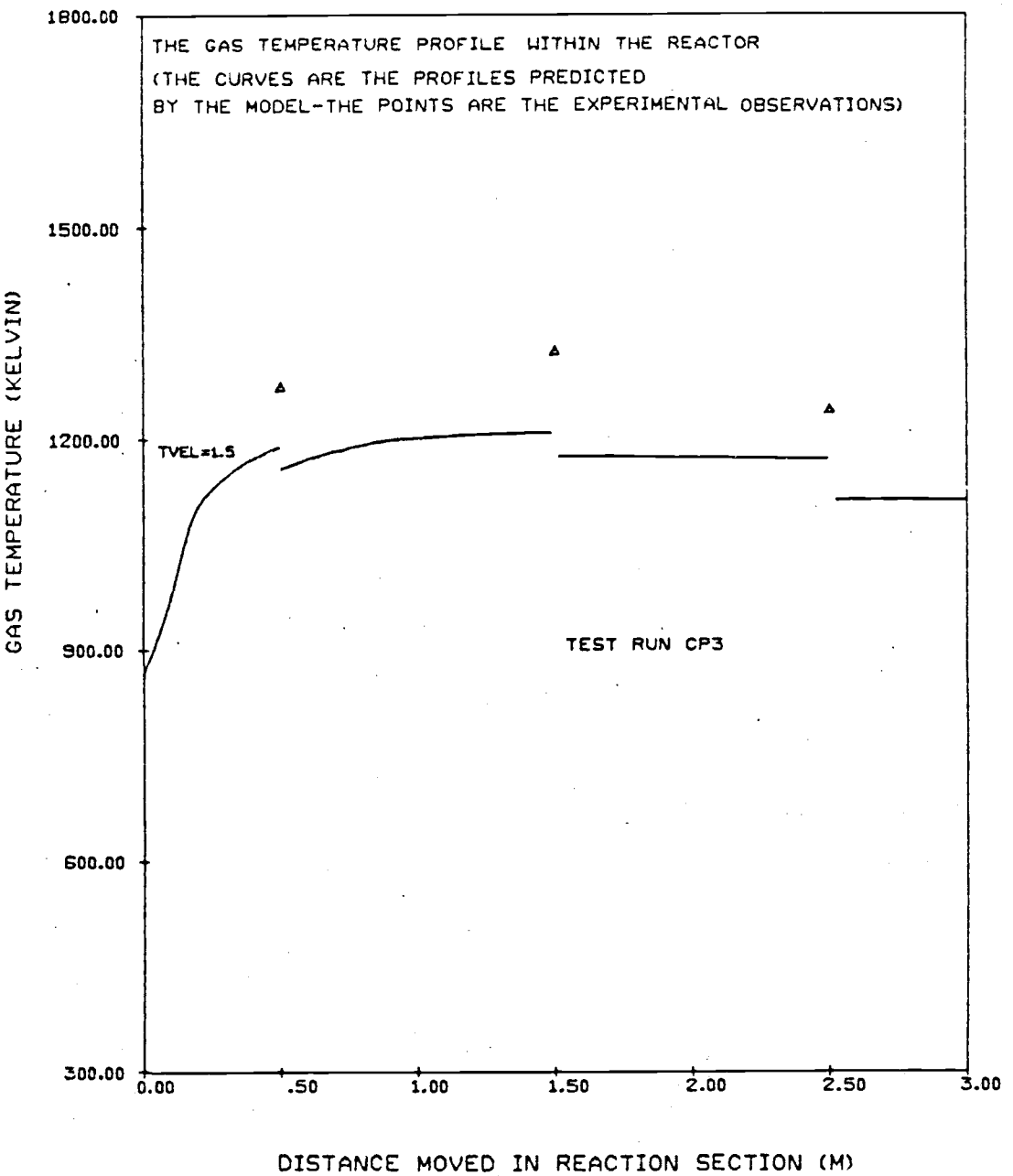

Figure 4.20. Comparison of experimental and predicted profiles, using a terminal velocity 1.5 times greater than the original correlation, for run CP3 (direct calculation of solids flow rate).

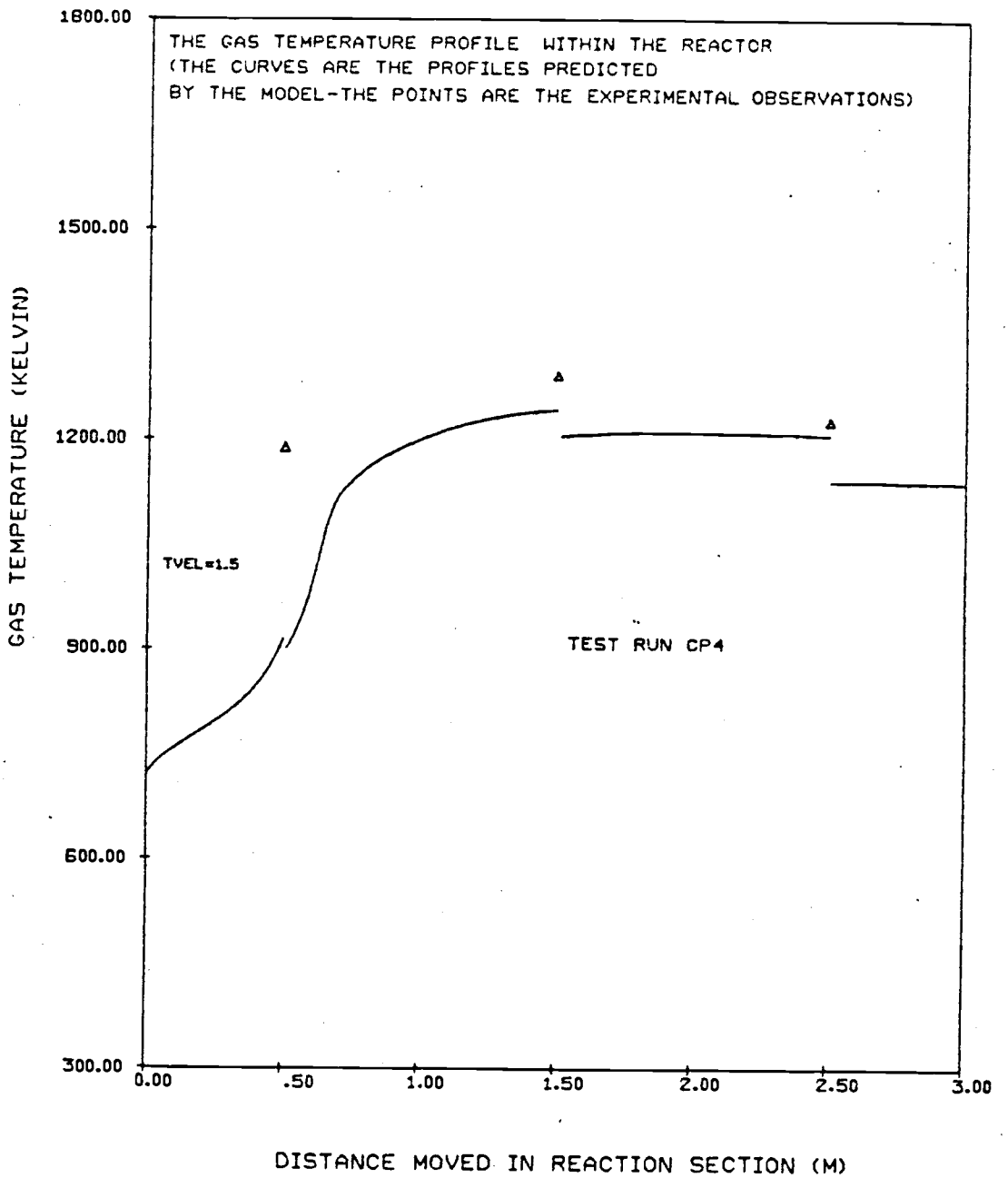

Figure 4.21. Comparison of experimental and predicted profiles, using a terminal velocity 1.5 times greater than the original correlation, for run CP4 (direct calculation of solids flow rate).

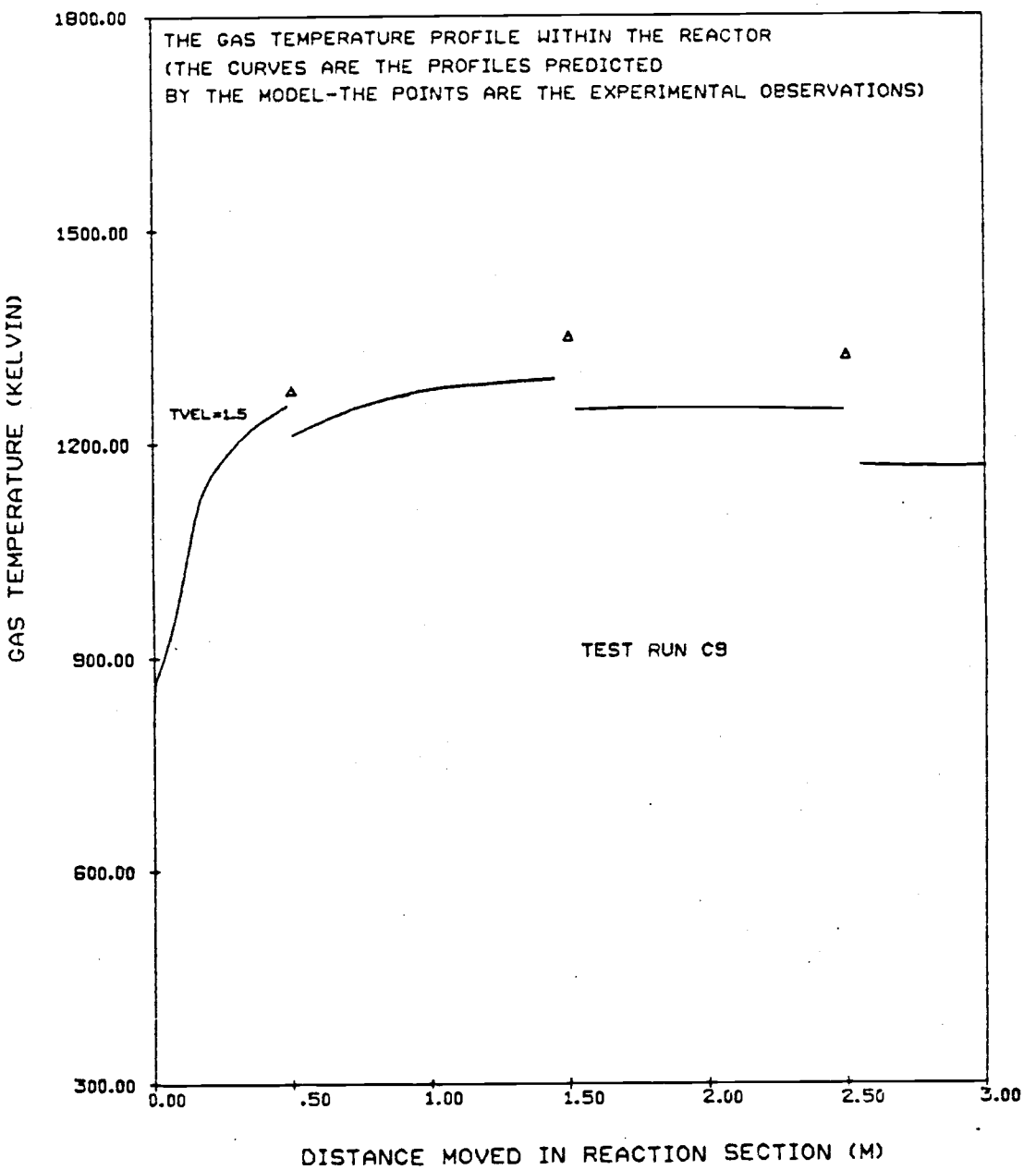

Figure 4.22. Comparison of experimental and predicted profiles, using a terminal velocity 1.5 times greater than the original correlation, for run C9 (direct calculation of solids flow rate).

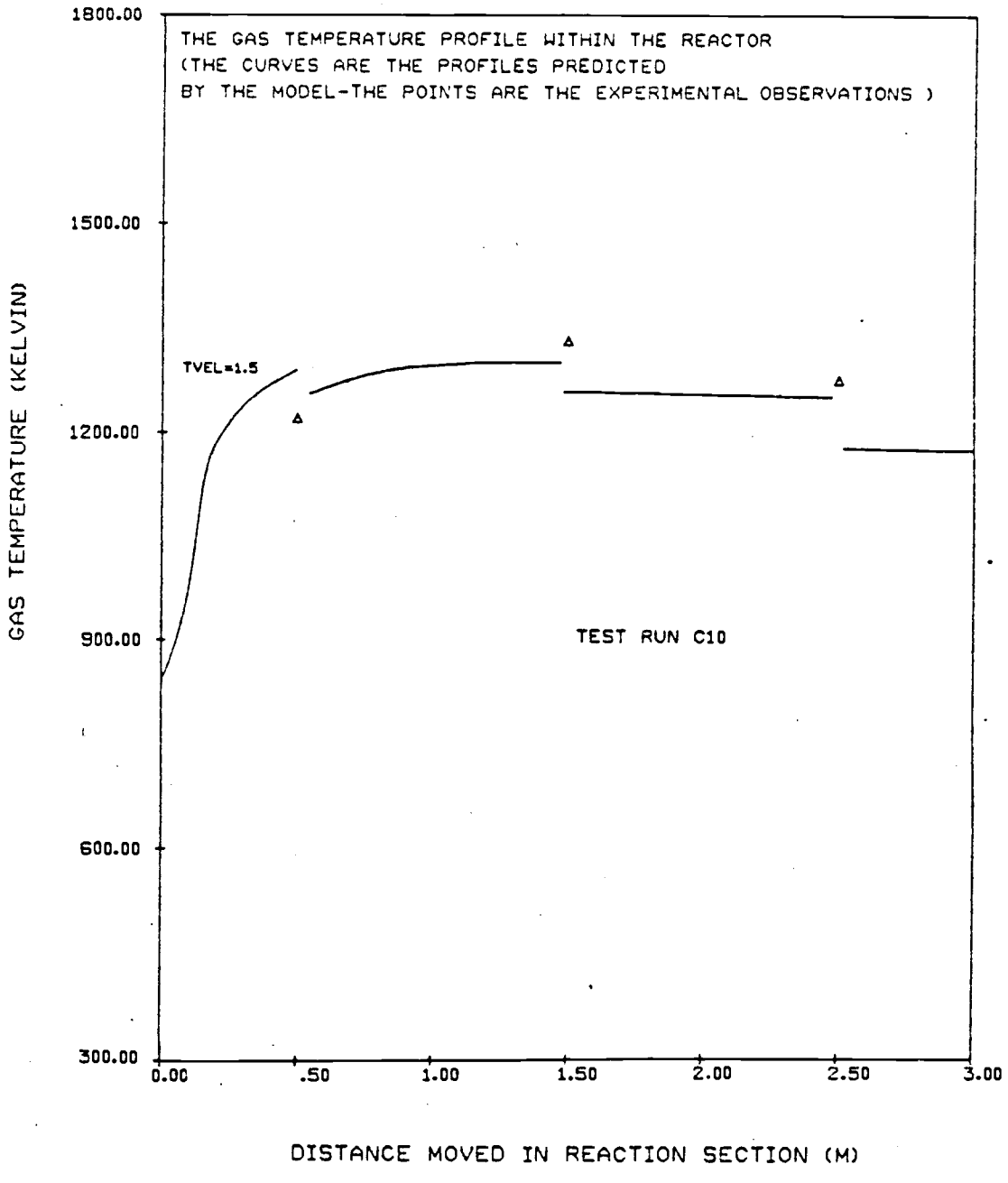

Figure 4.23. Comparison of experimental and predicted profiles, using a terminal velocity 1.5 times greater than the original correlation, for run C10 (direct calculation of solids flow rate).

the predicted profile is a good approximation to the actual observations. However, it should be pointed out that this is not really consistent with the assumptions of the model. Since the more combustion which takes place in the initial heat balance the greater the number of large particles present at the base of the reactor. This situation is probably better described by a mixed tank reactor than by an overall heat and mass balance. Since the effect of particles being elutriated has been ignored, the more large particles present in the bottom of the reactor the greater the error is in assuming no elutriation.

However the predicted profiles using the modified terminal velocity, seem to be consistent with the data and therefore this might be considered as a possible fitting parameter.

4.3. The Effect of the Split Parameters on the Predicted Profiles

Up to this point the gas and reactor split parameters, available as an option in the model (see 3.3.4) have been set to unity. This corresponds to both gas and solids travelling together in the reactor, with no bypassing of gas.

However it was originally hoped to model the effect of the tangential air inlet (as used in the C and CP series of runs) by using these parameters. Since both a gas flow rate and a reactor volume parameter were included in the model, the flow of gas through the

reaction zone and the gas velocity may be altered. By setting the gas split parameter (β) less than the reactor volume parameter (γ) the overall effect is to decrease the gas velocity in the reaction zone. This is equivalent to increasing the terminal velocity of the particles and the effects produced are the same as those described above in the terminal velocity discussion.

The results obtained by varying the values of the split parameters are presented in Figures 4.24-4.29 (and Tables J.37-J.43). The comparison between predicted and experimental results is not as good as it was for the modified terminal velocity case. A problem with this type of split parameter is that since a certain portion of the gas stream is bypassed the temperature drop at the point where the two streams (reactor and bypass) remix is dependent upon how much of the gas was bypassed. For this reason not more than 30% of the gas stream was allowed to bypass the reaction section. This is equivalent to setting a lower limit of the split parameter β to 0.7. The value of the reactor volume split was also not allowed to be set below a certain lower limit. This limit was chosen as 0.9 and corresponds to the physical situation where the annulus of gas and particles is 2/3 of the radius of the reactor thick.

Although the split parameters help explain what is physically happening, the do not predict the correct shape of the profile.

The large temperature drop which occurs at the final mixing

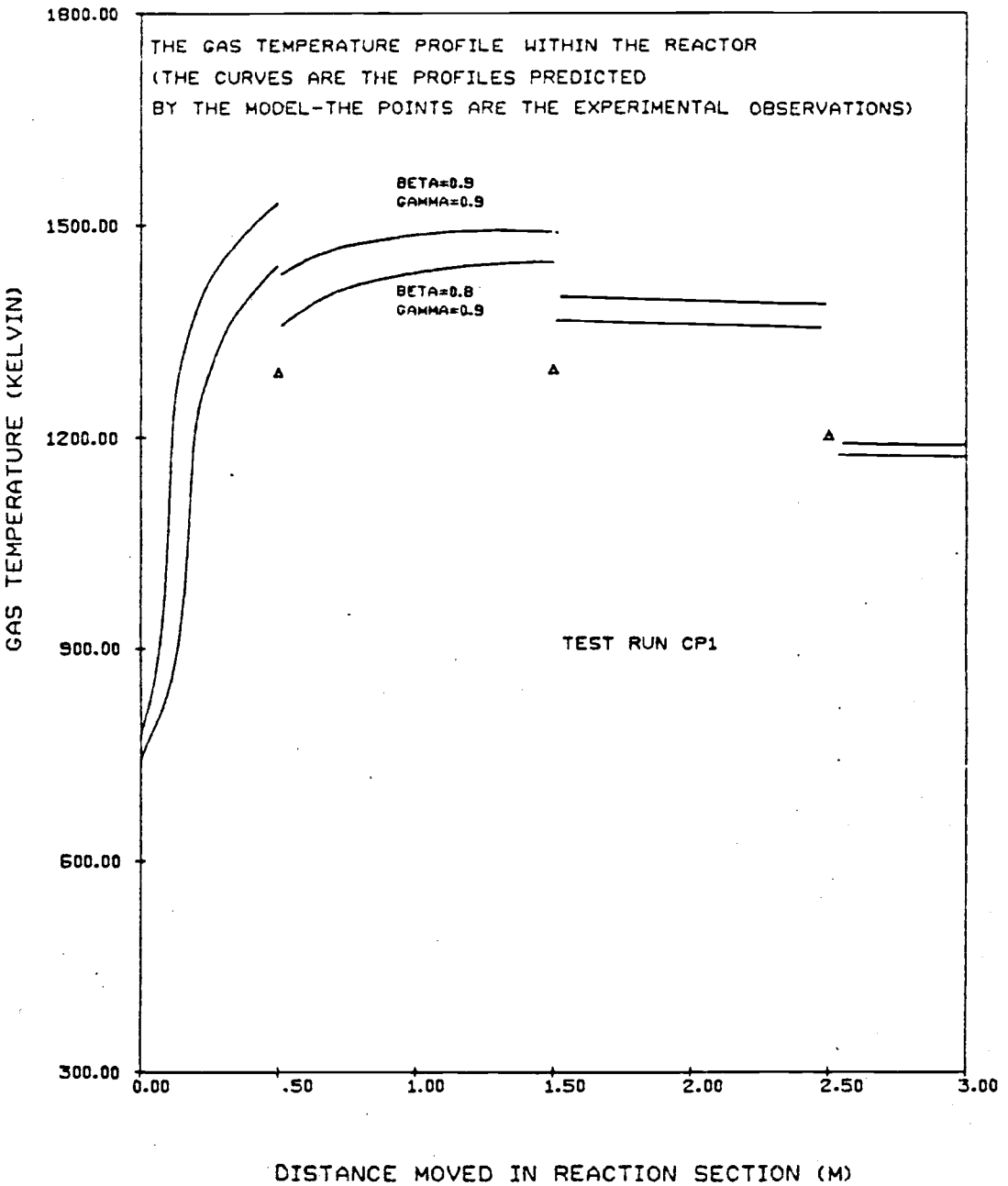

Figure 4.24. Comparison of experimental and predicted profiles, using different values of the gas (Beta) and reactor volume (Gamma) split parameters, for test run CP1 (direct calculation of solids flow rate).

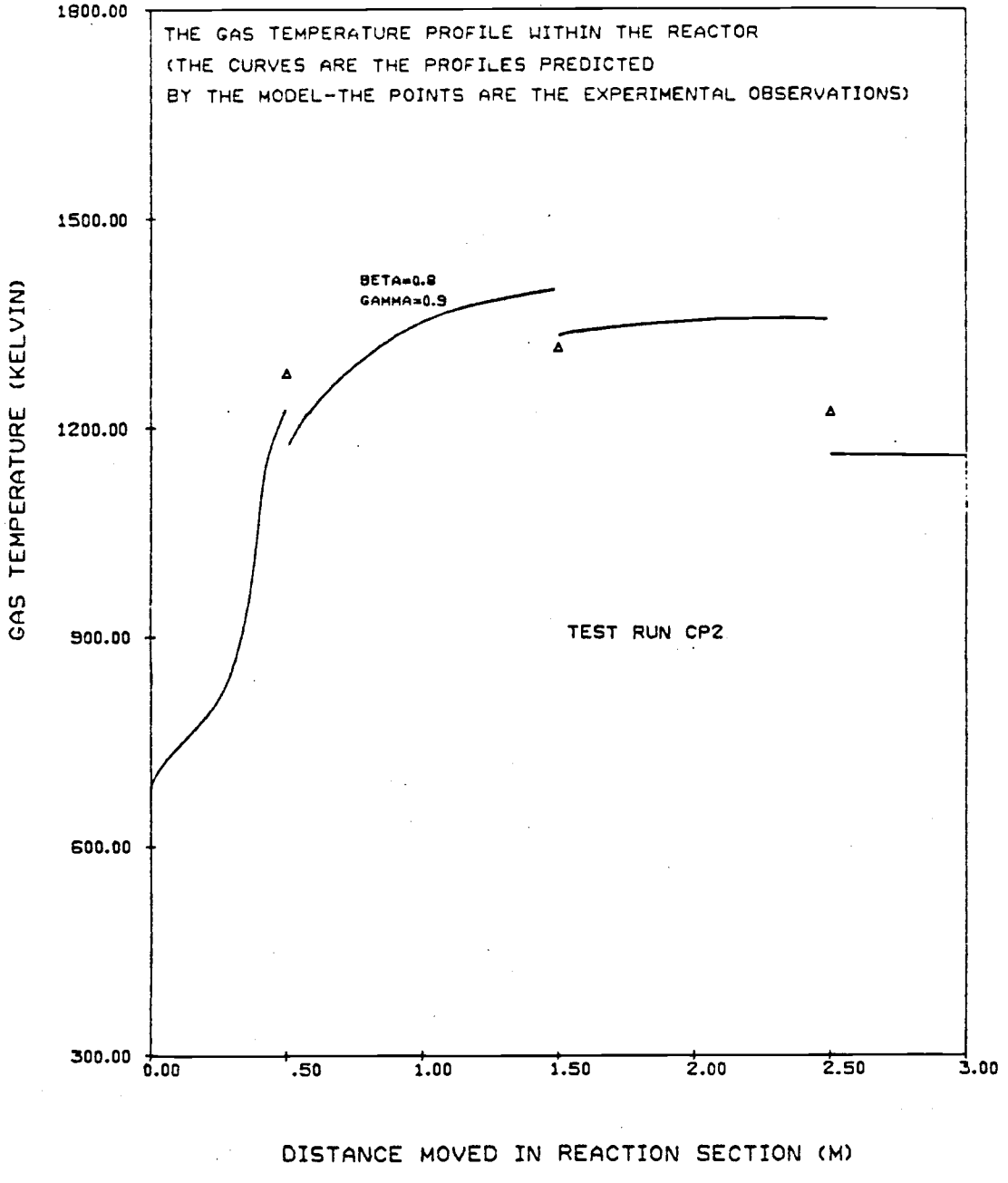

Figure 4.25. Comparison of experimental and predicted profiles, using different values of the gas (Beta) and reactor volume (Gamma) split parameters, for test run CP2 (direct calculation of solids flow rate).

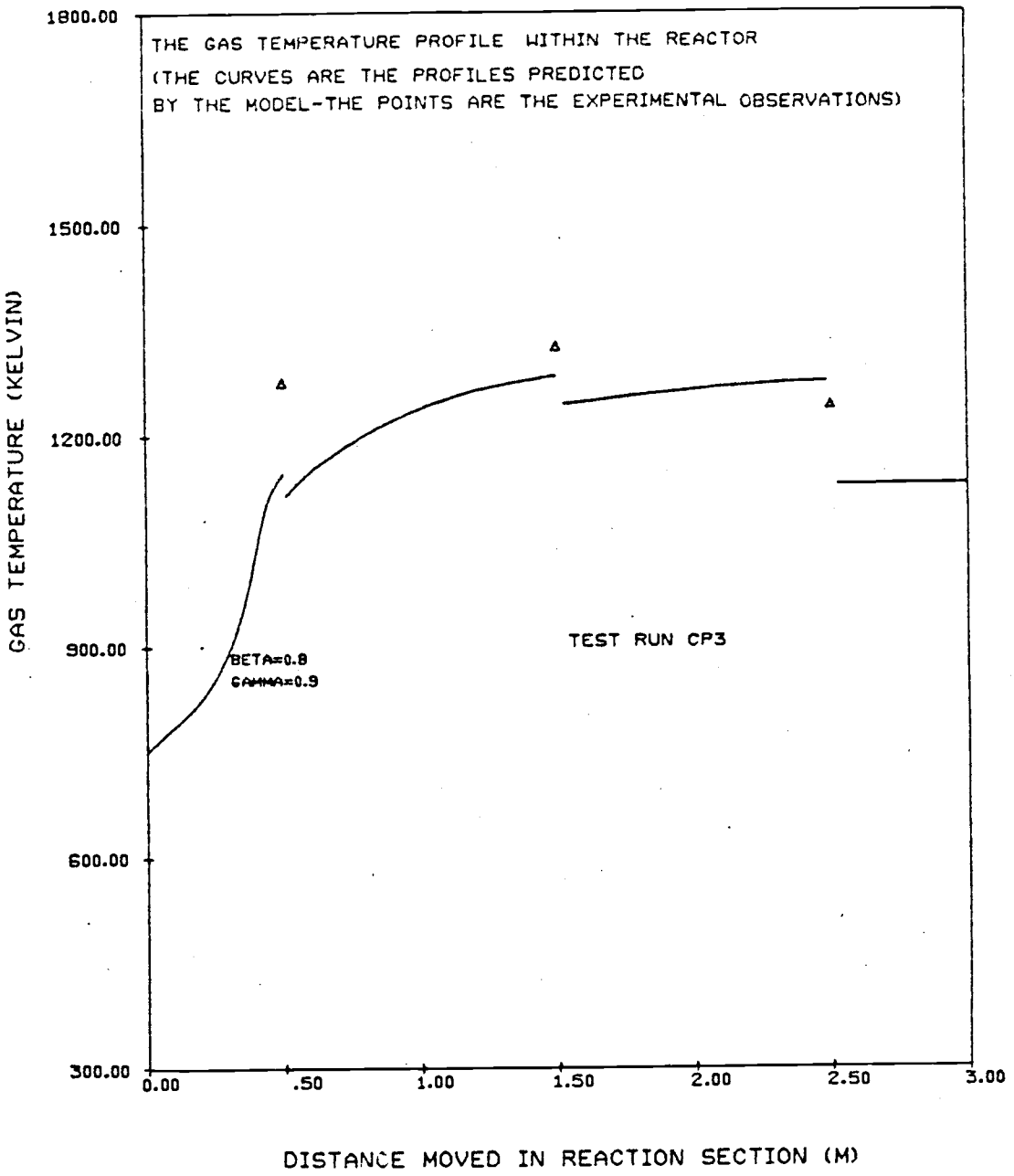

Figure 4.26. Comparison of experimental and predicted profiles, using different values of the gas (Beta) and reactor volume (Gamma) split parameters, for test run CP3 (direct calculation of solids flow rate).

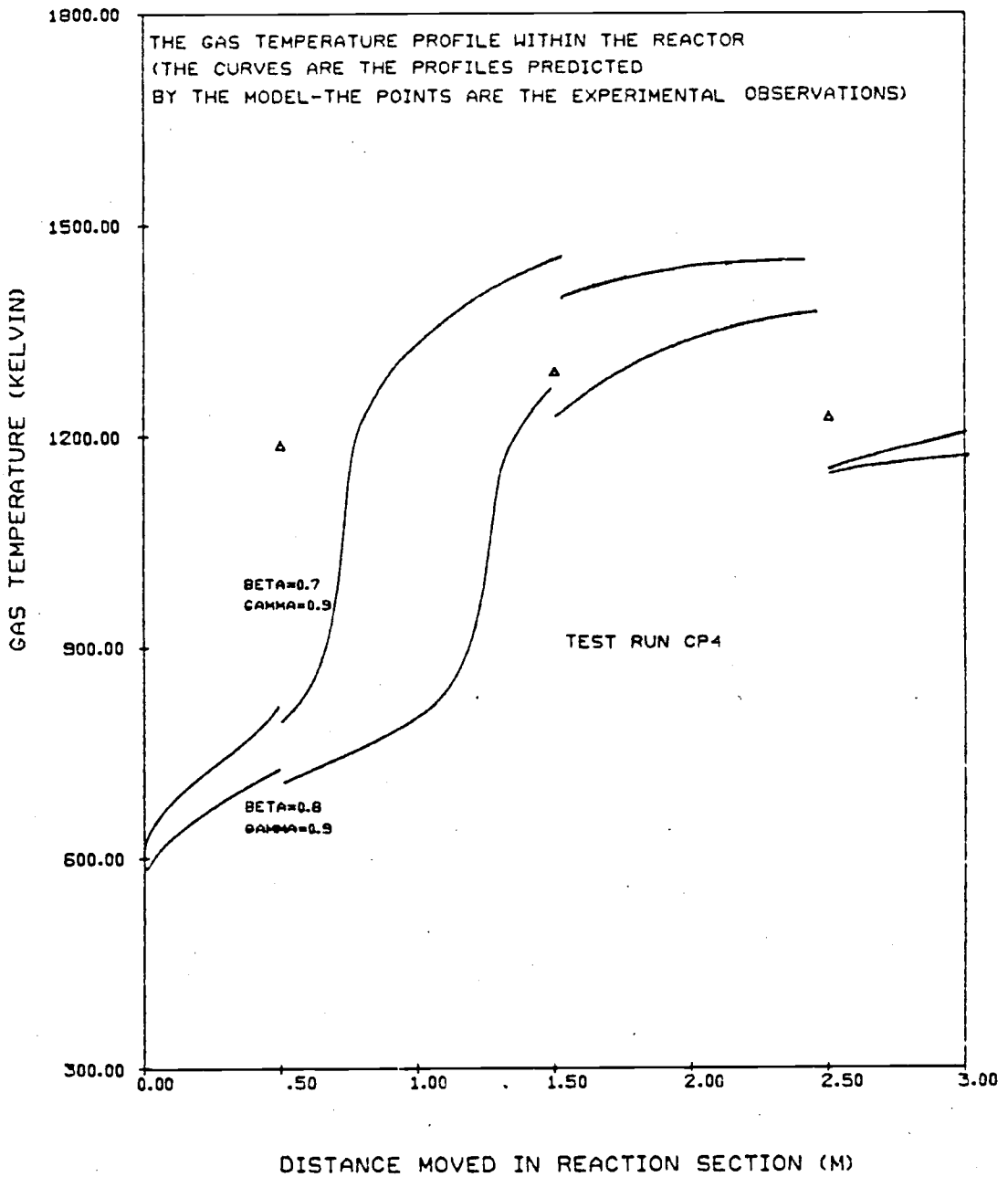

Figure 4.27. Comparison of experimental and predicted profiles, using different values of the gas (Beta) and reactor volume (Gamma) split parameters, for test run CP4 (direct calculation of solids flow rate).

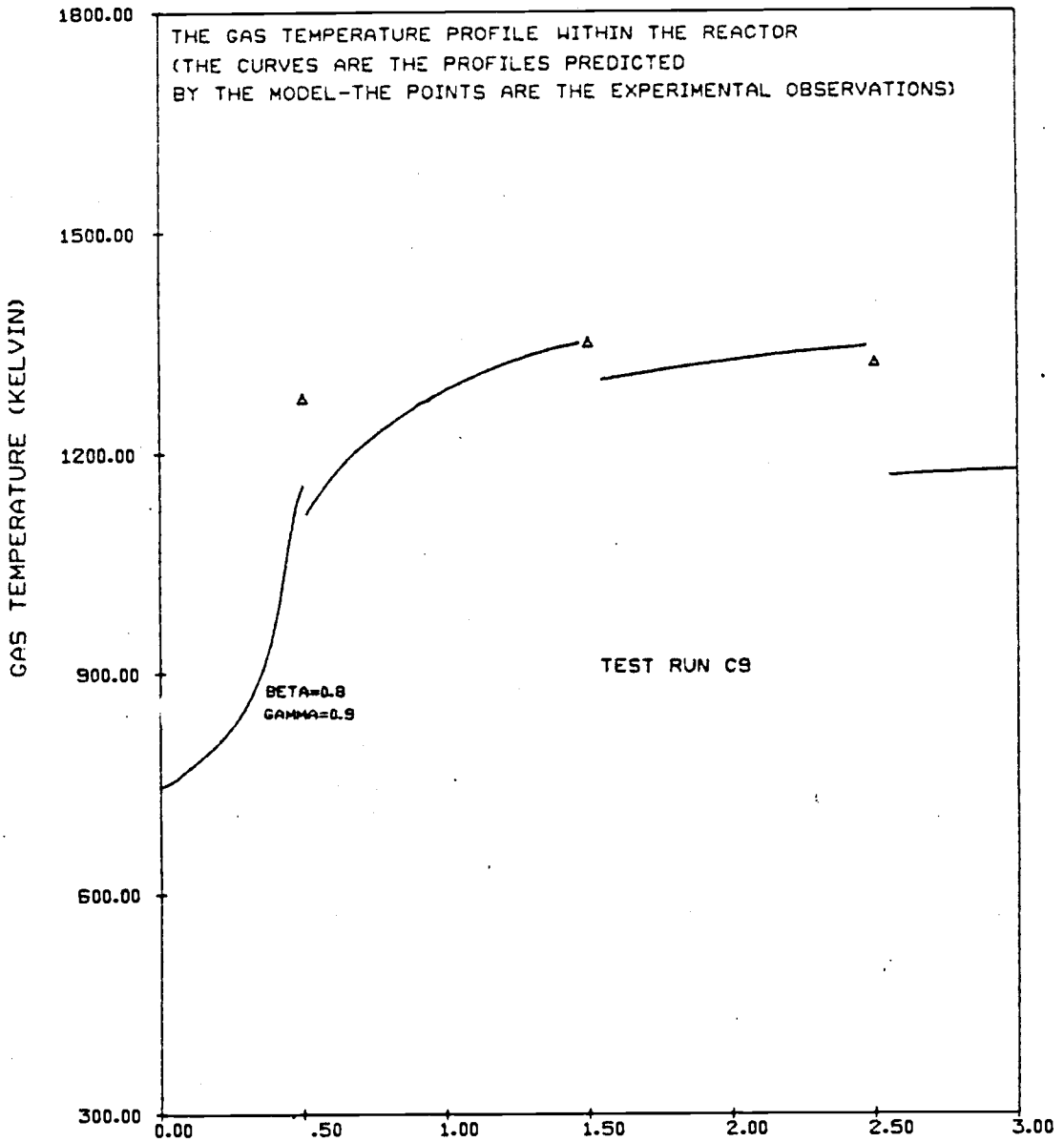

Figure 4.28. Comparison of experimental and predicted profiles, using different values of the gas (Beta) and reactor volume (Gamma) split parameters, for test run C9 (direct calculation of solids flow rate.

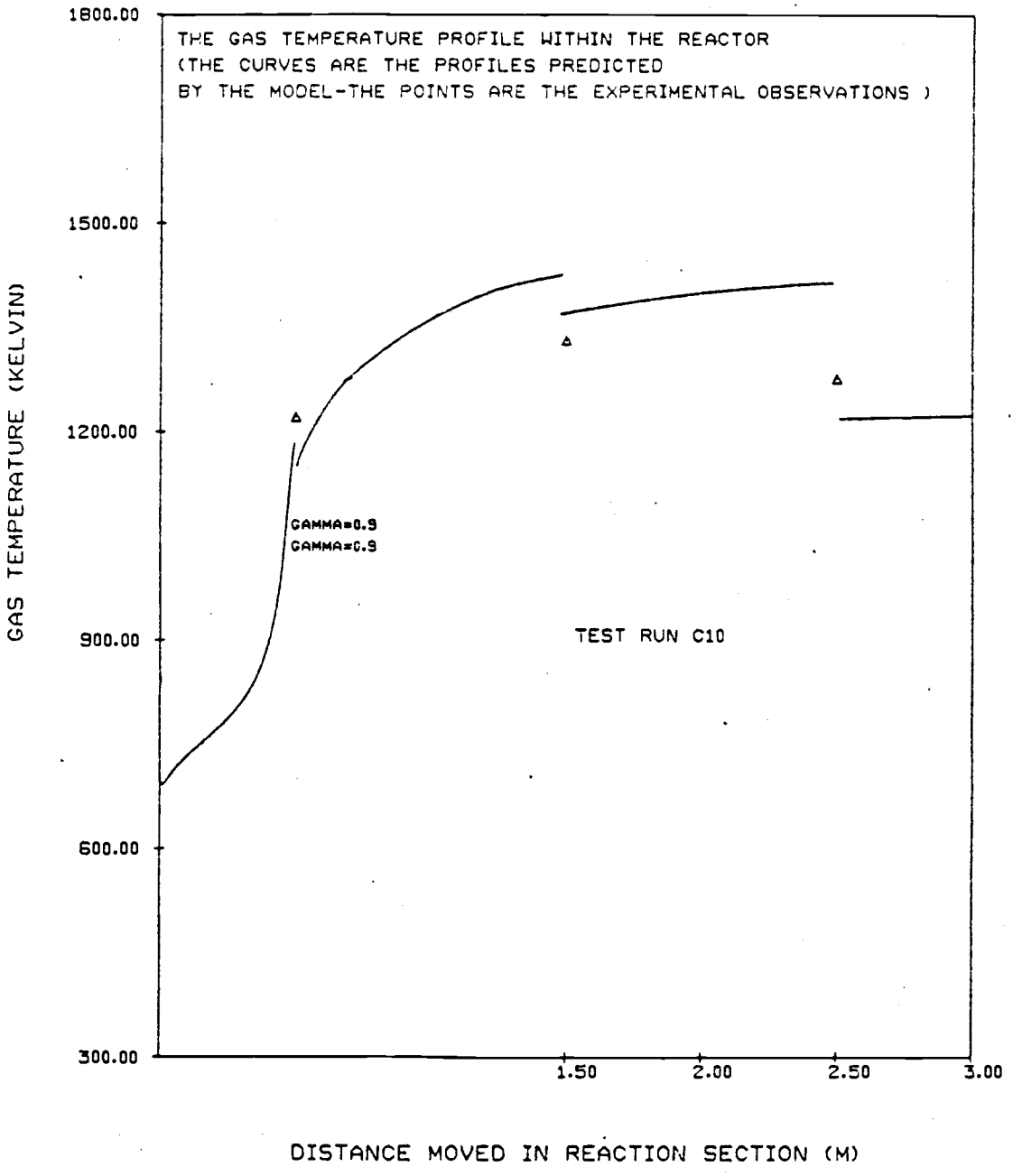

Figure 4.29. Comparison of experimental and predicted profiles, using different values of the gas (Beta) and reactor volume (Gamma) split parameters, for test run C10 (direct calculation of solids flow rate).

of the bypass and reactor streams, does not seem physically reasonable. One possible modification would be to include a remixing parameter. This would allow partial mixing between the bypass and reactor streams as they travelled through the reactor. However this would introduce a new parameter at every partial mixing point i.e. fraction of bypass stream which is remixed. This approach would then degenerate into a multiple regression problem and for that reason was not adopted in this work.

4.4. Other Parameters Effecting the Model

In formulating the model it was necessary to assume the values of certain parameters about which little experimental data were available. In this section the sensitivity of the model is checked against variations in these parameters.

The first parameter to be considered is the inside temperature of the reactor wall. For the previous computer runs the wall temperature has been assumed to be 1000 K. This value was used since it was estimated as the lowest value which seemed physically reasonable. The gas and solids are in general above 1250 K and so this estimate is believed to be a conservative one. The effect of increasing the wall temperature to 1100 K was investigated. The results for the input conditions of test run CP4 are presented in Table J.43. By comparing these results with those obtained with a wall temperature

of 1000 K (Table J.8) it can be seen that there is little difference between the two runs. Thus it would seem that the value of the wall temperature does not have a great effect on the temperature profile.

The second parameter which was studied was the step size used in the integration of the system of differential equations. The differential equations used to describe the situation occurring in the reaction zone are known to behave as a stiff system. The method of solving these equations used a crude variable step technique. This procedure allowed small increments to be made only when the temperature changed quickly and when the temperature change was slow larger step lengths were taken. This procedure allowed the integration to be carried out accurately but a the same time did not use an excessive number of function evaluations. The effect of halving the step size for any given region of integration was considered. The results for run CP4 are presented in Table J.44. It can be seen that at certain points in the profile there is as much difference as 40 K between this profile and the original profile in Table 4.10. This, however, should not cause too great a problem since the discrepancies occur mostly during the ignition region. This

means that although the computer profile may slightly under-predict what actually happens at ignition, the overall profile will give a very good indication of the process.

4.5 A Comparison of the Other Predictions Made by the Model

Although the model may predict the shape of the temperature profile reasonably well, its prediction of the conversion of carbon within the reactor is invariably too high. In 22 out of the 42 computer runs, the predicted conversion of the carbon in the feed stock was 100%. In 11 of the remaining 20 runs the predicted value was 98% or greater. The results are presented below in Table 4.3.

The results would indicate that in general the model under-predicts the temperature at the beginning of the reactor and over-predicts the final conversion of carbon. The first phenomena may be explained by an underestimation of the terminal velocity of the particle or possibly by the bypassing of some of the gas stream. Yet another explanation is that the assumption made in the model concerning the gas and particles being at the same temperature is wrong. It will be recalled that a particle was assumed to have a temperature either

colder than or equal to the the gas stream, but never hotter. This assumption was made in order to ease the numerical calculations. However, it is conceivable that large particles will rise to a temperature greater than the gas temperature and will accordingly react faster than predicted by the model.

The fact that the conversion predicted by the model is always higher than that found by experiment is puzzling. In Appendix F the combustion of carbon was considered and the model used to describe the combustion assumed that any ash formed, continually flaked off, leaving a spherical ball of unreacted carbon. During the course of the experiments it was possible to observe the combustion of single particles. It was noticed that when a particle burned it did not, in general, act like a shrinking sphere. Often the size of the particle did not change and a burning anulus was seen to travel through the particle, leaving an ash layer behind. Whenever an ash layer is formed, the resistance it offers to mass transfer is always greater than that due to diffusion through the stagnant gas film surrounding the particle. However in the model this resistance was not considered and hence the predicted reaction rate used will be too high. The reaction rate at the start will not be effected greatly since the ash layer will be thin. However as the unreacted core gets smaller and the ash layer gets thicker the reaction rate may deviate appreciably from that predicted, assuming only film diffusion resistance

Table 4.3. Comparison of the predicted and experimental conversion of wood char feed stock

Run number	Predicted value	Actual value
P1	1.0	0.951
	1.0	
	1.0	
P2	1.0	0.940
	0.9997	
	1.0	
P3	1.0	
	1.0	
	0.9696	0.946
	1.0	
	1.0	
	1.0	
P4	0.9407	0.868
	0.9650	
	0.9993	
	1.0	
Mean	0.992	0.926

Table 4.3. (Continued)

Run number	Predicted value	Actual value
CP1	1.0	.957
	1.0	
	1.0	
	1.0	
	1.0	
CP2	0.9999	.931
	0.9957	
	1.0	
	1.0	
CP3	1.0	.960
	0.9987	
	0.9690	
	0.9798	
CP4	0.9994	.941
	0.9265	
	0.9041	
Mean	0.986	.947

Table 4.3. (Continued)

C9	1.0	0.898
	0.9903	
	0.9675	
	0.9843	
C10	1.0	0.952
	1.0	
	0.9703	
	0.9828	
Mean	0.987	0.925

(and chemical reaction resistance). The effect of using an ash diffusion resistance was considered by modifying the original model. The results are presented in Figure 4.30 and Table J.45. The profile indicates that when the temperature reaches about 850 K (at about 0.3 M up the reactor) the ash layer becomes a significant resistance. The conversion of char leaving the reactor is 77% and this indicates that the actual reaction mechanism lies somewhere between the shrinking sphere and shrinking core extremes.

The second comparison which can be made is between the predicted and experimental gas profiles in the reactor. Although samples of gas were analyzed at 3 different positions in the reactor the results obtained were far from satisfactory.

One of the major problems encountered was the discrepancy in the combined volume fraction of oxygen, carbon dioxide and carbon monoxide. This should have been in the vicinity of 21% but was invariably around the 19% mark. It was originally thought that this was due to an error in the carbon dioxide analyzer, however on comparing the final exit temperatures with the adiabatic flame temperature (Table 4.1) and the corresponding mass balance (Table 4.2) the validity of the oxygen analysis equipment becomes suspicious. Another problem which arose with the analysis of the gas composition was the buildup of ash and char in the 2 micron filters and sample tubes. This meant that the conditions in the sample tubes might not be the same as that present

within the reactor i. e. burning within the sampling equipment might be possible.

For the above reasons, the gas profiles were not compared, it should be sufficient, however, to compare just the temperature profiles.

4.6 Possible Sources of Error

One possible source of error which has not been considered yet is the effect of carbon monoxide production.

In the model it was assured that carbon monoxide would not be produced. However, the results presented in Appendix D showed that there was on occasion a considerable amount of carbon monoxide produced (0.6%). This level of carbon monoxide is equivalent to about a five percent overestimation in the predicted temperature rise. However since the mass balance is not known to this accuracy this assumption should not cause any significant errors for the computed profiles.

Another point of interest is the correlation between the flow of solids into the reactor and the flow of solids leaving the reactor. A balance was made on the inorganic content for the experimental runs and the results are presented in Table 4.4. There is obviously a significant amount of inorganic content which cannot be accounted for. Some will of course escape to the atmosphere through the cyclone stack. However, it is hard to accept that this can account for such

Table 4.4. The mass balance on the inorganic content in the feed stream.

Run number	Wt of inorganic solids Inlet (kg)	Outlet (kg)	% Loss
P1	1.952	.482	75.3
P2	1.634	.795	51.4
P3	4.643	.843	81.8
P4	3.100	.9617	68.9
CP1	1.280	.449	64.9
CP2	1.166	.711	39.0
CP3	1.404	.977	30.4
CP4	2.156	1.035	52.0
C1	5.194	1.273	75.5
C2	5.053	1.561	69.1
C3	0.724	.653	9.8
C4	0.621	.545	12.3
C5	1.228	.352	71.4
C6	0.905	.550	39.2
C7	0.886	.961	-8.0
C8	2.070	.696	66.4
C9	4.205	1.004	76.1
C10	2.785	1.143	59.0

large deviations in the overall balance. There is a significant amount of ash buildup on the reactor walls but again it seems hard to believe that this amount of solids could be accumulated in this way. However there is no other explanation and thus the combination of stack loss and accumulation in the reactor must account for the loss of inorganic solids.

Finally, it should be noted that the predicted size distribution of solids at the reactor inlet might be in error. The effect of size distribution on the temperature profile was (however, considered. The profile for the original size distribution of char in run P3 was compared with the predicted distribution and this is shown in Figure 4.31 (Table J.46) . The results show that the ignition point in the reaction section occurs earlier for the original distribution than for the predicted distribution. This is as expected due to the greater number of large particles. Apart from this the profiles show a similar trend.

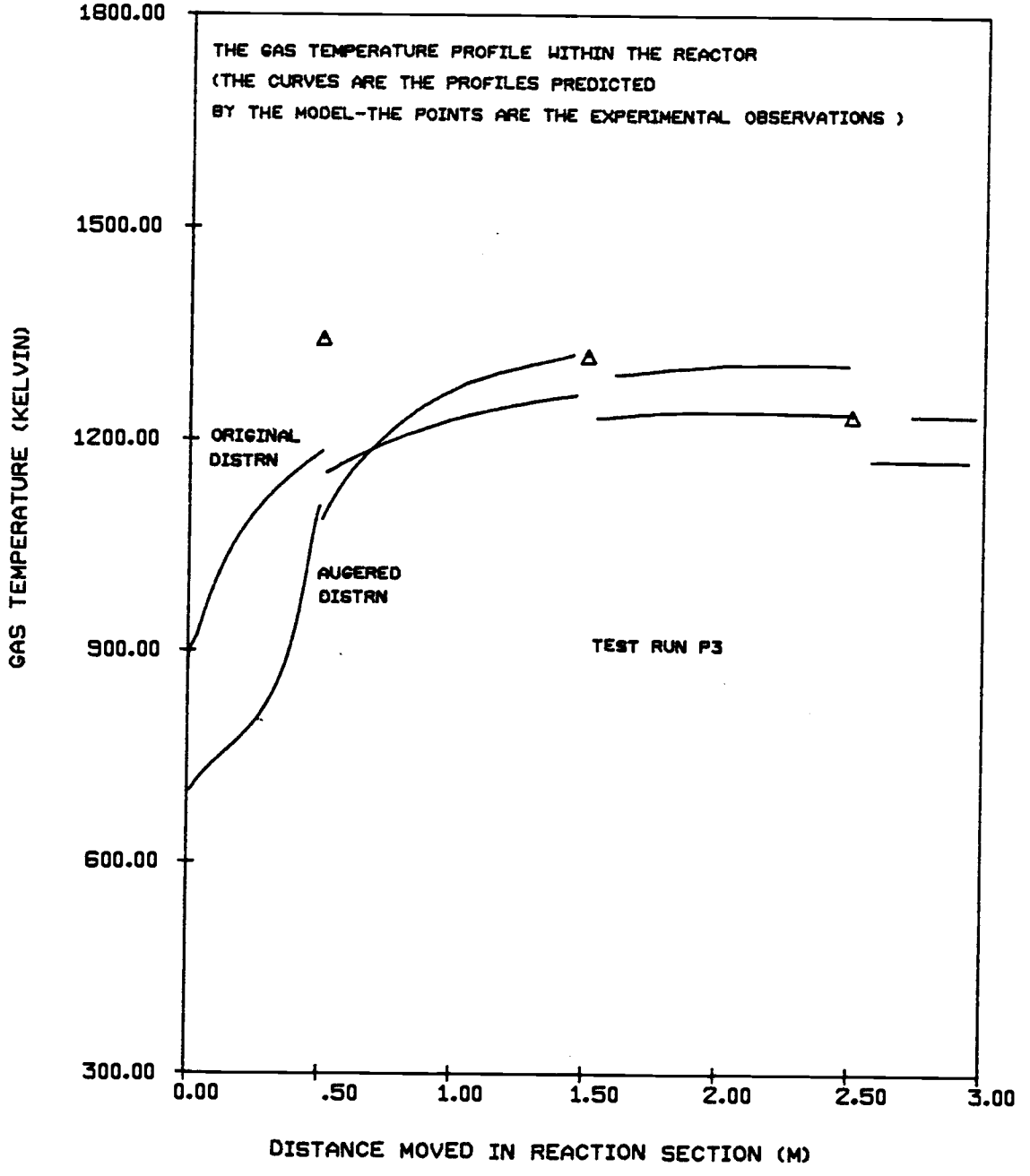

Figure 4.31. Comparison of experimental and predicted profiles, using the direct method to evaluate the solids flowrate and the Original Size Distribution for the char feed.

5. CONCLUSIONS

The important findings of the present study may be summarized as follows:

(a) The single most important factor in evaluating the validity of the combustion model is the overall material balance on the reactor system.

(b) The model of combustion presented in this work tends to underestimate the temperature in the lower 1/3 of the reactor.

(c) The combustion model tends to overpredict the final conversion of wood char leaving the reactor.

(d) The terminal velocity of a char particle is an important parameter in the combustion model. By adjusting the free fall velocity of the char particles, the predicted temperature profile may be fitted reasonably well to the experimental data.

(e) The temperature profiles predicted by the model are very sensitive to variations in the split parameters. For this reason only small variations were considered for these parameters.

(f) The experimental data did not indicate any appreciable difference between the different modes of operating the reactor. Although, it is felt by the author, that by introducing the inlet air through the tangential ports, the operation should prove superior to the radial introduction of the air.

(g) The temperature profile and final conversion of char are significantly effected by assuming that a layer of ash builds up around the particle.

(h) The temperature profile is effected by the amount of crushing which occurs in the solids transport system, i.e. the distribution of solids entering the reactor.

6. AREAS FOR POSSIBLE FUTURE WORK

The results of this study indicate that certain areas of the combustion process should be further examined in order to verify the validy of the model and to determine the flexibility of the reactor system. The areas for future examination are presented below:

(a) The solids feed system should be calibrated more accurately and a comprehensive study of the bulk density of char should be made.

(b) The combustion gas analysis equipment should be checked with a reliable chemical analysis method.

(c) Thermocouples should be placed in the refractory to determine the temperature profile within the insulating layer.

(d) A comprehensive laboratory study on the combustion of the wood char should be made with the aim of evaluating the burning times of different size particles.

(e) A more sophisticated technique should be adopted to solve the set of differential equations presented in the model.

BIBLIOGRAPHY

1. Nusselt, W., Z. Ver. dt. Ing., 68, 124, 1924.

2. Spalding, D. B. "Combination of Coal." Jnl. Inst. Fuel, 26, 289. (1953)

3. Essenhigh, R. H., "Predicted Burning Times of Solid Particles in an Idealized Dust Flame." Jnl. Inst. Fuel, 34, 239 (1961)

4. Frank-Kamenetskii, D. A., Diffusion and Heat Exchange in Chemical Reactions, Princeton University Press, 1955.

5. Field, M. A., D. W. Gill, B. B. Morgan, and P. G. W. Hawksley, "Combustion of Pulverized Fuel " The British Coal Utilization Research Association-Monthly Bulletin, 31, Part 6 (1967)

6. Yagi, S. and D. Kuni, 5th Symposium (International) on Combustion," Reinhold, New York, 1955.

7. Yagi, S. D. Kuni, K. Nagahara and H. Naito, "Axial Moving of Particles in Moving Beds," Chem. Eng. (Japan), 25, 469 (1961)

8. Levenspiel, O., Chemical Reaction Engineering, 2nd Edition, John Wiley and Sons, New York, 1972.

9. Parker, A. S. and H. C. Hottel, "Combustion Rate of Carbon," Ind. Engng. Chem., 28, 1334 (1936)

10. Tu, C. M., H. Davis and H. C. Hottel, "Combustion of Carbon," Ind. Engng. Chem., 26, 749 (1934)

11. Golovina, E. S., and G. P. Khaustovich, Eighth International Symposium on Combustion, 784, 1962.

12. Gray, M. D. and G. M. Kimber, "Reaction of Charcoal particles with carbon dioxide and water at temperatures up to 2800 K," Nature, 214, 797 (1967)

13. Froesling, N., Gerland Beitr., Geophys. 52, 170 (1938)

14. Walker, P. L., F. Rusinko, Jr., and L. G. Austin, "Gas Reactions of Carbon.± Advances in Catalysis, 11, 133 (1959)

15. Thiele, E. W., "Material or Heat Transfer between a Granular Solid and a flowing fluid," Ind. Eng. Chem., 31, 916 (1939)

16. Weiss, P. B., and C. D. Prater, "Interpretation of Measurements in Experimental Catalysis," Advances in Catalysis, 6,143 (1954)

17. Zenz, F. A. and D. F. Othmer, Fluidisation and Fluid-Particle Systems Reinhold, New York, 1960.

18. Knudsen, J. G., and D. L. Katz, Fluid Dynamics and Heat Transfer, McGraw-Hill, New Yor, 1958.

19. Brown, G. G., Unit Operations, John Wiley and Sons, New York, 1950.

20. Becker, H. A., "The Effects of Shape and Reynolds Number on Drag in the Motion of a Freely Orientated Body in an Infinite Fluid," Can. J Chem. Eng., 37, 85 (1959)

21. Welty, J. R., C. E. Wicks, and R. E. Wilson, Fundamentals of Momentum, Heat, and Mass Transfer, 2nd Edition, John Wiley and Sons, New York, 1976.

22. Rohsenow, W. M., and J. P. Hartnett (Editors), Handbook of Heat Transfer McGraw-Hill, New York, 1973.

23. Ranz, W. E. and W. R. Marshal, Jr., "Evaporation from Drops," Chem. Eng. Progr., 48, 141 (1952)

24. Colburn, A. P., "A Method for Correlating Forced Convection Heat Transfer Data with a Comparison with Fluid Flow," Trans. Amer. Inst. Chem. Eng. 29, 174 (1933)

25. Kuni, D. and O. Levenspiel, Fluidisation Engineering, Wiley, New York, 1969.

26. Gears, C. W., "The Automatic Integration of Ordinary Differential Equations," Comm. A.C.M., 14, 176 (1971)

27. Carnahan, B., H. A. Luther and J. O. Wilkes, Applied Numerical Methods, Wiley, New York, 1969.

28. Kayihan, F. A Personal Communication.

29. Smith, J M and H. C. Van Ness, Introduction to Chemical Engineering Thermodynamics, 3rd Edition, McGraw-Hill, 1975.

30. Perry, R. H. and C. H. Chilton (Editors), Chemical Engineers' Handbook, 5th Edition, McGraw-Hill, New York, 1973.

31. Pankhurst, R. C., and E. Ower. The Measurement of Air Flow. 4th Edit., Oxford, New York, 1966.

APPENDICES

APPENDIX A

SIZE DISTRIBUTIONS OF WOOD CHAR AND ASH PRODUCT

Eighteen experimental runs were carried out on the reactor. In all but one of these runs, samples of the wood char feedstock and the ash produced by combustion were taken. Only for run C4 were no samples taken. The particle size distribution for each sample was measured using AMERICAN STANDARD sieve trays. The original size analysis used the following set of 6 screens.

Apperture Size ($M \times 10^{-6}$)
1000
500
250
125
63
45

After the analysis had been carried out, it was discovered that between 41 and 89 percent by weight of the char samples were collected on the first screen (i.e., 1000 micron). It was decided that to eliminate errors due to extrapolating the distribution outside the measured range, the top fraction of the char samples (i.e., particles with size greater than 1000 micron) should be further subdivided. This subdivision was achieved by resieving the char samples using the following set of 3 screens:

Apperture Size ($M \times 10^{-6}$)
3327*
2000
1000

* #6 TYLER STANDARD screen

The fractions collected on each screen were then used to convert the weight of solid collected on the 1000 micron screen in the original analysis to three equivalent weights of solid. These three equivalent weights represent the fictitious weights of solid which would have been collected if the 3327 and 2000 micron screens had been used in the original analysis.

An example is given below to illustrate the principle and method of calculation.

EXAMPLE A. 1

The original results for run P1 are:

Apperture Size ($M \times 10^{-6}$)	Weight Collected ($Kg \times 10^{-3}$)
1000	26.81
500	8.75
250	2.52
125	1.07
63	0.53
45	0.20
PAN	0.14
	40.02

Results for the 3 screen analysis of the same wood char sample from run P1 are:

Screen Size ($M \times 10^{-6}$)	Weight Collected ($Kg \times 10^{-3}$)	% of Total
3327	0.70	4.48
2000	3.45	22.04
1000	11.50	73.48
	15.65	100.00

The results above are now used to convert the 26.81×10^{-3} kg collected on the 1000 micron screen in the original analysis to the 3 equivalent weights.

Screen Size ($M \times 10^{-6}$)	Equivalent Weight ($Kg \times 10^{-3}$)	% of Total
3327	1.20	4.48
2000	5.91	22.04
1000	19.70	73.48
	26.81	100.00

The complete adjusted screen analysis for Run P1 is given below.

Screen Size ($M \times 10^{-6}$)	Weight Collected ($Kg \times 10^{-3}$)	Cumulative Weight %
3327	1.20	100.00
2000	5.91	97.00
1000	19.70	82.23
500	8.75	33.01
250	2.52	11.14
125	1.07	04.85
63	0.53	02.17
45	0.20	00.85
PAN	0.14	00.35
	40.02	

The cumulative weight fraction represents the fraction of the total weight with size less than or equal to the size of the fraction being considered e.g., 82.23 % by weight of the sample has a size less than or equal to 1000 micron.

The procedure illustrated in example A.1 was used for all the samples of wood char feedstock. The three screen analysis was carried out for each sample and the adjusted size distribution was calculated

accordingly. Since the samples were the same for both the original 6 screen analysis and the subsequent 3 screen analysis, the errors due to readjusting the size distributions should be negligible.

The results for both carbon char and product ash samples are presented below in Tables A. 1-A. 6.

In order to present the results of the size distribution in the form of a histogram it is necessary to assign a mean particle size to each size cut. For convenience the mean particle size was taken as the arithmetic mean of the apperture size of the screen on which the solid was collected and the screen immediately above it. This approach assumes that the size distribution is linear in the given size cut. This assumption may not necessarily be a good one, however for most cases it is reasonable first approximation and eases the computation of the mean size.

Tables A. 7-A. 12 give the mean particle sizes and their associated weight fractions for all the char and ash samples.

The mean particle size for the wood char collected on the first screen (i. e., 3327 microns) was taken to be 4013 microns. This corresponds to the mean apperture size for a number 4 and number 6 TYLER STANDARD screen. Although a number 4 screen was not used in the analysis, a periodic check showed that virtually all the particles passed through this screen. Using a similar resieving,

the largest particle size for the product ash was chosen as 1500 microns.

Table A.1. The size distribution analysis for the wood char feedstock used in runs P1-P4.

Run number	P1	P2	P3	P4
Screen size ($M \times 10^{-6}$)	Cumulative weight fractions			
3327	1.0000	1.0000	1.0000	1.0000
2000	.9700	.9402	.9743	.9442
1000	.8223	.7009	.7722	.6512
500	.3301	.2438	.2912	.1539
250	.1114	.0668	.0570	.0208
125	.0485	.0314	.0198	.0097
63	.0217	.0138	.0087	.0064
45	.0085	.0018	.0020	.0
PAN	.0035	.0015	.0010	.0

Table A.2. The size distribution analysis for the wood char feedstock used in runs CP1-CP4.

Run number	CP1	CP2	CP3	CP4
Screen size ($M \times 10^{-6}$)	Cumulative weight fractions			
3327	1.0000	1.0000	1.0000	1.0000
2000	.9820	.9746	.9675	.9734
1000	.8332	.7844	.6375	.8067
500	.4122	.3156	.1482	.3812
250	.1787	.1176	.0401	.1486
125	.1057	.0453	.0328	.1029
63	.0653	.0212	.0183	.0717
45	.0348	.0113	.0052	.0360
PAN	.0179	.0071	.0016	.0110

Table A. 3. The size distribution analysis for the wood char feedstock used in runs C1-C10.

Run number	C1	C2	C3	C5	C6
Screen size ($M \times 10^{-6}$)	Cumulative weight fraction				
3327	1.0000	1.0000	1.0000	1.0000	1.0000
2000	.9825	.9850	.9801	.9733	.9653
1000	.8736	.8730	.8453	.7967	.7670
500	.5903	.5248	.5242	.3101	.2800
250	.3774	.3308	.3256	.0972	.0688
125	.3071	.2718	.2581	.0502	.0308
63	.2478	.2206	.1996	.0285	.0123
45	.1803	.1560	.1470	.0095	.0000
PAN	.0058	.0001	.0000	.0000	.0000

Run number	C7	C8	C9	C10
3327	1.0000	1.0000	1.0000	1.0000
2000	.9141	.9318	.9236	.9459
1000	.5916	.6274	.6183	.7070
500	.1577	.1901	.2225	.3116
250	.0365	.0505	.0605	.1206
125	.0247	.0316	.0321	.0873
63	.0118	.0200	.0193	.0634
45	.0000	.0083	.0069	.0305
PAN	.0000	.0050	.0037	.0129

Table A. 4. The size distribution analysis for the ash product from runs P1-P4.

Runs number	P1	P2	P3	P4
Screen size ($M \times 10^{-6}$)	Cumulative weight fraction			
1000	1.0000	1.0000	1.0000	1.0000
500	.9993	.9855	.9963	.9737
250	.9987	.9704	.9914	.9529
125	.9910	.9439	.9681	.9294
63	.8913	.8343	.8738	.8567
45	.7406	.6684	.7658	.7553
PAN	.1843	.1604	.3507	.4067

Table A. 5. The size distribution analysis for product ash from runs CP1-CP4.

Run number	CP1	CP2	CP3	CP4
Screen size ($M \times 10^{-6}$)	Cumulative weight fraction			
1000	1.0000	1.0000	1.0000	1.0000
500	0.9999	1.0000	1.0000	0.9970
250	0.9999	0.9983	0.9958	0.9944
125	0.9990	0.9876	0.9773	0.9822
63	0.9686	0.8985	0.8886	0.9060
45	0.8726	0.7648	0.7571	0.6644
PAN	0.3625	0.2747	0.1983	0.1345

Table A.6. The size distribution analysis for the ash product from runs C1-C10.

Run number	C1	C2	C3	C5	C6
Screen size ($M \times 10^{-6}$)	Cumulative weight fraction				
1000	1.0000	1.0000	1.0000	1.0000	1.0000
500	0.9997	0.9996	1.0000	1.0000	1.0000
250	0.9977	0.9963	0.9967	0.9997	0.9998
125	0.9791	0.9664	0.9653	0.9988	0.9984
63	0.8327	0.8504	0.8769	0.9525	0.9279
45	0.6262	0.6474	0.6330	0.8105	0.7482
PAN	0.2386	0.2994	0.0392	0.3139	0.2941

Run number	C7	C8	C9	C10
1000	1.0000	1.0000	1.0000	1.0000
500	1.0000	1.0000	0.9992	0.9967
250	0.9999	0.9995	0.9945	0.9955
125	0.9887	0.9806	0.9789	0.9903
63	0.8776	0.8276	0.8957	0.9217
45	0.6785	0.6122	0.6761	0.7163
PAN	0.2236	0.1040	0.2000	0.2389

Table A.7. The mean particle sizes and corresponding weight fractions for the carbon char from runs P1-P4.

Run number	P1	P2	P3	P4
Mean particle size ($M \times 10^{-6}$)	Weight fraction			
4013	.0300	.0598	.0257	.0558
3604	.1477	.2393	.2021	.2930
1500	.4922	.4571	.4810	.4973
750	.2187	.1770	.2342	.1331
375	.0629	.0354	.0372	.0111
187.5	.0268	.0176	.0111	.0033
96.0	.0132	.0120	.0067	.0064
54.0	.0050	.0003	.0010	.0000
22.5	.0035	.0015	.0010	.0000
Total	1.	1.	1.	1.

Table A.8. The mean particle size and corresponding weight fraction for the carbon char from runs CP1-CP4.

Run number	CP1	CP2	CP3	CP4
Mean particle size ($M \times 10^{-6}$)	Weight fraction			
4013	.0180	.0254	.0325	.0266
2664	.1488	.1902	.3300	.1667
1500	.4210	.4688	.4893	.4255
750.0	.2335	.1980	.1081	.2326
375.0	.0730	.0723	.0073	.0457
187.5	.0404	.0241	.0145	.0312
96.00	.0305	.0099	.0131	.0357
54.00	.0169	.0042	.0038	.0250
22.50	.0179	.0071	.0014	.0110
Total	1.	1.	1.	1.

Table A. 9. The mean particle sizes and corresponding weight fractions for the carbon char from runs C1-C10.

Run number	C1	C2	C3	C5	C6
Mean particle size ($M \times 10^{-6}$)	Weight fraction				
4013	.0175	.0150	.0199	.0267	.0347
2664	.1089	.1120	.1348	.1786	.1983
1500	.2833	.3482	.3211	.4846	.4870
750.0	.2129	.1940	.1986	.2129	.2112
375.0	.0703	.0590	.0675	.0463	.0380
187.5	.0593	.0512	.0585	.0224	.0185
94.00	.0676	.0646	.0526	.0190	.0123
54.00	.1745	.1559	.1479	.0095	.0000
22.50	.0058	.0001	.0000	.0000	.0000
Total	1.	1.	1.	1.	1.

Run number	C7	C8	C9	C10
4013	.0859	.0682	.0764	.0541
2004	.3225	.3044	.3053	.2389
1500	.4339	.4373	.3958	.3954
750.0	.1212	.1396	.1620	.1910
375.0	.0118	.0189	.0286	.0333
187.5	.0129	.0116	.0128	.0239
96.00	.0118	.0117	.0124	.0329
54.00	.0000	.0033	.0032	.0176
ww. tp	.0000	.0050	.0037	.0129
Total	1.	1.	1.	1.

Table A. 10. The mean particle size and corresponding weight fractions for the product ash from runs P1-P4.

Run number	P1	P2	P3	P4
Mean particle size ($M \times 10^{-6}$)	Weight fraction			
1500	.0007	.0145	.0037	.0263
750	.0006	.0151	.0049	.0208
375	.0077	.0265	.0233	.0235
187.5	.0997	.1096	.0943	.0727
94.0	.1507	.1659	.1080	.1014
54.0	.5563	.5080	.4151	.3486
22.5	.1843	.1604	.3507	.4067
Total	1.	1.	1.	1.

Table A. 11. The mean particle sizes and corresponding weight fractions for the product ash from runs CP1-CP4.

Run number	CP1	CP2	CP3	CP4
Mean particle size ($M \times 10^{-6}$)	Weight fraction			
1500	.0001	.0000	.0000	.0030
750	.0000	.0017	.0042	.0026
375	.0009	.0107	.0185	.0122
187.5	.0304	.0891	.0887	.0762
94.0	.0960	.1337	.1315	.2416
54.0	.5101	.4901	.5588	.5299
22.5	.3625	.2747	.1983	.1345
Total	1.	1.	1.	1.

Table A.12. The mean particle sizes and corresponding weight fractions for the product ash from runs C1-C10.

Run number	C1	C2	C3	C5	C6
Mean particle size ($M \times 10^{-6}$)			Weight fraction		
1500	.0003	.0004	.0	.0	.0
750	.0020	.0033	.0033	.0003	.0002
375	.0186	.0299	.0314	.0009	.0014
187.5	.1404	.1160	.0904	.0463	.0705
94.0	.2065	.2030	.2419	.1420	.1797
22.5	.2386	.2996	.0392	.3139	.2941
Total	1.	1.	1.	1.	1.

Run number	C7	C8	C9	C10
1500	0.	0.	.0008	.0033
750	.0001	.0005	.0047	.0012
375	.0112	.0129	.0156	.0052
187.5	.1111	.1590	.0832	.0686
94.0	.1991	.2154	.2196	.2054
54.0	.4549	.5082	.4761	.4774
22.5	.2236	.1040	.2000	.2389
Total	1.	1.	1.	1.

THE SIZE REDUCTION OF SOLIDS ON PASSING THROUGH THE SOLIDS FEED SYSTEM

Since the carbon char feed stock passes through approximately 15 meters of the transport system before it reaches the reactor, it was thought that a certain amount of size reduction might take place. This size reduction would also be aided by the low shear strength of the wood char.

Due to the above two factors, it was decided to investigate the size distributions of feed before and after passing through the auger transport system.

Four samples of wood char feed stock and four samples of augered feed were taken and analysed. These results are presented in Tables A. 13 and A. 14. The mean of both sets of distributions is also presented and this is plotted in Figure A. 1. The change in cumulative weight percent for a given mean particle size is also given in Table A. 15 and this is plotted in Figure A. 2.

Table A. 13. Particle size distribution for fresh wood char feed stock.

Tyler sieve no.	Screen aper-ture ($M \times 10^{-6}$)	Cumulative weight % passed through sieve Run 5	Run 6	Run 7	Run 8
6	3327	100.0	100.0	100.0	100.0
10	1651	99.7	96.8	97.8	97.5
20	833	70.4	70.0	75.2	61.1
28	595	36.6	37.5	39.9	20.7
48	295	24.0	25.1	23.1	11.0
80	177	9.6	10.9	6.2	4.9
150	104	5.3	6.7	3.2	3.6
200	74	3.6	4.3	2.3	2.8
270	53	3.0	3.5	2.0	2.4
325	44	2.4	2.8	1.6	1.9
PAN	PAN	1.7	2.0	1.2	1.3

The mean of the above four distributions

6	100.0
10	98.0
20	69.2
28	33.7
48	20.8
80	7.9
150	4.7
200	3.3
270	2.7
325	2.2
PAN	1.6

Table A.14. Particle size distribution of wood char after passing through the auger feed system.

Tyler sieve no.	Screen aperture ($M \times 10^{-6}$)	Cumulative weight % collected on sieve Run 1	Run 2	Run 3	Run 4
6	3327	100.0	100.0	100.0	100.0
10	1051	99.4	99.9	99.5	99.7
20	833	87.6	91.4	85.6	90.6
28	595	61.1	62.7	55.3	64.2
48	295	48.8	43.7	43.0	48.7
80	177	30.1	20.1	28.0	25.1
150	104	18.8	8.9	21.6	14.2
200	74	14.7	6.8	17.1	10.8
270	53	10.6	5.2	14.8	8.4
325	44	6.9	3.4	11.9	5.3
PAN	PAN	3.5	1.5	4.1	2.4

The mean of the above four distributions

6	100.0
10	99.6
20	88.8
28	60.8
48	46.1
80	25.8
150	15.9
200	12.4
270	9.8
325	6.9
PAN	3.1

Table A. 15. The change in cumulative weight per cent for a given mean particle size.

Mean particle size ($M \times 10^{-6}$)	Change in cumulative weight %
2489	1.6
1242	19.6
714.0	27.1
445.0	25.3
236.0	17.9
140.5	11.2
89.0	9.1
63.5	7.1
48.5	4.7
22.0	1.5

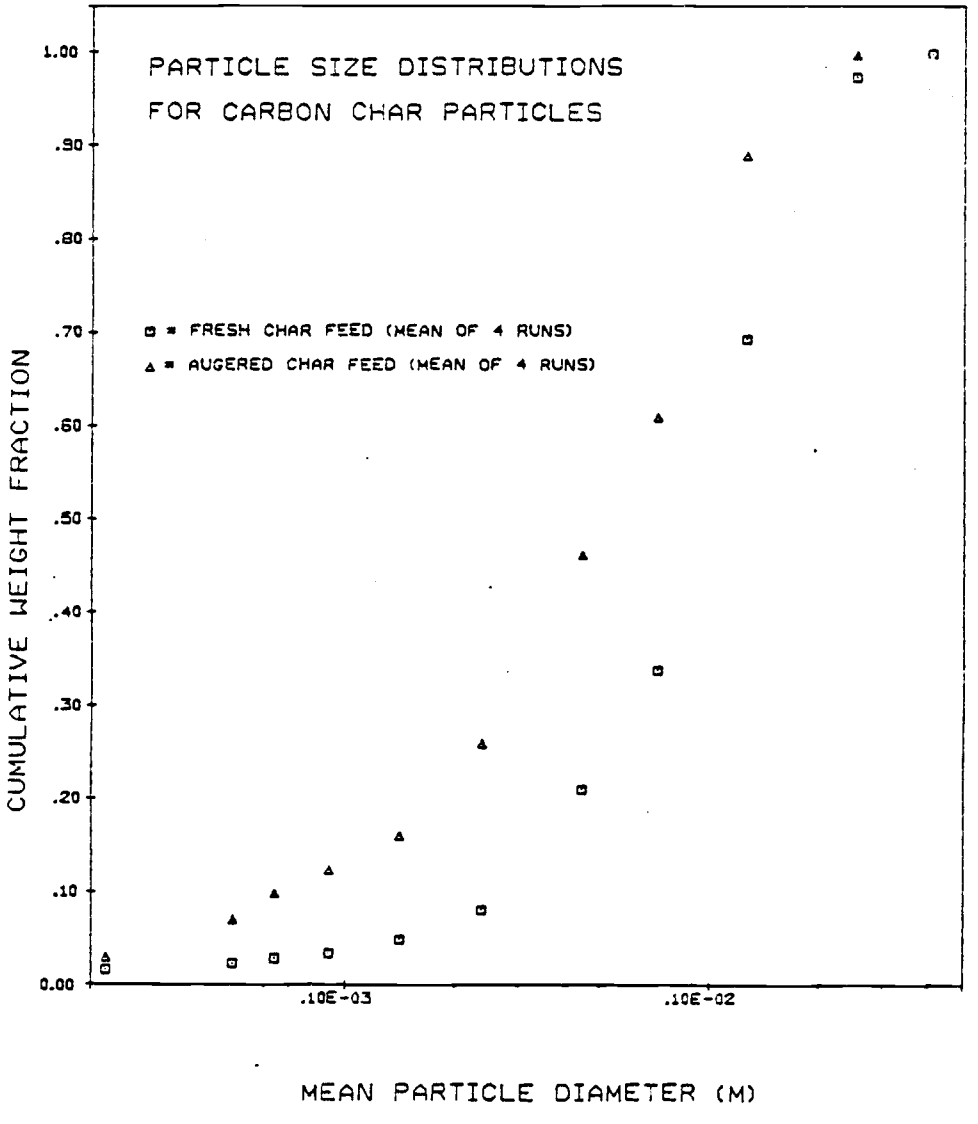

Figure A.1. Size Reduction of Feed Due to Crushing in the Auger.

THE EFFECT OF SIZE REDUCTION ON THE CHAR SAMPLES TAKEN FOR THE TEST RUN

From the results of the previous section it becomes apparent that as the carbon char feed stock is transported to the reactor a considerable change in the size distribution takes place. Thus the size distribution of wood char immediately prior to entering the reactor is different from the size distribution of the fresh feedstock.

The size distribution of solids entering the reactor may be an important parameter influencing the combustion of the wood char. It was thus decided to use the results from the preceding section to transform the size distribution for the char samples to an equivalent distribution at the reactor inlet. From Figure A.2 the % change in cumulative weight fraction for the mean particle sizes in the original distributions (Tables A.7-A.9) were found and are presented below in Table A.16.

The figures in Table A.16 may, at first, seem confusing. However, an example of a size distribution transformation is given below to illustrate the use of such a table.

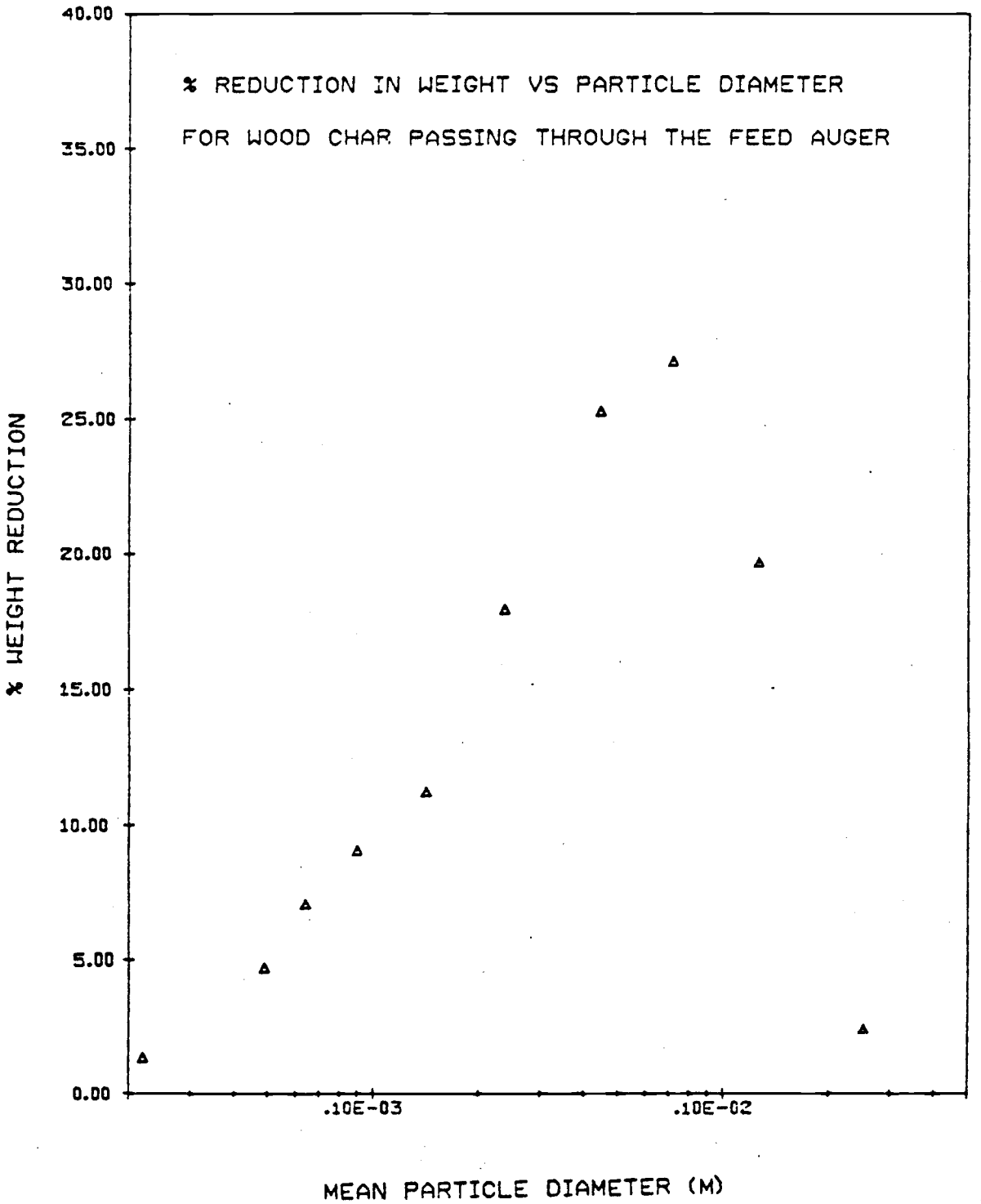

Figure A.2. The Degree of Size Reduction as a Function of Particle Size.

Table A.16. The % change in cumulative weight fraction for the mean particle sizes of the char samples.

Mean particle size ($M \times 10^{-6}$)	% Change in cumulative weight fraction
4013	0.
2664	2.
1500	13.
750	27.
375	21.
187.5	12.
94	9.
54	6.
22.5	2.

Example A.2 TRANSFORMATION OF A SIZE DISTRIBUTION.

From Table A.7 we can find cumulative weight fractions for the various size cuts for the char sample. Now using the values in Table A.16 we can estimate the cumulative weight fraction at the inlet of the reactor.

Mean particle size ($M \times 10^{-6}$)	Original cumulative weight fraction	$\Delta\%$	Transformed cum. wt. fr.	Wt fr
4013	1.0	0	1.	.0100
2664	.9700	+2	.9900	.0367
1500	.8223	+13	.9533	.3532
750	.3301	+27	.6001	.2787
375	.114	+21	.3214	.1529
187.5	.0485	+12	.1685	.0568
94.0	.0217	+9	.1117	.0432
54.0	.0085	+6	.0685	.0450
22.5	.0035	+2	.0235	.0235

The results for the complete set of char samples are presented in Tables A.17-A.19. It may be instructive to look at how much the size distribution changes. As fresh wood char enters the system it is partially crushed in the transport system and finally burnt in the reactor. The histograms for 3 representative runs are shown in Figures A.3-A.8. These figures show the size distributions of fresh char, char as it enters the reactor (predicted) and the ash produced by the combustion within the reactor.

Table A.17. Equivalent particle size distributions at the reactor inlet for char samples from runs P1-P4.

Run number	P1	P2	P3	P4
Mean particle size ($M \times 10^{-6}$)	Weight fraction			
4013	.0100	.0398	.0057	.0358
2664	.0367	.1293	.0921	.1830
1500	.3532	.3171	.3410	.3573
750	.2787	.2370	.2942	.1931
375	.1529	.1254	.1272	.1011
187.5	.0568	.0476	.0411	.0333
94.0	.0432	.0420	.0367	.0364
54.0	.0450	.0403	.0410	.0400
22.5	.0235	.0215	.0210	.0200
Total	1.	1.	1.	1.

Table A.18. Equivalent particle size distributions at the reactor inlet for char samples from runs CP1-CP4.

Run number	CP1	CP2	CP3	CP4
Mean particle size ($M \times 10^{-6}$)	Weight fraction			
4013	.0	.0054	.0125	.0066
2664	.0368	.0802	.2200	.0567
1500	.2810	.3288	.3493	.2855
750	.2935	.2580	.1681	.2926
375	.1630	.1623	.0973	.1357
187.5	.0704	.0541	.0445	.0612
94.0	.0605	.0399	.0431	.0657
54.0	.0569	.0442	.0438	.0650
22.5	.0379	.0271	.0214	.0310
Total	1.	1.	1.	1.

Table A. 19. Equivalent particle size distributions at the reactor inlet for char samples from runs C1-C10.

Run number Mean particle size (M x 10^{-6}	C1	C2	C3	C5	C6
	Weight fractions				
4013	0.	0.	0.	0.067	.0147
2664	0.	0.	.0247	.0686	.0883
1500	.1397	.2052	.1811	.3446	.3470
750	.2729	.2540	.2586	.2729	.2712
375	.1603	.1490	.1575	.1363	.1280
187.5	.0893	.0812	.0885	.0524	.0485
94.0	.0975	.0946	.0826	.0490	.0423
54.0	.2145	.1959	.1870	.0495	.0400
22.5	.0258	.0201	.0200	.0200	.0200
Total	1.	1.	1.	1.	1.

Run number	C7	C8	C9	C10
4013	.0659	.0482	.0564	.0341
2664	.2125	.1944	.1953	.1289
1500	.2939	.2973	.2558	.2554
750	.1812	.1996	.2220	.2510
375	.1018	.1089	.1184	.1233
187.5	.0429	.0416	.0428	.0539
94.0	.0418	.0417	.0424	.0629
54.0	.0400	.0433	.0432	.0576
22.5	.0200	.0250	.0237	.0329
Total	1.	1.	1.	1.

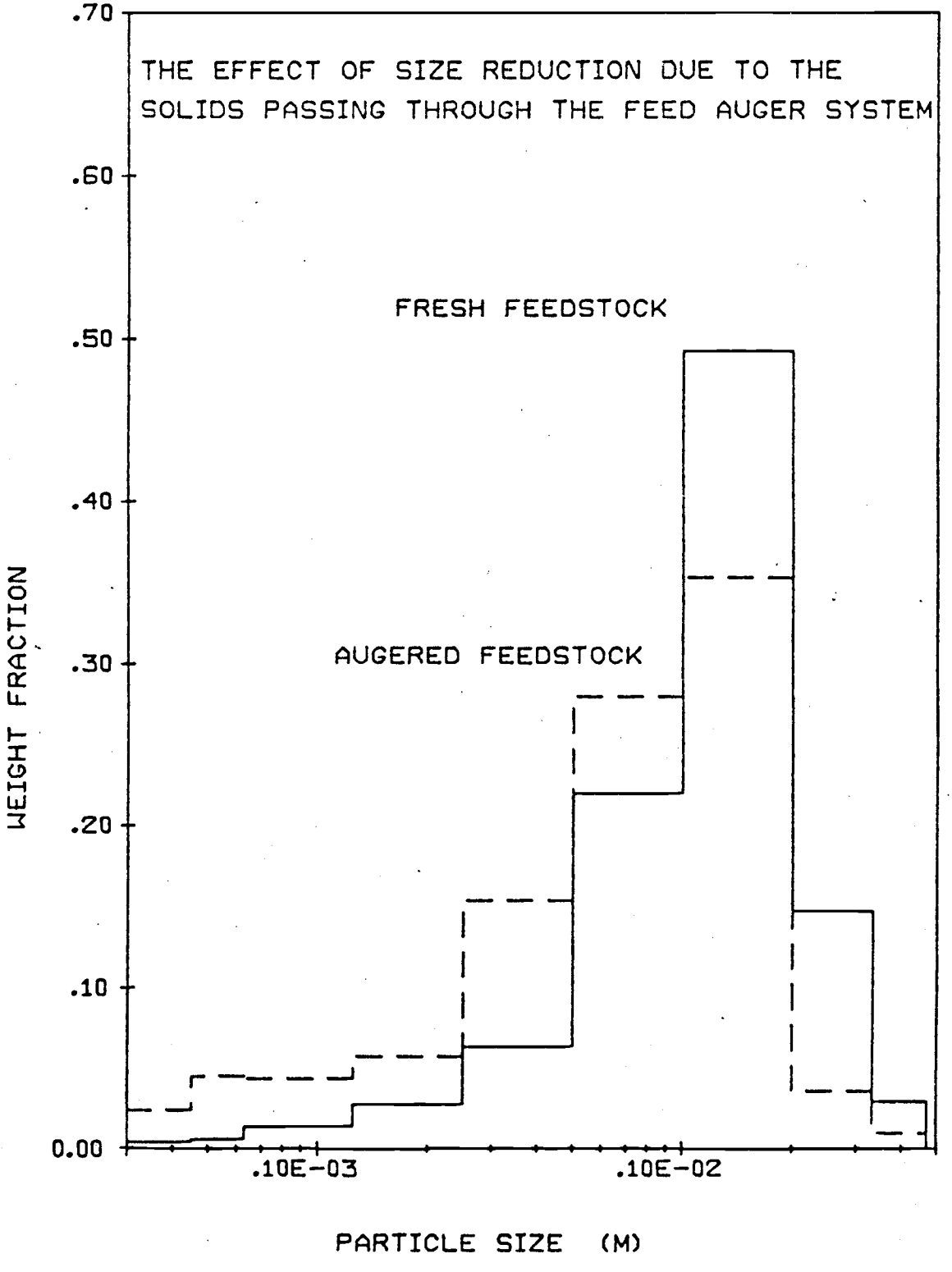

Figure A.3. Distributions for Run P1 (Feed Char).

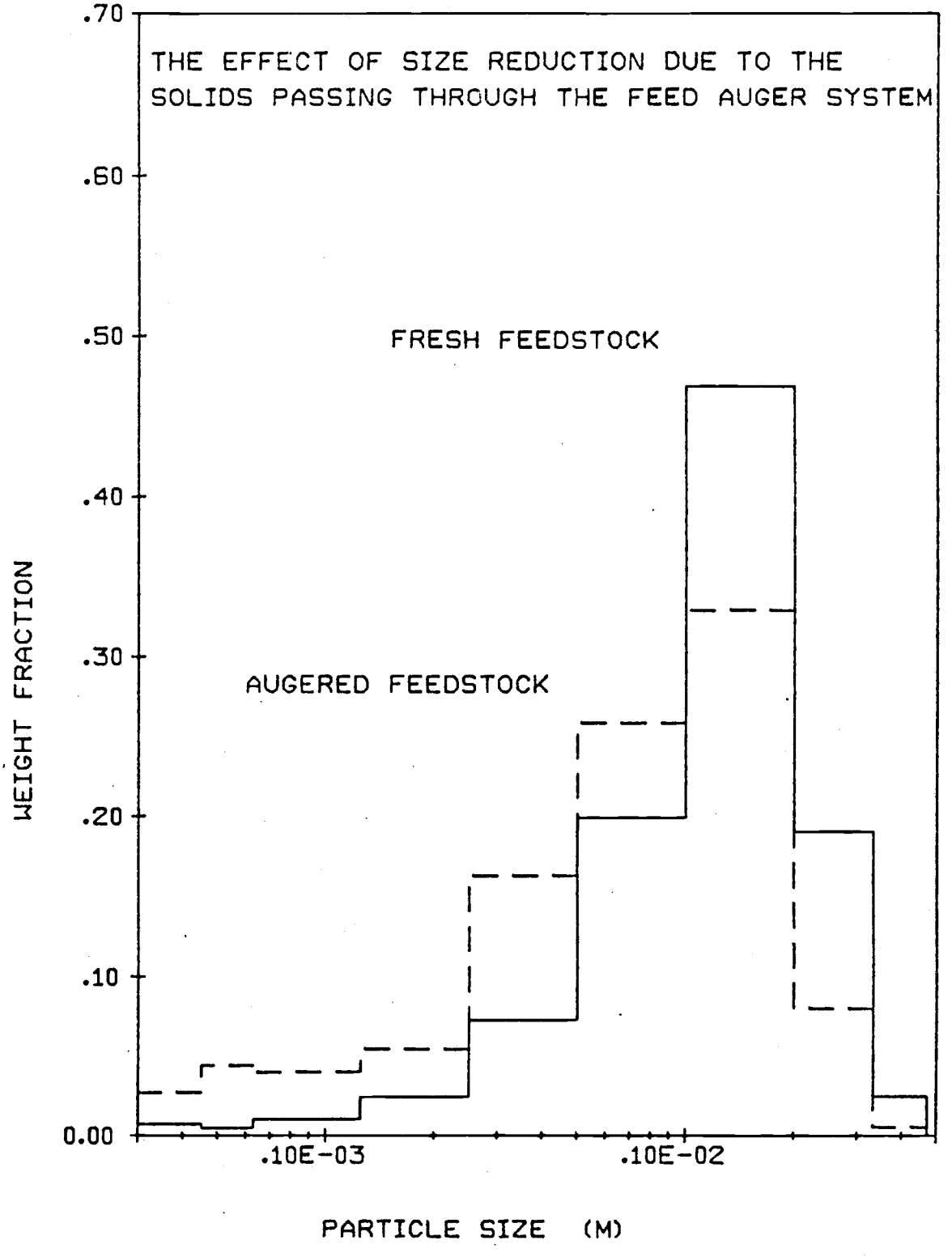

Figure A.4. Distributions for Run CP2 (Feed Char).

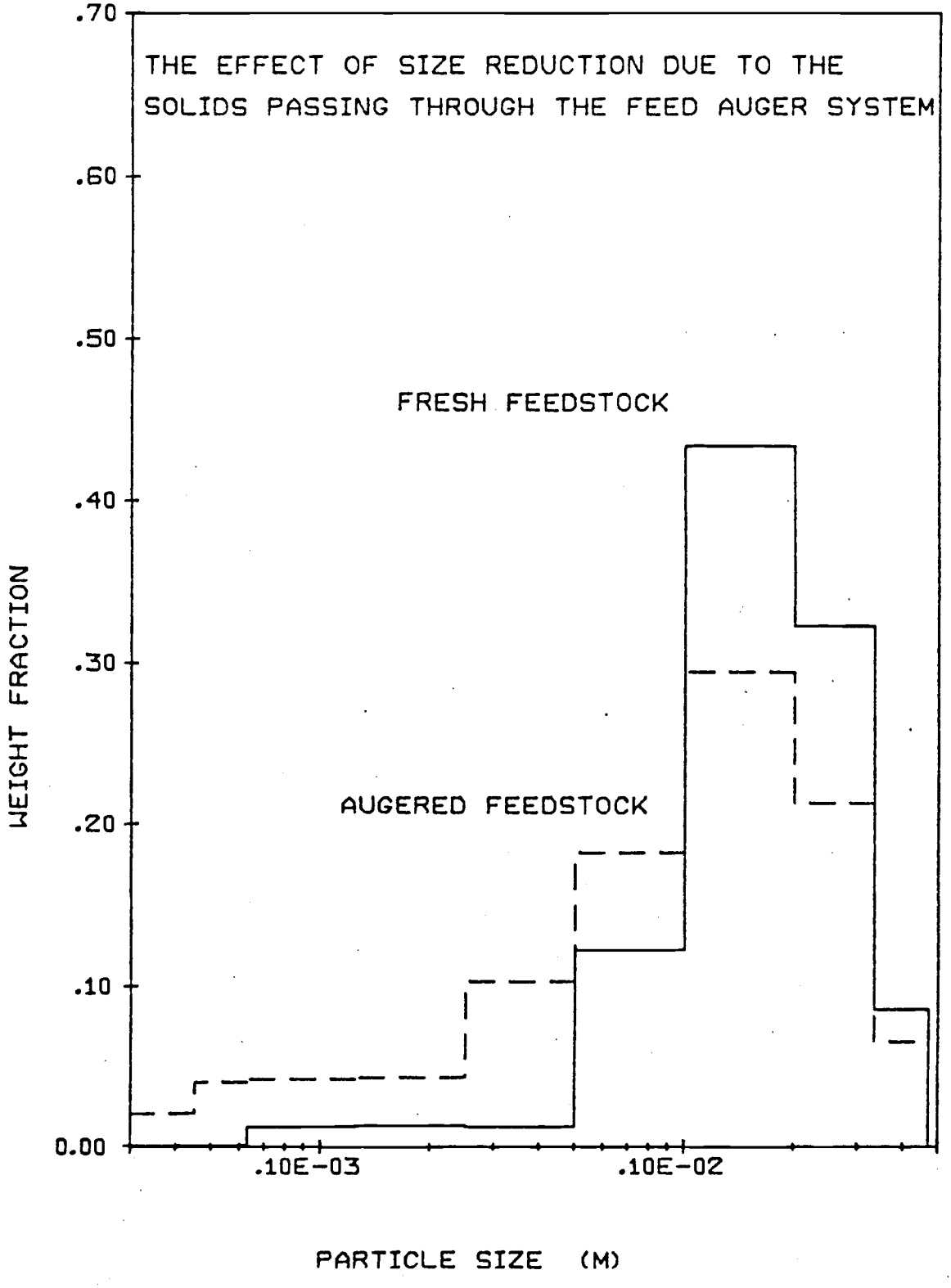

Figure A.5. Distributions for Run C7 (Feed Char).

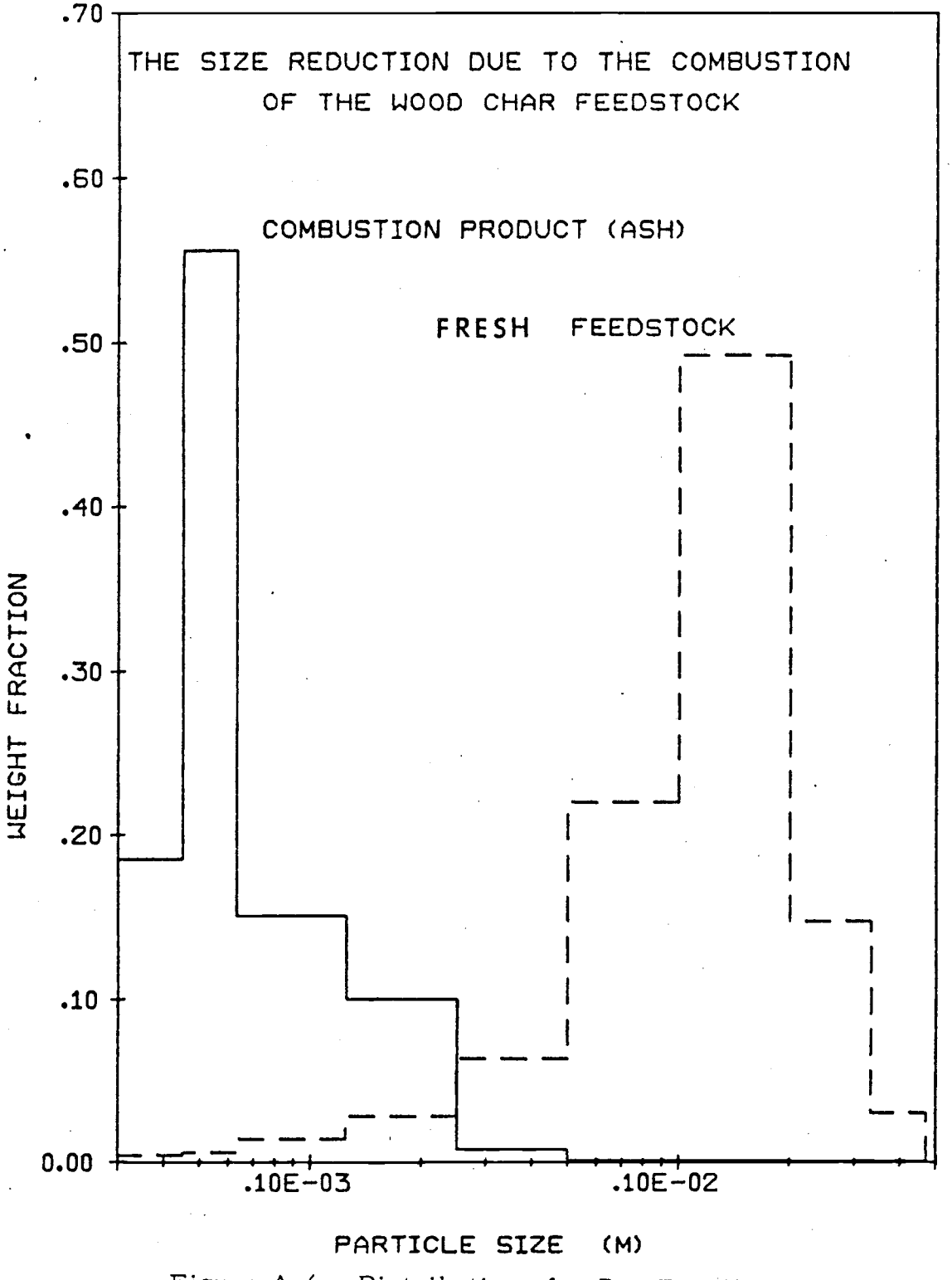

Figure A.6. Distributions for Run P1 (Char-Ash).

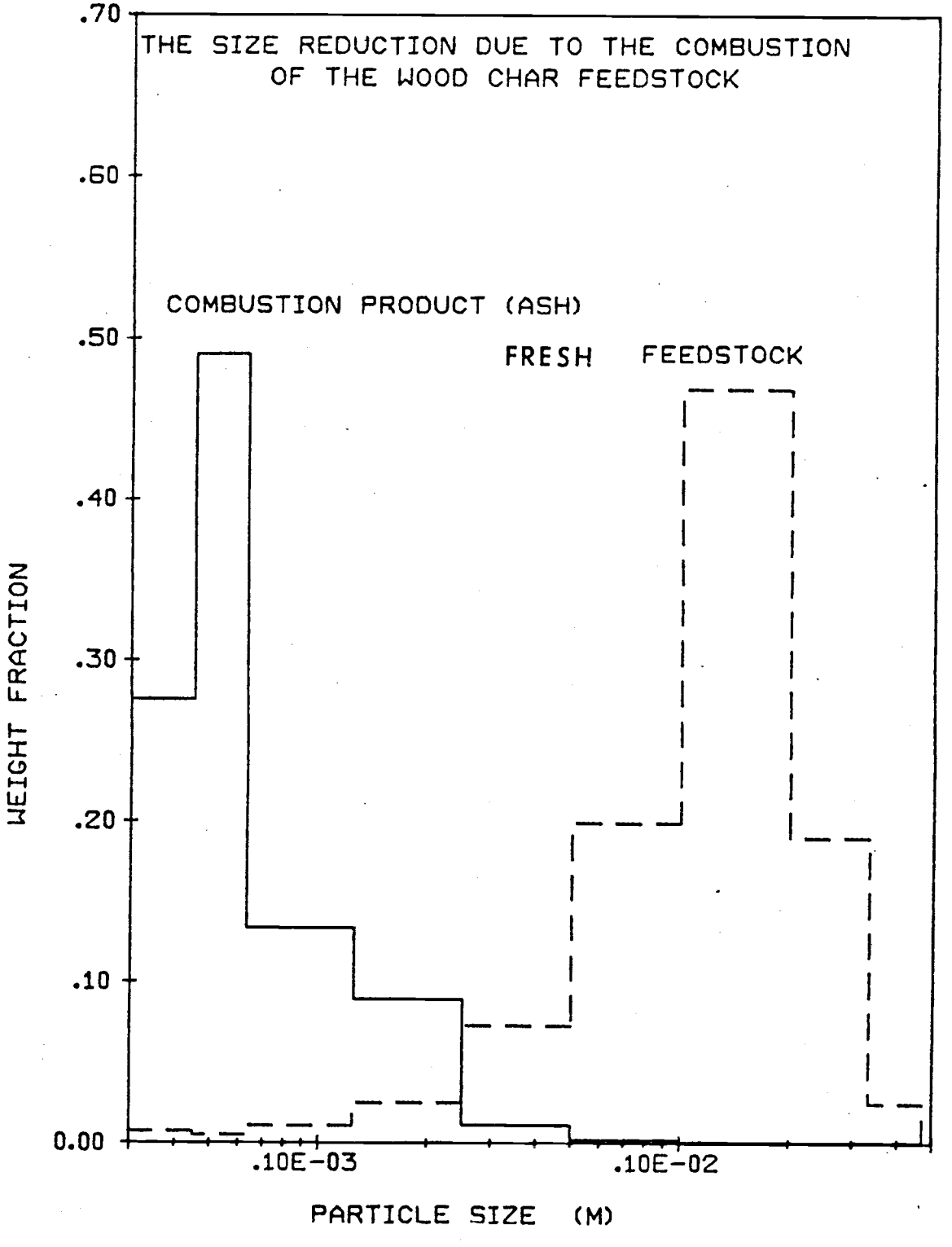

Figure A.7. Distribution for Run CP2 (Char-Ash).

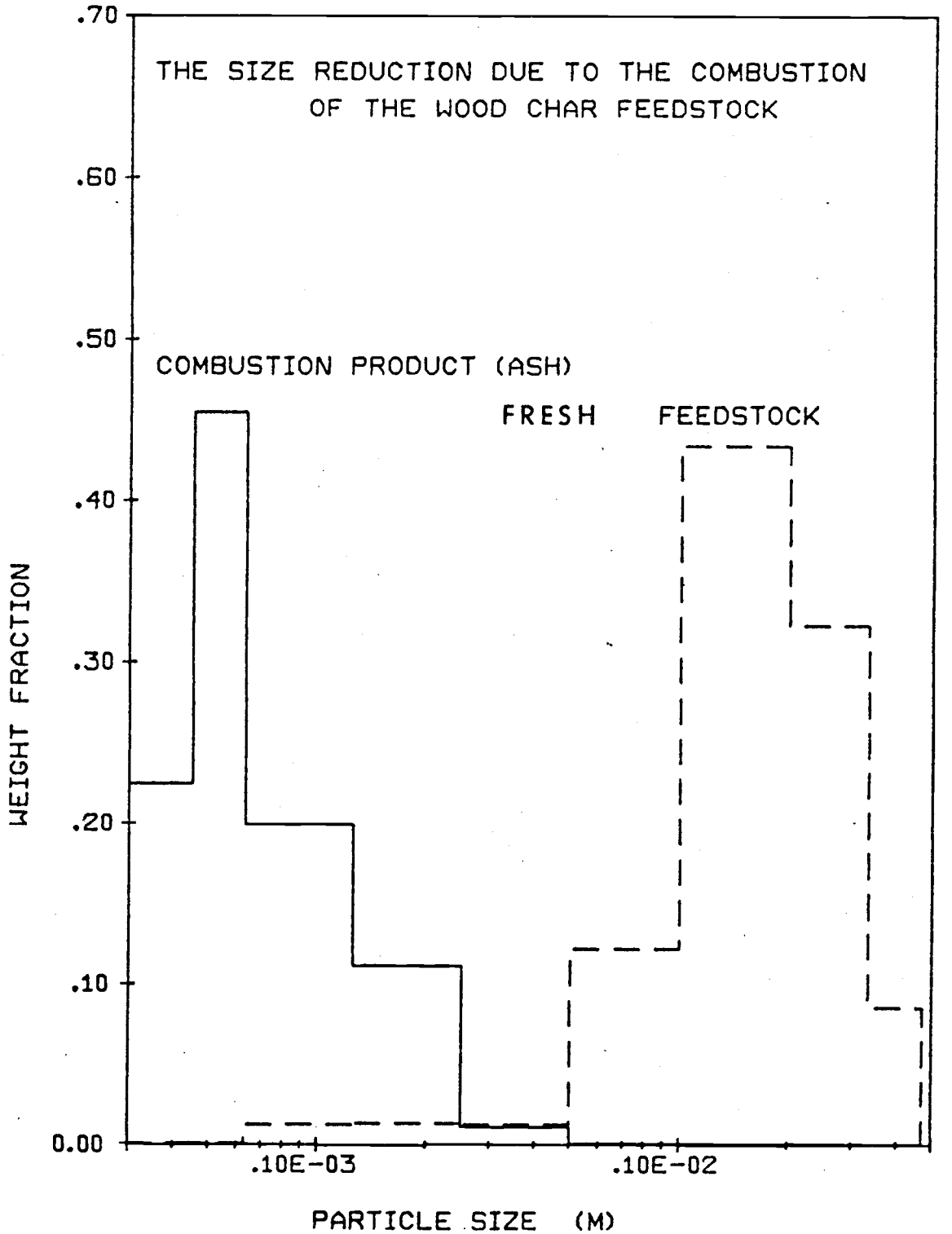

Figure A.8. Distributions for Run C7 (Char-Ash).

A NOTE ON MEAN PARTICLE SIZE

Throughout Appendix A both the terms mean particle size and mean particle diameter have been used. These terms are meant to mean the same thing, namely they refer to some characteristic length of a particle.

The term diameter may be confusing, since one normally associates the term diameter with a spherical object. This is not the case here.

Later on in the analysis it will become necessary, or at least convenient, to associate an equivalent spherical diameter with the particle. This is simply defined as

d_p = diameter of a sphere with the same volume as the particle considered.

This equivalent spherical diameter is not the same as the mean particle size but will be related by the following identity

$$d_p = A d$$

where d = mean particle size

and A = a constant for that particular particle.

The value of A may be above or below unity. However, for the work considered here the shape of most of the particles is well represented by a flat plate with a thickness about 1/6 of the characteristic length. This estimate is made from visual observation using an optical

microscope and corresponds to an A value of about 0.6.

The conversion value of 0.6 was used in the computer runs to estimate, from the mean particle size, the equivalent spherical diameter.

Further effects associated with shape and particle size are considered in Appendix E.

APPENDIX B

THE PHYSICAL PROPERTIES OF WOOD CHAR AND ASH PRODUCTS

THE PHYSICAL PROPERTIES OF WOOD CHAR AND THE ASH PRODUCED BY COMBUSTION

Since little information was available on the physical properties of the wood char feedstock used in all of the experimental test runs, it was decided to carry out some preliminary studies on such properties as apparent density, combustable content, etc.

The results obtained from these studies allowed certain correlations to be made which would be used in the computer simulated model of combustion.

THE APPARENT DENSITY OF WOOD CHAR

The wood char used as feedstock for the reactor is, what is commonly referred to as, fly ash. This fly ash was collected from the multiclone separators of a wood fired steam raising boiler, with the kind permission of WESTERN KRAFT INC. of Albany, Oregon.

The wood char is a light, fairly coarse material. It has low shear strength and is easily crushed in the hand.

The apparent density of a material has several meanings, however in this report the apparent density is defined as:

$$\text{Apparent Density} = \frac{\text{Weight of a Particle}}{\text{Volume of the Particle}}$$

Observations were made for various size particles using an optical microscope. It was found that for small sizes the shape of the

particles was fairly constant, however for the larger size particles there was a large variation in shape. In order to homogenize the shape of the larger particles the apparent density measurements were taken using the following procedure.

Firstly, the whole sample was screened and 3 representative sub samples were taken from each size cut (i.e., from each screen). The average size of the particles on a particular screen was approximated as the arithmetic mean aperture size of that screen and the screen immediately above it. Each sub sample was then crushed using a mortar and pestle and resieved through a #150 STANDARD TYLER SCREEN. The fraction of the sub sample which passed through the screen was used in the determination of apparent density.

This rather complicated procedure was adopted to try to avoid the errors involved in estimating a different average shape factor for each size cut.

Having obtained the desired sub sample the apparent density was found by measuring the volume of the sample using a graduated cylinder. The sample was gently vibrated in order to reorientate the particles and make them closely packed. The weight of this measured volume of sample was then taken and the voidage of the packed bed of particles in the measuring cylinder was estimated at 0.5 for all the runs. The apparent density was then calculated by:

$$\text{Apparent Density} = \frac{\text{Weight of Sample}}{\text{Volume Occupied x (1 - BED VOIDAGE)}}$$

The results for all the samples are given in Table B. 1 and the equation of the best straight line fit is also included. The results along with the correlation are plotted in Figure B. 1.

It can be seen from Figure B. 1 and Table B. 1 that the correlation and data are presented with the abscissa as $\log_{10}$ Particle Diameter. The word particle diameter is a little confusing here since a shape has not been assumed up to this point. Thus it may be instructive to think of the Particle Diameter as a characteristic dimension rather than to equate it with a spherical diameter.

The data is represented on a log scale for two reasons. Firstly, the correlation coefficient is greater for the log plot than for a non log plot. Secondly, the scatter about the correlation line for the log plot seems to be restricted to a uniform band. This is consistent with the assumption that the scatter is due to random error. For the non log plot this random error assumption looks suspect.

Table B.1. The variation of apparent density with particle size.

Mean particle size ($M \times 10^{-6}$)	Apparent density (kg/M^3)		
1290	402.8	478.3	452.2
1000	465.8	426.6	497.0
710	431.3	385.3	383.5
500	357.6	349.6	392.0
360	404.4	462.9	486.1
250	642.9	614.9	604.9
180	676.9	700.4	700.9
126	580.1	668.3	633.6
89	692.5	693.8	670.5
64	742.1	807.2	777.9
49	725.6	759.7	799.6
24	791.2	764.6	759.8

Correlation is of the form $\text{Density}^* = A + B \log_{10} \overline{D}_p$

where $A = -428.1 \quad kg/M^3$

$B = -277.8 \quad kg/M^4$

*This is only really correct for the particle range (1290 ~ 24) μ however it was used to extrapolate to 3000 μ.

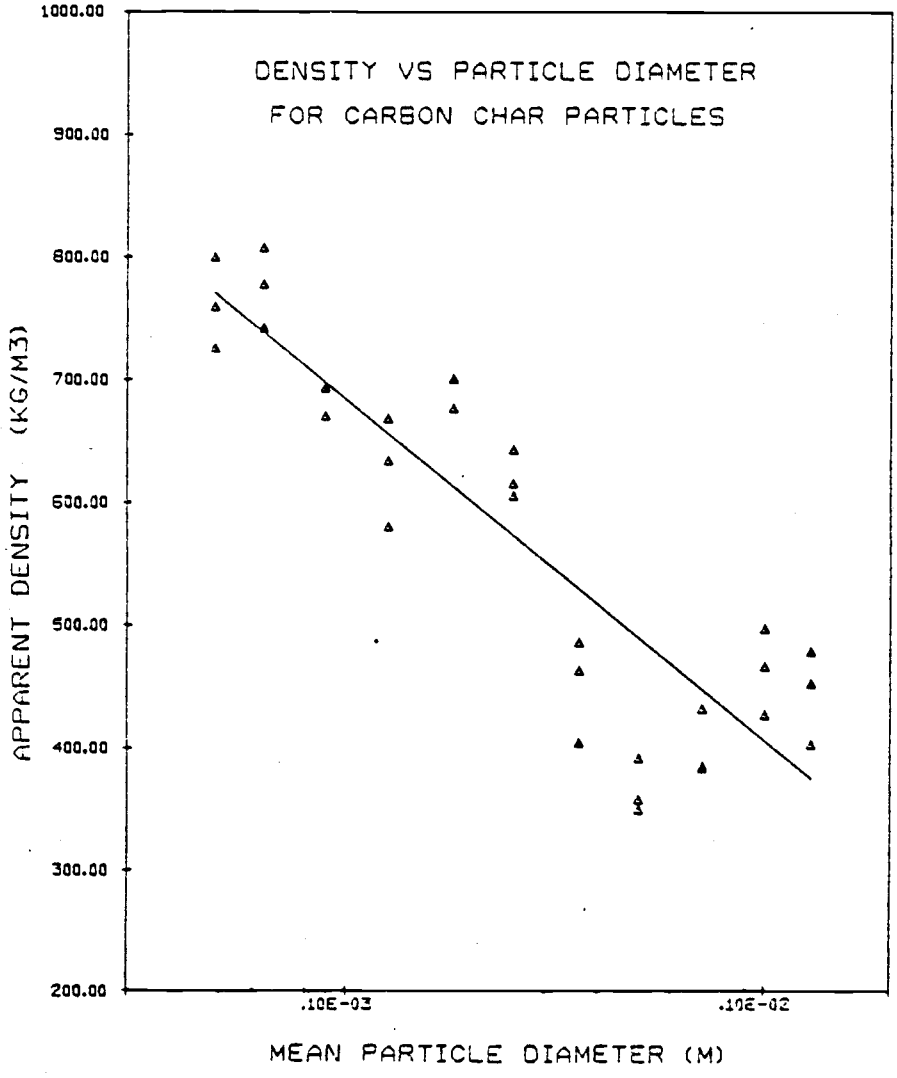

Figure B.1. Apparent Density Variation with Particle Size.

INTERNAL SURFACE AREA OF WOOD CHAR

The rate of reaction within a certain temperature range may be increased significantly by the presence of an appreicable internal surface area. For this reason the surface area for various size particles was investigated.

The internal surface area for various char samples was investigated by the low temperature physi-adsorption of nitrogen gas (i.e., at the normal boiling point of nitrogen 78 K.). The method consisted of placing a known weight of sample, of given size, in a small tin foil bucket which was then suspended from a very sensitive quartz spring. The whole system was sealed and then evacuated to less than 150 pascal absolute pressure. After equilibrium was attained the vertical position of the spring was measured. This was achieved by projecting the image of the spring onto a screen, since the spring is premarked the image of one of these marks can be drawn on the screen.

A small quantity of nitrogen is then introduced in the system which is again allowed to attain equilibrium. The vertical displacement of the spring, due to nitrogen adsorption, is then measured by again projecting the image of the spring onto the screen. The new position of the mark on the spring is recorded and the difference between the two marks on the screen is the displacement. Thus, by knowing the spring constant the change in weight of the sample can be calculated,

If also the pressure of nitrogen is recorded then the point on the adsorption isotherm may be plotted. By repeatedly introducing nitrogen and measuring the change in weight of the sample, the isotherm for the adsorption process can be plotted.

The isotherms for 25 different char samples are plotted in Figures B.2-B.5. The results are tabulated in Tables B.2 and B.3. The isotherms are presented as the weight of nitrogen on the sample divided by the weight of the sample versus the pressure (partial pressure) of nitrogen.

It can be seen that for all the isotherms there is a sharp knee in the curve, this knee is often referred to the "B" point. At the "B" point the surface of the sample has on it a monomolecular layer of nitrogen. Thus, the internal surface area may be evaluated from this point.

The "B" points and calculated surface areas are given in Tables B.4 B.5 and the results plotted as a function of mean particle diameter (logarithmic scale) in Figure B.6.

In Figure B.6 there are two points labelled outliers - these are results which seem not to follow the general trend of the plot. It was noticed, however, that during the experimental determination of surface area the sample buckets were rather high for these 2 runs and that they were close to the top of the liquid nitrogen bath in which

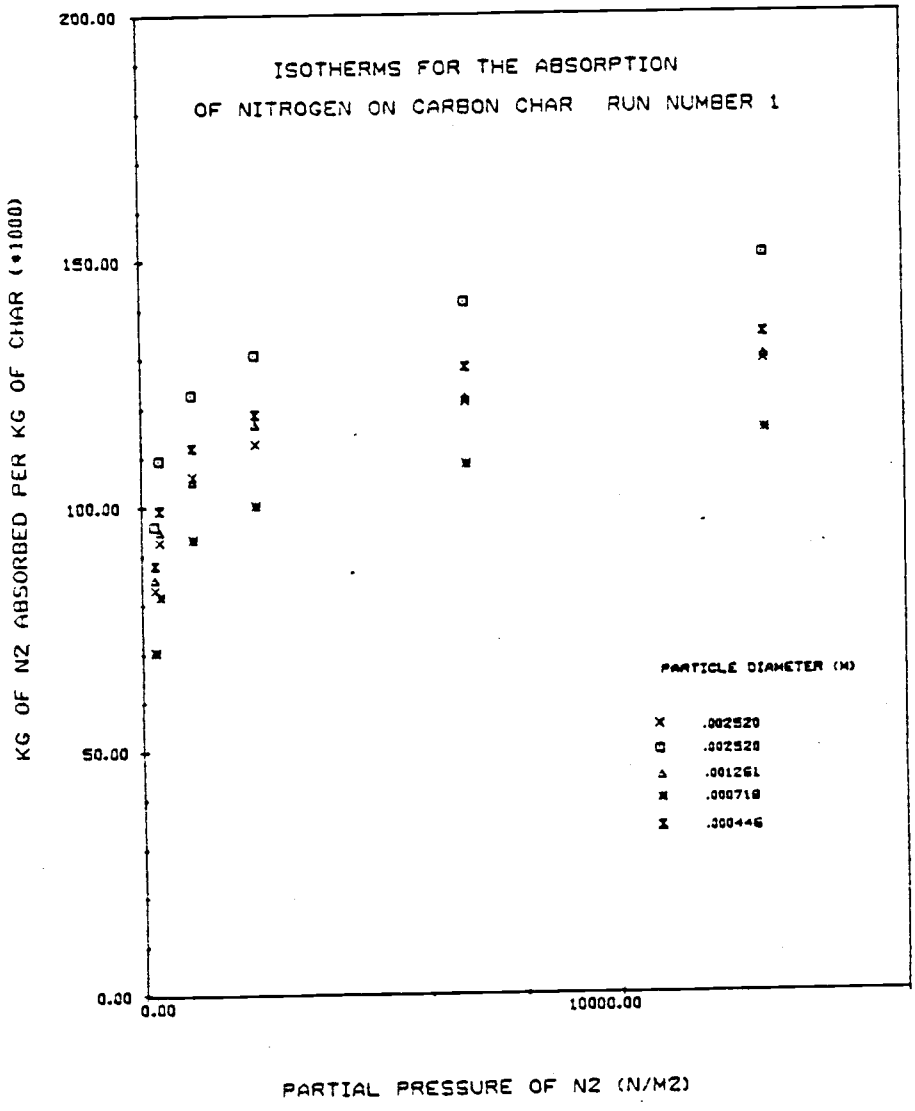

Figure B.2. Adsorption Isotherms for Run 1.

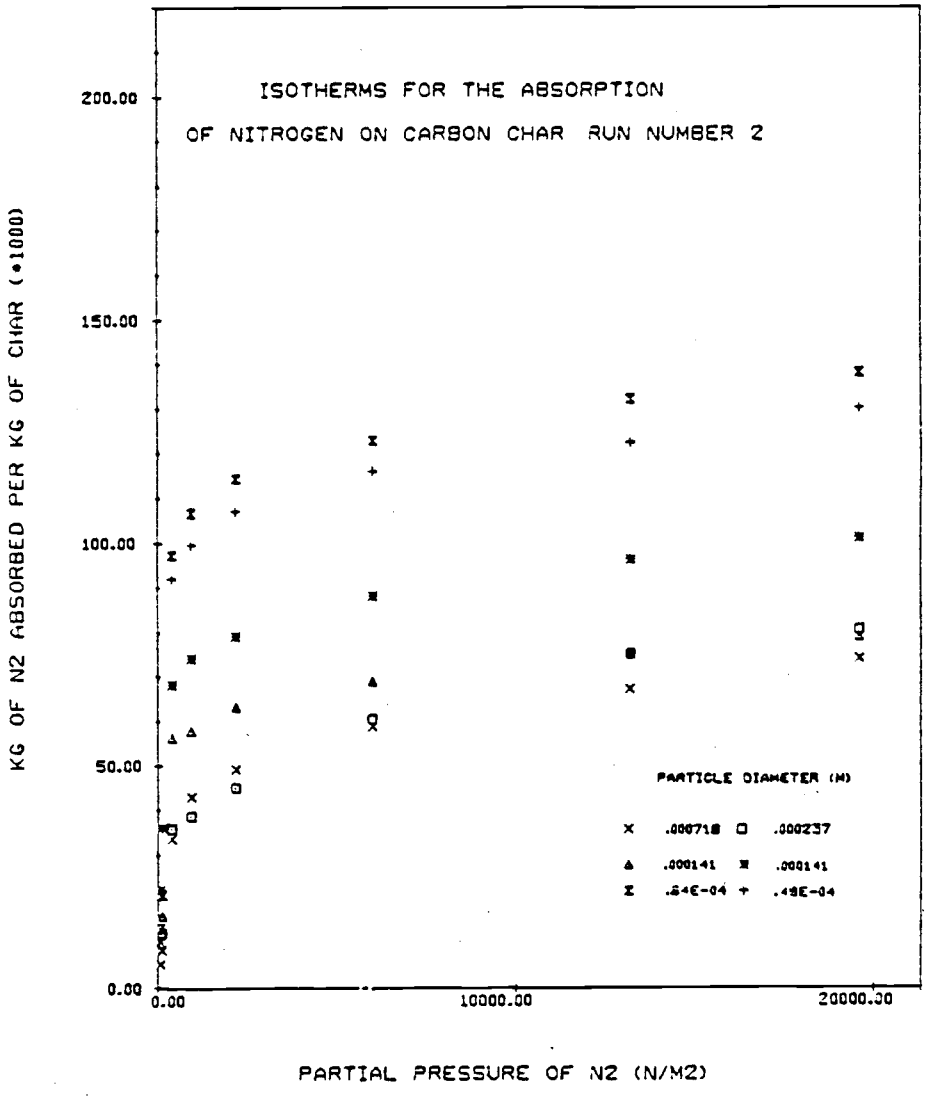

Figure B.3. Adsorption Isotherms for Run 2.

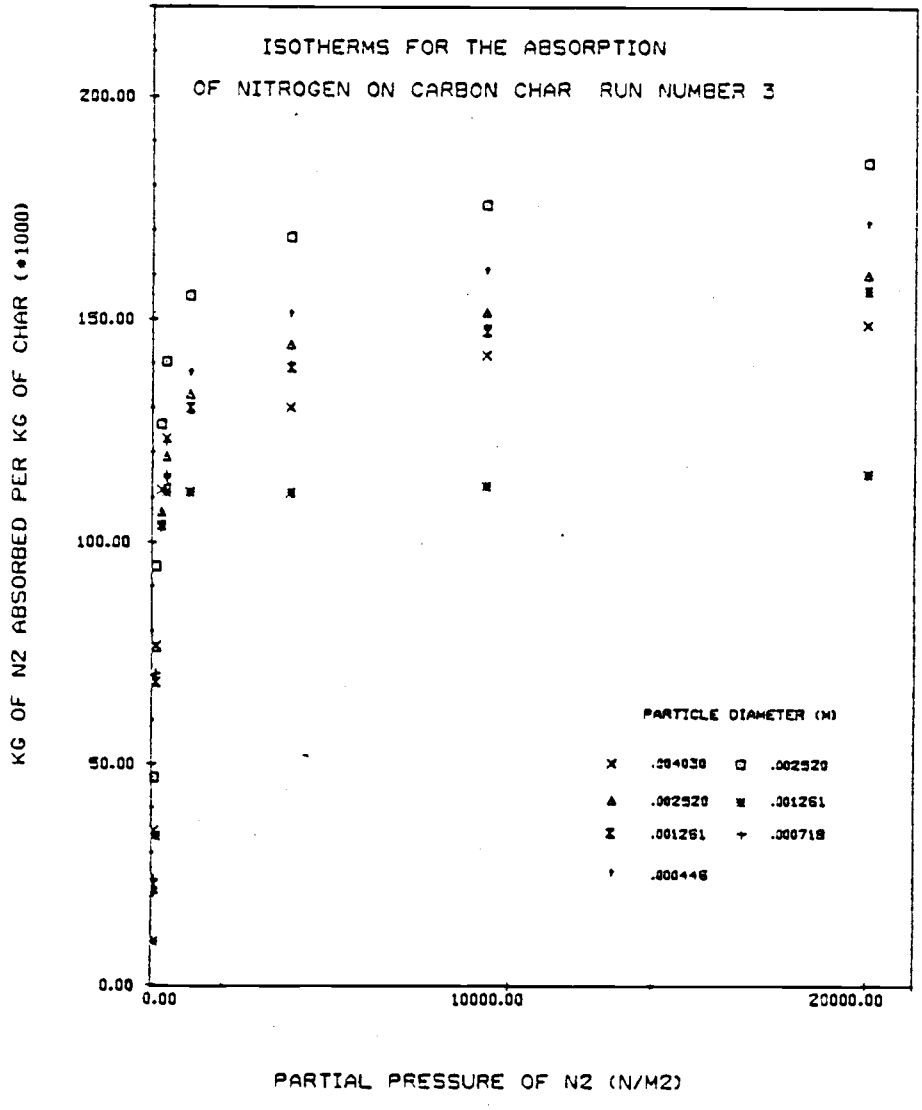

Figure B.4. Adsorption Isotherms for Run 3.

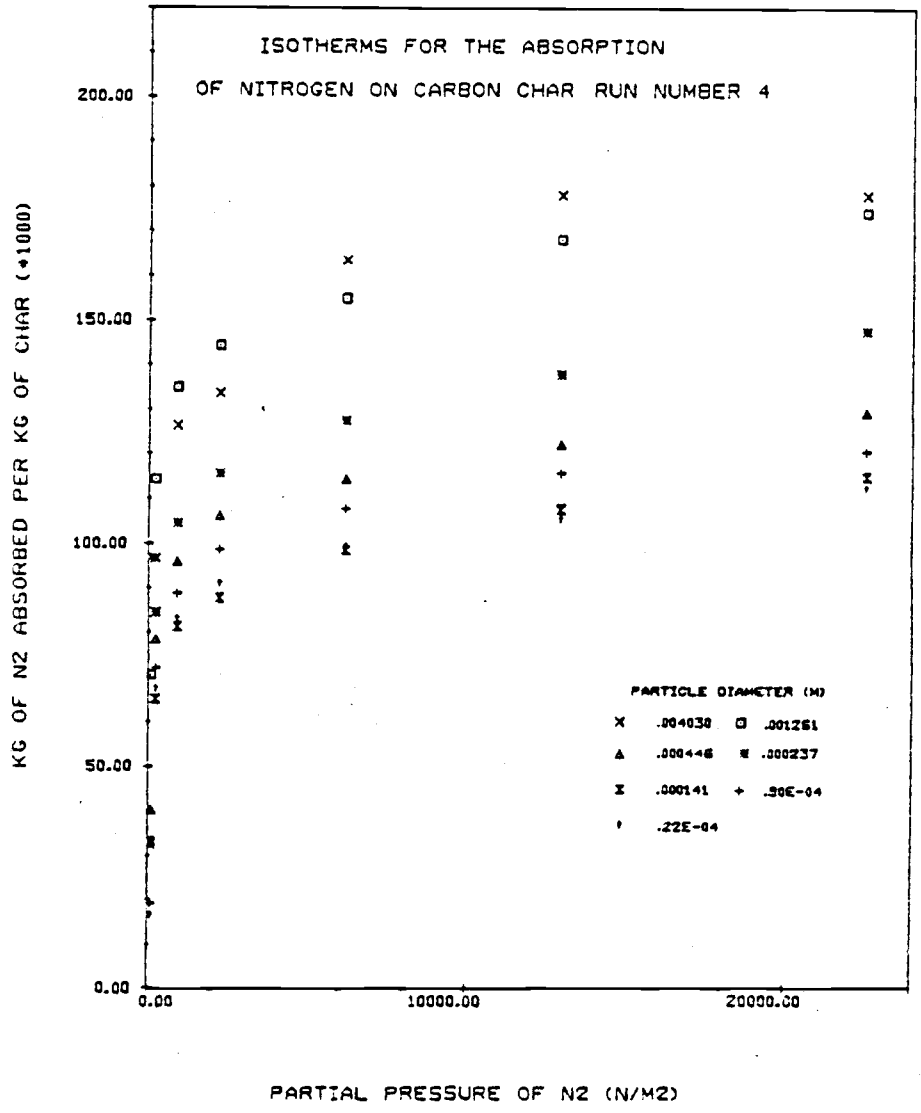

Figure B.5. Adsorption Isotherms for Run 4.

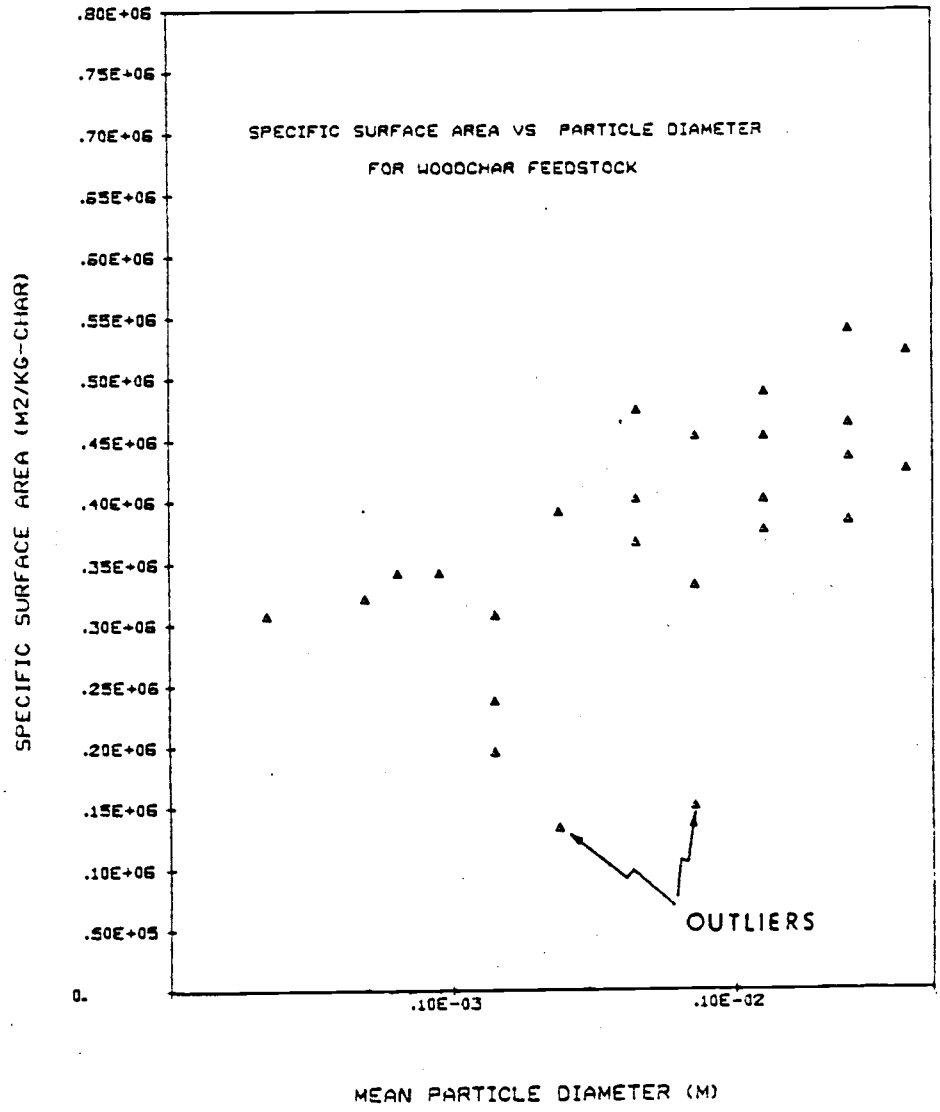

Figure B.6. Scatter Plot for the Variation of Surface Area with Particle Size.

all samples must sit.

By the end of the run, due to some of the liquid nitrogen evaporating, the samples were no longer sitting in the low temperature bath and for this reason it was decided to ignore these two points. The corrected plot along with the best fit straight line for the remaining points is given in Figure B. 7. The equation of the straight line correlation is also given at the bottom of Table B. 5.

The calculation of internal surface area from an isotherm is a straight forward procedure. An example of such a calculation is given below.

EXAMPLE B. 1

CALCULATION OF INTERNAL SURFACE AREA

For run number 1 the isotherms are plotted in Figure B. 2. The "B" point or knee of the curve for the 446 micron sample was estimated as:

$$\text{"B" point} = .115 \frac{\text{kg-}N_2}{\text{kg- char}}$$

Now 1 kg of nitrogen has $6.023 \times 10^{26}/28$ molecules and 1 nitrogen molecule covers a surface area of 16. 2 square angstrom.

$$\therefore \text{ 1 kg of nitrogen has a S. A.} = \frac{6.023 \times 10^{26} \times 16.2 \times 10^{-20}}{28}$$

$$= 3.4847 \times 10^{6} \text{ m}^{2}$$

At the "B" point we have a monolayer of nitrogen and hence the area

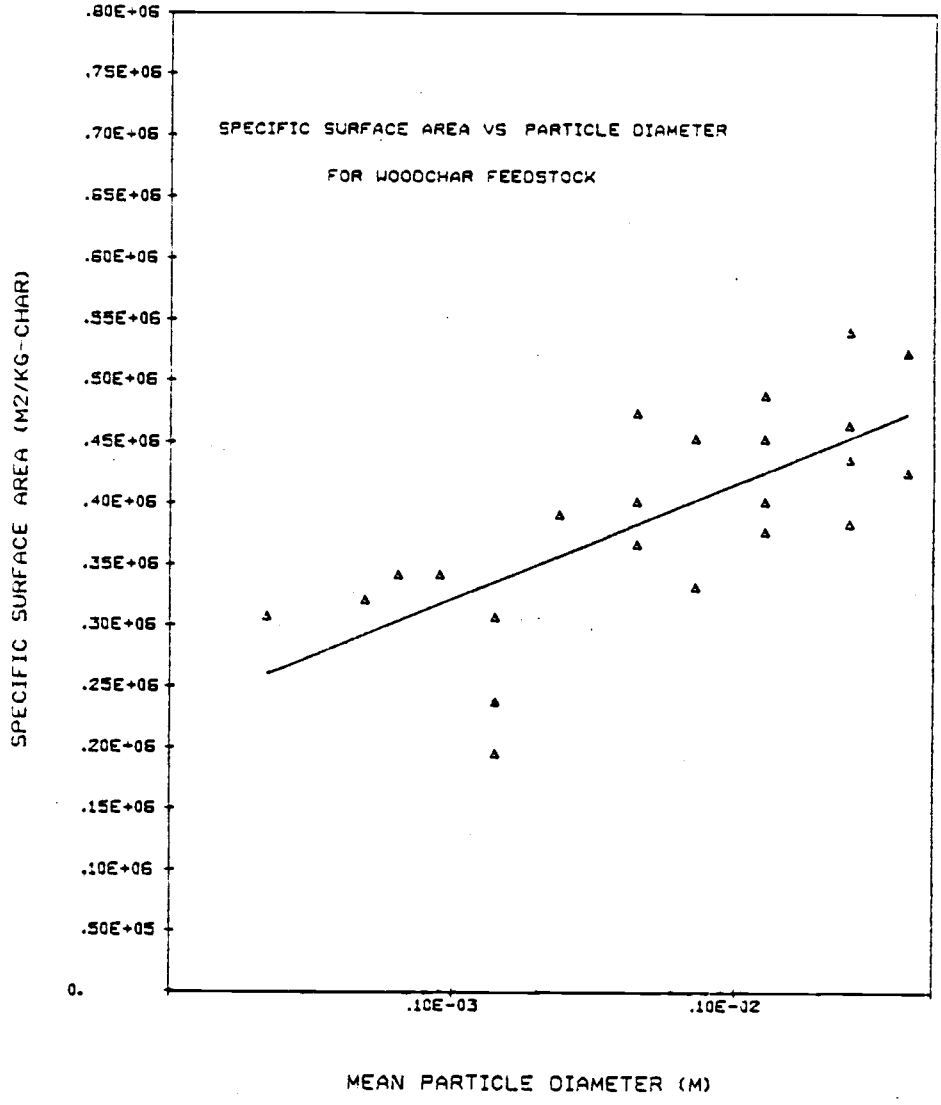

Figure B.7. Correlation between Surface Area and Particle Size.

covered by nitrogen molecules is the same as the internal surface area.

$$\therefore \text{ Surface Area of Char } = .115 \times 3.4847 \times 10^6 \ M^2/\text{kg-char}$$

$$= .40074 \times 10^5 \ M^2/\text{kg-char}$$

Table B.2. Adsorption isotherms for run 1 + 2.

Run 1						
Pressure of nitrogen $(N/M^2) \times 10^3$	.27	0.37	1.07	2.40	6.80	13.06
Mean particle size $(M \times 10^{-6})$			Wt. of nitrogen/wt. of sample $(kg\text{-}N_2/kg\text{-char}) \times 10^{-3}$			
2250	82.8	92.7	106.0	112.6	120.9	129.2
2520	95.9	109.3	122.6	130.6	141.3	150.6
1260.5	85.0	95.0	105.0	116.7	121.7	130.0
718.0	70.2	81.4	93.2	100.1	108.2	115.0
446.0	87.9	99.2	111.9	118.6	127.9	134.6

Run 2								
Pressure of nitrogen $(N/M^2) \times 10^3$	.08	.13	.40	.93	2.19	6.00	13.20	19.54
Mean particle size $(M \times 10^{-6})$			Wt. of nitrogen/wt. of sample $(kg\text{-}N_2/kg\text{-char}) \times 10^{-4}$					
718.0	5.5	8.6	33.5	42.8	49.1	58.8	67.0	74.0
237.0	11.9	12.4	35.7	38.5	44.9	6-.4	75.1	80.6
141.0	10.1	16.1	56.3	57.8	63.1	68.9	74.9	79.0
141.0	22.0	36.0	68.0	74.0	79.0	88.0	96.0	101.0
63.5	13.3	20.9	97.0	106.6	114.2	122.8	132.1	137.9
48.5	21.7	35.7	91.7	99.4	107.0	115.9	122.3	130.0

Table B.3. Adsorption isotherms for runs 3 + 4.

Run 3								
Pressure of nitrogen $(N/M^2) \times 10^3$	0.80	0.13	0.27	0.40	1.07	3.87	9.33	20.00
Mean particle size $(M \times 10^{-6})$	Wt. of nitrogen/wt. of sample $(kg\text{-}N_2/kg\text{-char}) \times 10^{-3}$							
4030	34.9	76.7	111.5	123.1	130.1	130.1	141.7	148.9
2520	46.7	94.4	126.2	140.2	155.2	168.3	175.7	185.1
2520	21.5	70.2	106.8	119.0	133.0	144.2	151.7	160.2
1260.5	9.8	33.7	103.8	110.9	110.9	110.9	112.3	115.1
1260.5	22.6	68.3	103.6	113.5	130.0	138.9	147.1	156.5
718.0	23.8	70.3	103.0	114.9	128.8	139.7	148.6	156.5
446.0	21.3	69.3	107.5	122.6	138.6	151.9	161.7	172.3

Run 4							
Pressure of nitrogen $(N/M^2) \times 10^3$	0.11	0.24	0.91	2.24	6.18	12.93	22.53
Mean particle size $(M \times 10^{-6})$	Wt. of nitrogen/wt. of sample $(kg\text{-}N_2/kg\text{-char}) \times 10^{-3}$						
4030	96.5	96.5	126.2	133.6	163.3	178.2	178.2
1260.5	70.2	114.1	134.8	144.2	154.9	168.0	174.3
446.6	40.0	78.4	95.9	106.3	114.2	122.1	129.6
237.6	32.3	84.4	104.6	115.4	127.5	137.8	147.7
141.0	32.8	64.9	81.3	87.7	98.4	107.7	116.9
89.5	18.9	71.8	88.8	98.6	107.7	115.6	120.5
22.5	17.0	67.9	83.7	91.6	100.1	106.3	113.1

Table B.4. 'B' points and calculated internal surface areas for runs 1 + 2.

Run 1

Mean particle size ($M \times 10^{-6}$)	'B' Point ($kg\text{-}N_2/kg\text{-}char) \times 10^{-3}$	Surface area ($M^2/kg\text{-}char) \times 10^5$
2520	125	4.3559
2520	110	3.8332
1260.5	115	4.0074
718.0	95	3.3105
446.0	115	4.0074

Run 2

Mean particle size ($M \times 10^{-6}$)	'B' Point ($kg\text{-}N_2/kg\text{-}char) \times 10^{-3}$	Surface area ($M^2/kg\text{-}char) \times 10^5$
718.*	43	1.4984
237 *	38	1.3242
141	56	1.9515
141	68	2.3696
64	98	3.4150
49	92	3.2060

*Disregarded in final analysis. See text.

Table B.5. 'B' Points and internal surface areas for runs 3 + 4.

Run 3

Mean particle size ($M \times 10^{-6}$)	'B' Point ($kg\text{-}N_2/kg\text{-}char$) $\times 10^{-3}$	Surface area ($M^2/kg\text{-}char$) $\times 10^5$
4030	122	4.2514
2520	155	5.4013
2520	133	4.6347
1261	108	3.7635
1261	130	4.5302
718	130	4.5302
446	136	4.7392

Run 4

Mean particle size ($M \times 10^{-6}$)	'B' Point ($kg\text{-}N_2/kg\text{-}char$) $\times 10^{-3}$	Surface area ($M^2/kg\text{-}char$) $\times 10^5$
4030	150	5.2271
1261	140	4.8786
446	105	3.6590
237	112	3.9029
141	88	3.0666
90	98	3.4150
22.5	88	3.0666

The correlation for internal surface area is

$$S.A. = A + B \log_{10} D_p \quad \text{where} \quad A = 69.8666 \times 10^4 \frac{M^2}{kg}$$

$$B = 9.4250 \times 10^4 \frac{M}{kg}$$

NON-COMBUSTIBLE CONTENT OF WOOD CHAR AND ASH PRODUCT

The non-combustible inorganic content of the wood char and ash samples, from the test runs, were evaluated.

The procedure used was similar to that suggested by the AMERICAN STANDARDS FOR TESTING OF MATERIALS (ASTM). A representative sample was taken and burnt in a muffle furnace, after suitable drying. The temperature was set at 973 K and the samples in crucibles were kept in the furnace for 6-10 hours until all combustible content was removed.

The results for both char and ash are given in Table B.6.

Table B.6. The non-combustible inorganic content for wood char and ash product for the various test runs.

Run #	Wood char % incombustible content			Ash product % incombustible content		
			Ave.			Ave.
P1	10.1	32.2	21.2	95.1	95.1	95.1
P2	24.0	23.9	24.0	95.2	92.8	94.0
P3	15.8	9.3	12.6	96.8	94.3	94.6
P4	20.9	22.5	21.7	95.3	88.3	91.8
CP1	12.0	15.7	13.9	95.6	95.8	95.7
CP2	12.8	8.6	10.7	96.2	90.0	93.1
CP3	18.2	4.1	11.2	95.4	96.6	96.0
CP4	13.9	21.3	17.6	94.1	94.0	94.1
C1	22.1	36.6	29.4	96.3	96.3	96.3
C2	23.1	34.1	28.6	93.2	93.4	93.3
C3	5.6	5.8	5.7	92.7	92.8	92.8
C5	8.8	20.0	14.4	93.8	93.7	93.8
C6	2.5	14.0	8.3	94.9	94.9	94.9
C4	5.2	7.1	6.2	95.2	95.1	95.2
C8	17.1	15.6	16.4	93.5	94.4	96.0
C9	25.4	22.2	23.8	89.7	89.8	89.8
C10	8.1	30.9	19.5	95.4	95.0	95.2

MOISTURE CONTENT OF WOOD CHAR

The moisture content for the wood char samples was found by placing a premeasured sample in a crucible and heating to 380 K for approximately 2 hours. The loss in weight was recorded and the moisture content calculated. The results are given in Table 8.7.

An average value for moisture content was calculated for each series of test runs (i.e., P, CD, and C series) and this mean value was used in the subsequent calculations.

Table B.7. The moisture content analysis for wood char feed stock.

Run #	% Loss in weight		Average
P1	4.1600	4.8940	4.5270
P4	5.3877	5.8360	5.6119
CP1	6.1503	5.8740	6.0122
CP3	3.4777	4.0120	3.7449
C3	3.2170	2.3539	2.7855
C9	6.5100	7.5873	7.0487
C10	4.9512	4.6570	4.8041
C12	4.7002	4.1936	4.4469

Average value for P series = 5.0695

CP series = 4.8786

C series = 4.7713

BULK DENSITY OF WOOD CHAR

The calibration of the solids feed system to the reactor will be discussed later. However, in order to find out how much feed material is arriving at the reactor inlet the "Bulk" density of the wood char must be found.

The term "Bulk" referred to here is simply the weight of a given volume of char. It is easily measured by filling a container of known volume with char and calculating the weight of char by difference. The "Bulk" density is then defined as the weight of char divided by the volume.

The bulk density of the char at the reactor inlet was calculated for several different samples and the results are given in Table B.8.

Table B.8. Bulk density measurement for wood char feed stock.

Run #	Wt. collected (kg)	Volume M^3	Density kg/M^3
1	2.4806	.02047	121.20
2	2.5373	"	123.97
3	2.6933	"	131.59
4.	2.3814	"	116.35
5	2.4806	"	121.20
6	2.7201	"	132.90
7	2.3991	"	117.22
8	2.8563	"	139.56
9	2.2111	"	108.03
10	2.3866	"	116.60
		Σ	1228.62
		$\overline{X}$	122.86 kg/m^3

Average bulk density of wood char = 122.86 kg/m^3

APPENDIX C

CALIBRATION OF THE SOLIDS AND AIR FEED SYSTEMS

SOLIDS FEED SYSTEM

The solids feed system is shown diagrammatically in Figure C.1.

The solids feed rate to the reactor is controlled by varying the speed of rotation of auger 2. The star valve and augers 3 and 4 are kept running at a constant speed during operation. This means that whatever solids auger 2 transports to the star valve, will be fed to the reactor.

The relay auger 1 keeps the supply bin fed with wood char and is set to operate automatically if the depth of solids in the bin falls below a certain level. Although the automatic operation is used under normal conditions it may be overridden and the whole supply process controlled manually.

The variable speed auger 2 is controlled by changing the motor current via a potentiometer mounted on the control panel. In order to convert setting on the potentiometer (scale 0-10) to volumetric flow rates of char, it was necessary to calibrate the solid feed system.

The calibration was achieved by measuring the time required to fill a certain volume, with char from the base of the reactor. The volumetric flow rate was then calculated and plotted against the potentiometer setting. The results are presented in Table C.1 and Figure C.2. The x-axis for Figure C.2 is labelled % of maximum and thus a reading of 30%, say, corresponds to a potentiometer setting of 3.

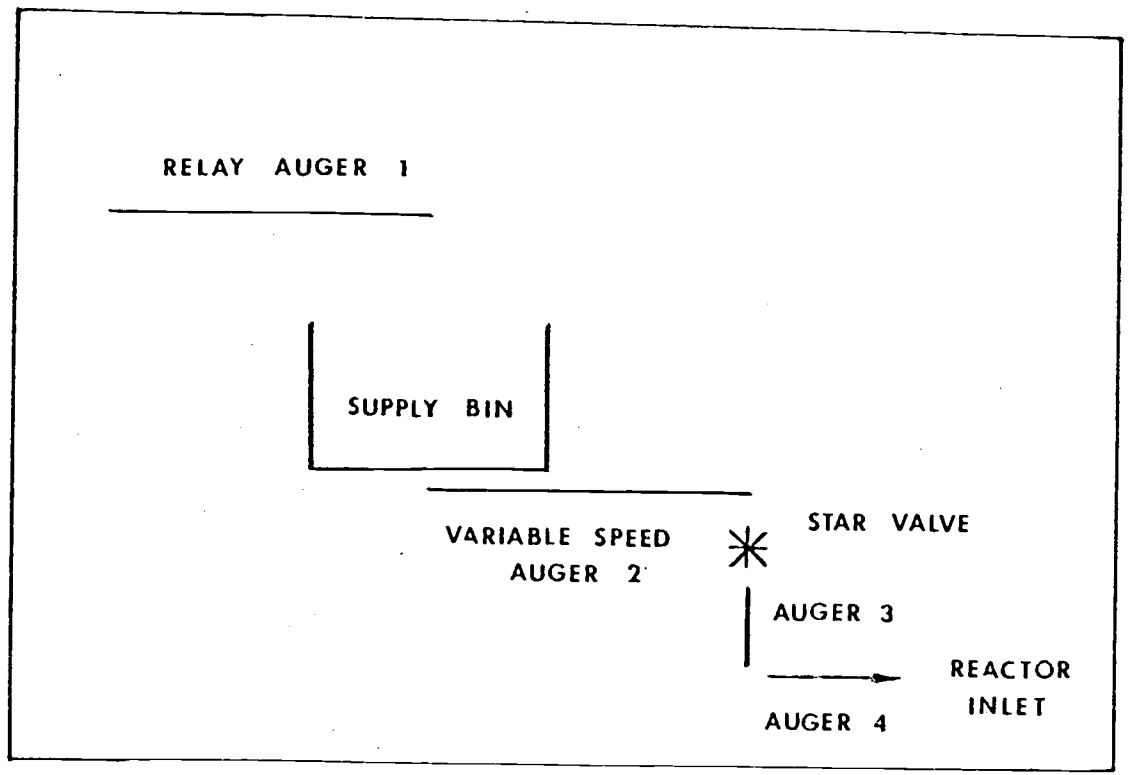

Figure C.1 SCHEMATIC DIAGRAM OF THE SOLIDS FEED SYSTEM

Table C.1. Calibration of the solids feed system.

Potentiometer setting	Volumetric flow rate $(M^3/s) \times 10^6$	Potentiometer setting	Volumetric flow rate $(M^3/s) \times 10^6$
10	132.70	10	157.5
9	111.30	9	142.7
8	88.12	8	121.4
7	89.22	7	100.6
6	70.45	6	85.47
5	63.42	5	61.54
4	55.28	4	56.53
3	35.27	3	35.42
2	14.62		

Calibration curve is:

$$\text{Vol flow rate} = B_1 \times (\text{pot setting}) + B_o$$

where $B_1 = 17.62 \times 10^{-6}$ M^3/s

$B_o = -19.39 \times 10^{-6}$ M^3/s

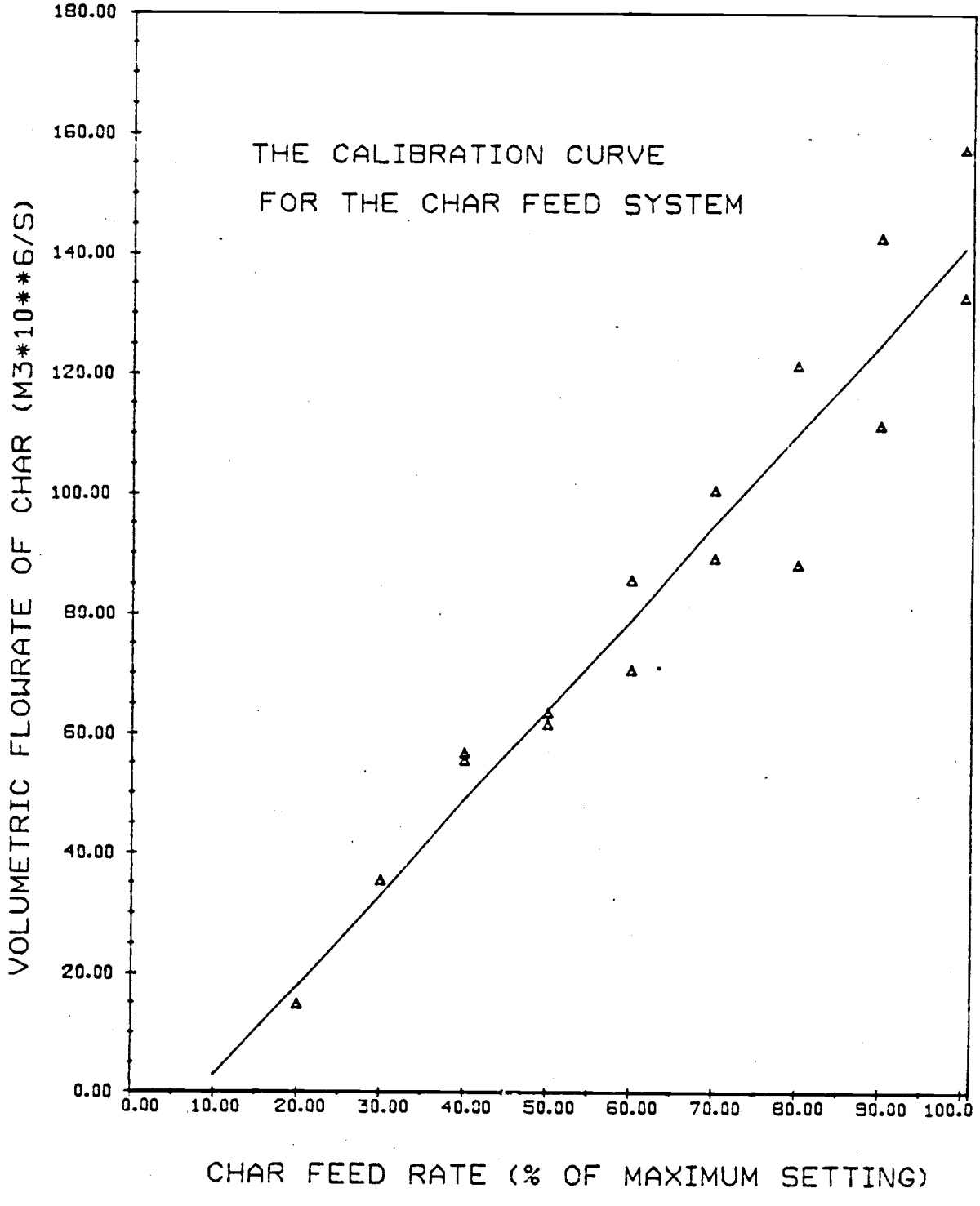

Figure C.2. Auger Calibration Curve.

THE CALIBRATION OF THE AIR FLOW METERS

Figure C.3 is a schematic diagram of the air feed system to the reactor. The diagram shows that there are 3 venturi flow meters and 1 orifice plate flow meter in the system. These flow meters must be calibrated correctly if flow rates are to be measured accurately.

ORIFICE PLATE FLOW METER CALIBRATION (VIEW PORT AIR)

For the latter half of the test runs the air supplied to the view ports was metered using a sharp edge flat plate orifice meter. The operating characteristics of the meter were established from theory and the approach was similar to that out-lined in Perry and Chilton (30). A table of results was generated using the digital computer and are presented in Table C.2. The operating curves were also calculated and these are presented in Figures C.4-C.7.

THE PREHEAT AND MAIN AIR -VENTURI FLOW METER CALIBRATIONS

The calibration for both these flow meters were again formulated from theory. The approach was, this time, taken from Pankhurst and Ower (31). The results are presented in Table C.3 and in Figures C.8-C.11.

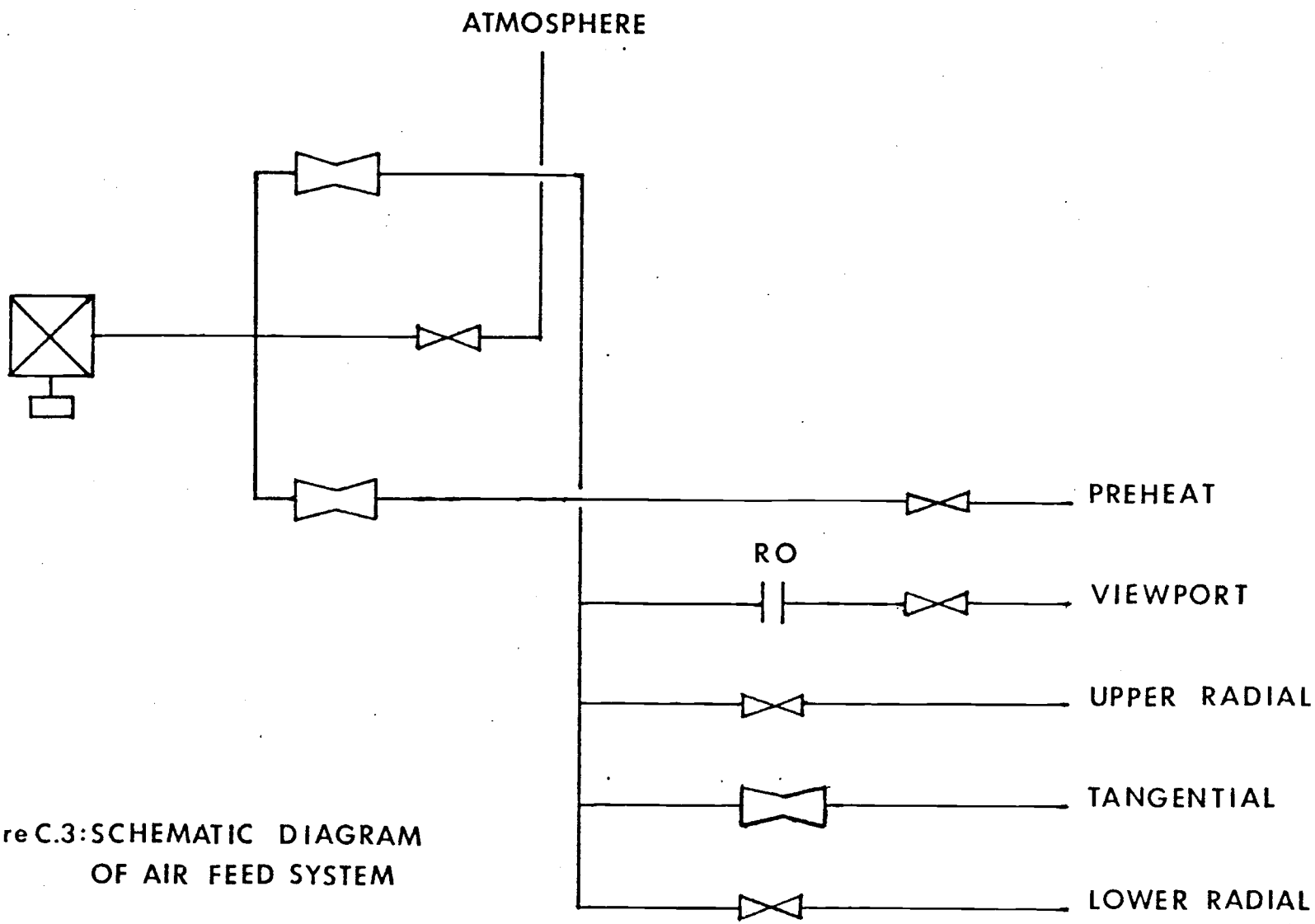

Figure C.3: SCHEMATIC DIAGRAM OF AIR FEED SYSTEM

Table C.2. Calibration results for the view port orifice flowmeter (computer generated).

```
*****************************************************************
TABLE OF CALCULATED FLOWRATES FOR THE VIEW PORT ORIFICE FLOWMETER
*****************************************************************

UPSTREAM PRESSURE =  .1083E+06  (N/M2)

PRESSURE DIFFERENCE (N/M2)=          0.0    1245.0    2490.0    3735.0    4980.0    6225.0

INLET AIR TEMPERATURE=290.0 (K)   0.00000    .01715    .02417    .02949    .03392    .03778
INLET AIR TEMPERATURE=300.0 (K)   0.00000    .01687    .02376    .02899    .03335    .03714
INLET AIR TEMPERATURE=310.0 (K)   0.00000    .01659    .02338    .02852    .03281    .03654
INLET AIR TEMPERATURE=320.0 (K)   0.00000    .01633    .02301    .02807    .03229    .03596
INLET AIR TEMPERATURE=330.0 (K)   0.00000    .01608    .02266    .02764    .03180    .03541

UPSTREAM PRESSURE =  .1153E+06  (N/M2)

PRESSURE DIFFERENCE (N/M2)=          0.0    1245.0    2490.0    3735.0    4980.0    6225.0

INLET AIR TEMPERATURE=290.0 (K)   0.00000    .01770    .02495    .03045    .03503    .03902
INLET AIR TEMPERATURE=300.0 (K)   0.00000    .01741    .02453    .02993    .03444    .03837
INLET AIR TEMPERATURE=310.0 (K)   0.00000    .01712    .02413    .02945    .03388    .03774
INLET AIR TEMPERATURE=320.0 (K)   0.00000    .01685    .02375    .02898    .03335    .03715
INLET AIR TEMPERATURE=330.0 (K)   0.00000    .01660    .02339    .02854    .03284    .03658

UPSTREAM PRESSURE =  .1223E+06  (N/M2)

PRESSURE DIFFERENCE (N/M2)=          0.0    1245.0    2490.0    3735.0    4980.0    6225.0

INLET AIR TEMPERATURE=290.0 (K)   0.00000    .01824    .02570    .03138    .03611    .04023
INLET AIR TEMPERATURE=300.0 (K)   0.00000    .01793    .02527    .03085    .03550    .03956
INLET AIR TEMPERATURE=310.0 (K)   0.00000    .01764    .02486    .03035    .03492    .03891
INLET AIR TEMPERATURE=320.0 (K)   0.00000    .01736    .02447    .02987    .03437    .03830
INLET AIR TEMPERATURE=330.0 (K)   0.00000    .01710    .02410    .02941    .03385    .03771

UPSTREAM PRESSURE =  .1293E+06  (N/M2)

PRESSURE DIFFERENCE (N/M2)=          0.0    1245.0    2490.0    3735.0    4980.0    6225.0

INLET AIR TEMPERATURE=290.0 (K)   0.00000    .01876    .02644    .03228    .03715    .04140
INLET AIR TEMPERATURE=300.0 (K)   0.00000    .01844    .02600    .03174    .03653    .04071
INLET AIR TEMPERATURE=310.0 (K)   0.00000    .01814    .02557    .03122    .03593    .04005
INLET AIR TEMPERATURE=320.0 (K)   0.00000    .01785    .02517    .03073    .03537    .03942
INLET AIR TEMPERATURE=330.0 (K)   0.00000    .01758    .02479    .03026    .03483    .03881
```

Table C.3. Calibration results for the main air and preheat air Venturi flowmeter (computer generated).

```
*****************************************************************************
TABLE OF CALCULATED FLOWRATES FOR THE MAIN AIR AND PREHEAT AIR VENTURI FLOWMETERS
*****************************************************************************

UPSTREAM PRESSURE = .1082E+06  N/M2

PRESSURE DIFFERENCE (N/M2)=              .0     2988.0     5976.0     8964.0    11952.0    14940.0

INLET AIR TEMPERATURE =290.0 (K)     .00000     .09097     .12650     .15227     .17273     .18960
INLET AIR TEMPERATURE =300.0 (K)     .00000     .08944     .12437     .14971     .16982     .18641
INLET AIR TEMPERATURE =310.0 (K)     .00000     .08798     .12234     .14727     .16705     .18337
INLET AIR TEMPERATURE =320.0 (K)     .00000     .08659     .12041     .14494     .16441     .18048
INLET AIR TEMPERATURE =330.0 (K)     .00000     .08527     .11857     .14273     .16190     .17772

UPSTREAM PRESSURE = .1151E+06  N/M2

PRESSURE DIFFERENCE (N/M2)=              .0     2988.0     5976.0     8964.0    11952.0    14940.0

INLET AIR TEMPERATURE =290.0 (K)     .00000     .09391     .13073     .15754     .17891     .19664
INLET AIR TEMPERATURE =300.0 (K)     .00000     .09233     .12853     .15489     .17590     .19333
INLET AIR TEMPERATURE =310.0 (K)     .00000     .09083     .12644     .15237     .17303     .19018
INLET AIR TEMPERATURE =320.0 (K)     .00000     .08939     .12444     .14996     .17030     .18717
INLET AIR TEMPERATURE =330.0 (K)     .00000     .08803     .12254     .14767     .16770     .18431

UPSTREAM PRESSURE = .1220E+06  N/M2

PRESSURE DIFFERENCE (N/M2)=              .0     2988.0     5976.0     8964.0    11952.0    14940.0

INLET AIR TEMPERATURE =290.0 (K)     .00000     .09677     .13484     .16264     .18489     .20343
INLET AIR TEMPERATURE =300.0 (K)     .00000     .09514     .13256     .15990     .18178     .20000
INLET AIR TEMPERATURE =310.0 (K)     .00000     .09359     .13040     .15730     .17882     .19675
INLET AIR TEMPERATURE =320.0 (K)     .00000     .09211     .12835     .15482     .17600     .19364
INLET AIR TEMPERATURE =330.0 (K)     .00000     .09070     .12638     .15245     .17330     .19068

UPSTREAM PRESSURE = .1289E+06  N/M2

PRESSURE DIFFERENCE (N/M2)=              .0     2988.0     5976.0     8964.0    11952.0    14940.0

INLET AIR TEMPERATURE =290.0 (K)     .00000     .09955     .13882     .16759     .19069     .21001
INLET AIR TEMPERATURE =300.0 (K)     .00000     .09787     .13648     .16477     .18748     .20647
INLET AIR TEMPERATURE =310.0 (K)     .00000     .09627     .13425     .16208     .18442     .20311
INLET AIR TEMPERATURE =320.0 (K)     .00000     .09475     .13214     .15952     .18151     .19990
INLET AIR TEMPERATURE =330.0 (K)     .00000     .09331     .13011     .15708     .17874     .19684
```

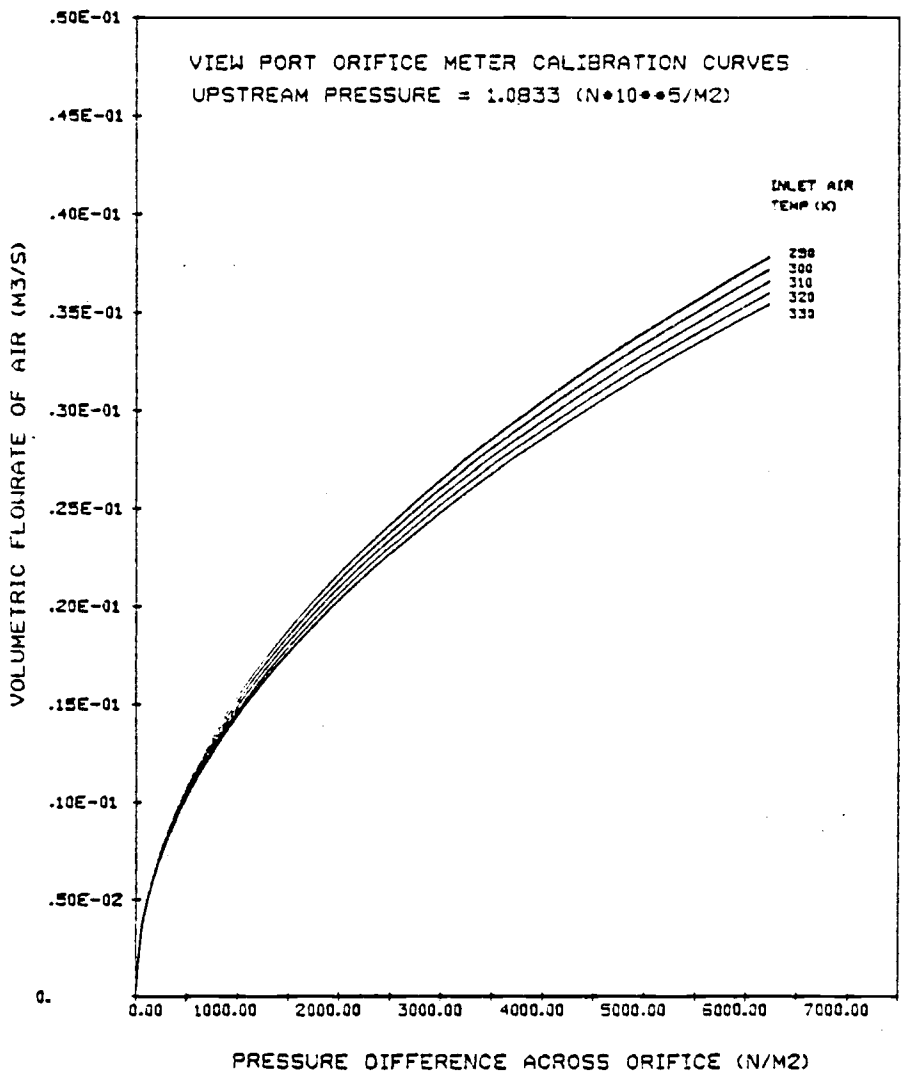

Figure C.4. Orifice Meter Calibration Curves.

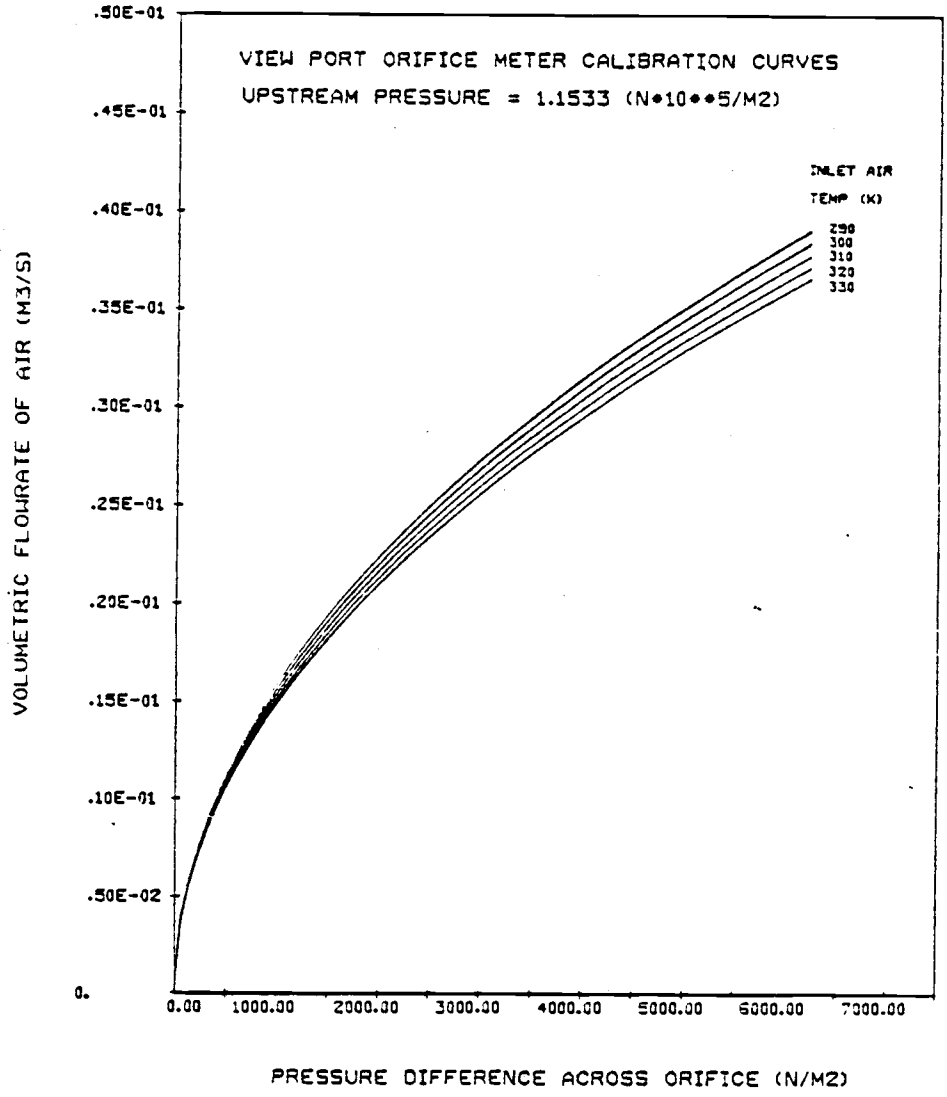

Figure C.5. Orifice Meter Calibration Curves.

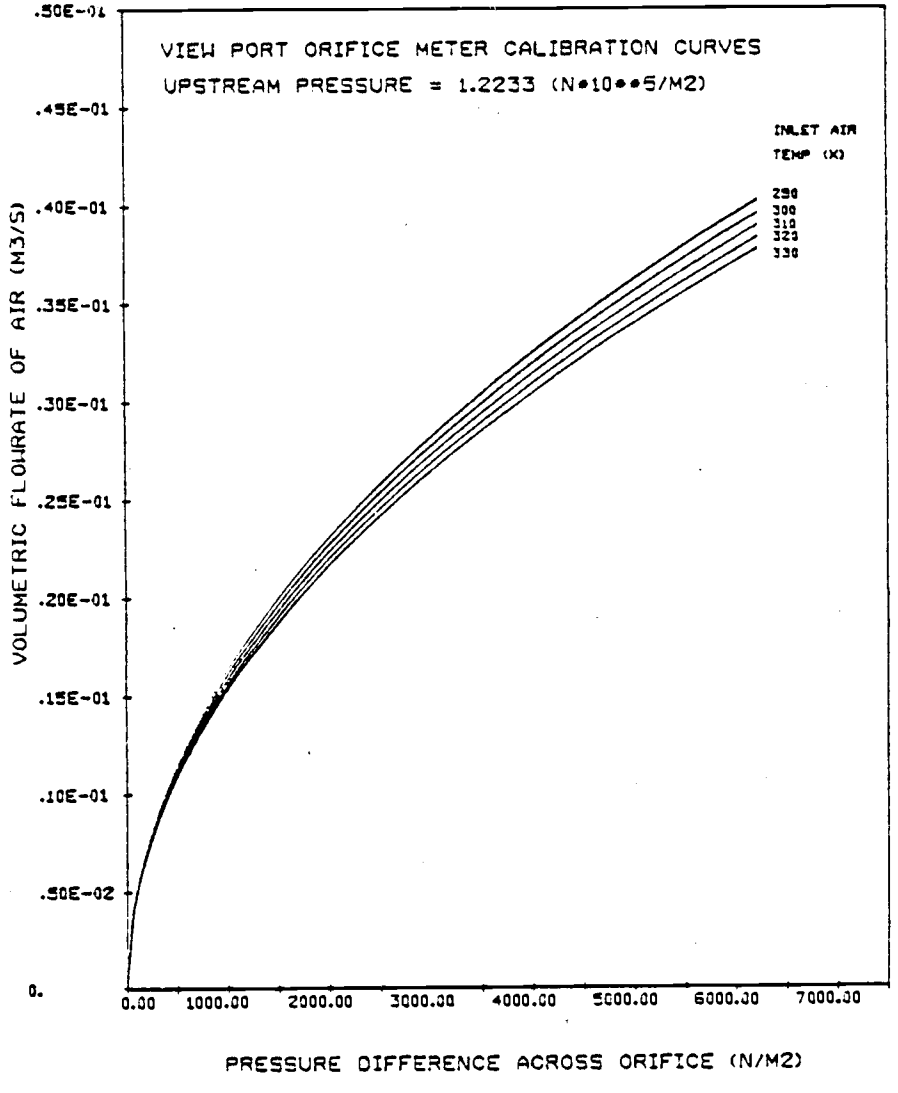

Figure C.6. Orifice Meter Calibration Curves.

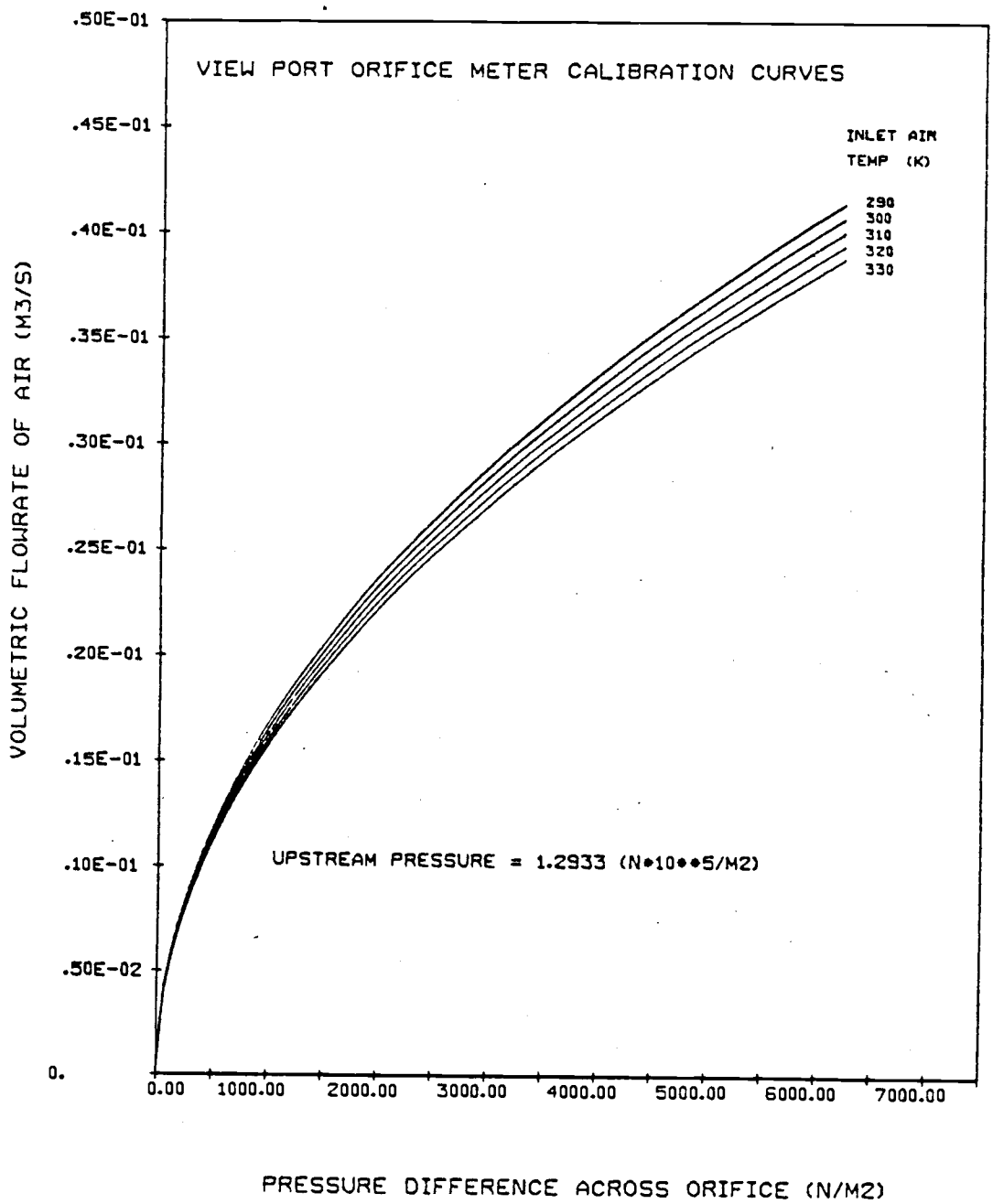

Figure C.7. Orifice Meter Calibration Curves.

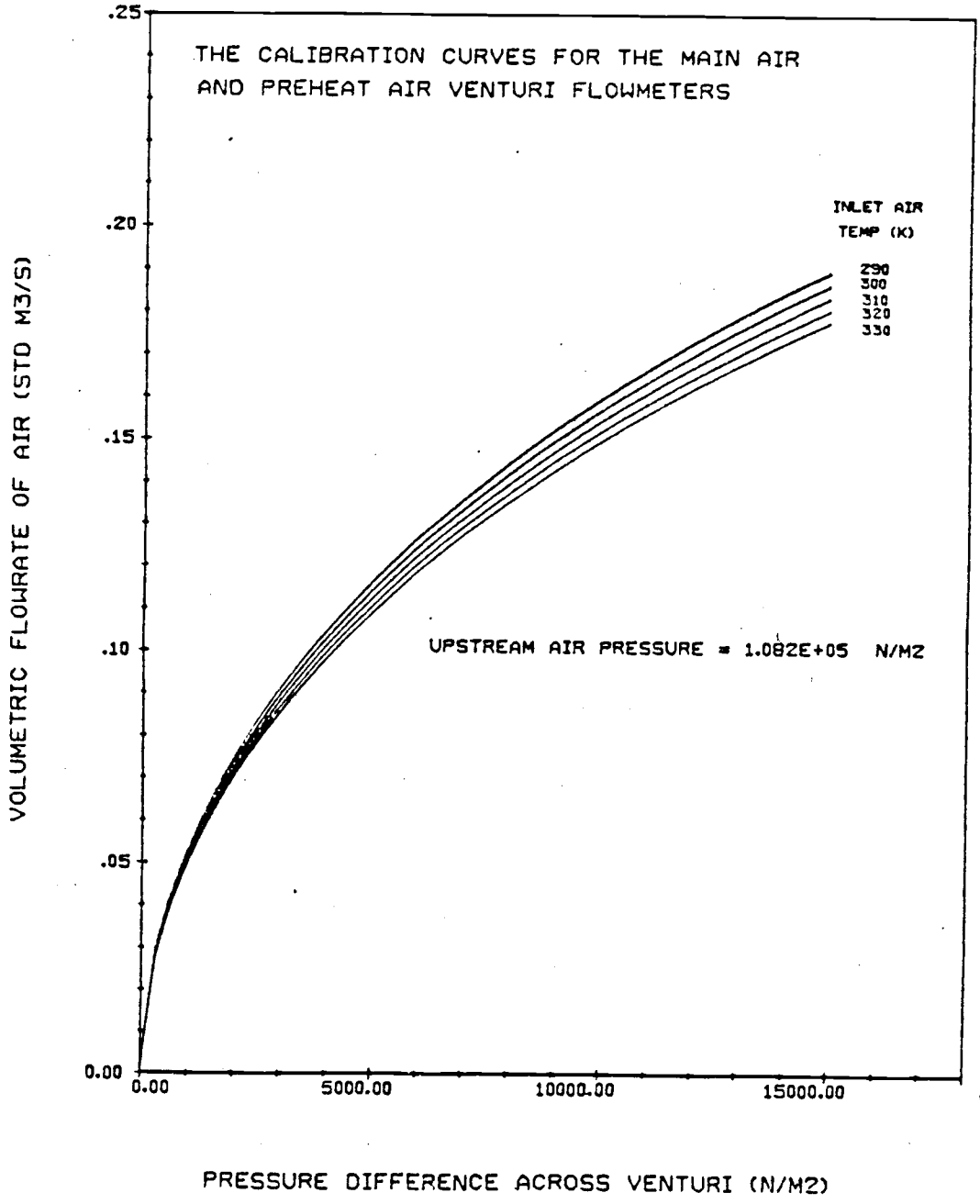

Figure C.8. Calibration Curves for Main Air Venturi Flowmeter.

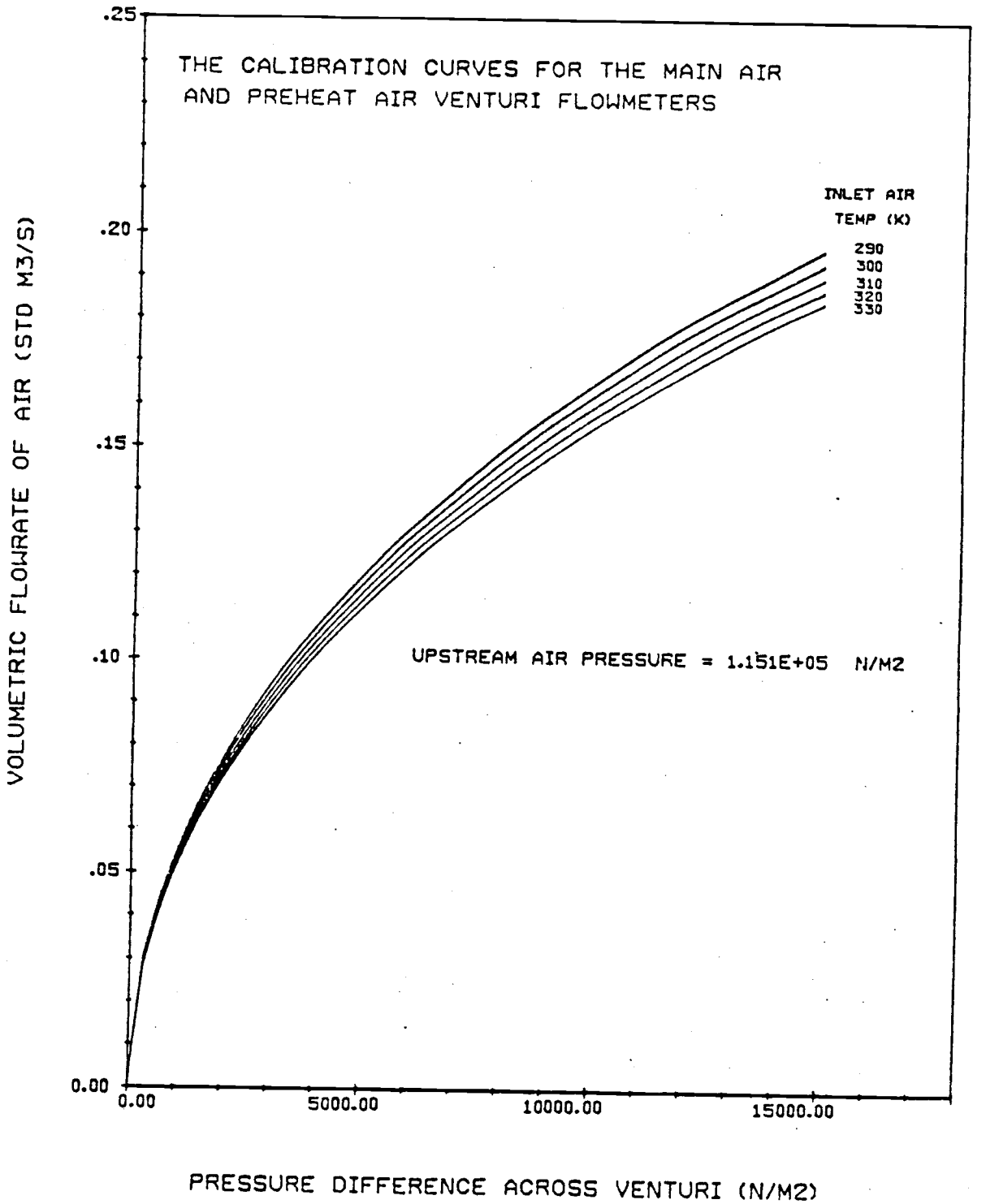

Figure C.9. Calibration Curves for Main Air Venturi Flowmeter.

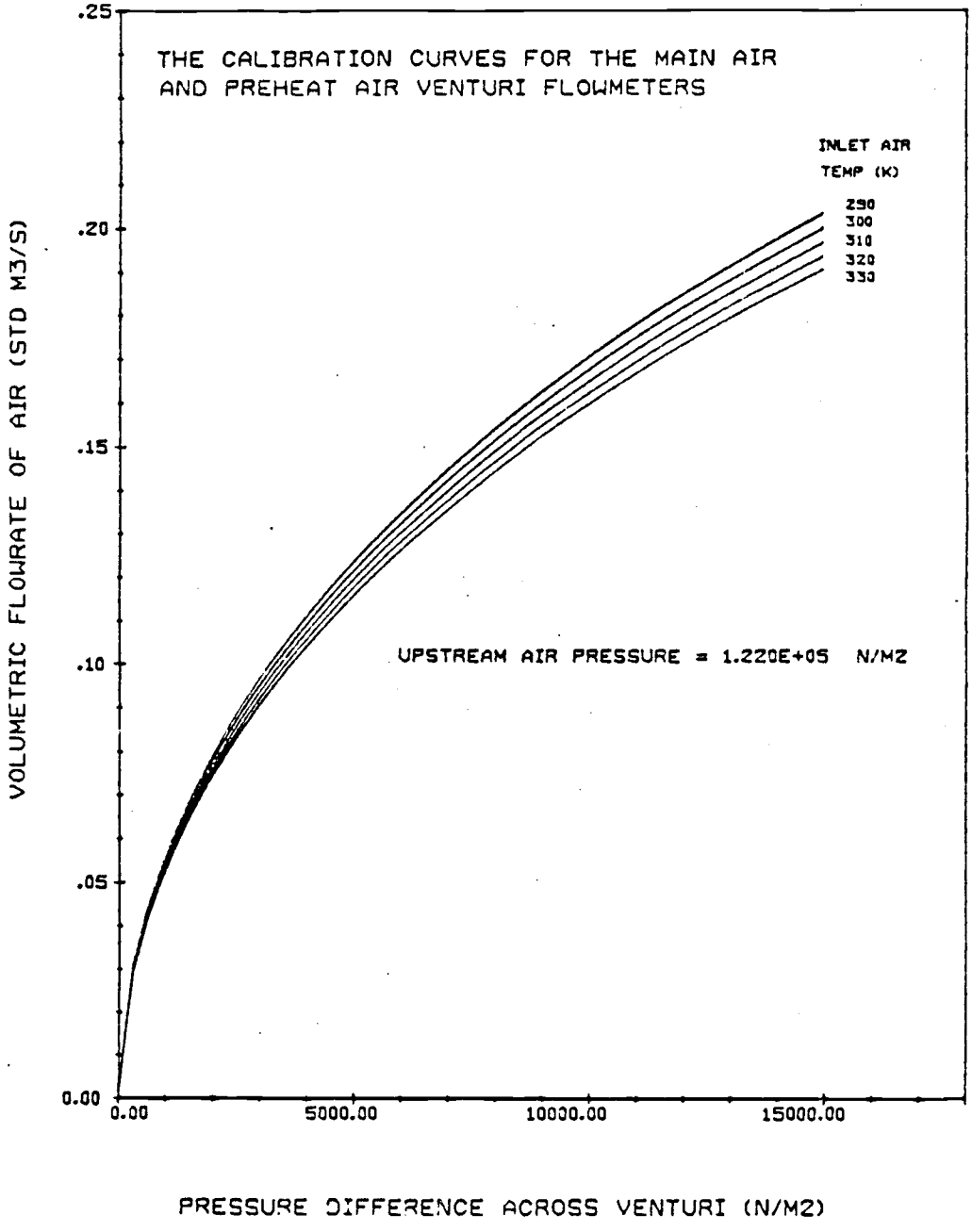

Figure C.10. Calibration Curves for Main Air Venturi Flowmeter.

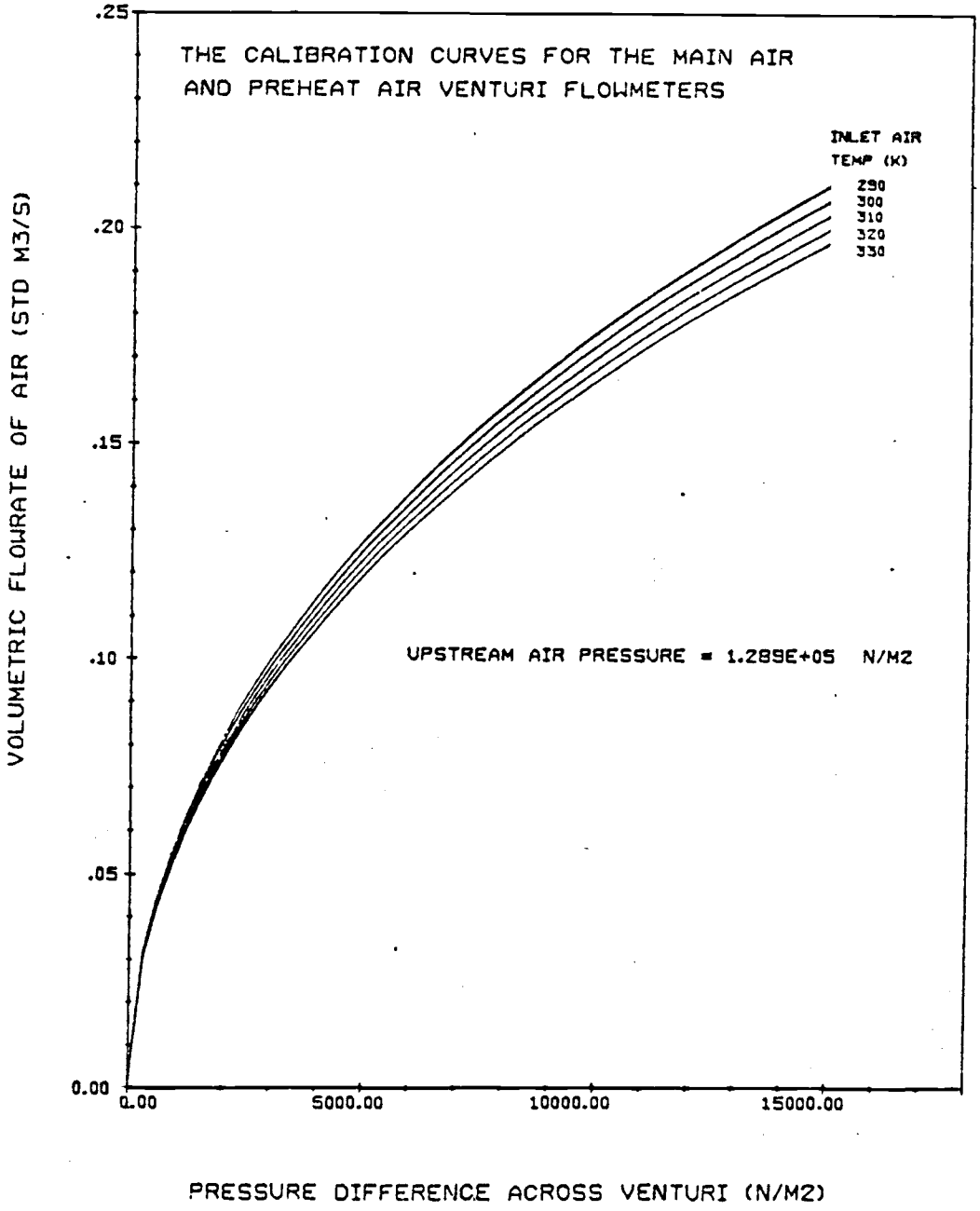

Figure C.11. Calibration Curves for Main Air Venturi Flowmeter.

TANGENTIAL AIR - VENTURI FLOWMETER CALIBRATION

This flowmeter was added to the system, as was the orifice meter described above, about halfway through the series of test runs.

The venturi flowmeter could not be located at a distance far enough downstream of a 90° bend, to allow the flow to become fully developed. Thus this flowmeter had to be calibrated *in situ*.

The calibration was achieved by fully opening the tangential air valve while closing both upper and lower radial air valves. Thus all the air passing through the tangential venturi flowmeter had also passed through the main air venturi. Since the main air venturi had been calibrated from theory, the calibration of the tangential air meter was a simple matter of comparing the two head losses for the two meters and noting the inlet air temperature.

The results for the calibration are given in Table C. 4 and Figure C. 12.

Table C. 4. Results for the calibration of the tangential air venturi flowmeter.

	Pressure difference (N/M^2)	Volumetric flow rate (std. M^3/s)	Pressure difference	Volumetric flow rate (std. M^3/s)
Upstream pressure (N/M^2)	1.085×10^5		1.220×10^5	
Upstream temperature (K)	300		310	
	1120.5	.06371	996.0	.06607
	1743.0	.08165	1867.5	.08495
	2490.0	.09911	2614.5	.10382
	3037.8	.11421	3311.7	.11940
	3610.5	.12600	3984.	.13214
	4233.0	.13686	4606.5	.14394
	4606.5	.14866	5303.7	.15479
	5229.0	.15716	5801.7	.16423
	5602.5	.16518	6349.5	.17367
	6225.0	.17320		

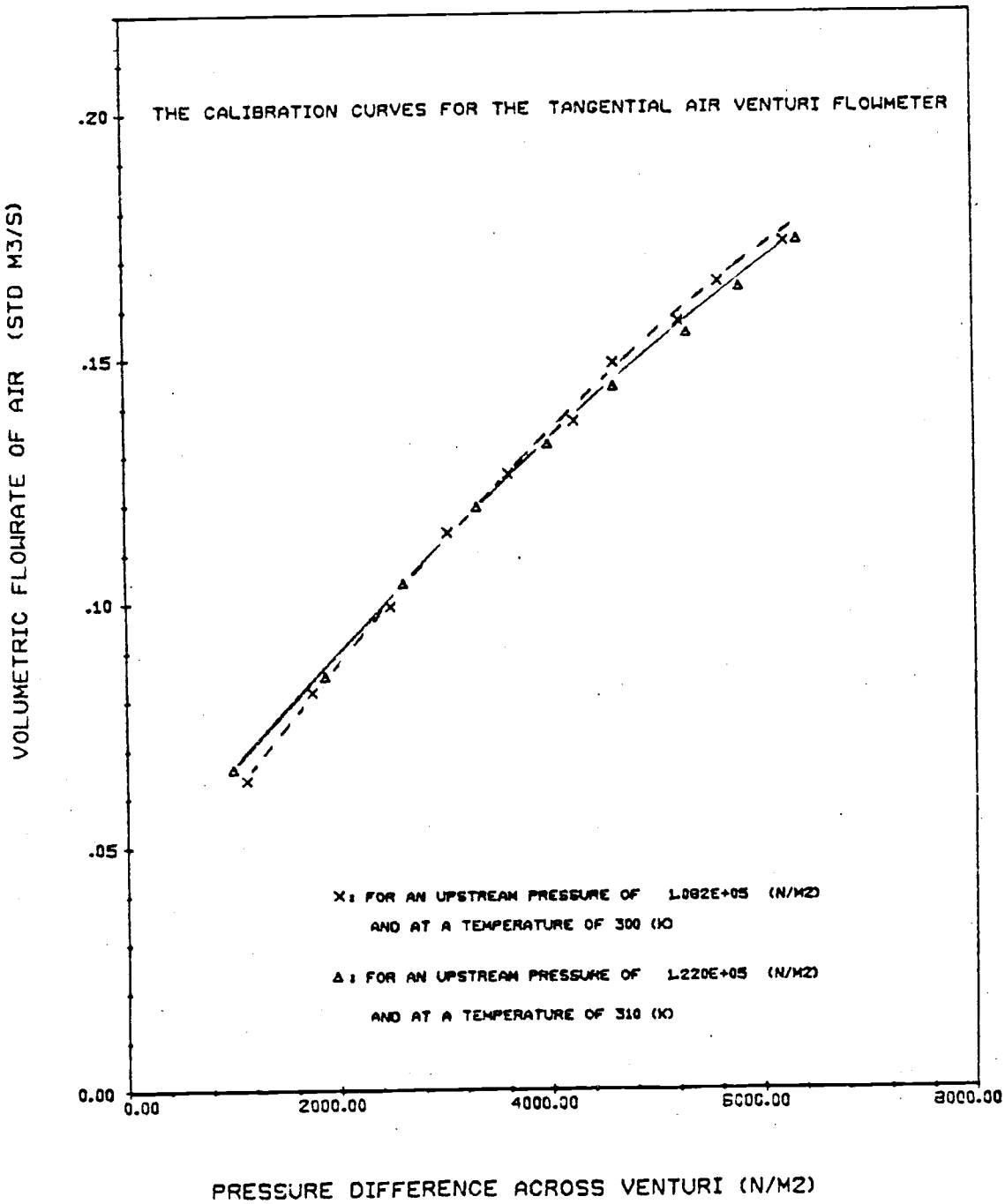

Figure C.12. Experimental Calibration Curves for the Tangential Air Venturi Flowmeter.

APPENDIX D

THE RESULTS FROM THE TEST RUNS

RESULTS FOR TEST RUNS ON THE REACTOR

In all, 18 test runs were carried out on the reactor. The performance of the reactor was tested under varying conditions of air flow rate, air flow distribution and solids flow.

There are basically two modes of air distribution which were considered. Either the bulk of the air was introduced in a radial direction into the conical section at the base of the reactor or it was fed tangentially into the bottom section. These two different modes of air feed are illustrated in Figure D. 1.

The letter of each run code gives an indication of how the main air is introduced into the reactor. For instance the P series (P1-P4) has all the main air introduced radially from the bottom, as illustrated in Figure D. 1 for radial mode. The CP and C series have the bulk of the main air introduced tangentially, see Figure D. 1. The difference between the CP and C series is that for the CP runs a small fraction of bottom radial air is introduced. This bottom radial air keeps the solids, which are not entrained by the tangential stream, continually moving and hence prevents the build up of a bed of unburnt wood char. In contrast the C series has virtually all the main air fed tangentially, although for a few runs some preheat air (radial) and some upper radial air (about two feet from bottom of reactor) was introduced to keep the temperature below 1350 K (the ash fusion point).

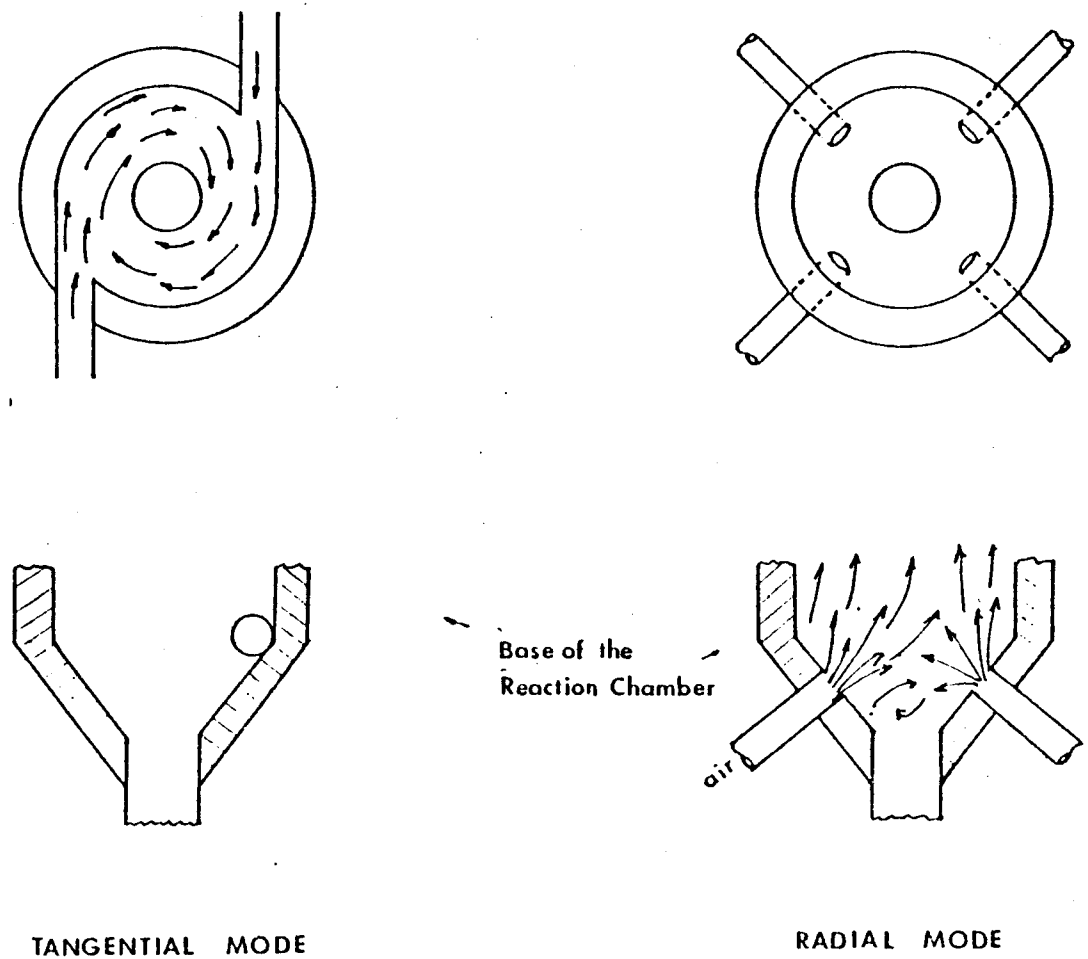

Figure D.1. The Two Different Modes of Introducing the Main Combustion Air.

The data for all the test runs is presented in Tables D.1-D.3. The results are given in the units which they were measured. However, the data is transformed into SI units with the aid of the calibration charts from Appendix C. The SI data is given in Tables D.4-D.6. Along with the size distributions of feed and physical properties of wood char and product ash given in appendices A and B this information is the main experimental data collected for this thesis and is used to compare the results given by the computer simulated combustion model and the observed data.

Table D.1. Results for the P-series of test runs.

Run number	Plug Flow Series (P) P1	P2	P3	P4
Solids feed rate (% max)	3.5	4.4	4.0	5.0
Total main air (ins. water)	14.0	23.0	25.5	54.0
Tangential air (ins. water)	0.0	0.0	0.0	0.0
View port air (ins. water)	4.3	24.0	8.5	5.5
Preheat air (ins. water)	0.0	0.0	0.0	0.0
Air temperature inlet (F)	105.0	90.0	80.0	90.0
Back pressure (psi)	3.0	1.0	0.5	2.0
Ave. top temperature (F)	1634.0	1815.0	1760.0	1723.0
Ave. mid temperature (F)	1772.0	1915.0	1910.0	1865.0
Ave. bot. temperature (F)	1741.0	1793.0	1954.0	1926.0
No. of readings taken	5	4	5	4
Ave. cyclone O_2 (% vol)	17.50*	18.00*	11.67	12.21
Ave. cyclone CO_2 (% vol)	2.63	1.90	6.43	5.63
Ave cyclone CO (% vol)	0.22	0.15	0.43	0.81
No. of readings taken	3	1	3	3
Ave. top O_2 (% vol)	16.20	-	11.80	12.40
Ave. top CO_2 (% vol)	3.85	-	7.60	6.70
Ave. top CO (% vol)	0.14	-	0.08	0.14
No. of readings taken	2	-	1	2
Ave. mid O_2 (% vol)	-	-	-	11.00
Ave. mid CO_2 (% vol)	-	-	-	6.60
Ave. mid CO (% vol)	-	-	-	0.30
No. of readings taken	-	-	-	1
Ave. bottom O_2 (% vol)	16.00	17.50	6.90	-
Ave bottom CO_2 (% vol)	3.10	2.20	11.30	-

Table D.1. (Continued)

Run number	Plug Flow Series (P) P1	P2	P3	P4
Ave. bottom CO (% vol)	0.40	0.15	0.08	-
No. of readings taken	1	1	2	-
Time of run (mins.)	30.0	30.0	30.0	30.0
Weight of ash collected (Kg)	0.5070	0.8460	0.8910	1.1080

*High values caused by the rupture of the seal on the vaccuum pump, used for sampling.

Table D.2. The results for the CP series of test runs.

Run number	Cyclone Plug Series (CP) CP1	CP2	CP3	CP4
Solids feed rate (% max)	3.5	4.0	4.5	5.0
Total main air (ins. water)	12.0	29.0	45.0	44.0
Tangential air (ins. water)	6.5	8.0	10.0	17.5
View port air (ins. water)	17.5	19.5	15.0	20.5
Preheat air (ins. water)	0.0	0.0	0.0	0.0
Inlet air temperature (F)	105.0	95.0	100.0	85.0
Back pressure (psi)	3.0	0.5	0.5	2.0
Ave. top temperature (F)	1703.0	1740.0	1773.0	1750.0
Ave. mid. temperature (F)	1875.0	1905.0	1928.0	1865.0
Ave. bot. temperature (F)	1866.0	1841.0	1833.0	1675.0
No. of readings taken	4	4	4	5
Ave. cyclone O_2 (%vol)	12.00	12.60	12.40	12.70
Ave. cyclone CO_2 (% vol)	8.40	6.20	8.10	5.23
Ave. cylcone CO (% vol)	0.00	0.16	0.12	0.88
No. of readings taken	2	3	3	3
Ave. top O_2 (% vol)	-	-	-	13.05
Ave. top CO_2 (% vol)	-	-	-	5.80
Ave. top CO (% vol)	-	-	-	0.10
No. of readings taken	-	-	-	2
Ave. mid. O_2 (% vol)	10.60	12.50	-	14.00
Ave. mid. CO_2 (% vol)	10.40	5.00	-	5.10
Ave. mid. CO (% vol)	0.10	0.20	-	0.25
No. of readings taken	2	1	-	1
Ave. bot. O_2 (% vol)	16.10	14.30	15.50	-

Table D.2. (Continued)

Run number	Cyclone Plug Series (CP)			
	CP1	CP2	CP3	CP4
Ave. bot. CO_2 (% vol)	3.75	5.30	4.00	-
Ave. bot. CO (% vol)	0.25	0.30	0.40	-
No. of readings taken	2	1	2	-
Time of runs (mins.)	30.0	30.0	30.0	30.0
Weight of ash collected (Kg)	0.4690	0.7640	1.0180	1.1000

Table D.3. The results for the C series of test runs.

Run number	Cyclone Series (C) C1	C2	C3	C4
Solids feed rate (% max.)	6.0	6.0	5.0	4.0
Total main air (ins. water)	30.0	41.0	42.0	10.0
Tangential air (ins. water)	*	*	*	*
View port air (ins. water)	*	*	*	*
Preheat air (ins. water)	2.0	2.0	0.0	0.0
Air temperature inlet (F)	70.0	70.0	70.0	60.0
Back pressure (psi)	1.0	1.0	0.5	4.0
Ave. top temperature (F)	1813.0	1813.0	1627.0	1760.0
Ave. mid. temperature (F)	1830.0	1857.0	1772.0	1893.0
Ave. bot. temperature (F)	1798.0	1637.0	1705.0	1800.0
No. of readings taken	4	3	3	3
Ave. cyclone O_2 (% vol)	-	-	13.50	12.20
Ave. cyclone CO_2 (% vol)	-	-	5.30	6.80
Ave. cyclone CO (% vol)	-	-	0.50	0.00
No. of readings taken	-	-	1	1
Ave. top O_2 (% vol)	7.50	10.17	8.00	11.45
Ave. top CO_2 (% vol)	10.38	10.10	11.50	7.75
Ave. top CO (% vol)	0.00	0.00	0.24	0.00
No. of readings taken	3	3	3	2
Ave. mid. O_2 (% vol)	-	-	-	-
Ave. mid. CO_2 (% vol)	-	-	-	-
Ave. mid. CO (% vol)	-	-	-	-
No. of readings taken	-	-	-	-
Ave. bot. O_2 (% vol)	8.08	12.00	0.77	14.40
Ave. bot. CO_2 (% vol)	10.33	6.47	16.00	4.80

Table D.3. (Continued)

Run number	Cyclone Series (C) C1	C2	C3	C4
Ave. Bot. CO_2 (% vol)	0.45	0.80	1.27	0.03
No. of readings taken	3	3	3	2
Time of runs (mins)	15.0	20.0	20.0	20.0
Weight of ash collected (Kg)	0.6623	1.1155	0.4689	0.3875

Run number	C5	C6	C7	C8
Solids feed rate (% max)	3.3	4.0	5.0	4.5
Total main air (ins. water)	10.0	16.0	28.0	28.0
Tangential air (ins. water)	*	*	*	*
View port air (ins. water)	*	*	*	*
Preheat air (ins. water)	0.0	0.0	0.0	0.0
Air temperature inlet (F)	100.0	95.0	80.0	80.0
Back pressure (psi)	4.0	4.0	0.5	2.0
Ave. top temperature (F)	1630.0	1766.0	1793.0	1724.0
Ave. mid. temperature (F)	1770.0	1860.0	1924.0	1861.0
Ave. bot. temperature (F)	1734.0	1738.0	1790.0	1733.0
No. of readings taken	4	4	4	4
Ave. cyclone O_2 (% vol)	14.00	13.40	14.17	15.07
Ave. cyclone CO_2 (% vol)	4.63	5.30	5.00	4.50
Ave. cyclone CO (% vol)	0.00	0.00	0.02	0.00
No. of readings taken	3	1	3	3
Ave. top O_2 (% vol)	13.40	12.20	12.75	12.70
Ave. top CO_2 (% vol)	5.40	6.40	6.55	6.10
Ave. top CO (% vol)	0.00	0.00	0.00	0.00
No. of readings taken	2	2	2	2

Table D.3. (Continued)

Run number	Cyclone Series (C) C5	C6	C7	C8
Ave. mid O_2 (% vol)	-	-	-	6.45
Ave. mid CO_2 (% vol)	-	-	-	14.25
Ave. mid CO (% vol)	-	-	-	0.10
No. of readings taken	-	-	-	2
Ave. bot. O_2 (% vol)	16.10	16.10	16.20	-
Ave. bot. CO_2 (% vol)	3.30	3.40	3.00	-
Ave. bot. CO (% vol)	0.10	0.14	0.23	-
No. of readings taken	3	2	2	-
Time of run (mins)	30.0	30.0	30.0	30.0
Weight of ash collected (Kg)	0.3750	0.5798	1.0070	0.7400

Run number	C9	C10
Solids feed rate (% max)	6.0	5.0
Total main air (ins. water)	46.0	34.0
Tangential air (ins. water)	17.0	12.5
View port air (ins. water)	26.0	16.5
Preheat air (ins. water)	0.0	0.0
Inlet air temperature (F)	85.0	90.0
Back pressure (psi)	1.0	1.0
Ave. top temperature (F)	1921.0	1838.0
Ave. mid. temperature (F)	1970.0	1938.0
Ave. bot. temperature (F)	1833.0	1738.0
No. of readings taken	4	4
Ave. cyclone O_2 (% vol)	13.70	11.17
Ave. cylcone CO_2 (% vol)	6.00	6.60

Table D.3. (Continued)

Run number	Cyclone Series (C) C9	C10
Ave. cyclone CO (% vol)	0.04	0.06
No. of readings taken	3	3
Ave. top O_2 (% vol)	12.05	11.80
Ave. top CO_2 (% vol)	6.90	7.00
Ave. top CO (% vol)	0.03	0.00
No. of readings taken	2	1
Ave. mid O_2 (% vol)	-	-
Ave. mid CO_2 (% vol)	-	-
Ave. Mid CO (% vol)	-	-
No. of readings taken	-	-
Ave. bot. O_2 (% vol)	17.50	15.40
Ave. bot. CO_2 (% vol)	1.90	3.85
Ave. bot. CO (% vol)	0.23	0.53
No. of readings taken	2	2
Time of run (mins)	30.0	30.0
Weight of ash collected (Kg)	1.1180	1.2010

*These readings could not be taken since the flowmeters were not installed at the time of the run

Table D.4. The results for the P-series of runs (SI units).

Run number	P1	P2	P3	P4
Flow rate of solids (kg/s) x 10^{-3}	5.1153	6.8072	6.0554	7.9355
Flow rate of main air (mole/s)	4.0335	5.0765	4.8713	7.4001
Flow rate of tangential air (mole/s)	0	0	0	0
Flow rate of view port air (mole/s)	0.6152	1.4500	0.8869	0.7349
Flow rate of preheat air (mole/s)	0	0	0	0
Average top temperature (K)	1163	1264	1233	1212
Average min temperature (K)	1240	1319	1316	1291
Average bottom temperature (K)	1222	1251	1341	1325
Average cyclone gas analysis				
% volume of oxygen	17.50	18.00	11.67	12.21
% volume of carbon dioxide	2.63	1.90	6.43	5.63
% volume of carbon monoxide	0.22	0.15	0.43	0.81
Average top gas analysis				
% volume of oxygen	16.20	-	11.80	12.40
% volume of carbon dioxide	3.85	-	7.60	6.70
% volume of carbon monoxide	0.14	-	0.08	0.14
Average mid gas analysis				
% volume of oxygen	-	-	-	-
% volume of carbon dioxide	-	-	-	-
% volume of carbon monoxide	-	-	-	-
Average bottom gas analysis				
% volume of oxygen	16.00	17.50	6.90	-
% volume of carbon dioxide	3.10	2.20	11.30	-
% volume of carbon monoxide	0.40	0.15	0.08	-
Collection rate of ash (kg/s) x 10^{-3}	0.2817	0.4700	0.4950	0.6156

Table D.5. The results for the CP-series of runs (SI units).

	CP1	CP2	CP3	CP4
Flow rate of solids (kg/s) x 10^{-3}	5.1153	6.0554	6.9954	7.9355
Flow rate of main air (mole/s)	3.7349	5.3115	6.4324	6.8050
Flow rate of tangential air (mole/s)	3.2094	3.6405	4.2153	5.7482
Flow rate of view port air (mole/s)	1.3272	1.3017	1.1107	1.3105
Flow rate of preheat air (mole/s)	0	0	0	0
Average top temperature (K)	1201	1222	1240	1227
Average mid temperature (K)	1297	1316	1326	1291
Average bottom temperature (K)	1292	1278	1274	1186
Average cyclone gas analysis				
% volume of oxygen	12.00	12.60	12.40	12.70
% volume of carbon dioxide	8.40	6.20	8.10	5.23
% volume of carbon monoxide	0.00	0.16	0.12	0.88
Average top gas analysis				
% volume of oxygen	-	-	-	13.05
% volume of carbon dioxide	-	-	-	5.80
% volume of carbon monoxide	-	-	-	0.10
Average mid gas analysis				
% volume of oxygen	10.60	12.50	-	14.00
% volume of carbon dioxide	10.40	5.00	-	5.10
% volume of carbon monoxide	0.10	0.20	-	0.25
Average bottom gas analysis				
% volume of oxygen	16.10	14.30	15.50	-
% volume of carbon dioxide	3.75	5.30	4.00	-
% volume of carbon monoxide	0.25	0.30	0.40	-
Collection rate of ash (kg/s) x 10^{-3}	0.2606	0.4244	0.5656	0.6111

Table D.6. The results for the C-series of runs (SI units).

	C1	C2	C3	C4
Flow rate of solids (kg/s) x 10^{-3}	9.8156	9.8156	7.9355	6.0554
Flow rate of main air (mole/s)	5.6191	6.5005	6.4529	3.7076
Flow rate of tangential air (mole/s)	*	*	*	*
Flow rate of view port air (mole/s)	*	*	*	*
Flow rate of preheat air (mole/s)	1.5085	1.5085	0	0
Average top temperature (K)	1262	1262	1159	1233
Average mid temperature (K)	1272	1287	1240	1307
Average bottom temperature (K)	1254	1165	1202	1255
Average cyclone gas analysis				
% volume of oxygen	-	-	13.50	12.20
% volume of carbon dioxide	-	-	5.30	6.80
% volume of carbon monoxide	-	-	0.50	0.00
Average top gas analysis				
% volume of oxygen	7.50	10.17	8.00	11.45
% volume of carbon dioxide	10.38	10.10	11.50	7.75
% volume of carbon monoxide	0.00	0.00	0.24	0.00
Average mid gas analysis				
% volume of oxygen	-	-	-	-
% volume of carbon dioxide	-	-	-	-
% volume of carbon monoxide	-	-	-	-
Average bottom gas analysis				
% volume of oxygen	8.08	12.00	0.77	14.40
% volume of carbon dioxide	10.33	6.47	16.00	4.80
% volume of carbon monoxide	0.45	0.80	1.27	0.03
Collection rate of ash (kg/s) x 10^{-3}	0.7359	0.9299	0.3908	0.3229

Table D.6. (Continued)

	C5	C6	C7	C8
Flow rate of solids (kg/s) x 10^{-3}	4.7393	6.0554	7.9355	6.9954
Flow rate of main air (mole/s)	3.5505	4.4716	5.2970	5.3878
Flow rate of tangential air (mole/s)	*	*	*	*
Flow rate of view port air (mole/s)	*	*	*	*
Flow rate of preheat air (mole/s)	0	0	0	0
Average top temperature (K)	1161	1236	1251	1213
Average mid temperature (K)	1239	1289	1324	1289
Average bottom temperature (K)	1219	1221	1250	1218
Average cyclone gas analysis				
% volume of oxygen	14.00	13.40	14.17	15.07
% volume of carbon dioxide	4.63	5.30	5.00	4.50
% volume of carbon monoxide	0.00	0.00	0.02	0.00
Average top gas analysis				
% volume of oxygen	13.40	12.20	12.75	12.70
% volume of carbon dioxide	5.50	6.40	6.55	6.10
% volume of carbon monoxide	0.00	0.00	0.00	0.00
Average mid gas analysis				
% volume of oxygen	-	-	-	6.45
% volume of carbon dioxide	-	-	-	14.25
% volume of carbon monoxide	-	-	-	0.10
Average bottom gas analysis				
% volume of oxygen	16.10	16.10	16.20	-
% volume of carbon dioxide	3.30	3.40	3.00	-
% volume of carbon monoxide	0.10	0.14	0.23	-
Collection rate of ash (kg/s) x 10^{-3}	0.2083	0.3221	0.5594	0.4111

Table D.6. (Continued)

	C9	C10
Flow rate of solids (kg/s) x 10^{-3}	9.8156	7.9355
Flow rate of main air (mole/s)	6.7014	5.8347
Flow rate of tangential air (mole/s)	5.6524	4.7902
Flow rate of view port air (mole/s)	1.5277	1.2284
Flow rate of preheat air (mole/s)	0	0
Average top temperature (K)	1322	1276
Average mid temperature (K)	1350	1333
Average bottom temperature (K)	1274	1221
Average cyclone gas analysis		
% volume of oxygen	13.70	11.17
% volume of carbon dioxide	6.00	6.60
% volume of carbon monoxide	0.04	0.06
Average top gas analysis		
% volume of oxygen	12.05	11.80
% volume of carbon dioxide	6.90	7.00
% volume of carbon monoxide	0.03	0.00
Average mid gas analysis		
% volume of oxygen	-	-
% volume of carbon dioxide	-	-
% volume of carbon monoxide	-	-
Average bottom gas analysis		
% volume of oxygen	17.50	15.40
% volume of carbon dioxide	1.90	3.85
% volume of carbon monoxide	0.23	0.53
Collection rate of ash (kg/s) x 10^{-3}	0.6211	0.6672

*These readings could not be taken since the flow meters were not installed at the time of the run.

CALCULATION OF THE SOLIDS FEED RATE

It is apparent that there are two methods of calculating the solids flow rate to the reactor.

The first method uses a direct approach. Since the bulk density of the char has been previously measured and the calibration of the auger system is known, the evaluation of the solids flow rate is straightforward.

The second method uses the oxygen concentration in the cyclone to evaluate the amount of carbon burnt. This method involves back calculating from the exit conditions of the reactor. The oxygen concentration is taken from the cyclone since the gases are assumed to be well mixed and represent the final gas composition.

Once the amount of carbon which has burnt has been evaluated it is necessary to correct for the conversion of carbon within the reactor. Thus the total carbon entering the reactor is known. The total solids feed rate may now be evaluated by simply dividing by the combustible content of the feed stream. The following equation gives the relationships between the known and unknown variables:

$$\text{Solids flow (kg/s)} = \frac{(0.21 - Y_{O_2}^{cyc}) \times F_g \times 12}{\beta \times (1-\alpha')} \qquad \text{D.1}$$

This formula (D.1) assumes that negligible carbon monoxide is produced in the combustion process. This is verified by the experimental observation eg maximum carbon monoxide reading was 0.8%.

The two methods of calculation described above should give the same results. Unfortunately this is not the case as Table D.7 illustrates.

The reason that only eight values are shown in the table is that these are the only runs in which either all the air flow was known or the cyclone oxygen reading was reliable. Since in runs C1-C8 the view port air was not monitored. For runs P1 and P2 the diaphragm on the vaccuum pump had ruptured and hence atmospheric air was introduced into the sampling system causing erroneously high oxygen concentrations.

The results summarized in Table D.7 show that the oxygen readings in the cyclone indicate a higher solids flow rate than was measured directly. The average percentage difference between the two sets of calculations was 27.56%. This difference is quite high and could represent a significant difference when the results are used in the computer simulated combustion model.

It was thus decided to compare the results for the simulated combustion using both the indirect and direct methods for solids flow. These results are given in chapter 4 of the main report.

Table D.7. Comparison of the methods of calculating the solids feed rate.

Run number	Solids flow rate (Kg/s) x 10^{-3} Direct calculation	Indirect calculation	Percentage difference
P3	6.0554	8.2775	+26.85
P4	7.9355	12.7643	+37.83
CP1	5.1153	7.0336	+27.27
CP2	6.0554	8.4816	+28.61
CP3	6.9954	9.6568	+27.56
CP4	7.9355	11.0808	+28.39
C9	9.8156	11.2383	+12.66
C10	7.9355	11.5565	+31.33
			Σ 220.5
			% 27.56

COMMENTS ON THE RESULTS FOR THE GAS ANALYSIS

It is evident from studying Tables D.1-D.6 that the volume fractions of oxygen carbon dioxide and carbon monoxide do not sum to 21%.

Since very little carbon monoxide is produced (< 0.8%) the total volume fraction that these gases should occupy is 21%. If appreciable carbon monoxide is produced then this value should be larger than 21%.

The total measured volume fraction for these gases is consistently around 19% and this presents a puzzling problem. One explanation would be the presence of volatile matter in the feed char. However, a periodic check showed that the volatile content of the wood char was negligible (<0.5% by weight) and so ruled out this possibility.

Another possible cause could be that the analysis equipment was faulty. The analyzers were, however, recalibrated at the beginning of each day and then checked at the end of the day to see how much "drift" had taken place. This "drift" was on the order of 0.5% for the oxygen and carbon dioxide test equipment and 0.05% for the carbon monoxide analyzer. The oxygen analyzer was also checked with another calibration gas and was found to be accurate to within ±0.5% . Thus for typical values found in the test runs (~12%) this represents an error of about 4.2%. Hence it would seem that the oxygen analysis equipment was fairly reliable. The other equipment

is, however, somewhat suspect although the results obtained were often checked with Fyrite chemical analysis and found to be in agreement.

There is still no explanation of why the gas analysis gives lower results than that predicted by the chemical stoichiometry.

APPENDIX E

THE TERMINAL VELOCITIES OF CARBON CHAR PARTICLES

TERMINAL VELOCITIES OF NON-SPHERICAL PARTICLES

Since the char particles used as feed stock in the reactor are, in general, non-spherical it is important to see the effect of non-sphericity on the terminal velocities of such particles.

Since the gas velocities in the reactor are less than 2 m/s we have fairly low Reynolds numbers for the particles. This does not mean that all the particles are described by Stokes Law. However the particles Reynolds Number (Re_s) will not, in general, exceed 200.

The approach adopted to evaluate the particle free fall velocity is based on that given by Becker ([30]).

We may write the drag force on a particle falling in a fluid as:

$$F_d = \frac{\pi d_p^2 V^2 \rho}{8\psi} \left(\frac{24}{Re_s} + C_1\right) \qquad \text{E.1}$$

and at the same time the net force on the particle due gravity is

$$F_g = M_p (\rho_p - \rho) g \qquad \text{E.2}$$

A particle falling under the influence of gravity will accelerate until the drag force just balances the gravitational force, after which it will continue to fall at a constant velocity. This is known as the terminal velocity. Thus by combining equations E.1 and E.2 we have

$$\frac{\pi d_p V_t^2 \rho}{8\psi} \left(\frac{24}{Re_s} + C_1\right) = M_p (\rho_p - \rho) g \qquad \text{E.3}$$

now $M_p = \frac{\pi}{6} d_p^3 e_p$ and substituting in E.3 we get

$$V_t = \sqrt{\frac{4}{3} \frac{d_p(\rho_p - \rho)\, g\psi}{(\frac{24}{Re_s} + C_1)}} \qquad \text{E.4}$$

The same approach as used above may be applied to spherical particles. In this case the surface sphericity will of course be unity and K_d may be expressed in a more convenient form.

From equation (E.4) it becomes obvious that to evaluate the terminal velocity of a given particle in a given fluid all that is required is the drag coefficient K_d.

where $$K_d = \frac{24}{Re_s} + C_1$$

There has been some work done on the evaluation of K_d by Knudsen and Katz (18) and Zenz and Othmer (17) however much of this work is related to particles having a Reynolds Number greater than about 1000. For Reynolds Number less than this the only reference found was by Becker (30). In this paper the drag coefficient for different ranges of Reynolds Number are presented. In Table E.1 taken from the above paper, the correlations for drag coefficients are given as well as information relating to the orientation and type of wake formed during motion.

Using the correlations for drag coefficient given above a computer

program was written to evaluate the terminal velocities for different size and density particles. The results are given in Figure E.1.

The dotted line in Figure E.1 represents the terminal velocity of the char particles - this curve uses the correlation for density vs. particle size and thus crosses the constant density curves at the particle diameter for which that density occurs.

There appears to be certain kinks in the curves of Figure E.1. These occur due to the different correlations used and can be accounted for by the fact that the correlations only give continuity in the terminal velocity function and not in its derivative. Hence there will be certain discontinuities in derivative at the points where the correlation changes - hence, the kinks.

The dotted line in Figure E.1 was used in the computer program to estimate the terminal velocities of the particles.

Table E.1. The correlations for C_1 for the various ranges of Reynolds Number.

Re_s	Flow regime	Wake	Free orientation	Inertial drag coefficient
0.1	Viscous	Irrotational	All orientations are stable when there are three or more perpendicular axes of symmetry	Inertial drag is negligible
0.1-5.5	Transition I			For angular bodies assume $C_1 = 2.25$
5.5-200	Transition II	Fixed vortices	Stable in position of maximum drag	$C_1 = 2.25 \left(\frac{5.5}{Re_s}\right)^{0.34\sqrt{\phi}}$ For non-stagnant fluid assume $C_1 = 2.53 - 0.283\, e^{2.3\psi}$ when this gives the greater value of C_1
200-500	Transition III	Periodic discharge of vorticity	Unpredictable discs and plates tend to wobble, while fuller blunt bodies tend to rotate	$C_1 = 2.53 - 0.283\, e^{2.3\psi}$ for $\psi < 0.8$
500-300	Transition IV	Increasing disorder		
$3\text{-}200 \times 10^3$	Inertial I	Fully turbulent	Rotation about axis of least inertia, frequently coupled with spiral translation	$C_1 = 2.53 - 0.283\, e^{2\psi}$
2×10^5	Inertial II	Boundary layer becomes turbulent. Wakes of rounded bodies narrow		Coefficients for rounded bodies decrease as the wake narrows

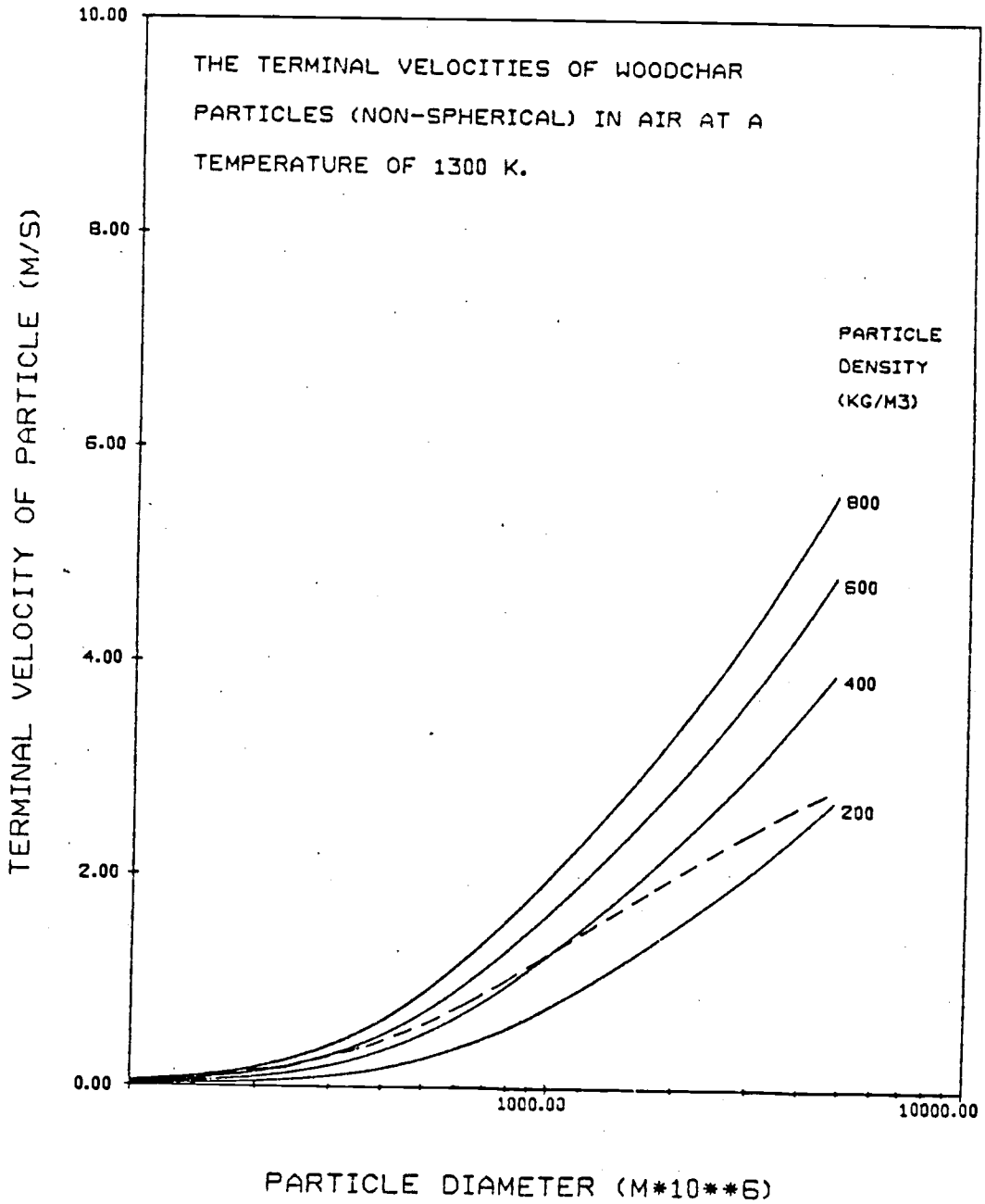

Figure E.1. The Terminal Velocity of Non-spherical Particles (Form Sphericity = 0.63 Surface Sphericity = 0.40).

APPENDIX F

REACTION RATES FOR THE COMBUSTION OF CARBON

THE REACTION RATES FOR COMBUSTION

When the design or simulation of a chemical reactor is considered, one of the most important factors is how fast will the desired reaction take place. The rate of reaction is dependent upon several factors and to accurately predict the reaction kinetics these factors must be understood and suitably combined.

For the case of heterogeneous reactions (i.e. between two or more different phases), the kinetic model may be quite complicated. Thus, the following discussion considers the situation for a solid gas reaction and the important points are outlined and briefly summarized.

There are several ways to describe the combustion of a wood char particle but these may be split, in general, into two classes. The first class of model considers the reaction between atmospheric oxygen and carbon to occur only on the exterior surface of the particle. While the second type of model allows for diffusion into the particle and hence reaction within the main bulk of the particle as well as at the exterior surface. These two types of model will be treated separately.

THE SHRINKING SPHERE MODEL (S.S.M.)

The shrinking sphere model assumes that the carbon particle may be considered as a solid ball of carbon with negligible internal pore

structure. The model assumes that any ash present in the original particle is uniformly distributed and continuously flakes off when exposed by reaction. Thus, the particle is seen to retain its spherical shape throughout its combustion history. A pictorial representation of what happens when the S.S.M. is obeyed is given in Figure F.1.

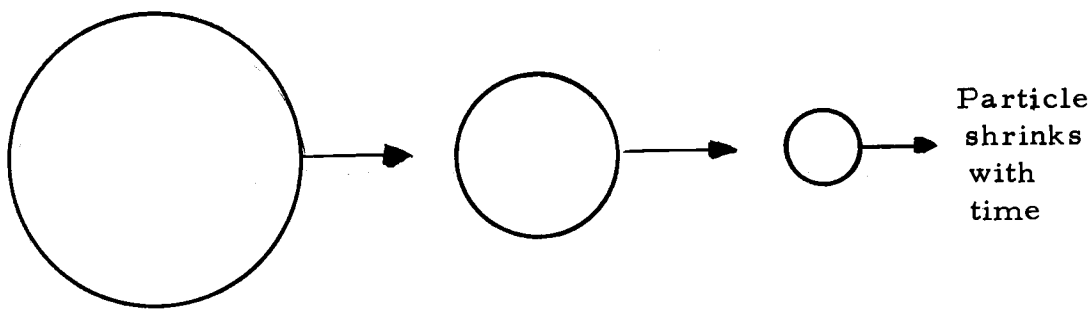

Figure F.1. Behavior in S.S.M.

If the original diameter of the particle was d_{P_o} and the diameter after combustion was d_p then the conversion for the single particle is given by

$$X_A = 1 - \rho_{p_o} d_{p_o}^3 / \rho_p d_p^3$$

For this model of combustion there are two resistances to reaction. The first resistance is that associated with the chemical absorption-desorption reaction which occurs at the exterior surface of the particle. The chemical reaction taking place is assumed to be

$$C + O_2 \rightarrow CO_2$$

The second resistance to reaction occurs when the oxygen diffuses

through the stagnant film of gas surrounding the particle. The rate constant for this mass transfer step is denoted k_{diff}.

If now an overall reaction rate coefficient k_{ov} is defined by:

$$\frac{\text{Rate of Reaction of Carbon}}{\text{Surface Area}} = -k_{ov}\, y_{o_2} \qquad \text{F.1}$$

Then it can easily be shown that the following relationships hold:

$$\frac{1}{k_{ov}} = \frac{1}{R_{chem}} + \frac{1}{k_{diff}} \qquad \text{F.2}$$

$$\overline{R}_{ov} = \overline{R}_{chem} + \overline{R}_{diff} \qquad \text{F.3}$$

Equation (F.3) shows that the resistances due to the two steps of the reaction (i.e. the mass transfer of gaseous reaction to the particle surface and the subsequent chemical reaction) act in series. Thus, the overall reaction rate must be smaller than either of the individual step rates.

There has been extensive work on the chemical reaction rates of carbon combustion. The most usual way to express such a reaction coefficient is in the form of an Arrhenius equation. The correlation used in this work was taken from Parker and Hottel ( ) and the form used is slightly different from the normal Arrhenius type since a $T_s^{-1/2}$ term is also included. The expression for the reaction rate is given by

$$K_{chem} = 7.9583 \times 10^3 \times P \times \exp(-44000/RT_s)/\sqrt{T_s}\ \frac{\text{moles}}{M^2 S} \qquad \text{F.4}$$

The diffusion coefficient is taken from an equation due to Ranz and Marshall (23) and is given below.

$$k_{diff} = \frac{D}{d_p} (2+0.6\ Re_p^{1/2}\ Sc^{1/3}) \times P/RT_g \quad \frac{moles}{M^2S} \qquad F.5$$

The terms used in equation (F.4+F.5) above are defined at the back of this work and the correlations used for the computer program are also given.

From the above 2 equations it can be seen that the chemical reaction term is very dependent upon temperature while the diffusion coefficient is relatively insensitive to temperature change. However, the diffusion coefficient is greatly effected by the size of particle (R_{chem} is not dependent upon size). Thus for relatively small particles at low temperatures--the rate controlling step is the chemical reaction at the particle surface. On the other hand for large particles at high temperatures the mass transfer step becomes controlling. When either of these two extremes takes place and one of the resistances becomes so small relative to the other, that it may be safely ignored. Then the burning times for complete conversion are given by simple analytical expressions (assuming constant gas composition and isothermal operation).

The subject of the shrinking sphere model and various other reaction models is dealt with extensively by Levenspiel (8). It is from this

reference that the following table (F. 1) of burning times is taken.

For the situation when neither of the two resistances can be ignored the burning time can be found by adding the burning times for the two different extremes. Thus we can write

$$\tau_{total} = \tau_{film\ only} + \tau_{reaction\ only} \qquad F.6$$

The overall reaction rates for this model is plotted in Figure F. 1 which shows the effect of different gas velocities, particle sizes and temperature.

Table F.1 The burning times of a carbon particle following the shrinking sphere model

Regime	Film diffusion controls	Reaction controls
Small particle Stokes Regime	$\frac{t}{\tau} = 1 - (1-X_A)^{2/3}$	$\frac{t}{\tau} = 1 - (1-X_A)^{1/3}$
	$\tau = \frac{\rho_p d_{p_o}}{4\, k_{diff} Y_{o_2}}$	$\tau = \frac{\rho_p d_{p_o}}{2\, k_{chem} Y_{o_2}}$
Large particle constant velocity	$\frac{t}{\tau} = 1 - (1-X_A)^{1/2}$	$\frac{t}{\tau} = 1 - (1-X_A)^{1/3}$
	$\tau = (\text{const}) \frac{d_{p_o}^{3/2}}{y_{o_2}}$	$\tau = \frac{\rho_p d_{p_o}}{2\, k_{chem} y_{o_2}}$

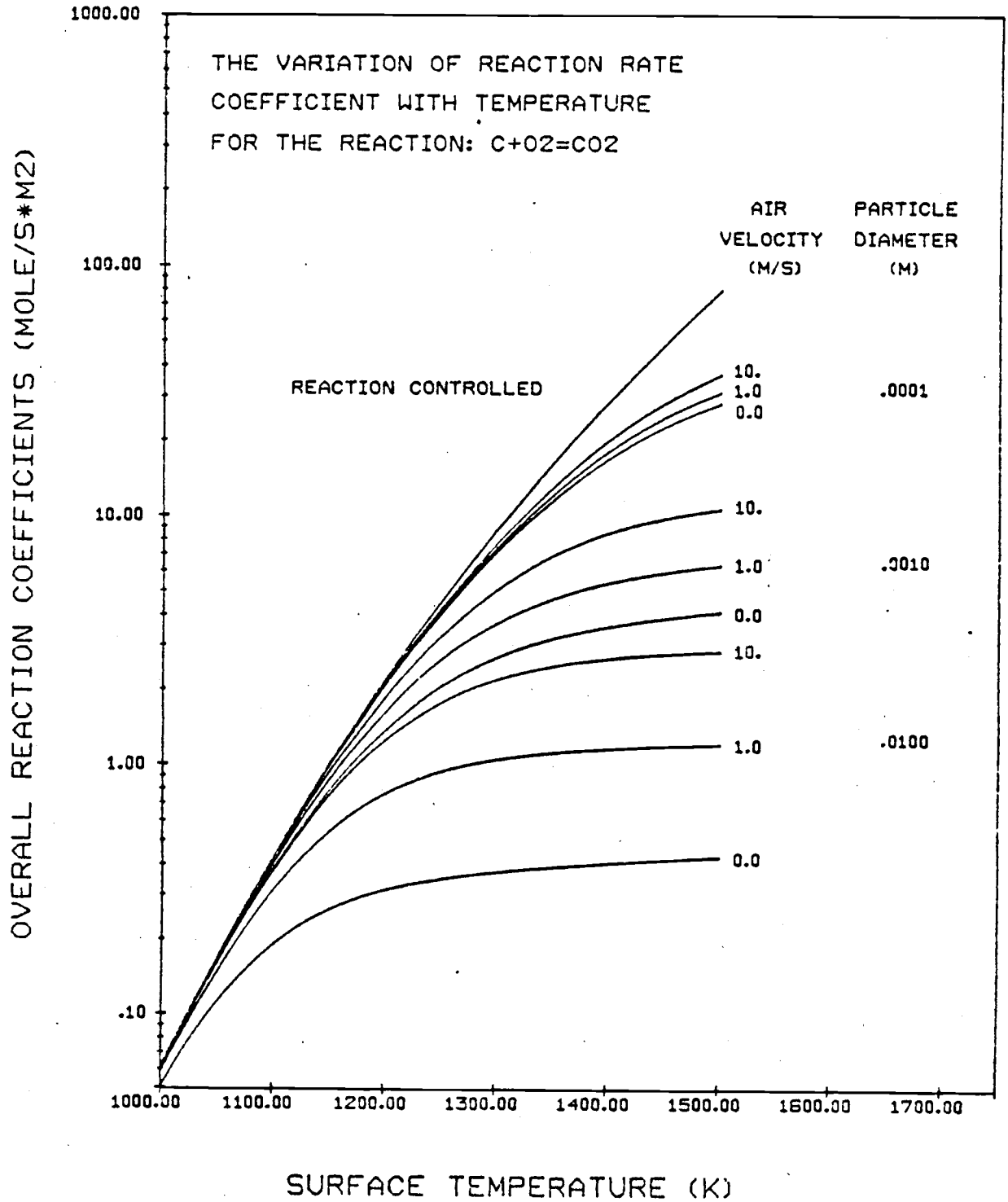

Figure F.2. Shrinking Sphere Kinetics.

THE EFFECT OF INTERNAL SURFACE AREA ON REACTION RATES

In the shrinking sphere model, only the chemical reaction taking place on the external surface of the particle, was considered. However, if extensive internal surface area exists within a particle then the chemical reaction rate predicted by the S.S.M. will be a gross underestimate. Therefore, for porous particles a new combustion model must be used, one which accounts for chemical reaction within the particle.

The chemical reaction rate coefficient may be expressed in the following form:

$$k'_{chem} = k_{chem} + \frac{r}{3} k_{chem} S_{int} \rho \varepsilon \qquad \text{F.7}$$

the first term on the right hand side of equation F.7 simply accounts for the reaction at the particle surface. The second term, however, accounts for the reaction within the particle. The R/3 term is simply the ratio of volume to surface ratio for a sphere and is necessary because the reaction coefficients must be computed on a surface area basis. The last term in equation F.7, namely ε, is known as the effective efficiency and reflects how much internal sufrace area is available for reaction. For low temperature and small particles, where the resistance to diffusion is small, the value of ε approaches unity.

This means that there is no concentration gradient within the pellet and the whole interior is bathed with gas at the bulk concentration existing in the main air stream.

The value of ε has quite a complicated form, which for spherical particles is most easily expressed as:

$$\varepsilon = \frac{3}{\delta}\left(\frac{1}{\tanh(\delta)} - \frac{1}{\delta}\right)$$

where $$\delta = \frac{d_p}{2}\sqrt{R_{chem} S_{int} / D_{eff}}$$

From equation F.7 it becomes obvious that the chemical reaction term will be very dependent upon the particle size and the internal surface area, two factors which were not considered in the S.S.M.

The overall reaction coefficient is given below, the mass transfer coefficient is the same as given in equation F.5 for the S.S.M.

The important point to be noted from the introduction of the internal surface area term is that the reaction term may be several orders of magnitude greater than for the S.S.M. This means that film diffusion will become limiting at much lower temperatures for a given particle size. This effect is shown quite clearly when Figures F.2+ F.3 are compared. Figure F.3 shows the variation of overall reaction rate when internal surface area affects are considered.

From the above discussion on reaction rates it becomes apparent

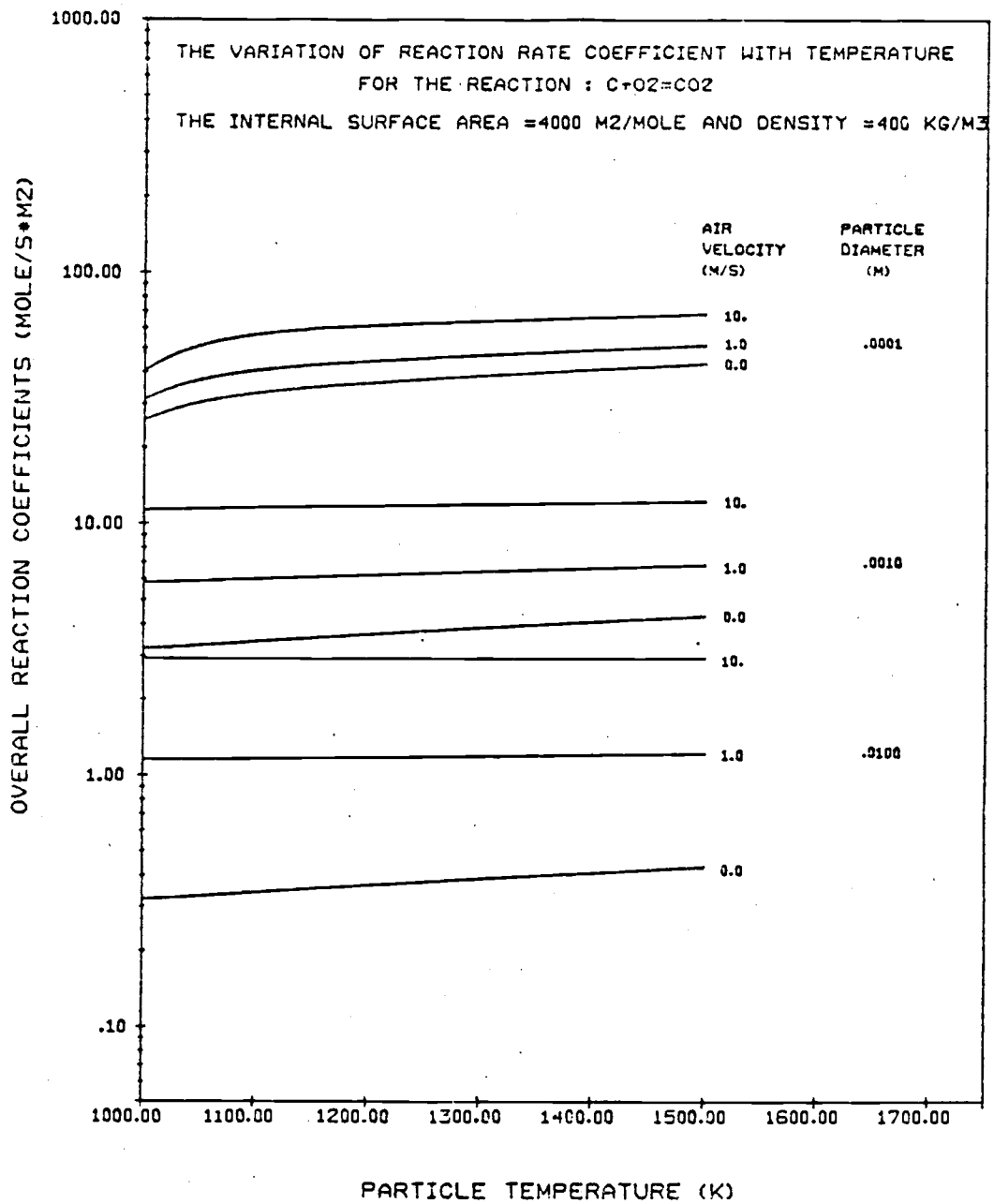

Figure F.3. The Reaction Rate for a Porous Carbon Particle.

that the internal surface area may have a profound effect on the rate of reaction for the wood char particles. This point is illustrated in the following example:

Example F.1

Calculate the time for complete combustion of a carbon particle 1 mm in diameter in a gas stream with $Y_{o_2} = 0.1$ at 1000 K (assume $e_p = 4.0 \times 10^4$ mole/M^3)

(A) If the particle is non-porous then we have from Table F.1

$$\tau = \frac{\rho_p d_{p_o}}{2\, k_{chem} y_{o_2}} = \frac{4.0 \times 10^4 \times 10^{-3}}{2 \times .1 \times 0.06} = \underline{55.6 \text{ mins}}$$

(B) If the particle is porous then we have from Table F.1

$$\tau = \frac{\rho_p d_{p_o}}{4\, k_{diff} y_{o_2}} = \frac{4.0 \times 10^4 \times 10^{-3}}{4 \times .1 \times 3.2} = \underline{31.3 \text{ secs}}$$

APPENDIX G

COMPUTER PROGRAMS

The object of this appendix is to list the computer programs which were used in this work and to briefly explain the terms used.

The Computer simulated combustion model. There are basically two programs used in the model. The main program, which is given in Table G. 1, contains the logic of putting the various elements of the model together. The second program, Table G. 2, contains the various elements of the model along with such functions as specific heats, thermal conductivities, reaction rates, etc.

The logic used in the main program is illustrated in the flow diagram of Figure G. 1. The terms used in both programs are listed below

The other programs used in the thesis. The programs used to calculate the orifice and venturi flow meter calibration table, the terminal velocity plot, and the reaction rate plot are listed in Tables G. 3-G. 6. Although certain other programs were used due to their simplicity it was decided not to include them here.

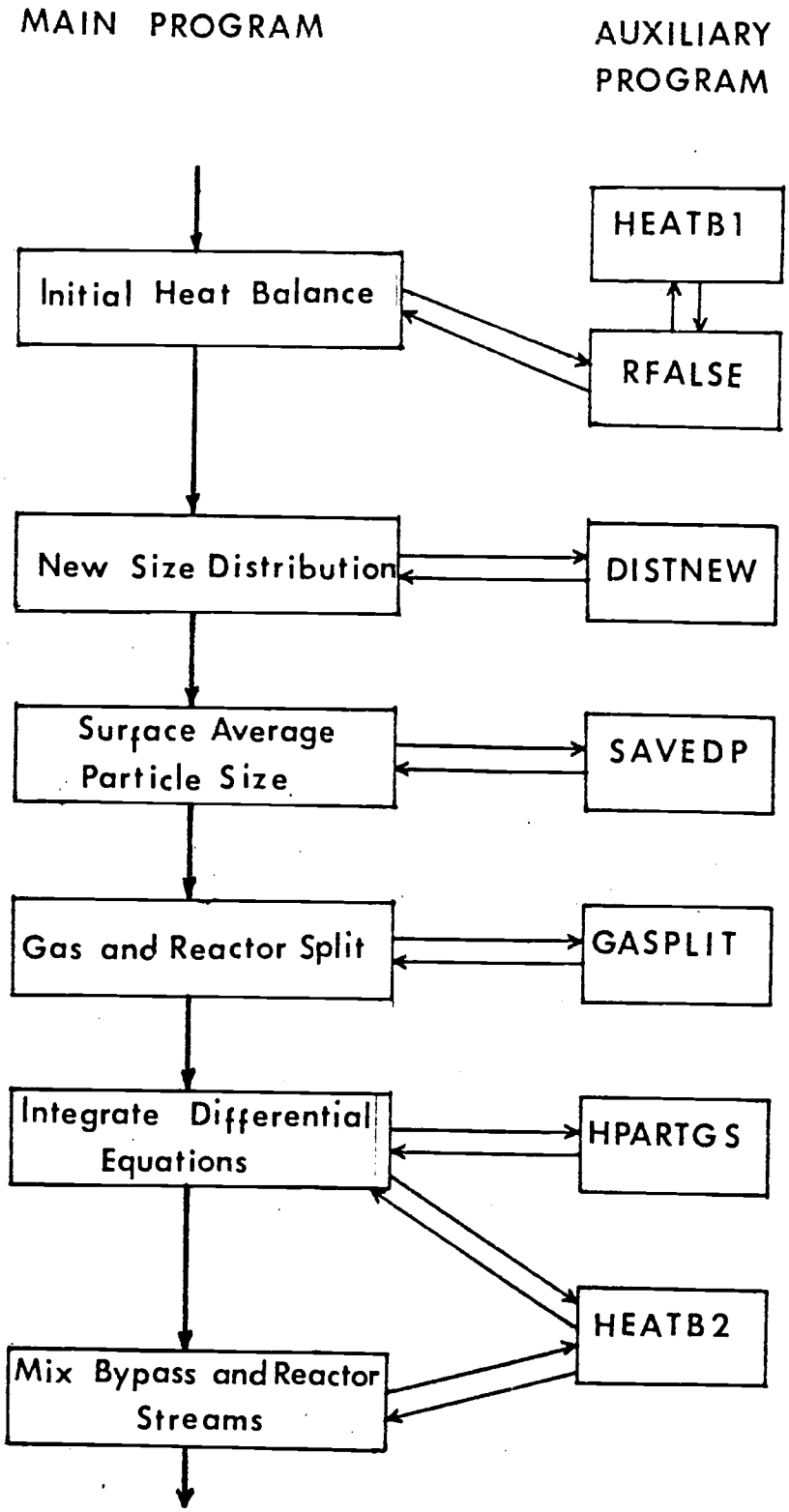

Figure G.1 : INFORMATION FLOW DIAGRAM FOR THE COMBUSTION PROGRAM

List of Input Parameters for the Main Program

FUDV - This is a parameter which alters the terminal velocity of a particle. The actual terminal velocity calculated is FUDV times the value predicted by the correlation (20).

LAB - This is a flag variable which when set less than two allows all the particles to move with the gas i.e. set the terminal velocity to zero.

DP - Vector of particle sizes used to describe the particle size distribution

WFR - Vector of weight fractions for the particle sizes stored in DP.

D2 - The inside diameter of the reactor

Fϕ - The mass flow rate of solids to the reactor

FRWATER - The weight fraction of water in the solids

Alpha - The weight fraction of combustible material (assumed to be carbon) in the solids.

TGAS - The temperature of incoming air.

TSOL - The temperature of incoming solids.

FGASM - The molar flow rate of the main combination air stream.

FVIEWG - Vector containing the molar flow rates of the view port air streams.

List of subprograms from the second part of the main program (Table G. 2)

SUBROUTINE HEAT B2

This subroutine solves the general heat and mass balance for the situation where a stream of hot gas and particles mix with a stream of cold gas.

The mass balance is solved explicitly, since it is assumed that reaction does not take place.

The heat balance, however, does not have an analytical solution. The temperature of the gas and solids leaving the mixing zone must be found by trial and error. This trial and error calculation is carried out within the subroutine using an interval halving technique. The temperature is found correct to the third significant figure.

The variables used in calling the subroutine are listed and briefly explained below.

HS - Molar flow of hot solids

HG - Molar flow of hot gas

HYO2 - On input - oxygen mole fraction in hot gas

On output - oxygen mole fraction in exit gas

HYN2 - On input - nitrogen mole fraction in hot gas

on output - nitrogen mole fraction in exit gas

HYCO2 - On input - carbon dioxide mole fraction in hot gas

On output - carbon dioxide mole fraction in exit gas

TH - Temperature of hot gas and solids

CG - Molar flow of cold gas

CYO2 - Oxygen mole fraction in cold gas

CYN2 - Nitrogen mole fraction in cold gas

CYCO2 - Carbon dioxide mole fraction in cold gas

Q - An additional heat input, if required.

TC - Temperature of cold gas

HTOT - Total gas flow leaving mixing zone

TF - The best estimate of the exit temperature.

The units used in the above subroutine and any of the following programs must be consistent.

SUBROUTINE GASPLIT

This subroutine simply evaluates the gas and reactor volume splits used in the model. The calling parameters are given as:

BETA - The gas split parameter

GAMMA - The reactor volume split parameter

F1 - Gas flow into the reaction section

F2 - Gas flow into the bypass section

RS1 - The cross sectional area of the reaction section

RS2 - The cross sectional area of the bypass section

The range of both beta and gamma is from zero to one.

SUBROUTINE DISTNEW

The particle size distribution entering the reaction section of the model is evaluated. The combustion in the initial heat balance (HEATB1) is accounted for and the new weight fractions for the various particle sizes are determined.

The calling parameters are:

SUM - The amount of carbon removed by the size reduction of larger particles to an entrainable particle size.

DPR - The largest particle entrained by the gas stream.

J - The index of the largest particle size in the original size distribution, which is entrained by the gas stream.

L - The index of the largest particle size, in the original size distribution, which does not completely burn in the initial heat balance.

SUMN - The amount of carbon removed by the combustion of the very small particles in the initial heat balance.

All the above parameters are evaluated in the initial heat balance (see HEATB1) and are transferred in the common block named 'DISTN'.

SUBROUTINE RFALSE

This subroutine evaluates the root of a given function, which is known to be between two points. The technique used to evaluate the

root of the function is an interval halving procedure. The calling parameters are:

X1 - The left hand guess at the root

X2 - The right hand guess at the root

XAPP - On output - the best estimate of the root

N - The maximum allowable function evaluations

ER - An error criterion. A root is found so that the absolute error in the root is less than ER.

FN - A user specified external function 0 the root of which is required. The function should be of the form of FN(X) where X is the guess at the root and the output value is the value of the function at X.

The values of the function for X1 and X2 must have different signs and the function must be unimodal for convergence to be guaranteed.

FUNCTION HEATB1

This function subprogram evaluates the error in the initial heat balance for a given input temperature. The correct temperature which satisfies this heat balance can be found by using this function in conjunction with a root finding technique (in this case it is most convent to use RFALSE).

FUNCTION SPECIF

This function evaluates the specific heat for a substance at a given input temperature. The relevant parameters are given below:

T - Input temperature

I - Index of the substance under consideration where:

I = 1 oxygen

I = 2 nitrogen

I = 3 water vapour

I = 4 carbon dioxide

I = 5 carbon (graphite)

A(I)
B(I)
C(I)

These are the coefficients required to evaluate the the specific heats. The values used here are taken from Smith and Van Ness (29).

FUNCTION CPHEAT

This function calculates the enthalpy change of a substance due to a change in temperature.

T1 - Final temperature

T2 - Initial temperature

I - Index of substance (see (SPECIF))

A(I), B(I), C(I) - (see SPECIF)

FUNCTION ENTHAL

This function evaluates the standard heat of reaction at a given temperature for the combustion of carbon yielding carbon dioxide.

T - Temperature at which reaction takes place.

FUNCTION HYPTANN

This function evaluates the hyperbolic tangent of a number.

FUNCTION SAVE DP

This function evaluates the surface average particle diameter for a discrete distribution of particles.

I - Is the index of the largest particle size in the distribution

L+1 - Is the index of the smallest particle size in the distribution.

FUNCTION RKOV

This function evaluates the overall reaction coefficient for the combustion of carbon to yield carbon dioxide.

T - The temperature of the particle.

TVEL - The relative velocity of the particle with respect to the gas.

DP1 - The equivalent spherical diameter of the particle.

FUNCTION TERVEL

This function evaluates the terminal velocity of a particle in air at a given temperature.

LAB - This is an index which when set less than two gives a zero terminal velocity. If LAB is greater than two then the terminal velocity is computed from a correlation given by Becker (20).

DPM - This is the equivalent spherical diameter of the particle.

T - The temperature of the gas.

VOLDPF - Form sphericity

SPHERIF - The reciprocal of the surface sphericity.

VISC - Viscosity of air. The correlation is taken from Perry and Chilton (30).

FUNCTION DPTERVL

This function calculates the equivalent spherical diameter of a particle given the air temperature and the particle terminal velocity.

LAB - This is an index which when set less than two gives a particle size greater than any in the particle size distribution. If Lab is greater than two then the particle size is found using the Becker Correlation (20).

VEL - The terminal velocity of the particle.

T - The gas temperature.

FUNCTION PDENSE

This function evaluates the density of a wood char particle of a given size.

DP1 - The size of the wood char particle.

FUNCTION PSAREA

This function evaluates the internal surface area of a wood char particle.

DP1 - The size of the wood char particle.

FUNCTION THCOND

This function evaluates the thermal conductivity of air at any required temperature.

FUNCTION HTCOGAS

This function evalautes the convective heat transfer coefficient from the walls of the reactor to the combustion gas. The Colburn (24) analogy is adopted and a friction factor of 0.01 is assumed.

T1 - Gas temperature.

T2 - Reactor wall temperature.

FUNCTION HEATTC

This function evaluates the heat transfer coefficient for a particle travelling in a gas.

The correlation used is the Ranz and Marshal equation (23).

T1 - Particle temperature

T2 - Gas temperature

V - The relative velocity of the particle and gas.

DP1 - The size of the particle.

SUBROUTINE HPARTGS

This subroutine contains the differential equations which describe the reaction process.

The subroutine integrates the various variables over a step length of given size.

TP - Vector of particle temperatures

DPART - Vector of particle sizes

XAPART - Vector of particle conversions

TG - Gas temperature

YO2G - Mole fraction of oxygen in the gas.

YCO2G Mole fraction of carbon dioxide in the gas.

DL - Step length for integration

RL - Total length travelled in the reactor.

FCϕ - Flow rate of solids initially entering the reactor section

FGϕ - Initial flow rate of gas entering the reactor section

Fϕl - Flow rate of solids entering the reactor.

XABAR - Overall conversion of carbon in the reactor.

Table G.1. The main program for the combustion simulation.

```
      PROGRAM   THES(INPUT,OUTPUT,TAPE6=OUTPUT,TAPE8,TAPE9)
      DIMENSION FVIEWG(3),XPOINTS(101),YPOINTS(101),YT(2)
      DIMENSION ZPOINTS(101),TP(10),RLENGTH(3),DPART(10),XAPART(10)
      DIMENSION APOINTS(101),BPOINTS(101),CPOINTS(101)
      EXTERNAL HEATB1
      COMMON/DAD/LAB
      COMMON/BROTH/FUDV
      COMMON/HTCOEF/A(5),B(5),C(5)
      COMMON/HEATER/QCONVEC,QRADIAT
      COMMON/PLUG/RNUMPAR,FG1,FG2,RSC1,RSC2
      COMMON/DISTN/SUM1,SUM2,JN1,JN2,YO2,YCO2,DP1
      COMMON/PARTCLE/DP(10),WFR(10)
      COMMON/REACTOR/D1,D2,RHT1
      COMMON/RINFO/DPP1,FGASM,FCAR,ALPHA,FO,TGAS,TSOL,DPBAR,FRWATER
      DATA(DP(I),I=1,9)/22.5E-06,54.E-06,94.E-06,
     * 188.E-06,375.E-06,750.E-06,1500.E-06,2665.E-06,4013.E-06/
      DATA (WFR(I),I=1,9)/.0329,.0576,.0629,.0539,.1233,.251,.2554,
     * .1289,.0341/
      DATA (FVIEWG(I),I=1,3)/3.071E-04,3.071E-04,6.142E-04/
      DATA D1,D2,RHT1/0.1524,0.762,0.508/
      DATA (A(I),I=1,5)/7.16,6.83,7.30,10.57,4.03/
      DATA (B(I),I=1,5)/1.E-03,.9E-03,2.46E-03,2.1E-03,
     * 1.14E-03/
      DATA (C(I),I=1,5)/-.4E+05,-.12E+05,0.0,-2.06E+05,
     * -2.04E+05/
      DATA FRWATER,FO,ALPHA,TGAS,TSOL,FGASM/0.0477,7.9355E-03
     * ,0.7573,305.2,285.,5.8347E-03/
      DATA (RLENGTH(I),I=1,3)/0.4999,1.4999,2.4999/
      DATA FUDV,LAB/1.5,3/
C
C
      FCAR=FO*ALPHA/12.
      CHINORG=1.-FRWATER-ALPHA
      WRITE(6,35)FO,TSOL,ALPHA,FRWATER,CHINORG,FGASM,TGAS,
     * (FVIEWG(I),I=1,3)
   35 FORMAT(//////2X,*THE RESULTS FOR THE SIMULATED COMBUSTION MODEL*,
     * * TEST RUN C10*,
     * //2X,*THE INLET CONDITIONS FOR AIR AND WOODCHAR*,//2X,
     * *FLOWRATE OF SOLIDS =*,E12.4,* KG/S*,/2X,*TEMPERATURE OF SOLIDS*,
     * *=*, F6.1,* K*,/2X,*COMBUSTIBLE CONTENT = *,F6.4,/2X,
     * *MOISTURE CONTENT    =*,X,F6.4,/2X,*INORGANIC CONTENT   =*,X,
     * F6.4, //2X, *MAIN AIR FLOWRATE   =*,X,E12.4,* KMOLE/S*,/2X,
     * *TEMPERATURE OF AIR   =*,2X,F6.1,* K*,/2X,
     * *AIR FOR VIEW PORT 1  =*,E12.4,* KMOLE/S*,/2X,
     * *AIR FOR VIEW PORT 2  =*,E12.4,* KMOLE/S*,/2X,
     * *AIR FOR VIEW PORT 3+4=*,E12.4,* KMOLE/S*,//)
C
      WRITE(6,36) (DP(I),I=1,9)
   36 FORMAT(2X,*THE INLET SIZE DISTRIBUTION FOR THE SOLIDS FEED*,
     * //2X,*MEAN DIAMETER (M)     *,9E11.4)
      DO 39 I=1,9
   39 DP(I)=DP(I)*0.6
      WRITE(6,38) (DP(I),I=1,9),(WFR(I),I=1,9)
   38 FORMAT(2X,*SPHERICAL DIAMETER (M)*,9E11.4,/2X,
     * *WEIGHT FRACTION   *,9E11.4,//)
C
      BETA=1.0
      GAMMA=1.0
      CALL GASPLIT(BETA,GAMMA,FG1,FG2,RSC1,RSC2)
```

```
      X1=290.
      F1=HEATB1(X1)
      X2=X1
   20 X2=X2+500.
      F2=HEATB1(X2)
      TS=F1*F2
      IF(X2.GT.1500.) GOTO 40
      IF(TS.LT.0.0) GOTO 30
      GOTO 20
   40 WRITE(6,45)
   45 FORMAT(2X,*THE INITIAL HEAT BALANCE DOES*,
     * *NOT HAVE A SOLUTION*,////)
      STOP
   30 NITER=50
      ERR=0.001
      CALL RFALSE(X1,X2,XAPP,NITER,ERR,HEATB1)
      WRITE(6,10) XAPP
   10 FORMAT(2X,*THE TEMPERATURE OF THE REACTANTS LEAVING *,
     * *THE INITIAL MIXING ZONE IS *,F6.1,* (K)*,//)
C
C
C     THE NEXT SECTION OF THE MAIN PROGRAM CALCULATES
C     THE NEW SIZE DISTRIBUTION AND EVALUATES THE
C     SURFACE AVERAGE PARTICLE DIAMETER.
C
      CALL DISTNEW(SUM1,DP1,JN1,JN2,SUM2)
      JNEW=JN1+1
      DPBAR=SAVEDP(JNEW,JN2)
      WRITE(6,15) DPBAR
   15 FORMAT(2X,*THE CALCULATED SURFACE AVERAGE PARTICLE *,
     * *DIAMETER IS *,E14.4,* (M)*,/)
C
C
C     THIS PART OF THE PROGRAM EVALUATES THE
C     GASFLOW RATES IN THE REACTION ZONE AND THE
C     BYPASS ZONE OF THE REACTOR.
C
      WRITE(6,55) FG1,RSC1,FG2,RSC2
   55 FORMAT(2X,*GAS FLOW INTO REACTION ZONE =*,F10.4,* KMOLE/S*,/2X,
     * *CSA OF REACTION ZONE        =*,F10.4,* M2*,/2X,
     * *GAS FLOW INTO BYPASS ZONE   =*,F10.4,* KMOLE/S*,/2X,
     * *CSA OF BYPASS ZONE          =*,F10.4,* M2*,//)
C
C
C     THE GASFLOW HAS NOW BEEN SPLIT AND THE
C     PLUG FLOW REACTION EQUATIONS MUST NOW BE SOLVED
C     THE EQUATIONS ARE STORED IN THE SUBROUTINE HPARTGS
C     AND ARE INTEGRATED IN A STEPWISE PROCEDURE WITHIN
C     THE SUBROUTINE
C
      WRITE(6,44)
   44 FORMAT(2X,*THE RESULTS FOR THE PLUG FLOW SECTION*,//)
C
      WRITE(6,43)
   43 FORMAT(/10X,*LENGTH*,5X,*TEMPERATURE*,5X,*CONVERSION*,6X,
     * *M F O2 *,6X,*M F CO2 *,6X,*M F N2 *,/)
C
      YM1=YO2
      YM2=YCO2
      TS1=XAPP
      M=1
```

```
      DO 61 I=1,7
      XAPART(I)=0.0
      IF(WFR(I).EQ.0.0) XAPART(I)=0.999999
      TP(I)=TSOL
      IF(DP(I).LT.100.E-06) TP(I)=XAPP
      IF(DP(I).EQ.DP1) TP(I)=XAPP
   61 DPART(I)=DP(I)
C
      NPTS=800
      DL=3.0/FLOAT(NPTS)
      RL=XPOINTS(1)=0.
      FCO=(FO-SUM1-SUM2)*ALPHA/12.
      YPOINTS(1)=XAPP
      ZPOINTS(1)=YO2
      APOINTS(1)=1.-FCO/FCAR
      BPOINTS(1)=YCO2
      CPOINTS(1)=YN2=0.79
      FG0=FG1
      FO1=FO
      DO 62 K=1,100
      DO 71 KL=1,2
      CALL HPARTGG(TP,DPART,XAPART,XAPP,YO2,YCO2,DL,RL,FCO,
     * FG0,FO1,XABAR)
C
      TEST=ABS((XAPP-YPOINTS(K))/DL)
      IF(TEST.LT.200.)  DL=.04
      IF(TEST.LT.100.)  DL=.04
      IF(TEST.GT.500.) DL=.008
      IF(TEST.GT.1000.) DL=.004
      IF(RL.GE.RLENGTH(M)) GOTO 65
      GOTO 63
   65 Z1=FCO*(1.-XABAR)
      Z2=FVIEWG(M)
      Z3=0.0
      YN2=0.79
      CALL  HEATB2(Z1,FG0,YO2,YN2,YCO2,XAPP,Z2,
     * 0.21,0.79,0.0,Z3,TGAS,Z4,Z5)
      FG0=Z4
      XAPP=Z5
      IF(M.EQ.3) GOTO 66
      GOTO 67
   66 CALL HEATB2(Z1,FG0,YO2,YN2,YCO2,XAPP,FG2,
     * YM1,0.79,YM2,0.0,TS1,Z4,Z5)
      FG0=Z4
      XAPP=Z5
   67 M=M+1
   63 CONTINUE
   71 CONTINUE
      XPOINTS(K+1)=RL
      YPOINTS(K+1)=XAPP
      ZPOINTS(K+1)=YO2
      APOINTS(K+1)=XABAR
      BPOINTS(K+1)=YCO2
      CPOINTS(K+1)=YN2
   62 CONTINUE
      WRITE(9,73) (XPOINTS(I),ZPOINTS(I),I=1,101)
      WRITE(8,73) (XPOINTS(I),YPOINTS(I),I=1,101)
   73 FORMAT(2X,2E14.4)
      WRITE(6,83)(XPOINTS(I),YPOINTS(I),APOINTS(I),
     * ZPOINTS(I),BPOINTS(I),CPOINTS(I),I=1,101,10)
   83 FORMAT(2X,6F14.4)
      WRITE(6,931)
  931 FORMAT(//////////)
      STOP
      END
```

Table G.2. Program containing subroutines for the combustion model.

```
      SUBROUTINE HEATB2(HS,HG,HYO2,HYN2,HYCO2,TH,CG
     * ,CYO2,CYN2,CYCO2,Q,TC,HTOT,TF)
      COMMON/RINFO/DPP1,FGASM,FCAR,ALPHA,FO,TGAS,TSOL,DPBAR,FRWATER
C
C     THIS SUBROUTINE SOLVES THE GENERAL HEAT AND MASS BALANCE
C     FOR HOT GAS (HG) AND SOLIDS (HS) ENTERING WITH COLD GAS (CO).
C     THE EXIT TEMPERATURE (TF) IS COMPUTED AS ARE THE RESULTING
C     MOLE FRACTIONS OF COMPONENT GASES.
C     AN EXTRA HEAT INPUT Q CAN ALSO BE ADDED TO THE HEAT BALANCE
C     THIS CAN TAKE ACCOUNT OF THE HEAT GAINED BY RADIATION AND
C     CONVECTION FROM THE REACTOR WALL.
C
      IF(CG.EQ.0.) GOTO 401
      GOTO 402
  401 TF=TH
      HTOT=HG
      RETURN
  402 I=0
      TF1=0.
      XA=TC
      XB=TH
  400 TF=(XA+XB)/2.
      I=I+1
      IF(I.GT.30) GOTO 410
      DELH1=HG*(HYO2*CPHEAT(TF,TH,1)+HYN2*CPHEAT(TF,TH,2)+
     * HYCO2*CPHEAT(TF,TH,4))+HS*CPHEAT(TF,TH,5)+FO*(1.-ALPHA-FRWATER)
     * *CPHEAT(TF,TH,5)/12.+ FO*FRWATER*CPHEAT(TF,TH,5)/18.
      DELH2=CG*(CYO2*CPHEAT(TF,TC,1)+CYN2*CPHEAT(TF,TC,2)
     * +CYCO2*CPHEAT(TF,TC,4))+Q
      DELHOUT=DELH1+DELH2
C
      TEST=ABS((TF-TF1)/TF)
      IF(TEST.LT.0.001) GOTO 420
      IF(DELHOUT.LT.0.0)  XA=TF
      IF(DELHOUT.GT.0.0) XB=TF
      TF1=TF
      GOTO 400
  410 WRITE(6,430) TF
  430 FORMAT(2X,*THE NUMBER OF ITERATIONS FOR HEATB2 HAS *,
     * *EXCEEDED THE MAXIMUM *,//2X,*THE BEST APPROXIMATION *,
     * *TO THE EXIT TEMPERATURE IS *,F10.2,* (K)*,//,//)
  420 HYO2=(HG*HYO2+CG*CYO2)/(HG+CG)
      HTOT=HG+CG
      HYN2=(HG*HYN2+CG*CYN2)/HTOT
      HYCO2=(HYCO2*HG+CYCO2*CG)/HTOT
      RETURN
      END
C
```

```
C
C
C
C
      SUBROUTINE  GASPLIT(BETA,GAMMA,F1,F2,RS1,RS2)
      COMMON/RINFO/DPP1,FGASM,FCAR,ALPHA,FO,TGAS,TSOL,DPBAR,FRWATER
      COMMON/REACTOR/D1,D2,RHT1
C
C     THIS SUBROUTINE EVALUATES THE SEPARATE GAS FLOWRATES
C     AND CROSS SECTIONAL AREAS FOR THE BYPASS AND REACTION
C     SECTIONS OF THE MAIN REACTOR
C
      F1=BETA*FGASM
      F2=(1.-BETA)*FGASM
      PI=3.14159
      RS1=GAMMA*PI*D2**2/4.
      RS2=(1.-GAMMA)*PI*D2**2/4.
      RETURN
      END
C
C
C
C
C
C
      SUBROUTINE  DISTNEW(SUM,DPR,J,L,SUMN)
      COMMON/PARTCLE/DP(10),WFR(10)
      COMMON/RINFO/DPP1,FGASM,FCAR,ALPHA,FO,TGAS,TSOL,DPBAR,FRWATER
C
C     THIS SUBROUTINE CALCULATES THE NEW WEIGHT FRACTIONS
C     AFTER THE INITIAL HEAT BALANCE AND STORES THEM IN
C     WFR(I).
C     SUM=LOSS IN WEIGHT DUE TO PARTICLE SHRINKAGE
C     J=INDEX OF THE LARGEST PARTICLE SIZE NOT AFFECTED
C     BY THE ENTRAINMENT REACTION
C
      ADD=0.
      JHIGH=J+1
      IF(JHIGH.GE.10) GOTO 640
      DO 600 I=JHIGH,9
  600 ADD=FO*WFR(I)+ADD
  640 FJ=ADD-SUM
      FTOT=FO-SUM-SUMN
      WFR(J+1)=FJ/FTOT
      DP(J+1)=DPR
      NP=L+1
      DO 610 I=NP,J
  610 WFR(I)=FO*WFR(I)/FTOT
      IF(L.LT.1) GOTO 650
      DO 620 I=1,L
  620 WFR(I)=0.0
  650 CONTINUE
      JP=JHIGH+1
      IF(JP.GE.10) RETURN
      DO 630 I=JP,9
  630 WFR(I)=0.0
C
      RETURN
      END
C
```

```
C
C
C
      SUBROUTINE  RFALSE(X1,X2,XAPP,N,ER,FN)
C
C     THIS SUBROUTINE EVALUATES THE ROOT OF A
C     FUNCTION (FN) WHICH IS KNOWN TO LIE BETWEEN
C     X1 AND X2 AND STORES THE ROOT IN XAPP.
C     ER IS AN ERROR CRITERION.....A ROOT IS FOUND
C     SO THAT THE ABSOLUTE ERROR IS LESS THAN ER.
C     N IS THE MAXIMUM FUNCTION EVALATIONS ALLOWED.
C
      TEST=(FN(X1)*FN(X2))
      IF(TEST.GT.0.0) GOTO 800
      I=0
      XN1=X1
  810 I=I+1
      IF(I.GE.N) GOTO 820
      XAPP=(X2+X1)/2.
      TEST=ABS( (XAPP-XN1)/XAPP)
      XN1=XAPP
      IF(TEST.LT.ER) GOTO 830
      A=FN(XAPP)*FN(X1)
      B=FN(XAPP)*FN(X2)
      IF(A.GT.0.0) X1=XAPP
      IF(B.GT.0.0) X2=XAPP
      GOTO 810
  820 WRITE(6,840)
  840 FORMAT(2X,*THE NUMBER OF ITERATIONS HAS EXCEEDED THE *,
     * *ALLOWABLE MAXIMUM*,/2X,*THE BEST APROXIMATION TO THE*,
     * *ROOT IS GIVEN BY XAPP*,//)
      GOTO 890
  800 WRITE(6,850)
  850 FORMAT(2X,*THE TWO STARTING VALUES GIVE THE SAME SIGN *,
     * //)
      STOP
  830 CONTINUE
  890 RETURN
      END
C
C
C
C
C
C
      FUNCTION HEATB1(TEMP)
      DIMENSION DEN(10)
      COMMON/REACTOR/D1,D2,RHT1
      COMMON/PLUG/RNUMPAR,FG1,FG2,RSC1,RSC2
      COMMON/DISTN/SUM1,SUM2,JN1,JN2,YO2,YCO2,DP1
      COMMON/RINFO/DPP1,FGASM,FCAR,ALPHA,F0,TGAS,TSOL,DPBAR,FRWATER
      COMMON/PARTCLE/DP(10),WFR(10)
      COMMON/DAD/LAB
```

```
C     THIS FUNCTION EVALUATES THE ERROR IN THE FIRST
C     HEAT BALANCE ON THE REACTOR.THIS TAKES ACCOUNT
C     OF THE PARTICLES WHICH ARE NOT ENTRAINED DUE TO
C     THEIR LARGE SIZE.
C
      PI=3.14159
      GASVEL=FG1*8.2102E-02*TEMP/RSC1
C
      DP1=DPTERVL(LAB,GASVEL,TEMP)
C
      DO 760 I=1,9
  760 IF(DP(I).LT.0.1E-04) JN2=I
      COUNT=0.
      IF (JN2.LT.1) GOTO 766
      DO 765 I=1,JN2
  765 COUNT=COUNT+F0*WFR(I)
      SUM2=COUNT
      BURNT=COUNT*ALPHA/12.
      GOTO 767
  766 SUM2=BURNT=0.
  767 CONTINUE
C
      M=0
      DO 700 J=1,9
      VELS=TERVEL(LAB,DP(J),TEMP)
      IF(VELS.GT.GASVEL) GOTO 710
  700 M=J
  710 IF(M.EQ.9)GOTO 730
C
      DENDP1=PDENSE(DP1)
      SUM=0.
      DO 705 IL=1,9
  705 DEN(IL)=PDENSE(DP(IL))
      DO 720 K=J,9
      PNUM=6.*WFR(K)*F0/(DEN(K)*PI*(DP(K)*.63)**3)
      SUM=SUM+PI*PNUM*(DEN(K)*(DP(K)*.63)**3-
     * DENDP1*(DP1*0.63)**3)/6.
  720 CONTINUE
C
      SUM1=SUM
      JN1=J-1
C
      CARLOST=SUM*ALPHA/12.+BURNT
      GOTO 750
  730 CARLOST=BURNT
      JN1=9
      SUM1=0.
  750 HEAT1=CARLOST*ENTHAL(TGAS)
      HEAT2=CARLOST*(1.-FRWATER)*CPHEAT(TGAS,TSOL,5)
      YN2=0.79
      YO2=0.21-CARLOST/FGASM
      YCO2=CARLOST/FGASM
      WLATENT=2256.1
      IF(TEMP.LT.373.0) WLATENT=0.
C
      HEAT3=FGASM*(YN2*CPHEAT(TEMP,TGAS,2)+
     * YO2*CPHEAT(TEMP,TGAS,1)+YCO2*CPHEAT(TEMP,TGAS,4))
     * +F0*FRWATER*(WLATENT+CPHEAT(TEMP,TSOL,3))/18.
C
      HEAT4=(F0*(1.-ALPHA-FRWATER)/12.)*CPHEAT(TEMP,TGAS,5)
C
      HEATB1=HEAT1+HEAT2+HEAT3+HEAT4
      RETURN
      END
```

```
C
C
      FUNCTION  SPECIF(T,I)
      COMMON/HTCOEF/A(5),B(5),C(5)
C
C     THIS FUNCTION EVALUATES THE SPECIFIC HEAT FOR
C     SUBSTANCE I AT A TEMPERATURE OF T (K)
C     WHERE I=1.......OXYGEN
C           I=2.......NITROGEN
C           I=3.......WATER VAPOUR
C           I=4.......CARBON DIOXIDE
C           I=5.......CARBON (GRAPHITE)
C
      SPECIF=4.18*(A(I)+B(I)*T+C(I)/(T*T))
      RETURN
      END
C
C
C
C
C
C
      FUNCTION  CPHEAT(T1,T2,I)
      COMMON/HTCOEF/A(5),B(5),C(5)
C
C     THIS FUNCTION CALCULATES THE ENTHALPY CHANGE
C     OF A SUBSTANCE (I) DUE TO A CHANGE IN TEMPERATURE
C     FROM T2 TO T1
C
      CPHEAT=4.18*(A(I)*(T1-T2)+B(I)*(T1**2-T2**2)/2.
     * -C(I)*(1./T1-1./T2))
      RETURN
      END
C
C
C
C
C
C
      FUNCTION ENTHAL(T)
      COMMON/HTCOEF/A(5),B(5),C(5)
C
C     THIS FUNCTION EVALUATES THE STANDARD HEAT
C     OF REACTION AT A TEMPERATURE T (K)
C     FOR THE REACTION  C+O2=CO2
C
      TAU=T/298.
      DELA=A(4)-A(1)-A(5)
      DELB=B(4)-B(1)-B(5)
      DELC=C(4)-C(1)-C(5)
      ENTHAL=4.18*(-94051.+298.*DELA*(TAU-1.)+298.**2*DELB
     * *(TAU**2-1.)/2.+DELC*(1.-1./TAU)/298.)
      RETURN
      END
C
C
```

```
C
C
      FUNCTION  RKOV(T,TVEL,DP1)
      COMMON/RINFO/DPP1,FGASM,FCAR,ALPHA,F0,TGAS,TSOL,DPBAR,FRWATER
C
C     THIS FUNCTION EVALUATES THE OVERALL REACTION
C     COEFFICIENT FOR THE REACTION  C+O2=CO2
C     THE DIFFUSION COEFFICIENT IS A CORRELATION
C     FROM RANTZ + MARSHALL .
C     THE SURFACE REACTION COEFFICIENT IS FROM A
C     PAPER BY PARKER + HOTTEL .THE TERM USED
C     ALSO INCLUDES A TERM ACCOUNTING FOR DIFFUSION
C     INTO THE PARTICLE (IE THIELE MODULUS)
C
      VOLDPF=0.63
      SPHERIF=2.5
      DIFF=7.381E-10*T**1.75
      RHOGAS=353.22/T
      VISC=18.E-07*T**1.5/(120.5+T)
      R=8.2102E-02
      P=1.
      RHO=PDENSE(DP1)
      SAINT=PSAREA(DP1)
      DEFF=9.5E-06*(1.-RHO/2268.)**2
      RE=DP1*SQRT(SPHERIF)*TVEL*RHOGAS/VISC
      SC=VISC/(RHOGAS*DIFF)
C
      RDIFF=DIFF*(2.+0.6*RE**.5*SC**(1./3.))*P/
     * (R*T*DP1)
C
      RCH=7.9583E+06*P*EXP(-(44000./(1.986*T)))/SQRT(T)
C
      PHI=DP1*VOLDPF*SQRT(RCH*SAINT/DEFF)/2.
      IF(PHI.LT.0.1) GOTO 201
      HTAN=HYPTANH(PHI)
      ENETA=3.*(1./HTAN-1./PHI)/PHI
      GOTO 202
  201 ENETA=1.0
  202 RCHEM=DP1*VOLDPF*RCH*SAINT*ENETA*RHO*ALPHA/72.+RCH
C
      RKOV=1./(1./RCHEM+1./RDIFF)
C
      RETURN
      END
C
C
```

```
C
C
C
      FUNCTION  HYPTANH(X11)
C
C     THIS FUNCTION EVALUATES THE HYPERBOLIC TANGENT OF X11
C
      HYPTANH=(EXP(X11)-EXP(-(X11)))/(EXP(X11)+EXP(-(X11)))
      RETURN
      END
C
C
C
C
C
C
      FUNCTION SAVEDP(I,L)
      COMMON/PARTCLE/DP(10),WFR(10)
C
C     THIS FUNCTION EVALUATES THE SURFACE AVERAGE PARTICLE
C     DIAMETER FOR A DISTRIBUTION OF PARTICLES HAVING I-L
C     SEPARATE WEIGHT FRACTIONS (DENSITY IS NOT ASSUMED
C     TO BE CONSTANT)
C
      WRITE(6,105) (DP(K),K=1,9),(WFR(K),K=1,9)
  105 FORMAT(2X,*THE SIZE DISTRIBUTION LEAVING THE INITIAL MIXING ZONE*,
     * //2X,*MEAN DIAMETER (M) *,9E12.4,/2X,*WEIGHT FRACTION   *,
     * 9F12.4,//)
      SUM=0.0
      COUNT=0.0
      MN=L+1
      IF(I.GT.9) I=9
C
      DO 100 J=MN,I
      RHO=PDENSE(DP(J))
      COUNT=COUNT+WFR(J)/RHO
  100 SUM=SUM+WFR(J)/(RHO*DP(J))
      SAVEDP=COUNT/SUM
      RETURN
      END
C
```

```
C
C
      FUNCTION  TERVEL(LAB,DP1,T)
      COMMON/BROTH/FUDV
C
C     THIS FUNCTION EVALUATES THE TERMINAL VELOCITY
C     OF A PARTICLE  (ASSUMED TO BE A DISC WITH A
C     DIAMETER:THICKNESS RATIO OF 5:1) IN AIR AT
C     A TEMPERATURE OF T (K)
C     THE CORRELATION IS FROM BECKER (1959)
C
      IF(LAB.LT.2) GOTO 991
      SPHERIF=2.5
      VOLDPF=0.63
      G=9.81
      RHOGAS=353.22/T
      VISC=18.E-07*T**1.5/(120.5+T)
      RHO=PDENSE(DP1)
      RE=0.1
  920 CD=24./RE+2.25*(5.5/RE)**0.2150
      V1=FUDV*(4.*G*DP1*(RHO-RHOGAS)/(3.*RHOGAS*CD*SPHERIF))**0.5
      RE1=DP1*SQRT(SPHERIF)*RHOGAS*V1/VISC
      TEST=ABS((RE1-RE)/RE1)
      RE=RE1
      IF(TEST.LT.0.001) GOTO 930
      GOTO 920
  930 IF(RE.LT.49.0) GOTO 990
  940 CD=24./RE+1.4051
      V1=FUDV*(4.*G*DP1*(RHO-RHOGAS)/(3.*RHOGAS*CD*SPHERIF))**0.5
      RE1=DP1*SQRT(SPHERIF)*RHOGAS*V1/VISC
      TEST=ABS((RE1-RE)/RE1)
      RE=RE1
      IF(TEST.LT.0.001) GOTO 990
      GOTO 940
  990 TERVEL=V1
      RETURN
  991 TERVEL=0.
      RETURN
      END
C
```

```
C
C
C
      FUNCTION  DPTERVL(LAB,VEL,T)
      COMMON/BROTH/FUDV
C
C     THIS FUNCTION CALCULATES THE DIAMETER OF A
C     PARTICLE WHOSE TERMINAL VELOCITY IN AIR AT A
C     TEMPERATURE=T IS VEL.
C
      FUDD=(1./FUDV)**2
      IF(LAB.LT.2) GOTO 501
      G=9.81
      SPHERIF=2.5
      VOLDPF=0.63
      RHOGAS=353.22/T
      VISC=18.E-07*T**1.5/(120.5+T)
      RHO=400.
      RE=0.1
  503 CD=24./RE+2.25*(5.5/RE)**0.2150
      DP1=FUDD*(VEL**2*3.*RHOGAS*CD*SPHERIF)/(4.*G*(RHO-RHOGAS))
      RHO=PDENSE(DP1)
      RE1=DP1*SQRT(SPHERIF)*VEL*RHOGAS/VISC
      TEST=ABS((RE1-RE)/RE1)
      RE=RE1
      IF(TEST.LT.0.001) GOTO 506
      GOTO 503
  506 IF(RE.LT.49.) GOTO 500
  507 CD=24./RE+1.4051
      DP1=FUDD*(VEL**2*3.*RHOGAS*CD*SPHERIF)/(4.*G*(RHO-RHOGAS))
      RHO=PDENSE(DP1)
      RE1=DP1*SQRT(SPHERIF)*VEL*RHOGAS/VISC
      TEST=ABS((RE1-RE)/RE1)
      RE=RE1
      IF(TEST.LT.0.001) GOTO 500
      GOTO 507
  500 DPTERVL=DP1
      RETURN
  501 DPTERVL=5.E-03
      RETURN
      END
C
C
C
C
C
C
      FUNCTION PDENSE(DP1)
C
C     THIS FUNCTION EVALUATES THE DENSITY OF A WOODCHAR
C     PARTICLE OF DIAMETER DP1
C
      PDENSE=-428.1-277.8*ALOG10(DP1)
      IF(PDENSE.LT.50.)  PDENSE=50.
      IF(PDENSE.GT.2000.) PDENSE=2000.
      RETURN
      END
```

```
C
C
C
C
      FUNCTION PSAREA(DP1)
C
C     THIS FUNCTION EVALUATES THE INTERNAL SURFACE AREA
C     FOR A WOODCHAR PARTICLE OF DIAMETER DP1
C
      PSAREA=8.384E+06+1.131E+06*ALOG10(DP1)
      IF(PSAREA.LT.10.0) PSAREA=10.0
      RETURN
      END
C
C
C
C
C
C
C
C
      FUNCTION THCOND(T)
C
C     THIS FUNCTION EVALUATES THE THERMAL CONDUCTIVITY OF AIR AT
C     A TEMPERATURE OF T KELVIN
C
      THCOND=(1.75+0.005*T)*1.E-05
      RETURN
      END
C
C
C
C
C
C
      FUNCTION HTCOGAS(T1,T2)
      COMMON/PLUG/RNUMPAR,FG1,FG2,RSC1,RSC2
C
C     THIS FUNCTION EVALUATES THE HEAT TRANSFER COEFFICIENT
C     FROM THE REACTOR WALLS (T2) TO THE GAS (T1). THE COLBURN
C     ANALOGY IS USED AND THE GS IS ASSUMED TO BE IN TURBULENT FLOW.
C     (C.F. P 339 WELTY-WICKS-WILSON)  (UNITS - KW/M2 K)
C
      TM=(T1+T2)/2.
      CP=(0.79*SPECIF(TM,2)+0.21*SPECIF(TM,1))
      CF=1.E-02
      PR=0.68
      HTCOGAS=PR**(-(2./3.))*FG1*CP*CF/(2.*RSC1)
      RETURN
      END
C
```

```
C
C
      FUNCTION HEATTC(T1,T2,V,DP1)
C
C     THIS FUNCTION EVALUATES THE HEAT TRANSFER COEFFICIENT
C     FROM A PARTICLE OF DIAMETER DP1 (T1) TO A GAS (T2),
C     WHILST TRAVELLING AT A VELOCITY V .
C     THE CORRELATION USED IS THE RANZ-MARSHALL EQUATION
C
      TM=(T1+T2)/2.
      VOLDPF=0.63
      SPHERIF=2.5
      RHOGAS=353.22/TM
      VISC=18.E-07*TM**1.5/(120.5+TM)
      RE=DP1*SQRT(SPHERIF)*V*RHOGAS/VISC
      TH=THCOND(TM)
      PR=0.68
      RTH=TH*(2.+0.6*RE**.5*PR**(1./3.))/(DP1*VOLDPF)
      HEATTC=RTH
      RETURN
      END
C
C
C
C
C
C
      SUBROUTINE HPARTGS(TP,DPART,XAPART,TG,YO2G,YCO2G,DL,RL,
     * FCO,FGO,FO1,XABAR)
      DIMENSION TP(10),DPART(10),XAPART(10),DENO(10),RNUMO(10),D(10),
     * FP1(10),PVEL(10),TAUP1(10)
      COMMON/PARTCLE/DP(10),WFR(10)
      COMMON/PLUG/RNUMPAR,FG1,FG2,RSC1,RSC2
      COMMON/DAD/LAB
      COMMON/HEATER/QCONVEC,QRADIAT
      COMMON/RINFO/DPP1,FGASM,FCAR,ALPHA,FO,TGAS,TSOL,DPBAR,FRWATER
C
C     THIS SUBROUTINE CLCULATES THE CHANGE IN TEMPERATURE,CONVERSION,
C     PARTICLE SIZE,GAS TEMPERATURE AND GAS MOLE FRACTIONS IN A LENGTH
C     INCREMENT UP THE REACTOR FOR THE PARTICLE SIZE DISTRIBUTION.
C
C
      VOLDPF=0.63
      RL=RL+DL
      DR=0.762
      PI=3.14159
      SIGMA=5.672E-11
      ETA=0.9
      TW=1000.
      VGAS=FGO*22.414*TG/(273.*RSC1)
      IF(RL.GT.DL) GOTO 301
      QRADIAT=QCONVEC=0.0
      CPW=SPECIF(1000.,3)
      DELH=ENTHAL(1000.)
      CPGAS=(0.21*SPECIF(1000.,1)+0.79*SPECIF(1000.,2))
      HGAS=HTCOGAS(1000.,TW)
      CP=SPECIF(1000.,5)
      DO 302 J=1,9
      DENO(J)=PDENSE(DP(J))/12.
  302 RNUMO(J)=FCO*WFR(J)*6./(ALPHA*DENO(J)*PI*DP(J)**3)
  301 CONTINUE
```

```
      DO 303 J=1,9
      PVEL(J)=VGAS-TERVEL(LAB,DPART(J),TG)
      IF(PVEL(J).LT.0.01) PVEL(J)=0.01
      VELOC=VGAS-PVEL(J)
      RK=RKOV(TP(J),VELOC,DPART(J))
      HP=HEATTC(TG,TP(J),PVEL(J),DPART(J))
      A=HP+SIGMA*ETA*(TW+TP(J))*(TW**2+TP(J)**2)-RK*YO2G*CP
      B=HP*TG+SIGMA*ETA*(TW+TP(J))*(TW**2+TP(J)**2)*TW-RK*YO2G*DELH
      C=PVEL(J)*PDENSE(DPART(J))*CP*DPART(J)*VOLDPF/72.
      FP1(J)=B/A
      TAUP1(J)=C/A
      D(J)=PVEL(J)*PDENSE(DPART(J))*DPART(J)*VOLDPF/(72.*RK*YO2G)
      IF(TP(J).GE.TG) GOTO 303
      QRADIAT=QRADIAT+RNUMO(J)*PI*DPART(J)**2*SIGMA*ETA*(TW**4
     * -TP(J)**4)*DL/PVEL(J)
  303 CONTINUE
C
C
      SUM=SUM2=SUM1=SUMM=SUN=SUMN=.0
      DO 304 J=1,9
      IF(TP(J).GE.TG) GOTO 323
      SUMMER=HEATTC(TG,TP(J),PVEL(J),DPART(J))*RNUMO(J)*PI
     * *DPART(J)**2/PVEL(J)
      SUM1=SUM1+SUMMER
      SUM2=SUM2+SUMMER*TP(J)
  323 SUM=SUM+WFR(J)*(1.-XAPART(J))/D(J)
      SUMN=SUMN+WFR(J)*XAPART(J)
      IF(TP(J).LT.TG) GOTO 304
      SUN=SUN+PI*RNUMO(J)*DPART(J)**2/PVEL(J)
      SUMM=SUMM+FCO*(1.-XAPART(J))*WFR(J)*CP
  304 CONTINUE
      DXABAR=SUM
      XABAR=SUMN
      QRADIAT=QRADIAT+SUN*SIGMA*ETA*(TW**4-TG**4)*DL
      QCONVEC=QCONVEC+HGAS*PI*DR*(TW-TG)*DL
      A1=SUM1+HGAS*PI*DR+SIGMA*ETA*(TW+TG)*(TW**2+TG**2)*SUN
      B1=SUM2-DXABAR*FCO=DELH+HGAS*PI*DR*TW+SIGMA*ETA*TW*(TW+TG)*
     * (TW**2+TG**2)*SUN
      C1=FGO*CPGAS+SUMM+FO1*(1.-ALPHA-FRWATER)*CP/12.
     * +FRWATER*FO1*CPW/18.
      F2=B1/A1
      TAUG1=C1/A1
C
C
      TGC1=TG
      TG=TG+(F2-TG)*(1.-EXP(-DL/TAUG1))
      DO 305 J=1,9
      IF(TP(J).GE.TGC1) GOTO 306
      TP(J)=TP(J)+(FP1(J)-TP(J))*(1.-EXP(-DL/TAUP1(J)))
      IF(TP(J).GT.TG) TP(J)=TG
      GOTO 312
  306 TP(J)=TG
  312 CONTINUE
      IF(XAPART(J).GE.0.999999) GOTO 307
      XAPART(J)=XAPART(J)+(1.-XAPART(J))*(1.-EXP(-DL/D(J)))
      IF(XAPART(J).GE.1.0) XAPART(J)=0.999999
  307 CONTINUE
      IF(DPART(J).LE.1.E-10) GOTO 308
      DPART(J)=DP(J)*(DENO(J)*(1.-XAPART(J))*12./PDENSE(DPART(J)))
     * **(1./3.)
```

```
      IF(DPART(J).LE.1.E-10) DPART(J)=1.E-10
  308 CONTINUE
  305 CONTINUE
C
C
      XABAR=1.-(1.-XABAR)*FCO/FCAR
      YO2G=0.21-XABAR*FCAR/FGO
      YCO2G=0.21-YO2G
      RETURN
      END
```

Table G.3. Program to calculate the orifice flowmeter calibration curves.

```
      PROGRAM   ORIFICE(OUTPUT,TAPE6=OUTPUT,TAPE10=0)
      DIMENSION DELP(60),Q(5,60),T(5)
      DATA (T(I),I=1,5)/290.,300.,310.,320.,330./
C
      WRITE(6,110)
  110 FORMAT(2X,65("*"))
      WRITE(6,100)
  100 FORMAT(2X,*TABLE OF CALCULATED FLOWRATES FOR THE *,
     * *VIEW PORT ORIFICE FLOWMETER*)
      WRITE(6,120)
  120 FORMAT(2X,65("*"),//)
C
      DO 10 L=1,4
      P1=1.0133E+05 + 7000.*FLOAT(L)
      NPTS=5
      DP=25.*249./FLOAT(NPTS)
      DO 20 I=1,5
      M=NPTS+1
      DO 30 J=1,M
      DELP(J)=FLOAT(J-1)*DP
   30 Q(I,J)=(3.0051+1.4741*(P1-DELP(J))/P1)*2.8316E-02
     * *SQRT(P1*DELP(J)/(T(I)*2.5231E+07))
   20 CONTINUE
      WRITE(6,40) P1
   40 FORMAT(/2X,*UPSTREAM PRESSURE = *,E10.4,2X,*N/M2*,/)
      WRITE(6,50) (DELP(J),J=1,5)
   50 FORMAT(2X,*PRESSURE DIFFERENCE (N/M2)=*,4X,5F10.1,/)
      DO 70 N=1,5
      WRITE(6,60) T(N),(Q(N,J),J=1,5)
   60 FORMAT(2X,*INLET AIR TEMPERATURE=*,F5.1,* (K)*,5F10.5)
   70 CONTINUE
   10 CONTINUE
      WRITE(6,55)
   55 FORMAT(////////2X)
C
      STOP
      END
/
```

Table G.4. Program to calculate the venturi flowmeter calibration curves.

```
      PROGRAM   VENT(OUTPUT,TAPE6=OUTPUT,TAPE10=0)
      DIMENSION DELP(60),Q(5,60),T(5)
      DIMENSION DELPCON(60).TF(5),QCONV(5,60)
      DATA (T(I),I=1,5)/290.,300.,310.,320.,330./
C
      WRITE(6,110)
  110 FORMAT(2X,81("*"))
      WRITE(6,100)
  100 FORMAT(2X,*TABLE OF CALCULATED FLOWRATES FOR THE *,
     * *MAIN AIR AND PREHEAT AIR VENTURI FLOWMETERS*)
      WRITE(6,120)
  120 FORMAT(2X,81("*"))
C
      DO 10 L=1,4
      P1=14.697+FLOAT(L)
      P1CONV=P1*1.0133E+05/14.697
      NPTS=5
      DP=60./FLOAT(NPTS)
      DO 20 I=1,5
      M=NPTS+1
      DO 30 J=1,M
      DELP(J)=1.E-20+FLOAT(J-1)*DP
      DELPCON(J)=DELP(J)*249.
      DS=2.4414
      FA=1.
      F=1.0342
      C=0.984
      P2=P1-.03613*DELP(J)
      R=P2/P1
      SY1=R**1.429
      SY2=3.5
      SY3=(1.-R**.2857)/(1.-R)
      BETA=0.50505050
      SY4=(1.-BETA**4)/(1.-BETA**4*SY1)
      YA=SQRT(SY1*SY2*SY3*SY4)
      TF(I)=(T(I)-273.)*1.8+32.
      GA=0.0862*459.7/(TF(I)+459.7)
      G=GA*P1/14.697
      WM=5.983*C*F*DS*FA*YA*SQRT(DELP(J)*G)
      ACFM=WM/G
      Q(I,J)=ACFM*529.*P1/(14.697*(TF(I)+459.))
   30 QCONV(I,J)=Q(I,J)*4.7194E-04
   20 CONTINUE
      WRITE(6,40) P1CONV
   40 FORMAT(/2X,*UPSTREAM PRESSURE =*,E10.4,2X,*N/M2*,/)
      WRITE(6,50) (DELPCON(J),J=1,6)
   50 FORMAT(2X,*PRESSURE DIFFERENCE (N/M2)=*,5X.6F10.1./)
      DO 70 N=1,5
      WRITE(6,60) T(N),(QCONV(N,J),J=1,6)
   60 FORMAT(2X,*INLET AIR TEMPERATURE =*,F5.1,* (K)*.6F10.5)
   70 CONTINUE
   10 CONTINUE
      WRITE(6,55)
   55 FORMAT(///////2X)
      STOP
      END
/
```

Table G.5. Program to plot terminal velocity bs. particle size.

```
      PROGRAM  RRATE(INPUT,OUTPUT,TAPE6=OUTPUT,TAPE10=0)
      DIMENSION DIAM(3),VEL(3),RKOV(4,4,51)
      DIMENSION LABX(3),LABY(5),TITLE1(3),TITLE2(3),TITLE3(3)
     * ,LABEL2(6),LABEL1(6)
      DATA (DIAM(I),I=1,3)/1.E-02,1.E-03,1.E-04/
      DATA (VEL(I),I=1,3) /10.,1.,0.0/
      DATA (LABX(I),I=1,3)/# SURFACE TEMPERATURE (K)       #/
      DATA(LABY(I),I=1,5)/#OVERALL REACTION COEFFICIENTS (MOLE/S*M2)#/
      DATA (TITLE1(I),I=1,3)/#THE VARIATION OF REACTION RATE#/
      DATA (TITLE2(I),I=1,3)/#COEFFICIENT WITH TEMPERATURE  #/
      DATA (TITLE3(I),I=1,3)/#FOR THE REACTION: C+O2=CO2    #/
      DATA (LABEL1(I),I=1,6)/#AIR#,#VELOCITY#,#(M/S)#,#PARTICLE#,
     * #DIAMETER#,#(M)#/
      DATA(LABEL2(I),I=1,3)/# REACTION CONTROLLED           #/
C
      RCONST=8.2102E-02
      NPTS=50
      TMAX=1500.
      TMIN=1000.
      DELT=(TMAX-TMIN)/FLOAT(NPTS)
      DO 10 I=1,3
      DO 20 J=1,3
      DO 30 L=1,51
      T=TMIN+DELT*FLOAT(L-1)
      P=1.
      DIFF=7.381E-10*T**1.75
      RHO=353.6/T
      VISC=18.E-07*T**1.5/(120.5+T)
      RE=DIAM(I)*VEL(J)*RHO/VISC
      SC=VISC/(RHO*DIFF)
      RDIFF=DIFF*(2.+0.6*RE**0.5*SC**0.3333)*P/(RCONST*T*DIAM(I))
      RCHEM=7.9583E+06*P*EXP(-(44000./(1.986*T)))/SQRT(T)
      RKOV(I,J,L)=1000./(1./RDIFF+1./RCHEM)
      RKOV(4,4,L)=1000.*RCHEM
   30 CONTINUE
   20 CONTINUE
   10 CONTINUE
      WIDTH=7.
      HEIGHT=9.
      ICODE=4
      CALL PLOTYPE(ICODE)
      CALL TKTYPE(4014)
      CALL SIZE(WIDTH+2.,HEIGHT+2.)
      CALL ERASE
      XLOW=XORG=TMIN
      XHIGH=TMAX+250.
      YLOW=YORG=5.E-02
      YHIGH=1000.
      XTIC=100.
      YTIC=1.E-02
      YMAX=ALOG10(YHIGH)
      YMIN=ALOG10(YLOW)
      XFACT=WIDTH/(XHIGH-XLOW)
      YFACT=HEIGHT/(YMAX-YMIN)
      CALL SCALE(XFACT,YFACT,1.5,1.5,XLOW,YMIN)
      CALL AXISL(XLOW,XHIGH,XORG,YLOW,YHIGH,YORG,XTIC,YTIC,
     * 0,0,1,1,1.,1.,0.1,1)
      CALL PLOT(XLOW,YMAX,1,0)
      CALL PLOT(XHIGH,YMAX,1,0)
      CALL PLOT(XHIGH,YMIN,1,0)
```

```
      DO 50 I=1,3
      DO 60 J=1,3
      CALL POINTS
      DO 70 L=1,51
      XP=TMIN+DELT*FLOAT(L-1)
      YP=ALOG10(RKOV(I,J,L))
      CALL PLOT(XP,YP,1,0)
   70 CALL VECTORS
   60 CONTINUE
   50 CONTINUE
      CALL POINTS
      DO 110 L=1,51
      XP=TMIN+DELT*FLOAT(L-1)
      YP=ALOG10(RKOV(4,4,L))
      CALL PLOT(XP,YP,1,0)
  110 CALL VECTORS
      ICHAR=IGRINPT(X,Y)
      CALL SYMBOL(X,Y,0.,0.15,30,LABX)
      ICHAR=IGRINPT(X,Y)
      CALL SYMBOL(X,Y,90.,0.15,50,LABY)
      ICHAR=IGRINPT(X,Y)
      CALL SYMBOL(X,Y,0.,0.12,30,TITLE1)
      ICHAR=IGRINPT(X,Y)
      CALL SYMBOL(X,Y,0.,0.12,30,TITLE2)
      ICHAR=IGRINPT(X,Y)
      CALL SYMBOL(X,Y,0.,0.12,30,TITLE3)
      DO 80 I=1,5
      ICHAR=IGRINPT(X,Y)
   80 CALL SYMBOL(X,Y,0.,0.10,8,LABEL1(I))
      DO 90 I=1,3
      ICHAR=IGRINPT(X,Y)
      CALL NUMBER(X,Y,0.,0.10,6,DIAM(I))
      DO 100 J=1,3
      ICHAR=IGRINPT(X,Y)
      CALL NUMBER(X,Y,0.,0.10,4,VEL(J))
  100 CONTINUE
   90 CONTINUE
      ICHAR=IGRINPT(X1,Y1)
      CALL SYMBOL(X1,Y1,0.,0.1,30,LABEL2)

      CALL PLOTEND
      STOP
      END
```

Table G.6 The computer program to evaluate the terminal velocity of various sized carbon particles.

```
      DIMENSION DP(60),VEL(5,60),RHO(5),RE1(5,60)
      DIMENSION LABX(3),LABY(4),LAB1(4),LAB2(4),LAB3(4),LABEL(7)
      DATA (LABX(I),I=1,3)/" PARTICLE DIAMETER (M*10**6)  "/
      DATA (LABY(I),I=1,4)/" TERMINAL VELOCITY OF PARTICLE (M/S)"/
      DATA (LAB1(I),I=1,4)/" THE TERMINAL VELOCITIES OF WOODCHAR  "/
      DATA (LAB2(I),I=1,4)/"PARTICLES (NON-SPHERICAL) IN AIR AT A "/
      DATA (LAB3(I),I=1,4)/"TEMPERATURE OF 1300 K.            "/
      DATA (LABEL(I),I=1,7)/"PARTICLE","DENSITY","(KG/M3) ",
     * "900     ","600     ","400     ","200    "/
C
      NPTS=20
      DO 10 I=1,NPTS
      DP(I)=(((100.-10.)/NPTS)*FLOAT(I-1)+10.)*1.E-06
      DP(I+NPTS)=(((1000.-100.)/NPTS)*FLOAT(I-1)+100.)*1.E-06
   10 DP(NPTS+NPTS+I)=(((5000.-1000.)/NPTS)*FLOAT(I-1)+1000.)*1.E-06
      DO 20 I=1,5
   20 RHO(I)=200.+FLOAT(I-1)*200.
C
      DO 30 I=1,5
      RE=0.
      DO 40 J=1,60
      RHO(5)=-428.1 -277.8*ALOG10(DP(J))
      TEMP=1300.
      RHOGAS=29.*273./(22.414*TEMP)
      G=9.81
      RE=0.01
      VISC=18.*TEMP**1.5/(TEMP+120.5)*1.E-07
C
  199 CD=24./RE
      VEL(I,J)=(4.*G*DP(J)*(RHO(I)-RHOGAS)/(3.*RHOGAS*2.5*CD))**0.5
      RE1(I,J)=SQRT(2.5)*DP(J)*RHOGAS*VEL(I,J)/VISC
      TEST=ABS( (RE1(I,J)-RE)/RE1(I,J) )
      RE=RE1(I,J)
      IF(TEST.LT.0.001) GOTO 350
      GOTO 199
  350 IF(RE1(I,J).LT.0.1) GOTO 60
   90 CD=24./RE1(I,J)+2.25
      VEL(I,J)=(4.*G*DP(J)*(RHO(I)-RHOGAS)/(3.*RHOGAS*2.5*CD))
     * **0.5
      RE=DP(J)*SQRT(2.5)*RHOGAS*VEL(I,J)/VISC
      TEST=ABS((RE-RE1(I,J))/RE)
      RE1(I,J)=RE
      IF(TEST.LT.0.001) GOTO 60
      GOTO 90
   70 IF (RE.LT.5.5) GOTO 60
   80 CD=24./RE+2.25*(5.5)**0.2150
      VEL(I,J)=(4.*G*DP(J)*(RHO(I)-RHOGAS)/
     * (3.*RHOGAS*2.5*CD))**0.5
      RE=DP(J)*SQRT(2.5)*RHOGAS*VEL(I,J)/VISC
      TEST=ABS((RE-RE1(I,J))/RE)
      RE1(I,J)=RE
      IF(TEST.LT.0.001) GOTO 150
      GOTO 80
  150 IF(RE.LT.49.) GOTO 60
  180 CD=24/RE+1.4051
      VEL(I,J)=(4.*G*DP(J)*(RHO(I)-RHOGAS)/
     * (3.*RHOGAS*2.5*CD))**0.5
      RE=DP(J)*SQRT(2.5)*RHOGAS*VEL(I,J)/VISC
      TEST=ABS((RE-RE1(I,J))/RE)
      RE1(I,J)=RE
      IF(TEST.LT.0.001) GOTO 60
      GOTO 180
   60 CONTINUE
   40 CONTINUE
```

```
      WD=7.
      HT=9.
      IC=4
      CALL PLOTYPE(IC)
      CALL TKTYPE(4014)
      CALL SIZE(WD+2.,HT+2.)
      CALL ERASE
      XLOW=XORG-100.
      XHIGH=10000.
      YLOW=YORG=0.
      YHIGH=10.
      XTIC=10.
      YTIC=2.
      XMAX=ALOG10(XHIGH)
      XMIN=ALOG10(XLOW)
      XFACT=WD/(XMAX-XMIN)
      YFACT=HT/(YHIGH-YORG)
      CALL=SCALE(XFACT,YFACT,1.5,1.5.XMIN.YORG)
      CALL AXISL(XLOW,XHIGH.XORG.YLOW,YHIGH,YORG,XTIC,YTIC,
     * 0,0,1,1,1.,1.,0.1,2)
      CALL PLOT(XMIN,YHIGH,1.0)
      CALL PLOT(XMAX,YHIGH,1,0)
      CALL PLOT(XMAX,YLOW,1.0)
C
      DO 100 I=1,4
      CALL POINTS
      DO 200 J=21,60
      XP=ALOG10(DP(J)*1.E+06)
      YP=VEL(I,J)
      CALL PLOT(XP,YP.1,0)
  200 CALL VECTORS
  100 CONTINUE
      CALL POINTS
      DO 300 J=21,60,3
      I=5
      XP=ALOG10(DP(J)*1.E+06)
      YP=VEL(I,J)
      CALL PLOT(XP,YP,1.0)
  300 CALL DASHES
      ICHAR=IGRINPT(X,Y)
      CALL SYMBOL(X,Y.0..0.15,30,LABX)
      ICHAR=IGRINPT(X,Y)
      CALL SYMBOL(X,Y,90.,0.15,40,LABY)
      ICHAR=IGRINPT(X,Y)
      CALL SYMBOL(X,Y,0.,0.12.40.LAB1)
      ICHAR=IGRINPT(X,Y)
      CALL SYMBOL(X,Y,0.,0.12,40,LAB2)
      ICHAR=IGRINPT(X,Y)
      CALL SYMBOL(X,Y,0.,0.12,40,LAB3)
      DO 110 I=1,7
      ICHAR=IGRINPT(X,Y)
      CALL SYMBOL(X.Y.0..0.1,8,LABEL(I))
  110 CONTINUE
      CALL PLOTEND
      STOP
      END
```

APPENDIX H

PHOTOGRAPHS OF WOOD CHAR PARTICLES USING AN ELECTRON SCAN MICROSCOPE

Throughout this work the importance of the internal surface area of the wood char, has been stressed.

In Appendix B the internal surface area was estimated by the low temperature physi-adsorption of nitrogen. The results indicated that for all the particles studied, the internal surface area was very large.

The importance of this internal surface area becomes apparent in the discussion of reaction rates given in Appendix F. This importance stems from the fact that the surface available for reaction in a porous particle is several orders of magnitude greater than for a non-porous particle. The increase in the surface reaction rate tends to push the combustion reaction into the diffusion controlling regime. Consequently the time required to burn a particle of given size and at a given temperature, is greatly reduced.

The purpose of this appendix is to directly illustrate the vast internal surface structure which may be present in a wood char particle.

The results of a study on various sizes of wood char particle using an electron-scan microscope are presented. The samples used, were treated with a fine metal fibre which allowed the surface structure to be seen more clearly.

The wood char used in the experimental test runs was, in general, produced by pyrolysing Douglas Fir chips. However, during

the course of operation it is conceivable that Ponderosa Pine and Alder Bark derivative may be used as fuel. However, there was no visual difference between the various types of wood char and this is illustrated by the following photographs.

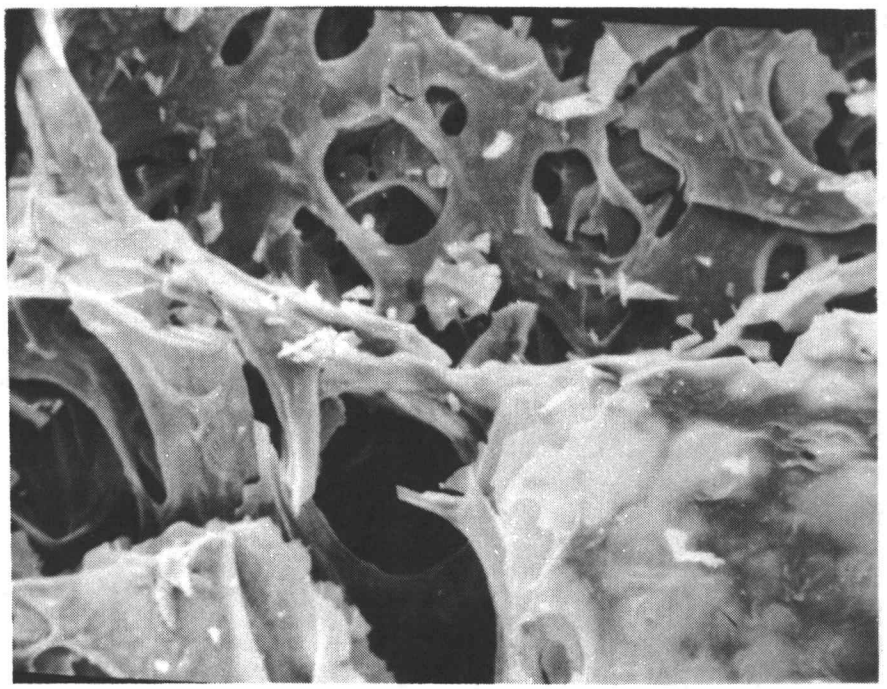

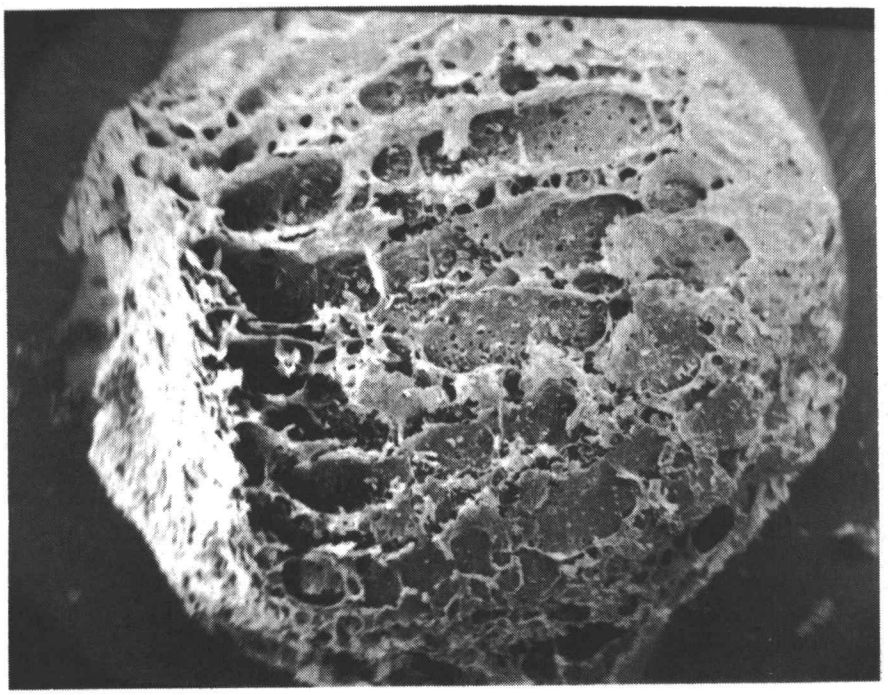

Figure H. 1. Particle collected on a #6 Tyler standard screen. The magnification is x30 (bottom) and x400 (top) (Douglas fir derivative)

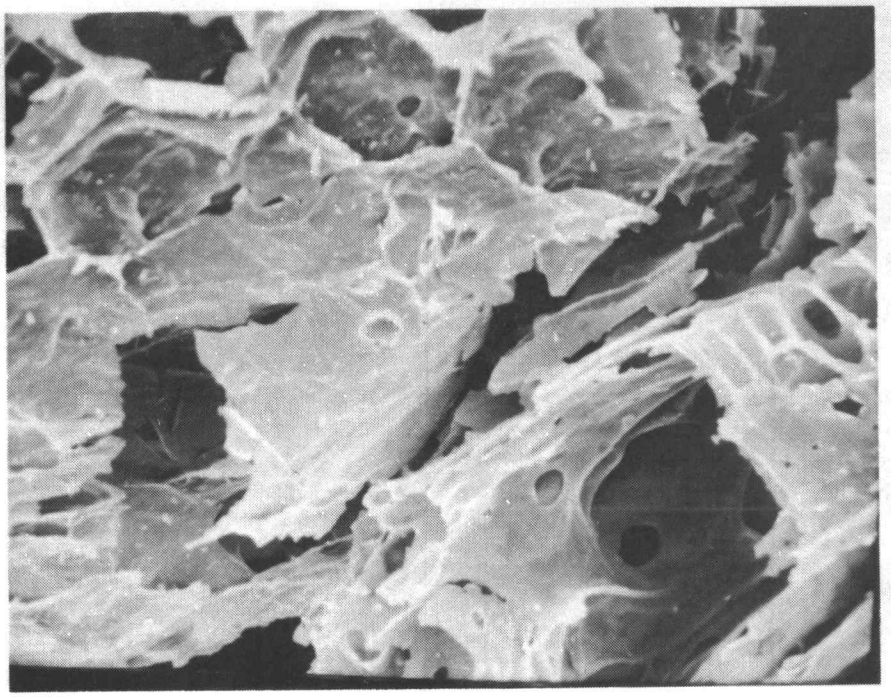

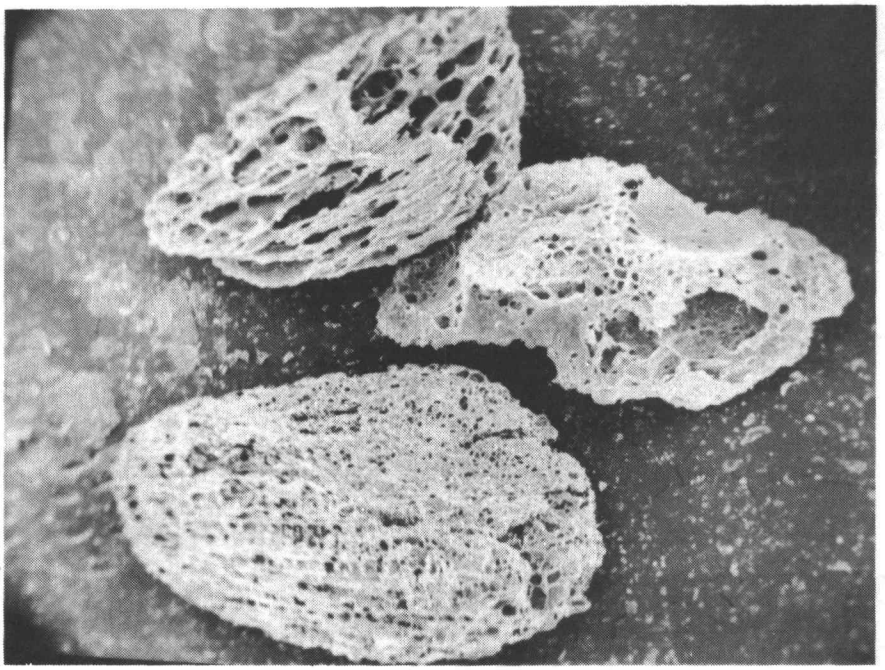

Figure H. 2. Particles collected on a #20 Tyler standard screen. The magnification is x30 (bottom) and x400 (top) (Douglas Fir derivative)

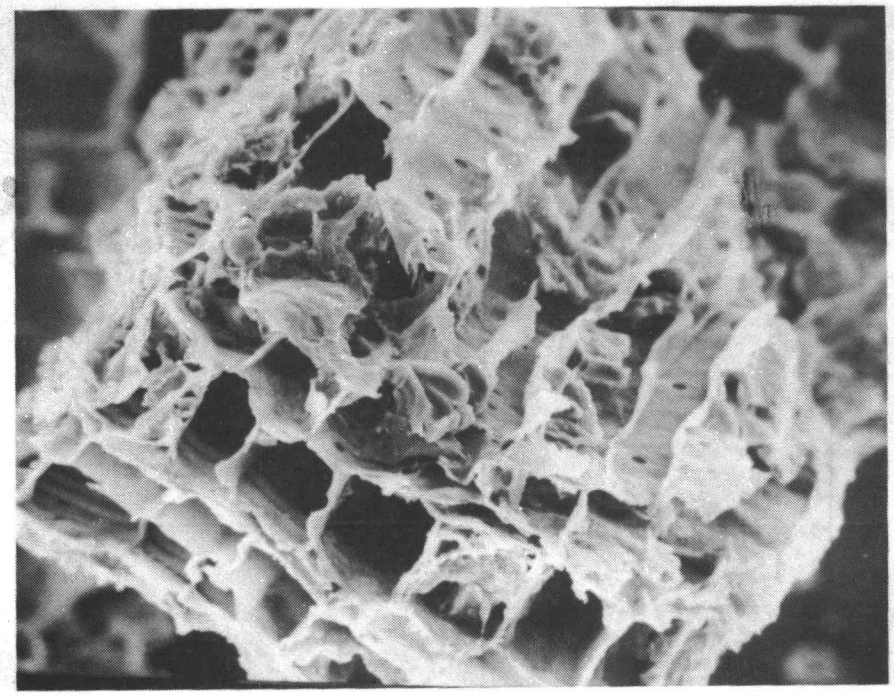

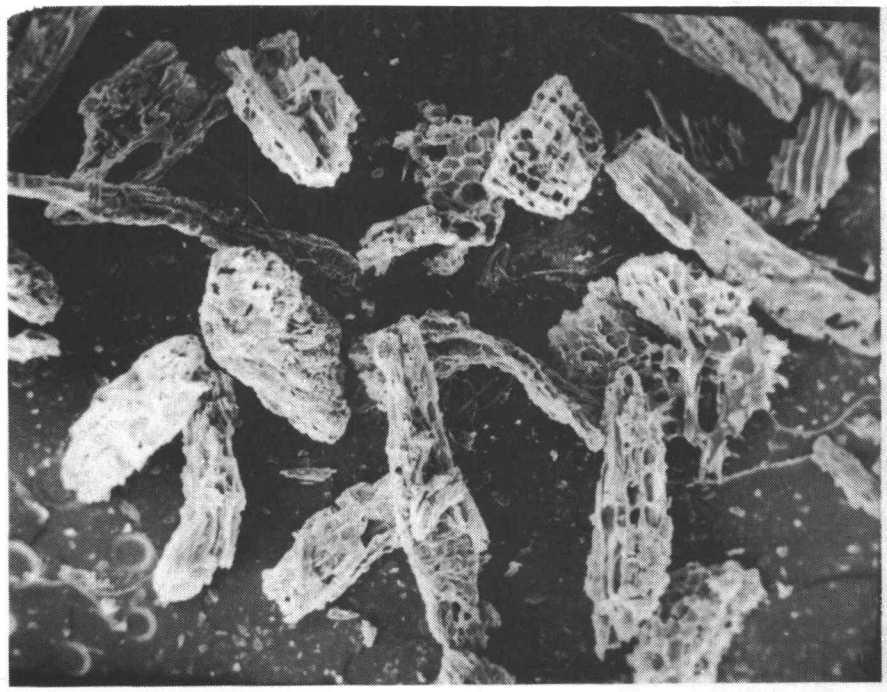

Figure H. 3. Particles collected on a #80 Tyler standard screen. The magnification is x50 (bottom) and x400 (top) (Douglas Fir derivative)

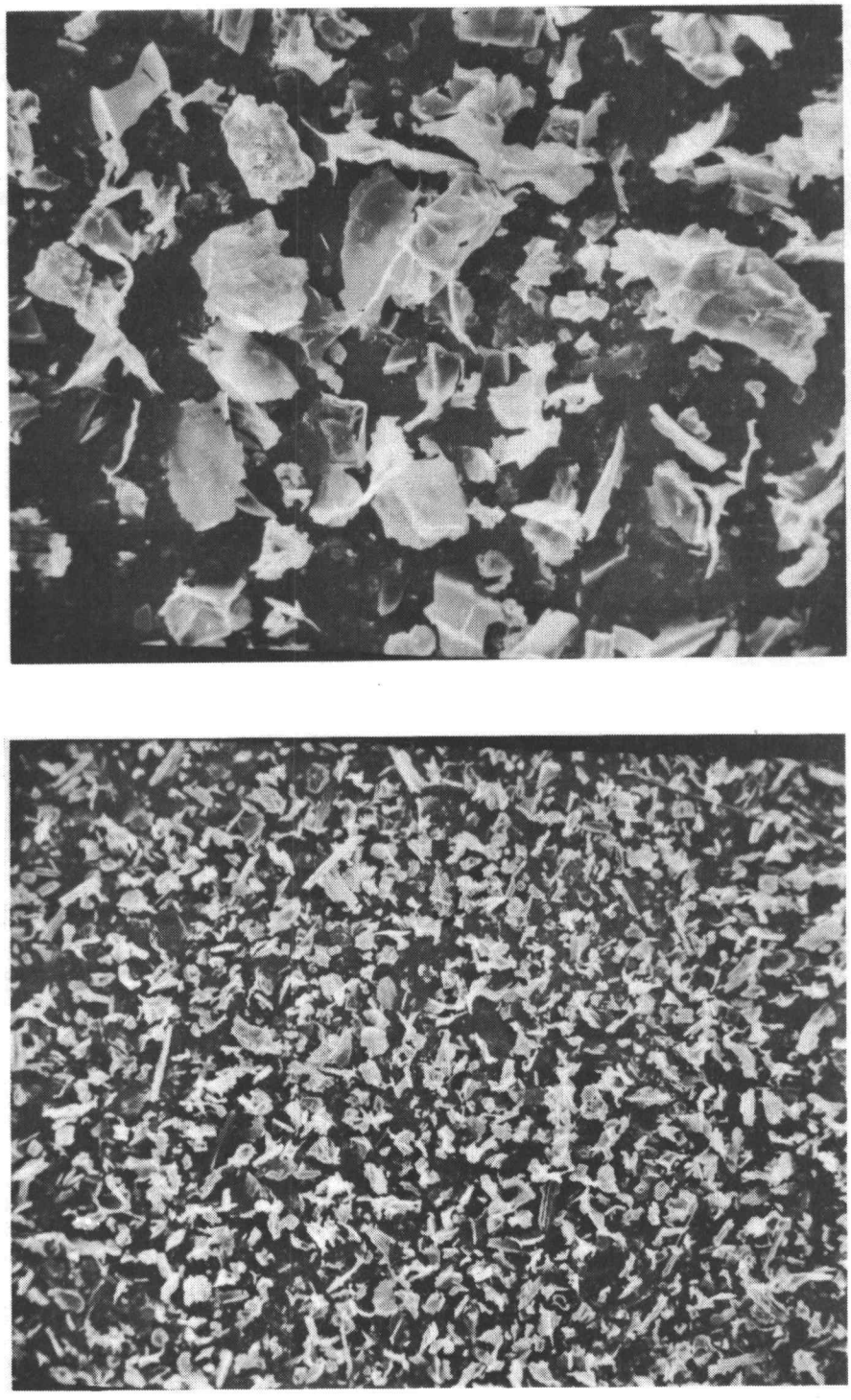

Figure H.4. Particles passing through a #325 Tyler standard screen. The magnification is x100 (bottom) and x400 (top) (Douglas Fir derivative)

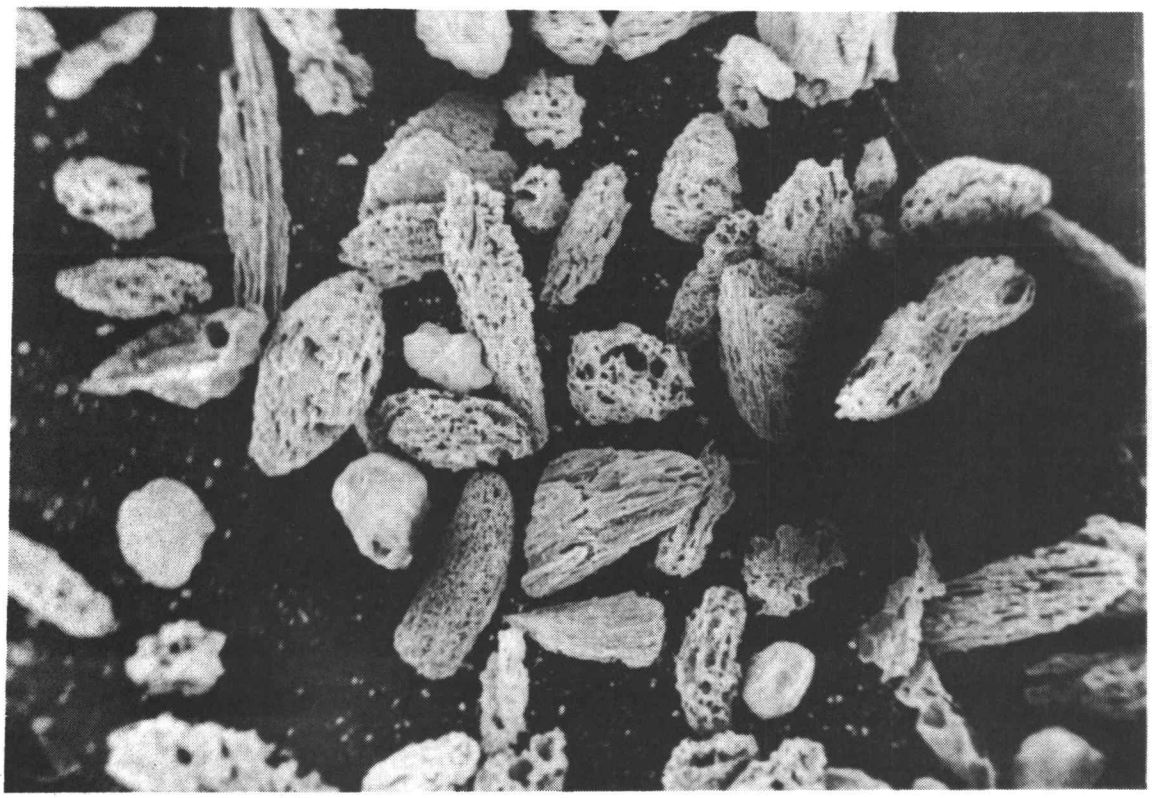

Figure H.5. 250 micron particles at a magnification of x30 (Alder Bark derivative)

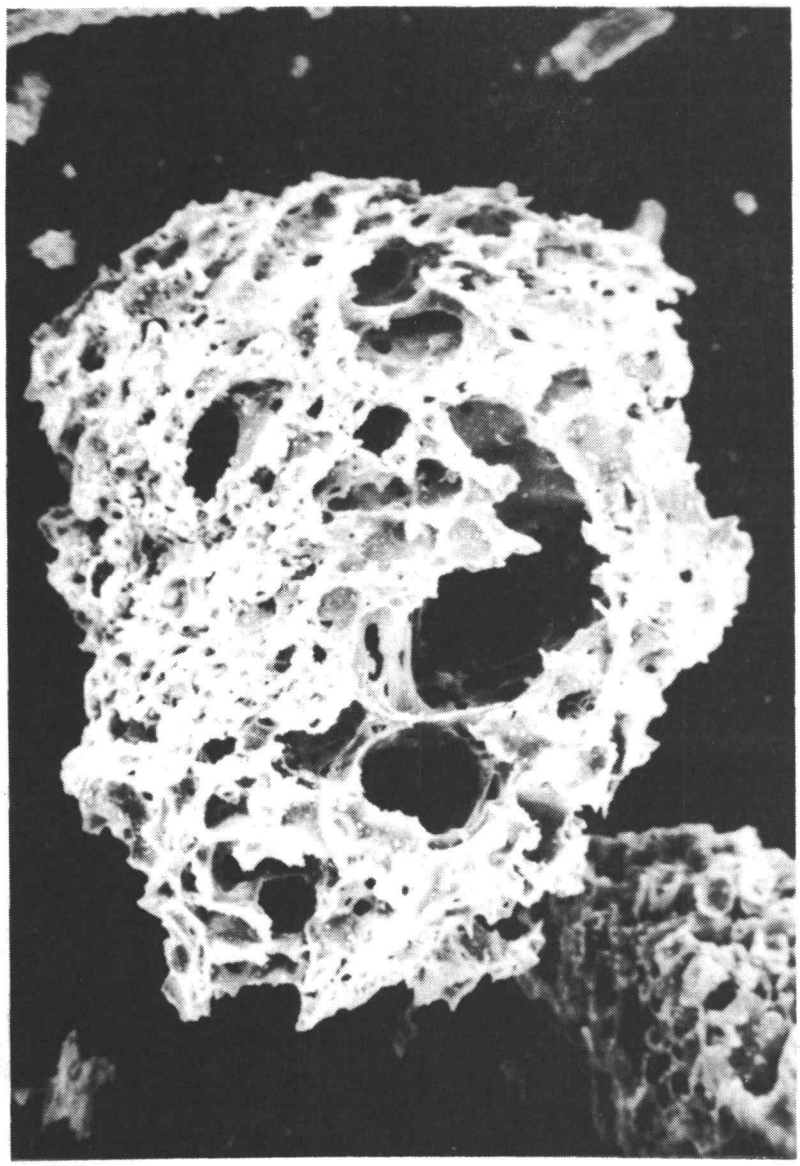

Figure H.6. A 250 micron particle at a magnification of x200. (Alder Bark derivative)

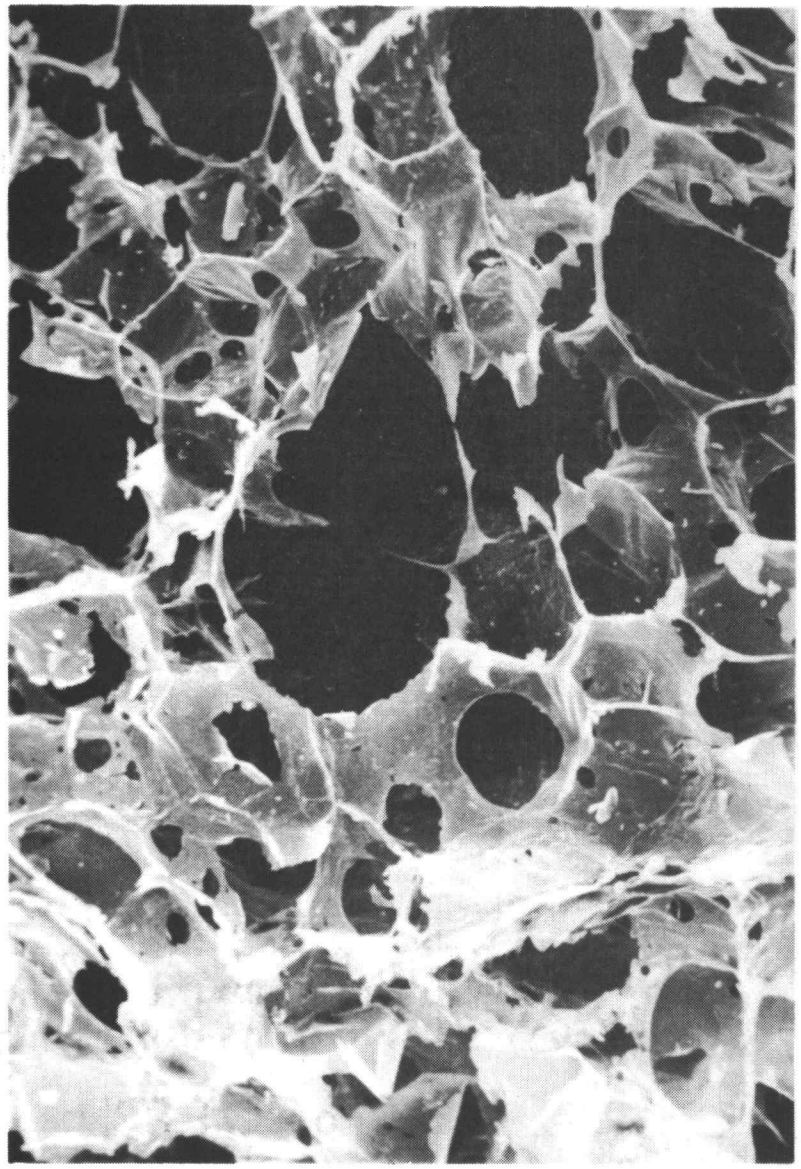

Figure H. 7. Figure H. 7. A 125 micron particle at x400 magnification. (Ponderosa Pine derivative)

APPENDIX I

DESCRIPTION OF CHAR BURNER

The wood char burner used in the experimental part of this work is illustrated in Figure I. 1. The unit is situated, along with an experimental wood-fired boiler, at the research facility at Fairplay, Oregon.

The char burner was built during the latter half of 1978 and completion was achieved by February 1979. The purpose of this unit was to satisfy the need for a basic experimental setup to study the combustion of wood char. The equipment was originally designed by D. Junge[1] with the help of F. Kayihan[2] and the author. The original design specifications were based on a maximum flow of char into the reactor of 6.3×10^{-3} kg/s (50 lb/hr). During operation however, it was found that the maximum flow rate of char which could be successfully handled was almost 60% greater than the design figure. In fact the air flow rate was the limiting factor in the operation of the burner.

The experimental setup consists of a cylindrical refractory lined, combustion chamber approximately 3 meters high and 0.75 meters inside diameter. The refractory lining is 0.1523 meters (6 inches) thick and covers the whole inside surface of the chamber. The shell of the chamber is constructed from 6.35 mm (1/4 inch) stainless steel.

The combustion products are led out of the top of the reactor and into a cyclone via 0.2032 M (8 inches) diameter pipe. This piping

---

[1] Associate Professor, Mechanical Engineering Dept., OSU
[2] Assistant Professor, Chemical Engineering Dept., OSU

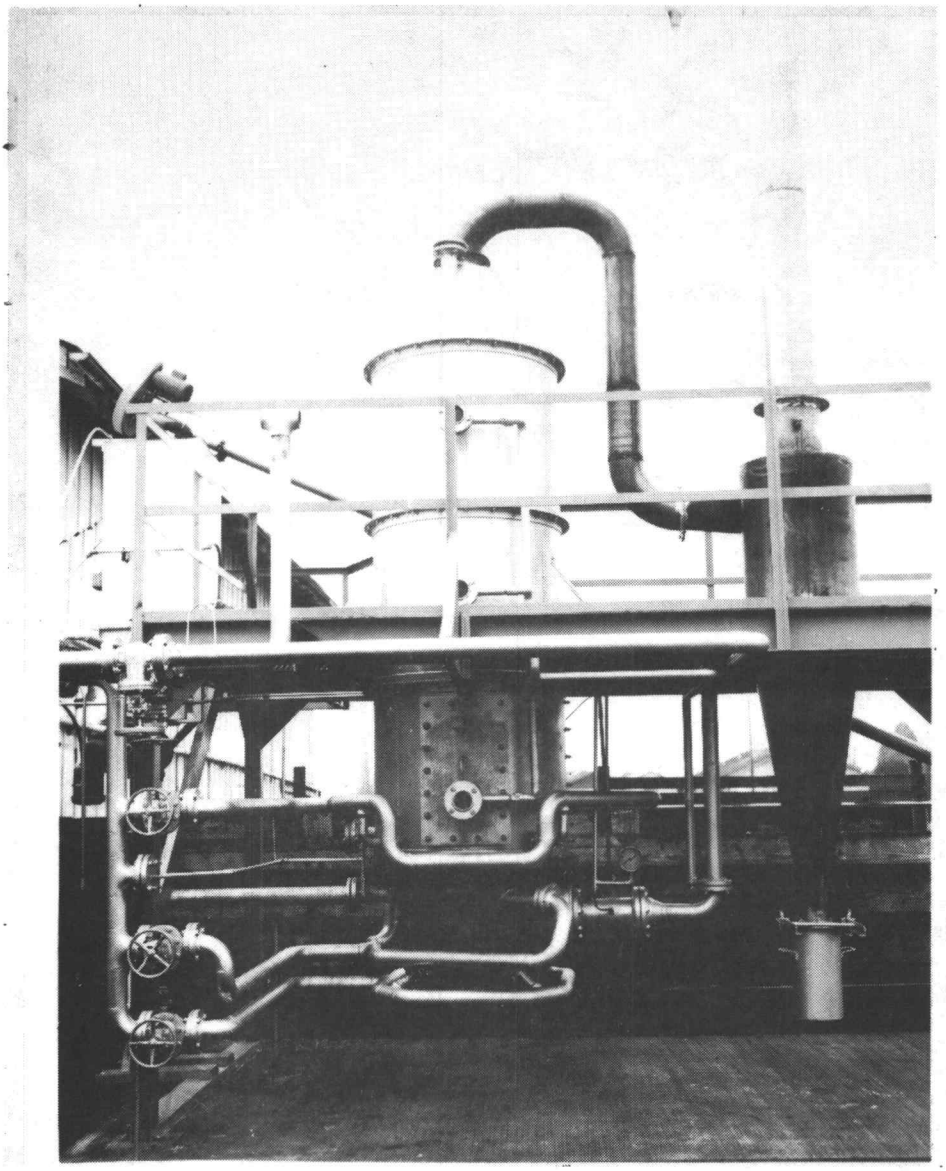

Figure I. 1. Photograph showing the main elements of the char burner.

along with the cyclone is again constructed from 6.35 mm stainless steel.

The overall dimensions and plan of the reactor and cyclone are illustrated in Figure I.1 and in the drawings of figures I.2 and I.3.

The method of introducing char and air into the system along with the procedure used to preheat the reactor are discussed in some detail, below.

I.1 The Char feed system

The wood char used as feed stock to the reactor was supplied by Western Kraft Inc of Albany.

The char was collected in barrels (ranging from 20 to 80 gallons) and stored at the Fairplay facility. A shed was constructed for the storage of char and this provided adequate protection from the rain and direct sunlight.

Some of the physical characteristics of the wood char were studied and the results were presented in Appendix B. To summarize, the wood char may be described as a light (density in the range 200-800 kg/M^3) fibrous material having a low shear strength e.g. the particles may easily be crushed by hand. The combustible content of the char varied from 50 to 90% by weight while the average moisture content was around 5% by weight.

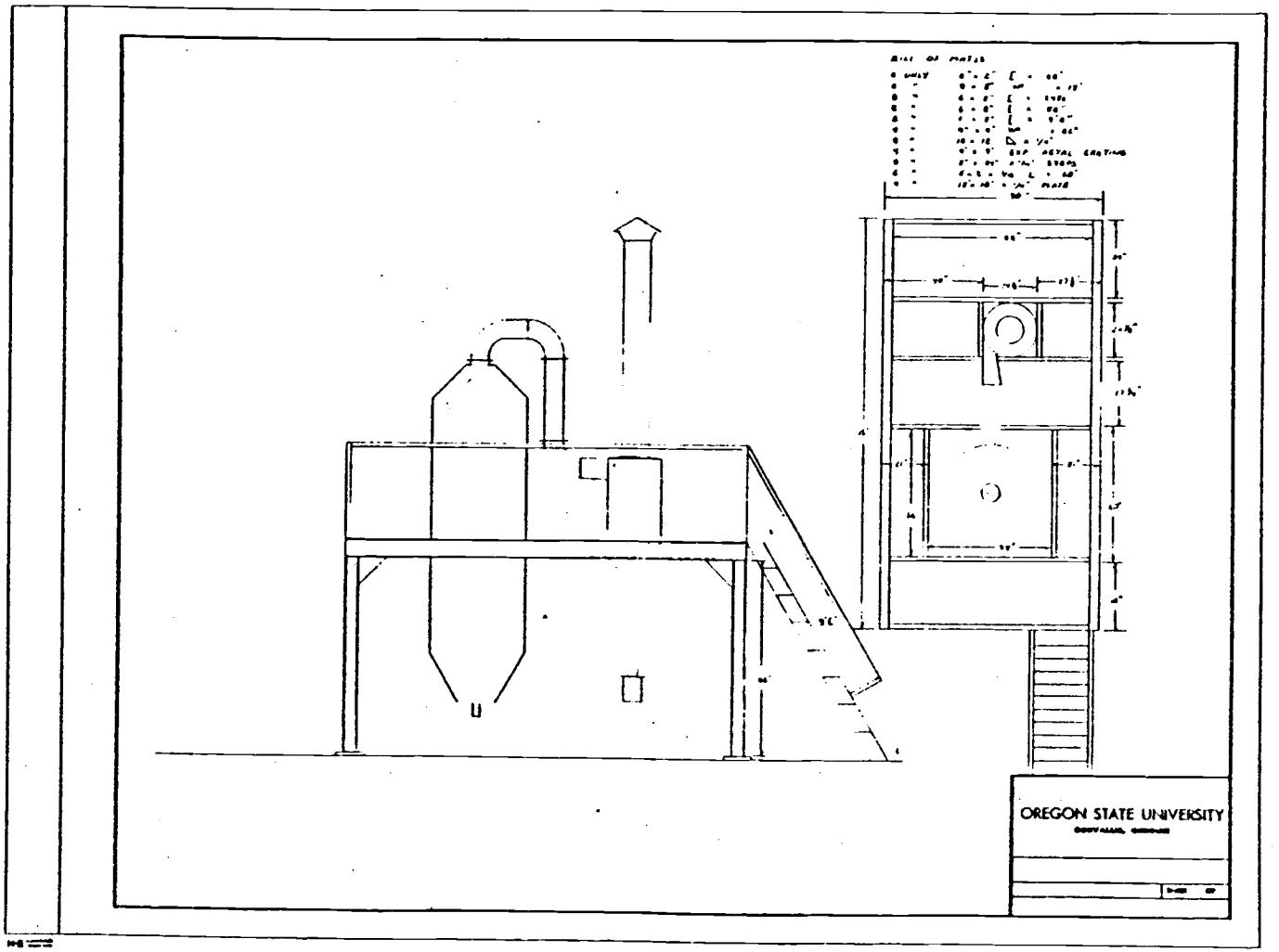

Figure I. 2. The overall plan of the char burner

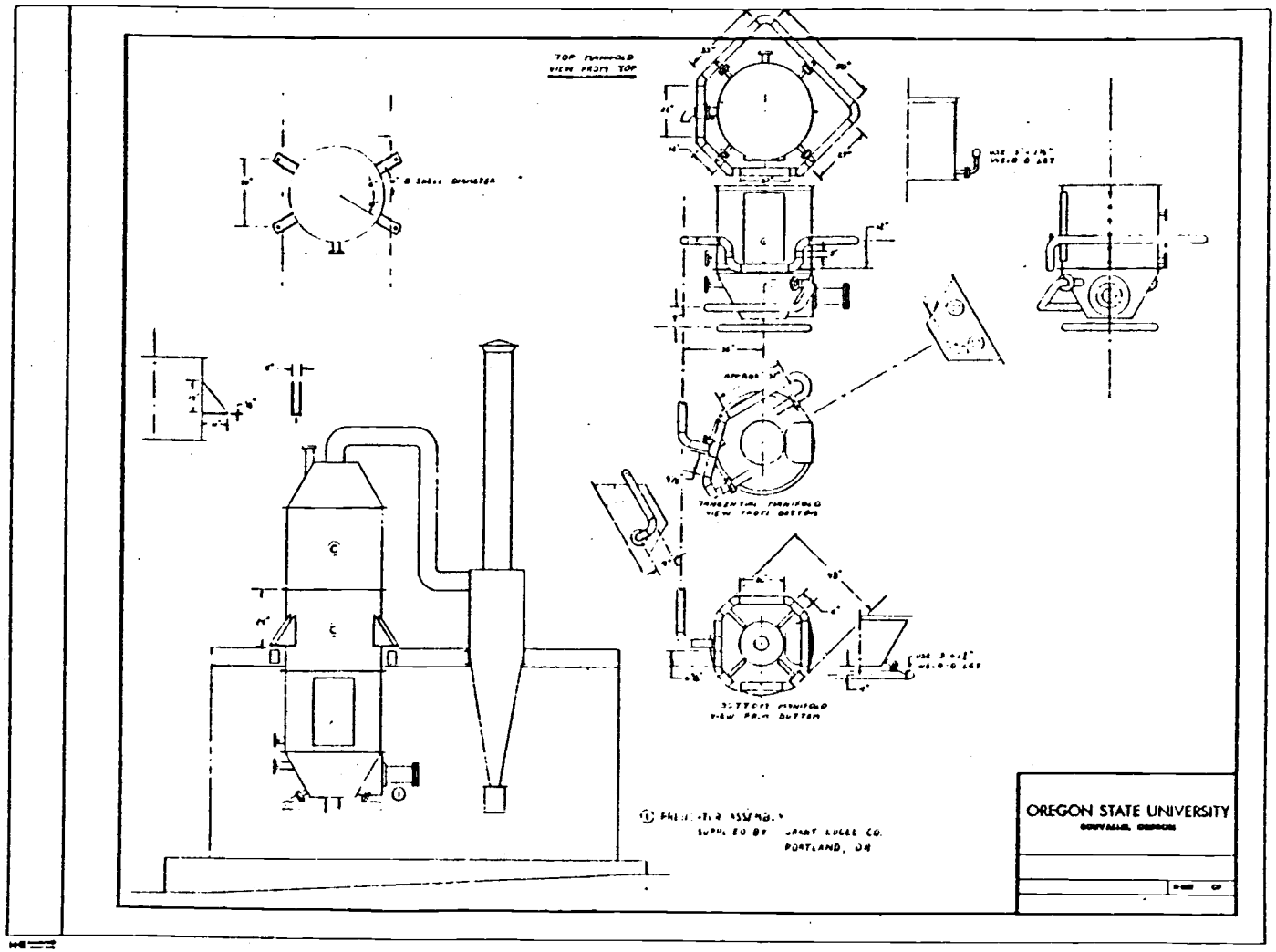

Figure I. 3. The char burner air feed system and the cyclone

When the wood char was used in its original dry condition few problems arose in its transportation. However, if the char was allowed to get wet (i. e. saturated by rain) then transportation became a problem.

The individual aspects of the char feed system are considered below and where appropriate comments are made to possible trouble spots and means of improvement.

The Relay Auger

It was mentioned previously that the wood char was stored in a shed close to the cyclone. In general only one or, at most, two days supply of char could be stored in the shed. This meant that a new load of char was required every day. Assuming that char was available the first part of the solids transportation system is the relay auger.

The purpose of the relay auger is to move solids from the storage shed to a surge bin situationed on the upper level of the support platform. The relay auger is illustrated in Figure 1.4, along with the auger motor and surge bin.

The auger itself is 0.1020 m (4 inches) in diameter and is driven by a 1 horsepower .1740 rpm motor which is mounted above the auger and surge bin, at the top of the shaft. The motor and auger are coupled together through a belt drive, with a 6:1 reduction ratio.

Figure I. 4. Photograph showing the relay auger, motor drive, and supply bin.

The relay auger represents the weak point of the solids transport system. There are basically two contributing factors to this weakness.

Firstly, due to the long distance spanned by the auger (approximately 7 meters) - the alignment of the auger shaft and casing is a problem. The inexact alignment coupled with the length of span causes the relay system to vibrate considerably. This vibration is a great problem when the relay auger is empty. Since in this condition, the vibrations become so intense that it can be operated for only a few seconds without damage occurring. However, when the auger is full of wood char the vibrations are greatly reduced as the char helps damp these out. Thus once the relay auger has been charged with char it is good practice to ensure the system remains in this condition and never runs dry. For the reasons given above the relay auger was operated manually from an extension switch situated in the storage shed. This allowed the operator to check that the relay auger was only used when the supply hopper, in the storage shed, was full.

The second problem with the relay auger concerned the motor mounting at the top of the auger shaft. Since the motor was mounted directly above the shaft with no extra support, the drive system was very susceptible to vibration. Since the mounting consisted of a piece of sheet metal attached directly to the auger case the vibrations in

the auger quickly caused the bolts securing the motor to become loose. It was also found that during the course of the experimental runs one of these bolts had sheared nearly in two and that the screw attaching the belt reduction to the shaft became loose several times.

It is felt that the problems encountered in this part of the transport system are due to the inadequate mounting of the motor coupled with the incorrect alignment of the auger. An improvement of either of the above factors should greatly increase the reliability of this part of the system.

The surge bin

The surge bin is situated on the upper platform and is fed by the relay auger previously described.

The main purpose of the bin is to even out any fluctuations in the flow of wood char and essentially operates as a buffer tank.

To ensure that bridging of the wood char does not occur within the supply bin an unlodading system was designed. This consists of five horizontal augers situated at the bottom of the bin. These augers are continually rotated by a 1.5 horsepower, 1750 rpm motor via three different gear reductions. The surge bin unloading system is shown in the drawings of Figure I.5 and I.6 and the mechanical mounting of the bin is shown in Figure I.7. The base of the surge bin feeds the horizontal auger which in turn feeds the rotary air-lock (see Figure

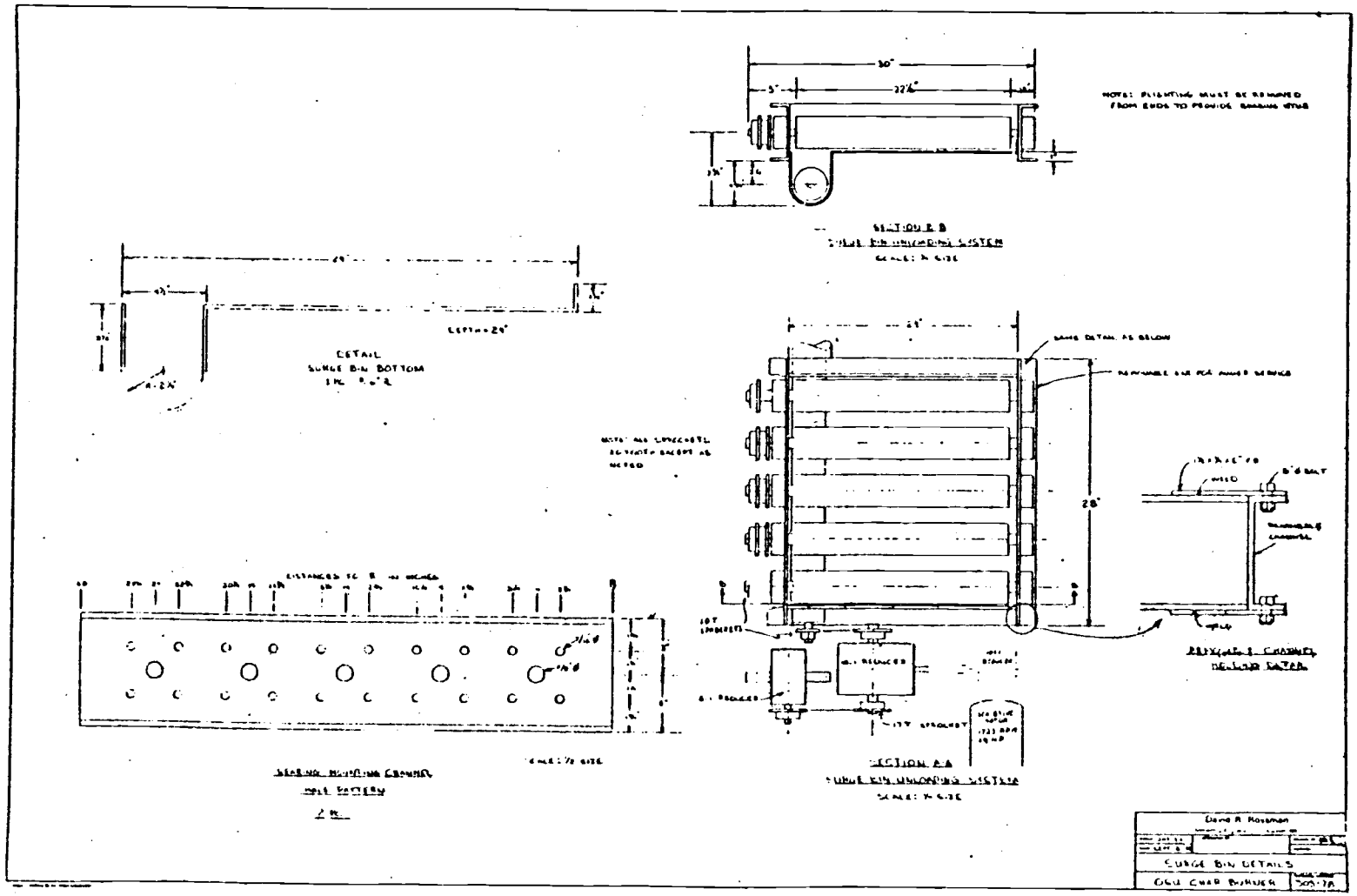

Figure I. 5. Details of the surge bin used in the solids feed system

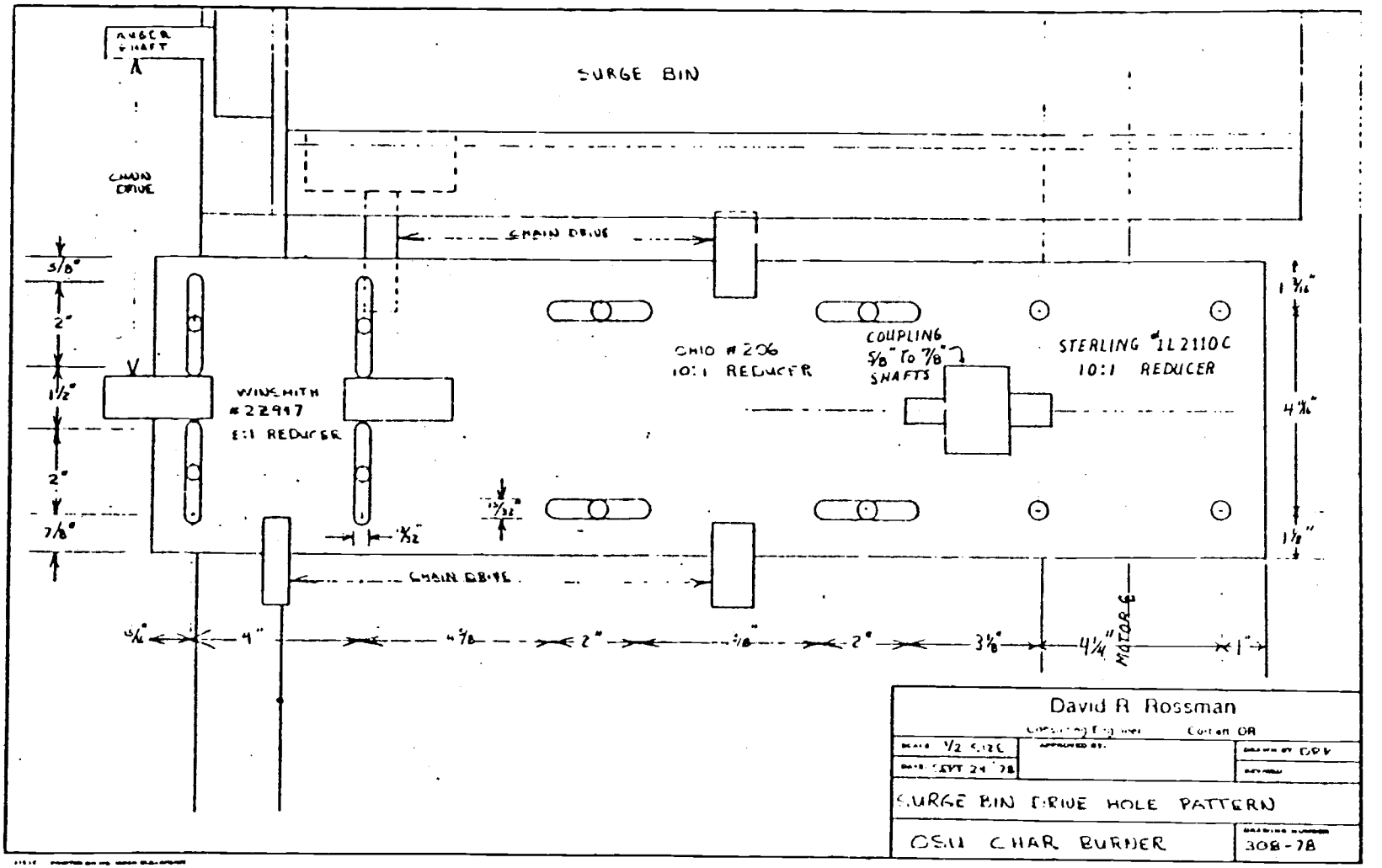

Figure I.6. The surge bin drive hole pattern

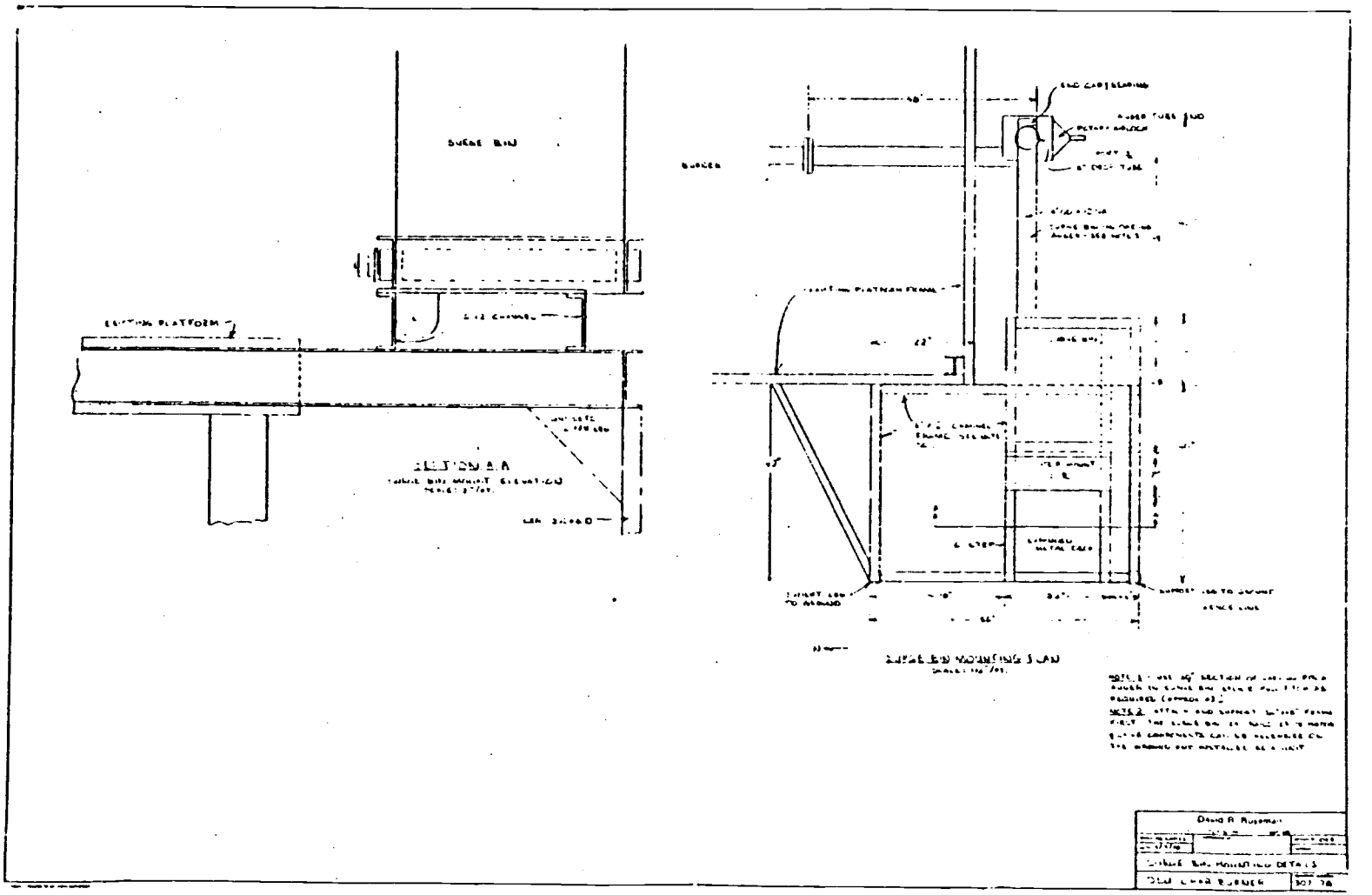

Figure I. 7. The surge bin mounting details

Blank

I. 7). The operation of the positive feed system from the bottom of the surge bin proved very reliable during the experimental work. The only time when problems arose was when the view port at the top of the surge bin was left open overnight. This allowed rain to saturate the char in the bin and when the unit was next operated considerable bridging occurred. This problem was alleviated by flushing the remaining char, with water, out of the bottom of the bin and through the sample port situated on the horizontal auger feeding the air lock. Apart from this single incident, the supply bin was wholly reliable throughout the period of operation.

The level of char in the surge bin was measured with two bindicators (high and low level) situated on the sides of the bin (see Figure I. 8). It was originally hoped to use these level indicators to automatically control the relay auger.

Thus when the level of solids dropped below the low level indicator the relay auger would be turned on, while if the level exceeded the top indicator it would be turned off.

However, due to the reasons previously mentioned, it was necessary to keep the relay auger fully charged with char. Since this would require an operator to continually check the level of the hopper at the base of the auger - it was decided to abandon the original operating procedure. Instead it was found to be more convenient to override

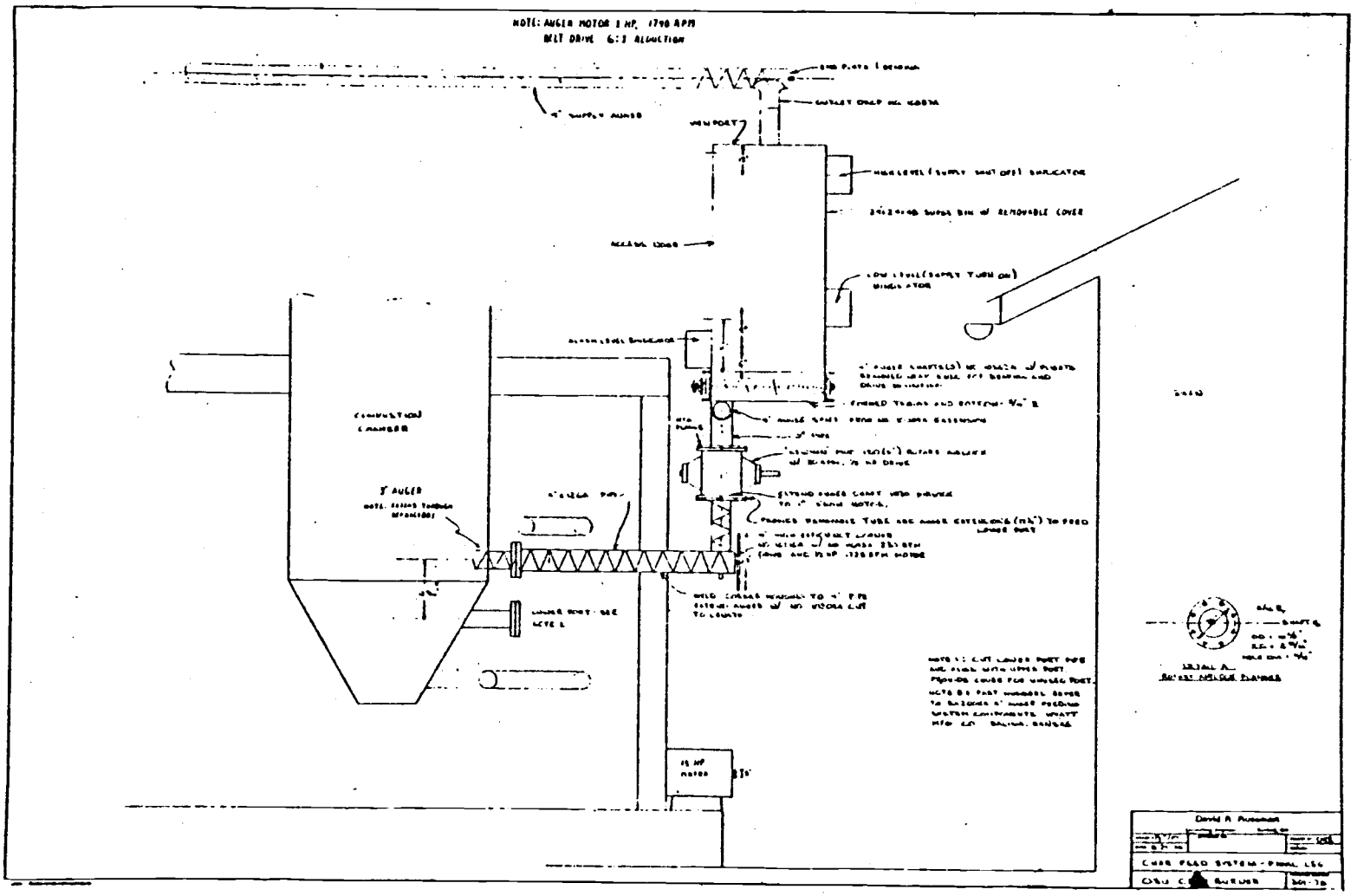

Figure I.8. The final leg of the char feed system

the bottom bindicator signal with a manual one. An extension switch was installed in the shed for this purpose. Thus the relay auger was only operated when someone was around to check the level of solids in the hopper. The only foreseeable problem with this method of operation was the possibility of the surge bin running dry. However, the lower bindicator was wired up to the alarm system. This meant that when the solids level got too low the operator had an instant audible indication and could operate the relay auger accordingly.

Variable speed auger

The horizontal auger connecting the base of the surge bin with the rotary airlock was controlled by the 1.5 horsepower motor, used to operate the augers at the base of the surge bin. The speed of rotation of this motor was in turn controlled by a potentiometer mounted on the control panel (the control panel is shown in Figure I.9 and the potentiometer is the second from the bottom in the second column from the left). Thus the rate at which solids are fed to the rotary airlock, and hence the reactor, is directly controlled by the setting on the potentiometer.

In Appendix C the calibration of this potentiometer, in relation to the solids feed rate, is given.

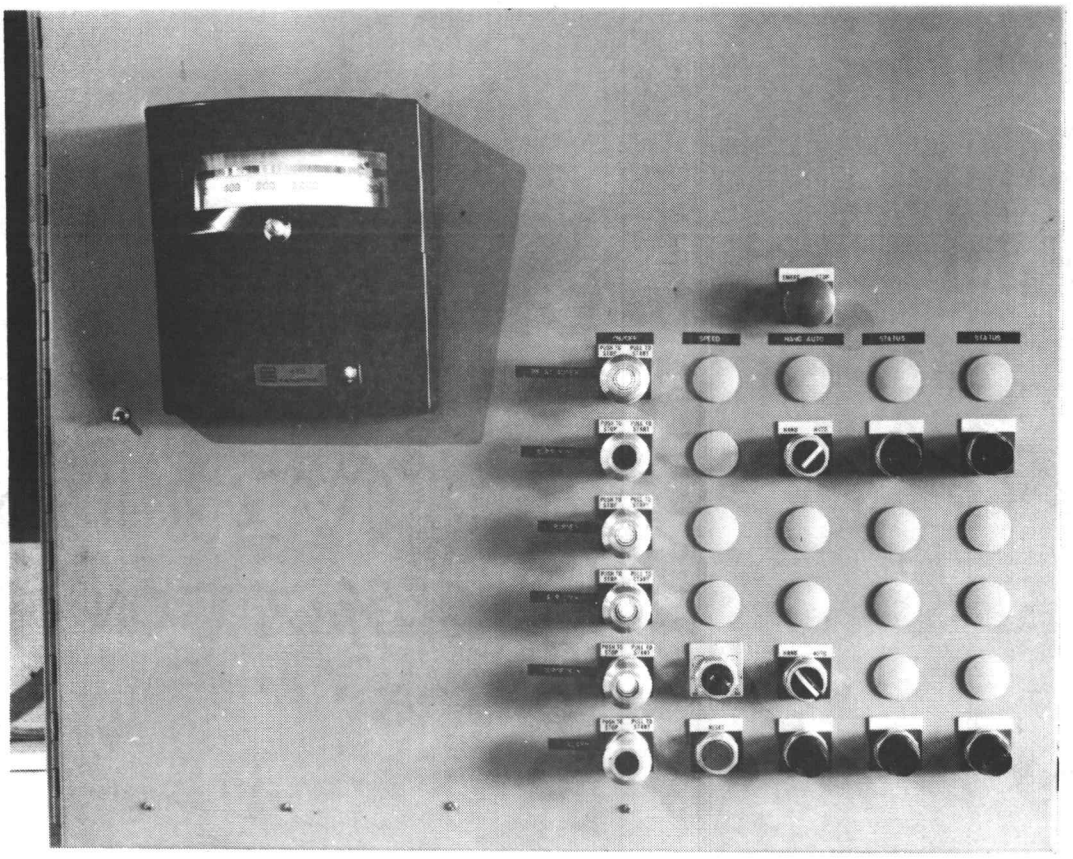

Figure I. 9. The control panel for the operation of the char burner.

The rotary airlock and burner augers

The remaining part of the solids transport system is shown in the drawing of Figure I. 8 and the photograph of Figure I. 10.

The rotary airlock and burner augers are run by two separate motors and operate at such a speed that any feed rate of char to the airlock may be successfully handled.

Again this part of the transport system was fairly reliable. Although towards the end of the runs, the bearings for the burner auger motor had to be replaced, due to excessive wear.

The above discussion covers the major points of the solids transport system. It is worth pointing out that in Figure I. 10 the horizontal burner auger is connected to the upper feed port, while the lower part is blocked off. This was not the usual situation however, and for the majority of the experiments the lower feed port was used. In Figure I. 10 it can also be seen that there is a small air line connected to each solids inlet port. This air line is used to prevent the solids packing in the burner auger and it is important to keep the air line open, especially if the char is slightly damp.

The next section discusses the air feed system and the released instrumentation.

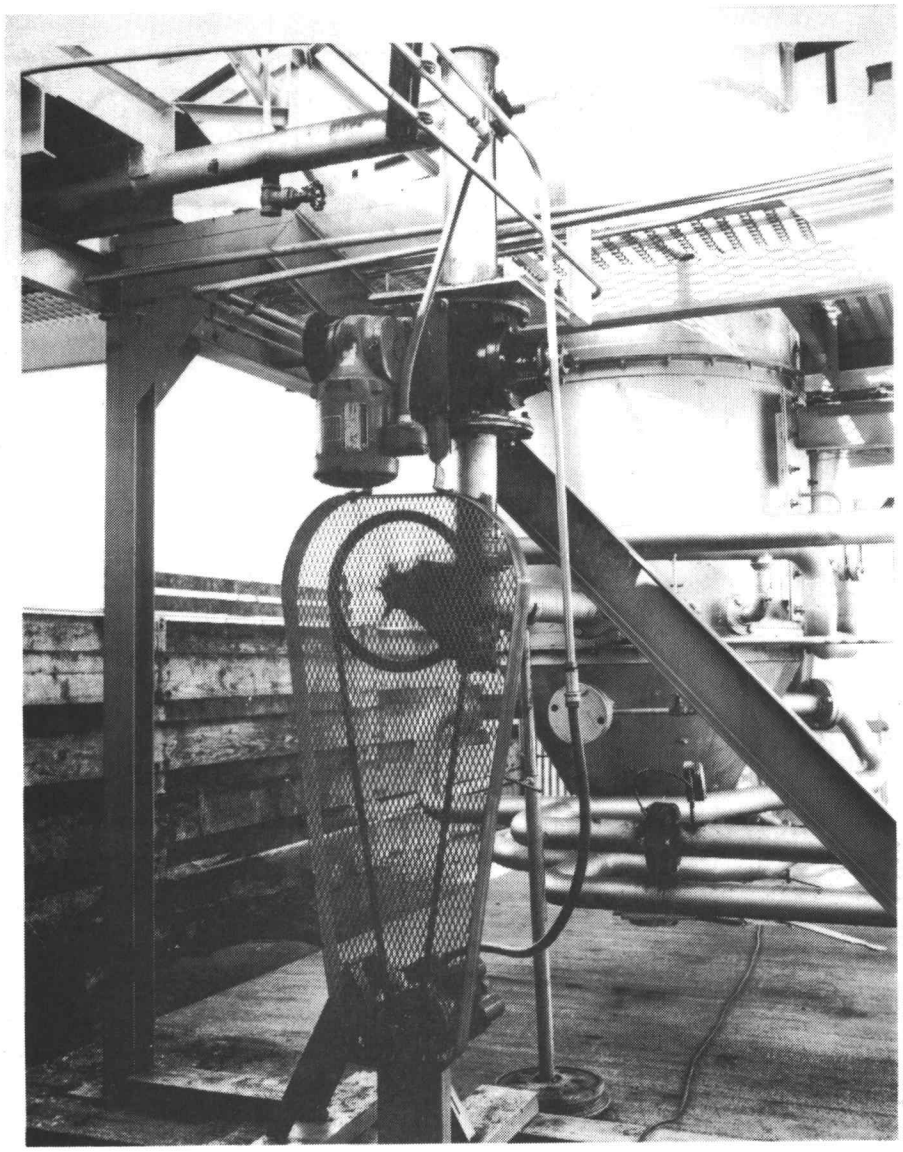

Figure I. 10. Photograph showing the rotary air lock, burner auger, and the tangential air venturi flow meter.

I.2. The Air Feed System

All the air supplied to the reaction chamber is produced by the Roots Blower situated in the main storage building at Fairplay. The blower is shown in Figure I. 11 and again in the air flow diagram of Figure I. 12.

A supply of air is required when the reactor is preheating as well as when it is operating with a char feed. Thus the blower is operating whenever the reactor is in use.

The amount of air entering the combustion chamber as well as the position at which it enters, may be chosen by adjusting the valves illustrated in Figures I. 12 and I. 13.

Excluding the preheat air, there are three main sets of ports through which the air may enter the combustion chamber.

Firstly, the air may be directed into the conical base of the reaction chamber in a radial direction. This would be achieved by opening the lowest valve in Figure I. 13. The four radial ports are positioned symmetrically around the axis of the reaction chamber i. e. at 90° to each other and the incoming air is subjected to considerable mixing on entry. The mixing of inlet air will occur rapidly in this mode since the four separate streams will be directed toward a common point.

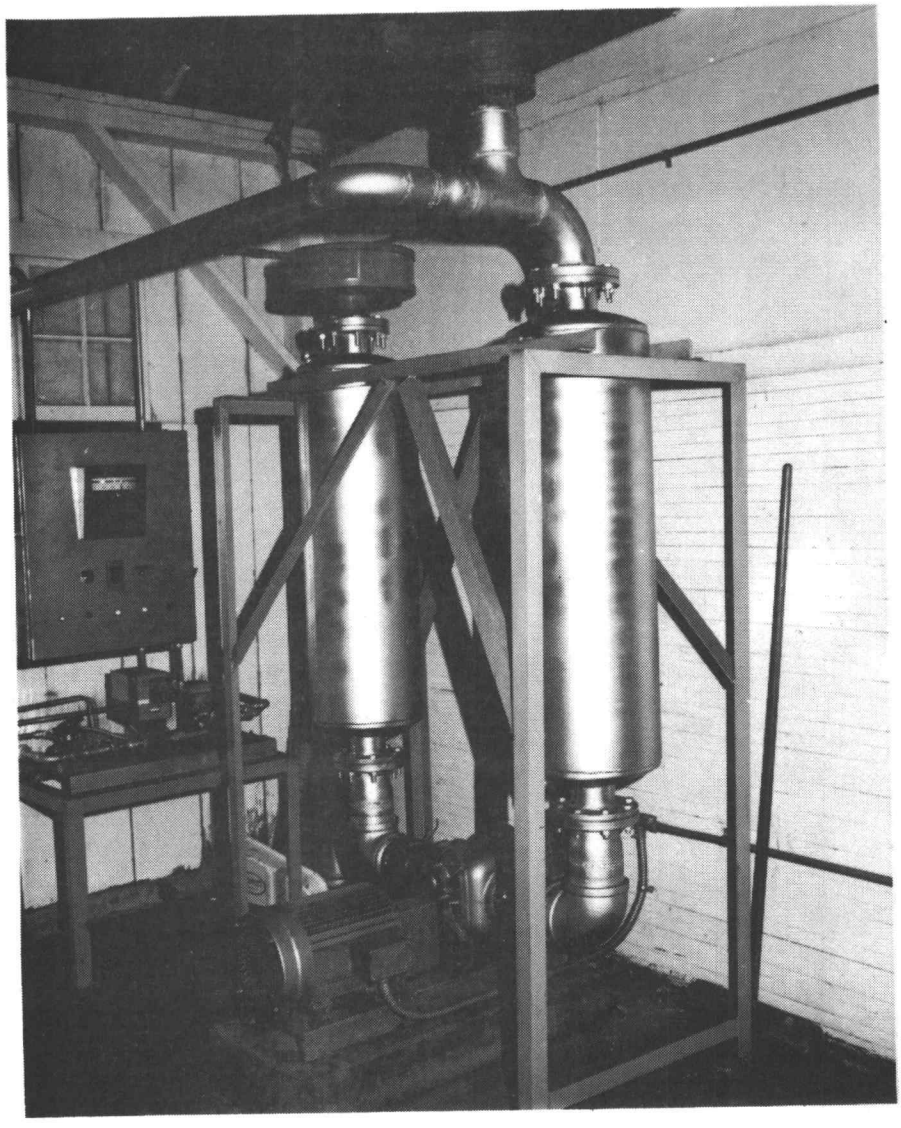

Figure I. 11. Roots blower (350 gj) with 10 H. P. motor and Stoddard (F64-4) silencer.

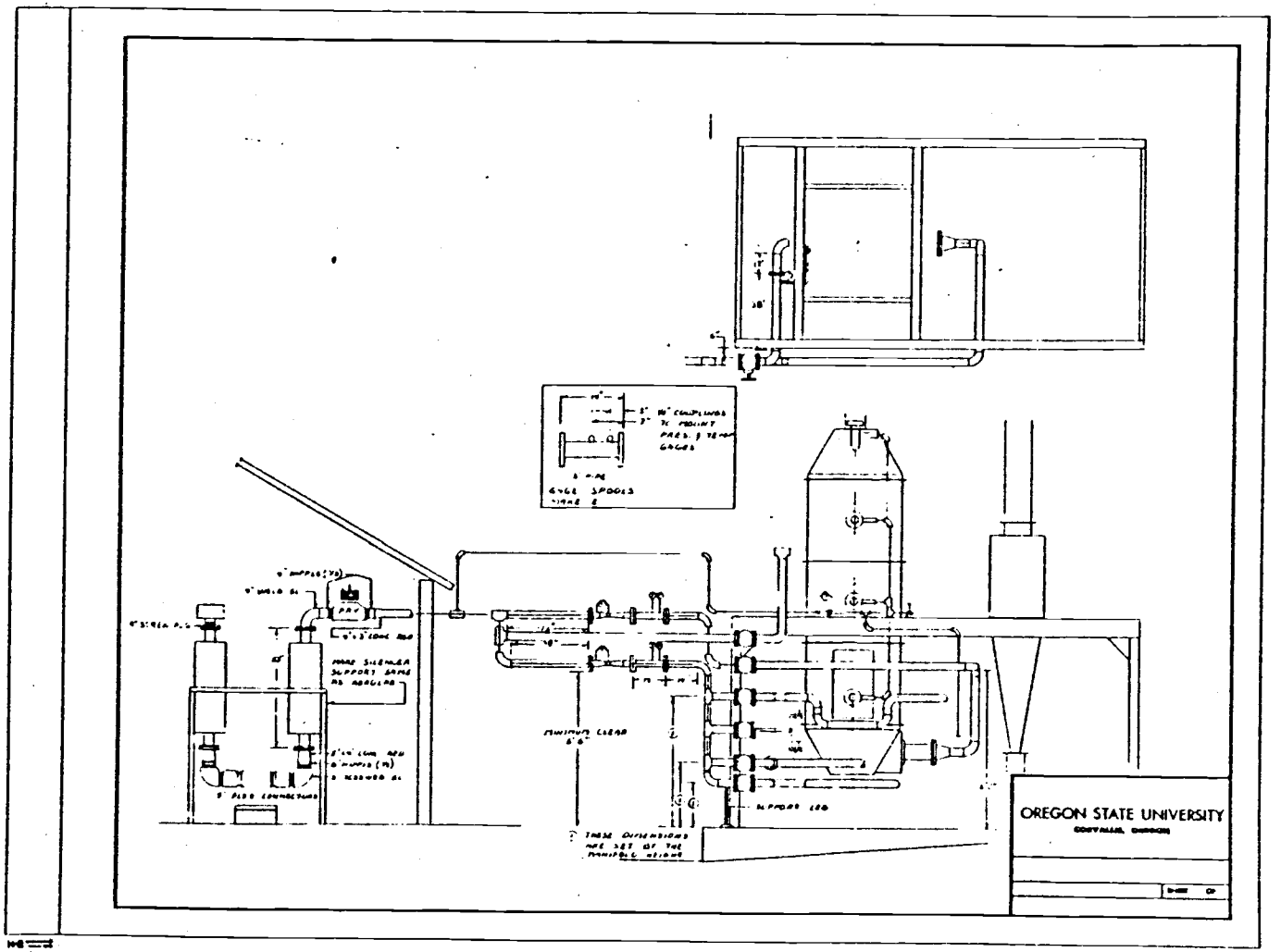

Figure I. 12. The char burner air feed system

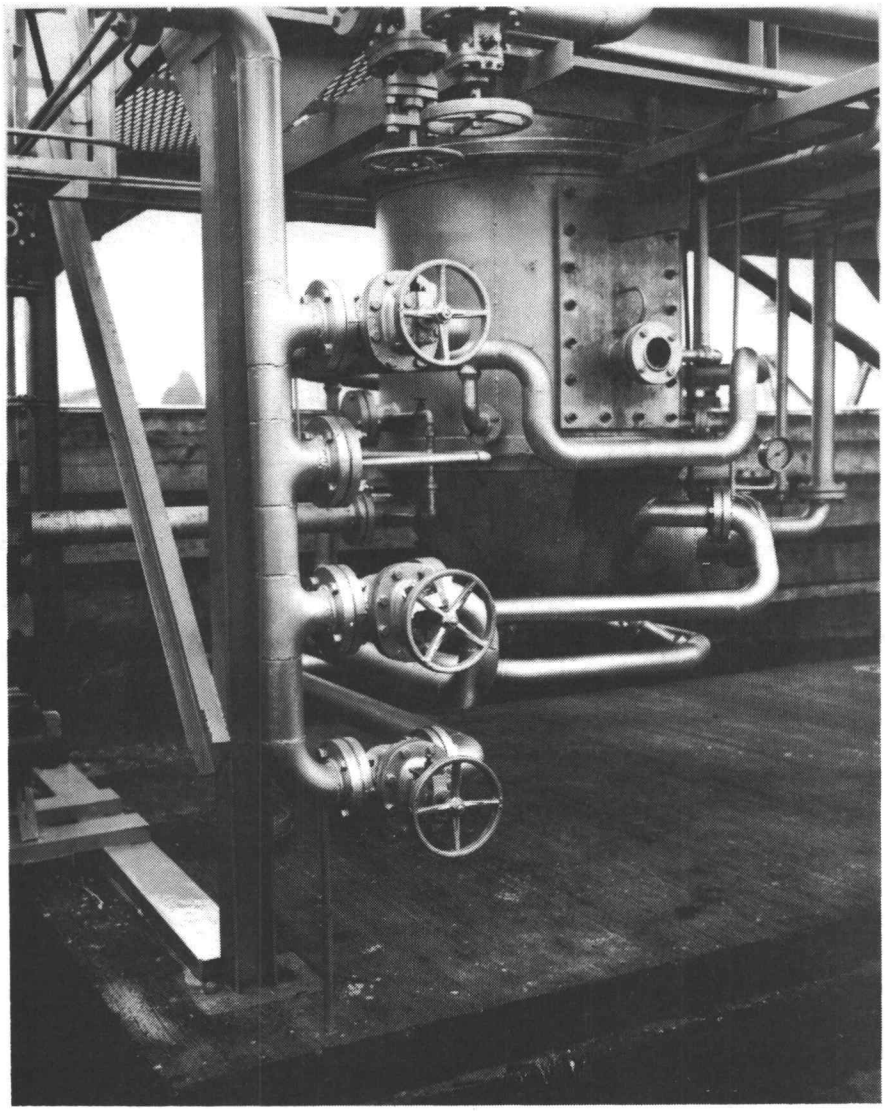

Figure I. 13. The valves controlling the flow rate and direction of air entering the reactor.

The second set of ports which may be used to direct the main air are the two tangential inlets. Since the two incoming air streams are parallel and offset from the center a turning moment about the center of the reactor is seen to occur. Thus the air travels in a spiral towards the exit and the situation is similar to that occurring in a cyclone. The tangential air valve is the second from the bottom of Figure I. 13.

The final mode of introducing the main air into the reactor is through the upper radial ports. These are situated at the top of the conical base section and have the same radial positions as the lower radial ports. The main difference between the upper and lower radial ports is that the air is introduced above the solids feed point in the upper case and below it in the lower case. Another difference between the above two modes is that the air entering via the lower radial ports has an upward velocity component to it which helps to entrain the solids. This is not the case for the upper radial air since it is introduced horizontally. The upper radial air is controlled by the third valve from the bottom in Figure I. 13. The different modes of introducing air into the reactor are shown in the diagram of Figure I. 14.

The only air flow which has not been mentioned so far is via the viewports. This air is required in order to stop the buildup of char and ash in the view ports which would obscure part of the view into the

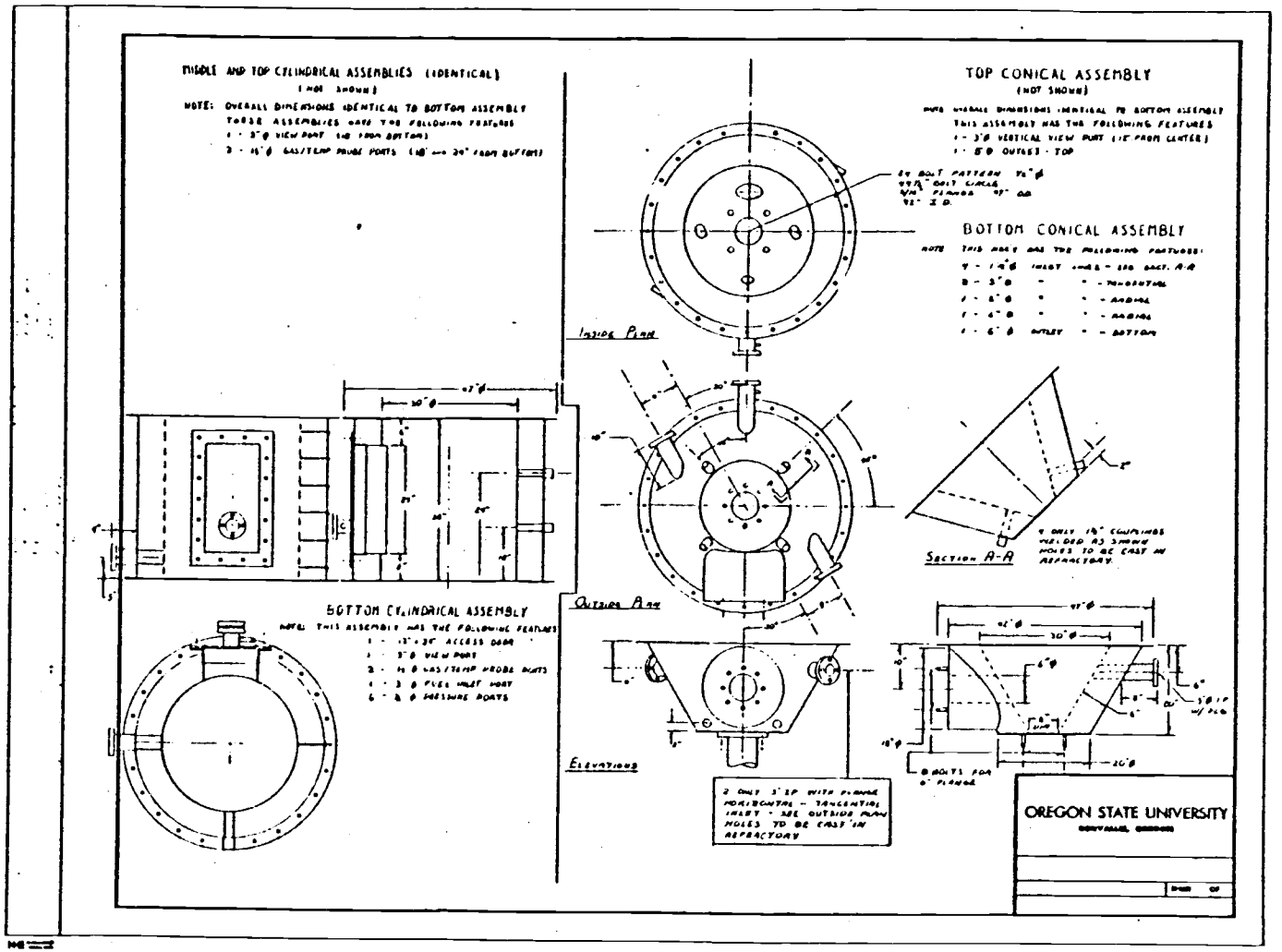

Figure I. 14. Details of the inlet air lines to the char burner

reactor.

In the original design only the bottom three ports were supplied with air. However, during operation it was found that the uppermost view port (looking down from the top of the reactor) was getting clogged with ash. Therefore an extension was added to this upper view port which helped reduce the ash accumulation.

The instrumentation of the air flow

Since the amount of air flowing into the reactor is an important parameter in the evaluation of the reactor's performance it was decided to measure the air flow rate using various flow meters.

In the original design only the main air and preheat air flows were measured using venturi flow meters. A photograph showing the pressure tappings, the temperature meter and gage pressure meter is given in Figure I. 15. Both these flow meters were calibrated by C. Gosmeyer[3] and the results are presented in Appendix C.

The view port air was not originally metered. However, approximately halfway through the series of test runs an orifice meter was added to this line. The orifice along with the vena-contracta pressure tappings and associated pressure gauge are shown in Figure I. 16. This flow meter was calibrated from theory and the results are again presented in Appendix C of this work.

[3]Graduate student, Chemical Engineering, OSU

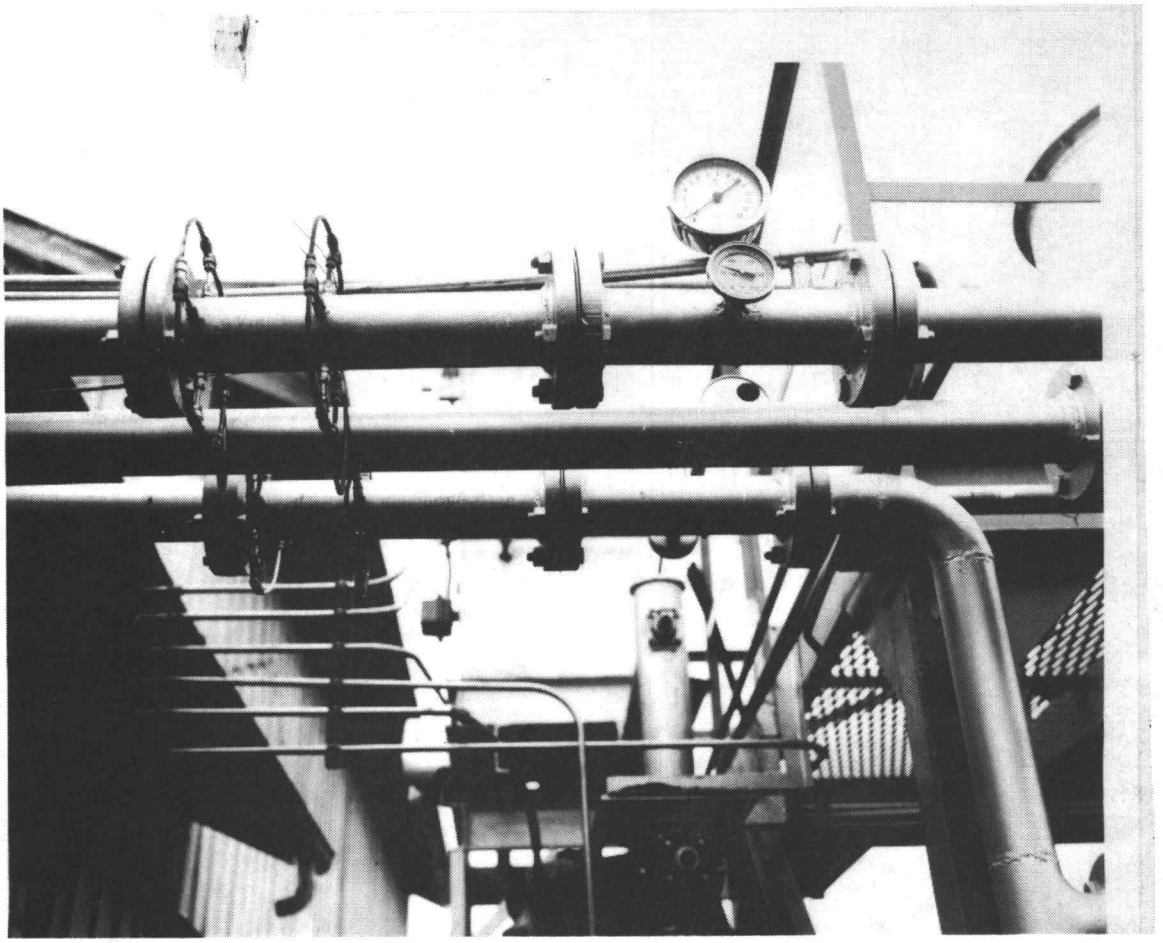

Figure I. 15. Pressure difference, temperature and gauge pressure measurements on the main air and preheat air streams.

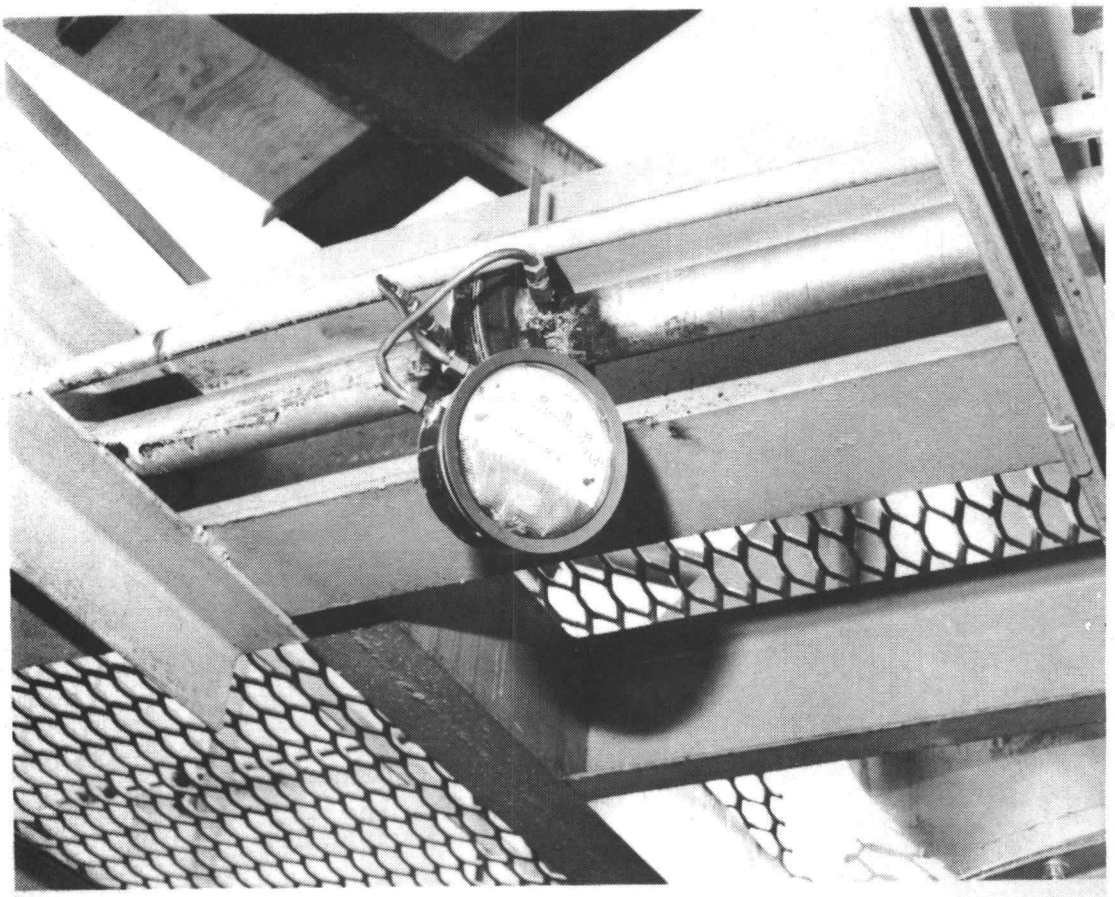

Figure I. 16. Orifice flow meter and associated pressure taps for the view port air line.

Finally at the same time that the above orifice meter was added a flow meter was also added to the tangential air line. This flow meter was shown in Figure I. 10. Unfortunately the only possible position was directly following a 90° lead in the air line. Thus the calibration of this meter could not be accurately calculated from theory. Thus, it was calibrated in situ and the results are presented in Appendix C.

I. 3. The Preheat System

Before the reactor may be used in its normal operating mode i. e. using wood char and inlet air at atmospheric conditions, the reaction chamber must be preheated. This preheating is necessary since at atmospheric conditions the rate of combustion of wood char is virtually zero. Hence, satisfactory operation cannot be achieved by simply introducing char and air into a cold reaction chamber.

The method of preheating the reactor uses propane gas as its source of fuel. The preheating system was designed by G. Edgel Co., Portland. The main principle of operation is to ignite a mixture of propane and air as it enters the reaction chamber. The photograph of Figure I. 17 shows the main propane line and the pilot line joining the preheat air line.

The control system used in the preheating system is shown in Figure I. 18 and the information flow diagram is presented in Figure I. 19.

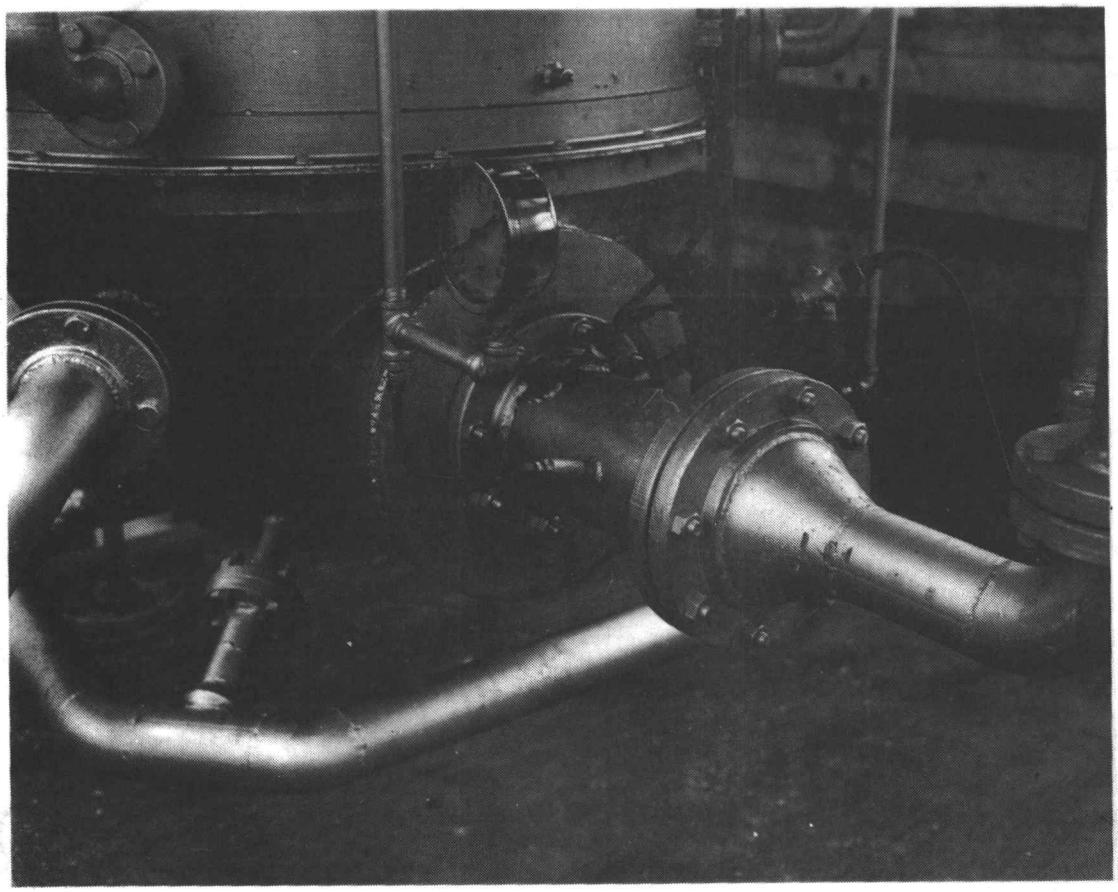

Figure I. 17. The propane pilot line (right) and the main propane line (left) joining the preheat air line.

The procedure used in the preheating cycle, along with the procedure for fuel changeover (propane to char), preheat restart and shutdown is given in Table I. 1 at the end of this Appendix.

I. 4. Experimental Operation

During the course of a test run certain measurments are recorded which allow the performance of the burner to be analyzed.

After the solids feed rate has been set the direction and flow rate of combustion air is adjusted to give a satisfactory operating point. This operating point must be such that the temperature within the reaction chamber does not exceed 1370 K (approximately 2000°F) at which point the ash produced by combustion starts to melt.

The temperature within the reactor is measured at three points, with platinum resistance thermocouples. The readout for these measuring instruments is via two analog displays situated in the main storage building. The first display is situated by the control panel (see Figure I. 9) and is used to read the middle and top thermocouple. A selector switch is provided to the left of the display and is used to select the desired thermocouple reading. The second display is used solely to read the temperature of the bottom thermocouple and it is situated above the preheat control system (see Figure I. 18).

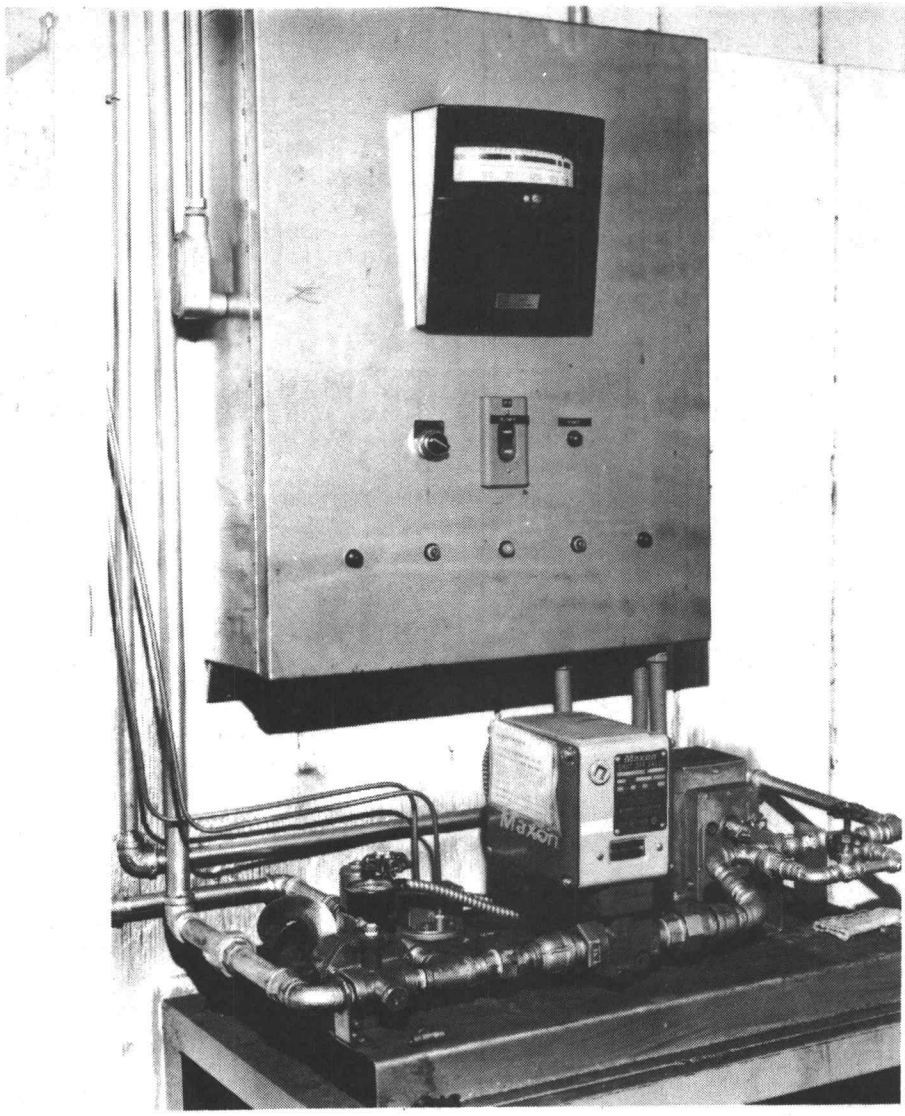

Figure I. 18. Photograph of the preheat control system.

The three thermocouples are spread through the length of the reaction chamber at a distance of approximately one meter apart. The first one is approximately a half a meter above the lower solids feed port. At every thermocouple location there is a gas sampling port close by. The gas sampling equipment consists of a length of 6.34 mm stainless steel tubing projecting into the reactor, with a 2 micron filter attached to it. The tubing is bent away from the gas stream in order to minimize the amount of ash and char sucked into the sampling system. The bulk of any material entering the system is then stopped by the 2 micron filter. The thermocouple and gas sampler are illustrated in Figure I.20.

The gas sample is sucked through a system of 6.35 mm brass tubing via a vaccuum pump and into the gas analysis equipment. Before the gas reaches the analysis equipment it is fed through a refrigerator and two filters in order to remove the water vapour present.

This method of gas sampling was not particularly reliable since it did not take long for the 2 micron filters to become clogged and there seemed to be a permanent error in the gas analysis results, which may have been due to faulty equipment. Another problem, which may have been due to the filters clogging, was the wear on the vaccuum pump and the diaphragm had to be replaced on one occasion.

Finally, during the operation of the reactor a bed of unburnt char

particles would build up at the base of the reactor. In order to conveniently remove this bed at the end of each day's operation a system of two valves was added to the base of the reactor (see Figure I.21). This also allowed the formation of slag to be checked periodically and proved a very useful addition.

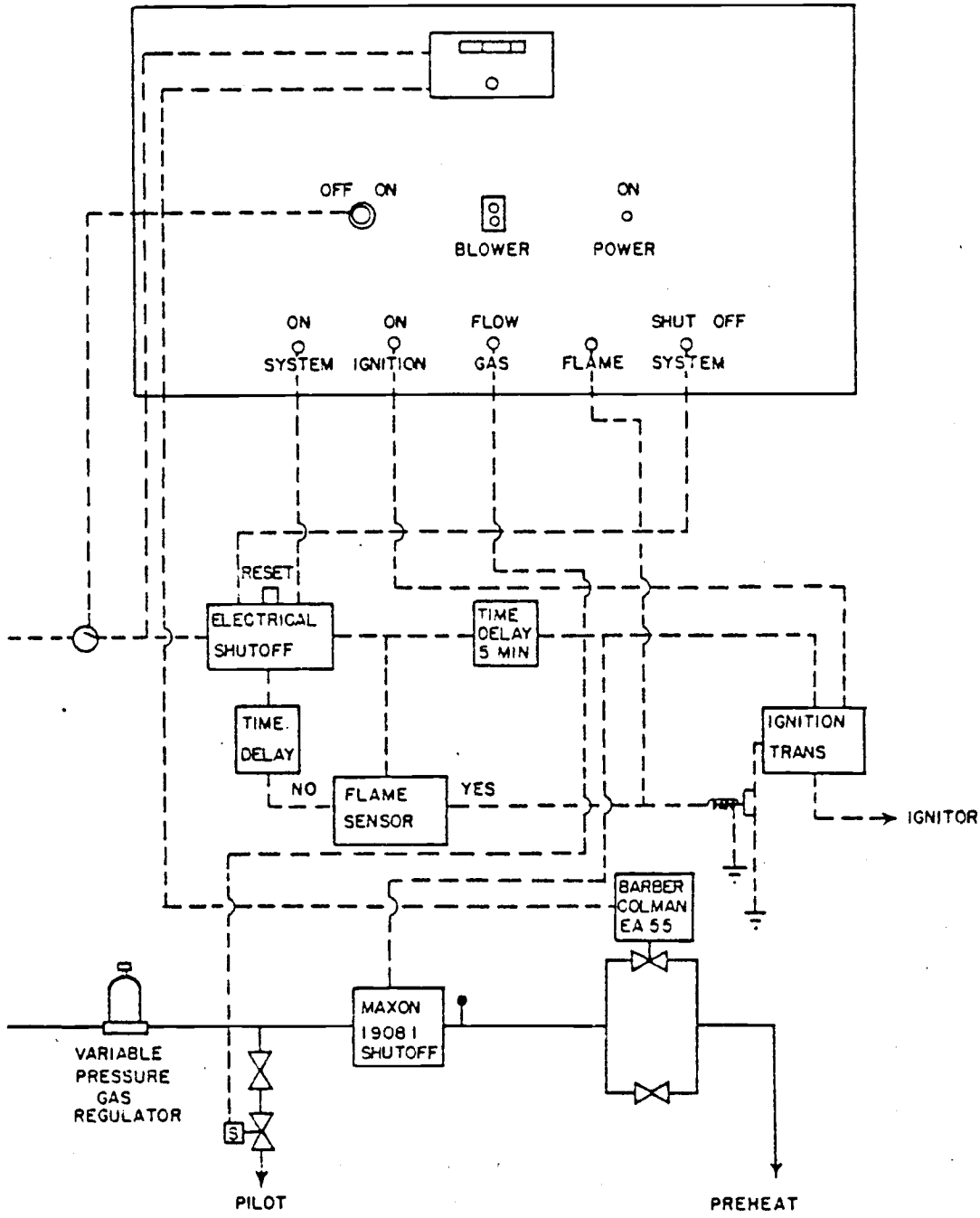

Figure I.19. The preheater control schematic diagram

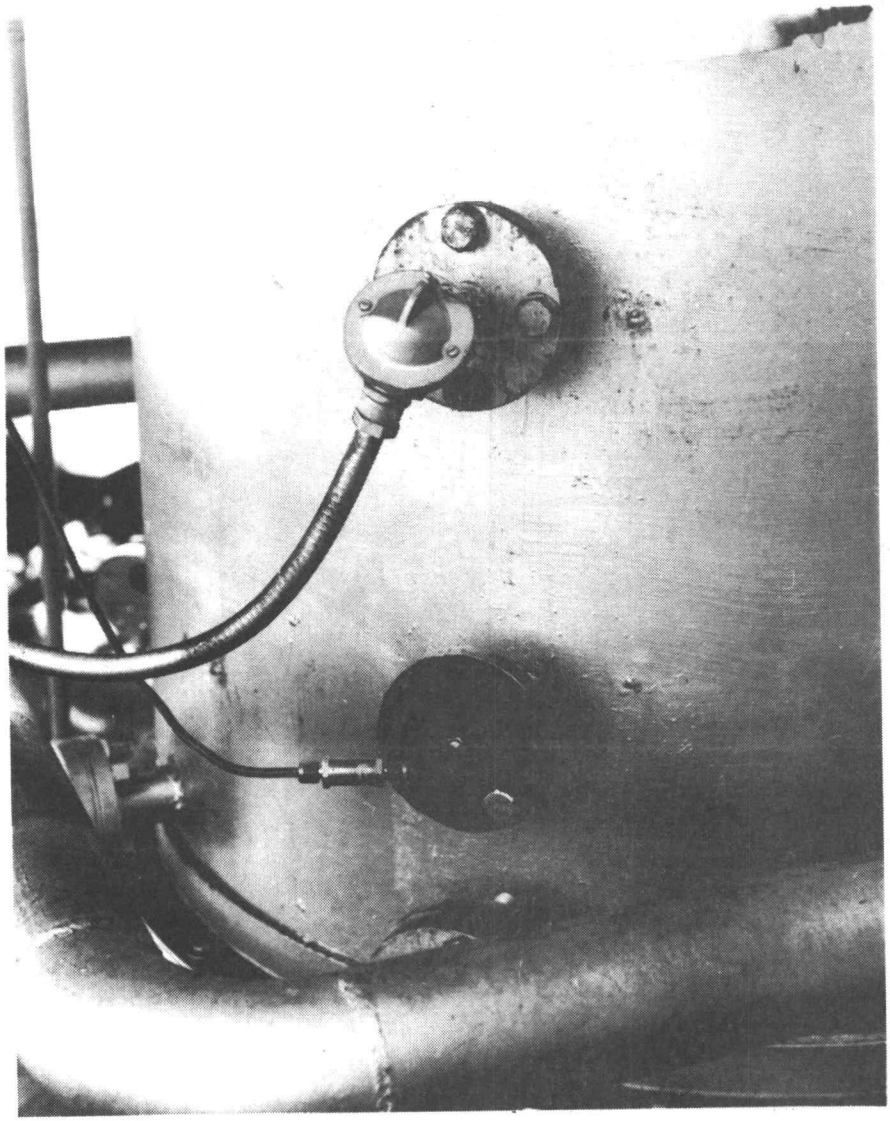

Figure I.20. Thermocouple port (top) and gas sample port (bottom) with the in line 2 micron filter.

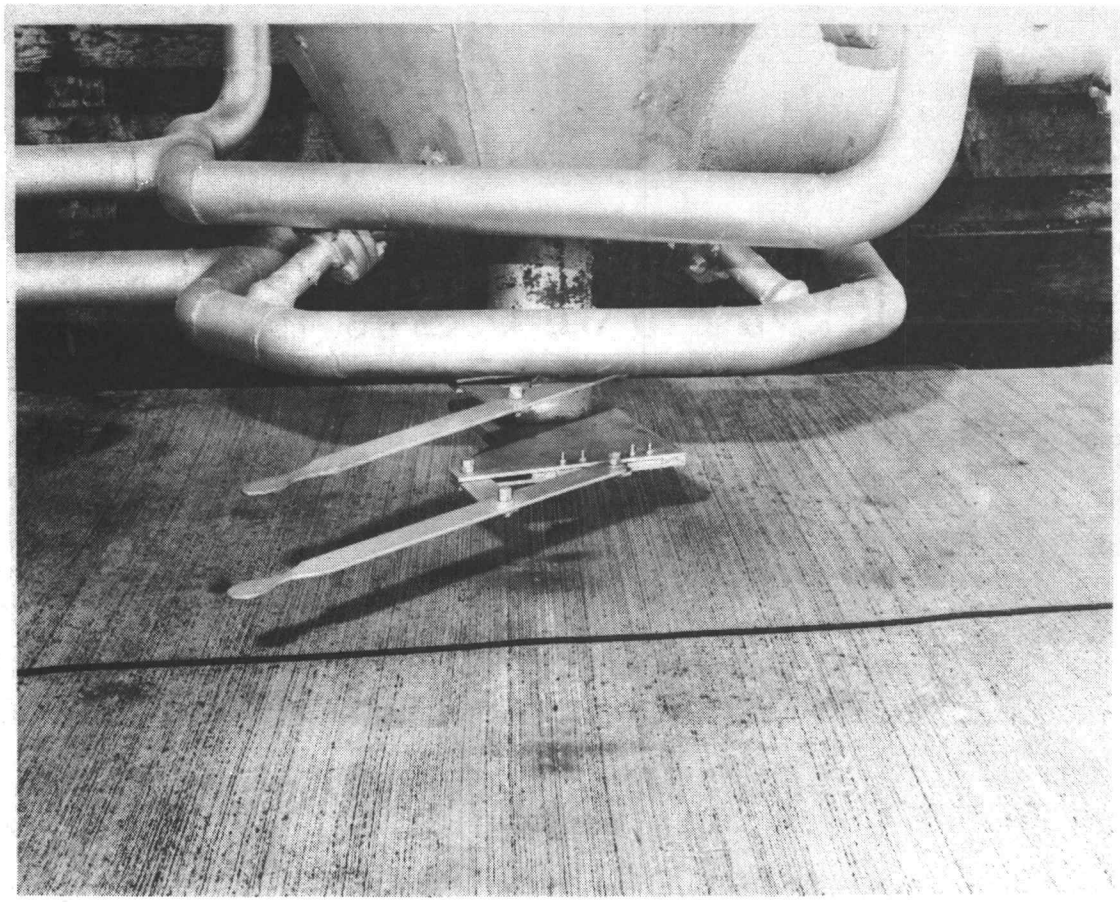

Figure I.21. Two valve system to remove unwanted build up from the bottom of the reaction chamber.

Table I. 1. Char burner run procedures.

Preheat

1. Gas tank valve - open
2. Gas pressure regulator - 1 to 2 psi
3. Pilot gas valve - open
4. Air valves
   a. Blower circuit breaker - on
   b. Blower - start
   c. Air bypass - set 1 to 2 psi
   d. Main air (upper, tangential, radial) - closed
   e. Preheater combustion air - set 1" to 2"
   f. View port air - set less than 5"
5. Gas system switch - on (five minute delay)

   NOTE: Light off automatic. If stable ignition not achieved adjust gas pressure and air flow. If system shut down indicator comes on, reset system using red button in panel.

   Indicator lights
   1. green - system activated
   2. white - ignition activated
   3. orange - pilot gas shut off open
      preheat gas valve armed
   4. white - combustion occurring
   5. red - system shut down
6. Maintain desired temperature - stabilize @ 420 K, increase 60 K to 120 K per hour until 1150 K
   a. Preheater combustion air - minimum to maintain good flame
   b. Gas regulator pressure - increase as necessary
   c. Temperature controller - set
   d. Preheat gas valve - on
   e. Preheat gas bypass - as required to maintain temperature controller valve near mid range.

Fuel changeover

1. Char management circuit breaker - on
2. Fuel inlet air valve - on at inlet in use
3. Main air valves - as required
4. Burner auger - on
5. Air lock - on
6. Surge bin auger - on

   } Check operation visually
7. Preheat system switch - off
8. Preheat combustion air - off
9. Burner auger - adjust feed rate to maintain desired temperatures. Allow fuel bed to form then decrease feed rate.

Table I. 1. (Continued)

Preheat restart (high combustion chamber temperatures)

1. Preheat system switch - on
2. Preheater combustion air - 5" to 7"
3. Gas regulator pressure - 5 to 7 psi
4. Stable combustion - light on, temperature rising
5. Char feed system - off
   a. Surge bin auger - off
   b. Air lock - off
   c. Burner auger - off
      NOTE: Do not turn off air to fuel feed port at any time when burner auger is running.
6. Main air - off
7. Bypass air - 1 to 2 psi back pressure
8. View port air - less than 5"
9. Maintain desired temperature
   a. Temperature controller - set
   b. Preheat gas valve - on
   c. Gas regulator pressure - as required
      NOTE: Chamber temperature will tend to decrease with time. Set pressure so controller gas valve is initially fully closed, with preheat gas bypass closed.

Shut down

1. Char feed system - off
   a. Surge bin auger - off
   b. Air lock - off
   c. Burner auger - off
2. Gas system - off
   a. Preheat system switch - off
   b. Tank valve - off
3. Blower - off
4. Circuit breakers - off

Table I.2. Mechanical components.

Name: Air System

Roots Blower 350 gJ with 10 hp motor
Stoddard F64-4 silencer

Fuel System:

Relay Auger Motor, 1 hp, 1740 rpm, w/6:1 belt reduction
Surge Bin Auger, 1.5 hp, 1750 rpm, DC-SCR
w/Sterling 142110C 10:1
Ohio 206
Winsmith 2Z947
} gear reduction
Rotary Air Lock, Newman, Valve type 150 cc
Chaindrive
1/2 hp motor w/internal reduction to 30 rpm
Burner Auger, 1-1/2 hp, 1750 rpm, w/6.5:1 belt reduction

APPENDIX J

COMPUTER GENERATED RESULTS FOR THE COMBUSTION MODEL

Table J.1. Computer results for Test Run P1 using the direct method to calculate the solids flowrate.

THE RESULTS FOR THE SIMULATED COMBUSTION MODEL TEST RUN P1

THE INLET CONDITIONS FOR AIR AND WOODCHAR

FLOWRATE OF SOLIDS = .5115E-02 KG/S
TEMPERATURE OF SOLIDS= 285.0 K
COMBUSTIBLE CONTENT = .7373
MOISTURE CONTENT = .0507
INORGANIC CONTENT = .2120

MAIN AIR FLOWRATE = .4033E-02 KMOLE/S
TEMPERATURE OF AIR = 313.6 K
AIR FOR VIEW PORT 1 = .1538E-03 KMOLE/S
AIR FOR VIEW PORT 2 = .1538E-03 KMOLE/S
AIR FOR VIEW PORT 3+4= .3076E-03 KMOLE/S

THE INLET SIZE DISTRIBUTION FOR THE SOLIDS FEED

MEAN DIAMETER (M)	.2250E-04	.5400E-04	.9400E-04	.1880E-03	.3750E-03	.7500E-03	.1500E-02	.2665E-02	.4013E-02
SPHERICAL DIAMETER (M)	.1350E-04	.3240E-04	.5640E-04	.1128E-03	.2250E-03	.4500E-03	.9000E-03	.1599E-02	.2408E-02
WEIGHT FRACTION	.0235	.0450	.0432	.0568	.1529	.2787	.3532	.0367	.0100

THE TEMPERATURE OF THE REACTANTS LEAVING THE INITIAL MIXING ZONE IS 717.2 (K)

THE SIZE DISTRIBUTION LEAVING THE INITIAL MIXING ZONE

MEAN DIAMETER (M)	.1350E-04	.3240E-04	.5640E-04	.1128E-03	.2250E-03	.4146E-03	.9000E-03	.1599E-02	.2408E-02
WEIGHT FRACTION	.0400	.0767	.0736	.0968	.2605	.4524	0.0000	0.0000	0.0000

THE CALCULATED SURFACE AVERAGE PARTICLE DIAMETER IS .1292E-03 (M)

GAS FLOW INTO REACTION ZONE = .0040 KMOLE/S
CSA OF REACTION ZONE = .4560 M2
GAS FLOW INTO BYPASS ZONE = 0 KMOLE/S
CSA OF BYPASS ZONE = 0 M2

THE RESULTS FOR THE PLUG FLOW SECTION

LENGTH	TEMPERATURE	CONVERSION	M F O2	M F CO2	M F N2
0	717.2461	.4131	.1778	.0322	.7900
.1195	788.5182	.4396	.1757	.0343	.7900
.2395	868.7139	.5077	.1704	.0396	.7900
.3595	1098.4542	.7457	.1519	.0581	.7900
.4795	1196.1278	.8571	.1432	.0668	.7900
.5995	1212.6105	.9107	.1416	.0684	.7900
.7195	1242.8525	.9471	.1389	.0711	.7900
2.6835	1194.0889	1.0000	.1424	.0676	.7900
5.0835	1181.0887	1.0000	.1424	.0676	.7900
7.4835	1168.9547	1.0000	.1424	.0676	.7900
9.8835	1157.6302	1.0000	.1424	.0676	.7900

Table J.2. Computer results for Test Run P1 using the indirect method to calculate the solids flowrate.

THE RESULTS FOR THE SIMULATED COMBUSTION MODEL TEST RUN P1

THE INLET CONDITIONS FOR AIR AND WOODCHAR

FLOWRATE OF SOLIDS = .6525E-02 KG/S
TEMPERATURE OF SOLIDS= 285.0 K
COMBUSTIBLE CONTENT = .7373
MOISTURE CONTENT = .0507
INORGANIC CONTENT = .2120

MAIN AIR FLOWRATE = .4033E-02 KMOLE/S
TEMPERATURE OF AIR = 313.6 K
AIR FOR VIEW PORT 1 = .1538E-03 KMOLE/S
AIR FOR VIEW PORT 2 = .1538E-03 KMOLE/S
AIR FOR VIEW PORT 3+4= .3076E-03 KMOLE/S

THE INLET SIZE DISTRIBUTION FOR THE SOLIDS FEED

MEAN DIAMETER (M)	.2250E-04	.5400E-04	.9400E-04	.1880E-03	.3750E-03	.7500E-03	.1500E-02	.2665E-02	.4013E-02
SPHERICAL DIAMETER (M)	.1350E-04	.3240E-04	.5640E-04	.1128E-03	.2250E-03	.4500E-03	.9000E-03	.1599E-02	.2408E-02
WEIGHT FRACTION	.0235	.0450	.0432	.0568	.1529	.2787	.3532	.0367	.0100

THE TEMPERATURE OF THE REACTANTS LEAVING THE INITIAL MIXING ZONE IS 763.1 (K)

THE SIZE DISTRIBUTION LEAVING THE INITIAL MIXING ZONE

MEAN DIAMETER (M)	.1350E-04	.3240E-04	.5640E-04	.1128E-03	.2250E-03	.4411E-03	.9000E-03	.1599E-02	.2408E-02
WEIGHT FRACTION	.0389	.0707	.0679	.0892	.2402	.4951	0.0000	0.0000	0.0000

THE CALCULATED SURFACE AVERAGE PARTICLE DIAMETER IS .1399E-03 (M)

GAS FLOW INTO REACTION ZONE = .0040 KMOLE/S
CSA OF REACTION ZONE = .4560 M2
GAS FLOW INTO BYPASS ZONE = 0 KMOLE/S
CSA OF BYPASS ZONE = 0 M2

THE RESULTS FOR THE PLUG FLOW SECTION

LENGTH	TEMPERATURE	CONVERSION	M F O2	M F CO2	M F N2
0	763.1445	.3634	.1739	.0361	.7900
.1197	995.8933	.5332	.1570	.0530	.7900
.2397	1257.7047	.7606	.1344	.0756	.7900
.3597	1333.5003	.8326	.1272	.0828	.7900
.4797	1383.1552	.8813	.1224	.0876	.7900
.5997	1383.5546	.9170	.1222	.0878	.7900
1.0817	1439.1912	.9756	.1166	.0934	.7900
2.4917	1413.6593	1.0000	.1176	.0924	.7900
3.8997	1336.4200	1.0000	.1238	.0862	.7900
5.3997	1322.3218	1.0000	.1238	.0862	.7900
6.8997	1308.7977	1.0000	.1238	.0862	.7900

Table J.3. Computer results for Test Run P2 using the direct method to calculate the solids flowrate.

THE RESULTS FOR THE SIMULATED COMBUSTION MODEL TEST RUN P2

THE INLET CONDITIONS FOR AIR AND WOODCHAR

FLOWRATE OF SOLIDS = .6807E-02 KG/S
TEMPERATURE OF SOLIDS= 285.0 K
COMBUSTIBLE CONTENT = .7093
MOISTURE CONTENT = .0507
INORGANIC CONTENT = .2400

MAIN AIR FLOWRATE = .5077E-02 KMOLE/S
TEMPERATURE OF AIR = 305.2 K
AIR FOR VIEW PORT 1 = .3625E-03 KMOLE/S
AIR FOR VIEW PORT 2 = .3625E-03 KMOLE/S
AIR FOR VIEW PORT 3+4= .7250E-03 KMOLE/S

THE INLET SIZE DISTRIBUTION FOR THE SOLIDS FEED

MEAN DIAMETER (M)	.2250E-04	.5400E-04	.9400E-04	.1880E-03	.3750E-03	.7500E-03	.1500E-02	.2665E-02	.4013E-02
SPHERICAL DIAMETER (M)	.1350E-04	.3240E-04	.5640E-04	.1128E-03	.2250E-03	.4500E-03	.9000E-03	.1599E-02	.2408E-02
WEIGHT FRACTION	.0215	.0403	.0420	.0476	.1254	.2370	.3171	.1293	.0398

THE TEMPERATURE OF THE REACTANTS LEAVING THE INITIAL MIXING ZONE IS 716.3 (K)

THE SIZE DISTRIBUTION LEAVING THE INITIAL MIXING ZONE

MEAN DIAMETER (M)	.1350E-04	.3240E-04	.5640E-04	.1128E-03	.2250E-03	.4500E-03	.5026E-03	.1599E-02	.2408E-02
WEIGHT FRACTION	.0368	.0689	.0719	.0814	.2145	.4055	.1210	0.0000	0.0000

THE CALCULATED SURFACE AVERAGE PARTICLE DIAMETER IS .1441E-03 (M)

GAS FLOW INTO REACTION ZONE = .0051 KMOLE/S
CSA OF REACTION ZONE = .4560 M2
GAS FLOW INTO BYPASS ZONE = 0 KMOLE/S
CSA OF BYPASS ZONE = 0 M2

THE RESULTS FOR THE PLUG FLOW SECTION

LENGTH	TEMPERATURE	CONVERSION	M F O2	M F CO2	M F N2
0	716.2695	.4155	.1771	.0329	.7900
.1185	751.8458	.4236	.1764	.0336	.7900
.2385	786.3502	.4396	.1752	.0348	.7900
.3565	833.3220	.4753	.1723	.0377	.7900
.4785	927.2442	.5664	.1651	.0449	.7900
.5985	1024.4897	.7191	.1568	.0532	.7900
.7185	1110.7578	.8204	.1493	.0607	.7900
.8385	1149.1477	.8664	.1459	.0641	.7900
.9585	1177.5093	.9008	.1434	.0666	.7900
2.5745	1116.0580	1.0000	.1483	.0617	.7900
4.9745	1109.0652	1.0000	.1483	.0617	.7900

Table J.4. Computer results for Test Run P2 using the indirect method to calculate the solids flowrate.

THE RESULTS FOR THE SIMULATED COMBUSTION MODEL TEST RUN P2

THE INLET CONDITIONS FOR AIR AND WOODCHAR

FLOWRATE OF SOLIDS = .8684E-02 KG/S
TEMPERATURE OF SOLIDS= 285.0 K
COMBUSTIBLE CONTENT = .7093
MOISTURE CONTENT = .0507
INORGANIC CONTENT = .2400

MAIN AIR FLOWRATE = .5077E-02 KMOLE/S
TEMPERATURE OF AIR = 305.2 K
AIR FOR VIEW PORT 1 = .3625E-03 KMOLE/S
AIR FOR VIEW PORT 2 = .3625E-03 KMOLE/S
AIR FOR VIEW PORT 3+4= .7250E-03 KMOLE/S

THE INLET SIZE DISTRIBUTION FOR THE SOLIDS FEED

MEAN DIAMETER (M)	.2250E-04	.5400E-04	.9400E-04	.1880E-03	.3750E-03	.7500E-03	.1500E-02	.3665E-02	.4013E-02
SPHERICAL DIAMETER (M)	.1350E-04	.3240E-04	.5640E-04	.1128E-03	.2250E-03	.4500E-03	.9000E-03	.1599E-02	.2406E-02
WEIGHT FRACTION	.0215	.0403	.0420	.0476	.1254	.2370	.3171	.1293	.0398

THE TEMPERATURE OF THE REACTANTS LEAVING THE INITIAL MIXING ZONE IS 794.4 (K)

THE SIZE DISTRIBUTION LEAVING THE INITIAL MIXING ZONE

MEAN DIAMETER (M)	.1350E-04	.3240E-04	.5640E-04	.1128E-03	.2250E-03	.4500E-03	.5569E-03	.1599E-02	.2406E-02
WEIGHT FRACTION	.0354	.0663	.0691	.0783	.2064	.3901	.1543	0.0000	0.0000

THE CALCULATED SURFACE AVERAGE PARTICLE DIAMETER IS .1501E-03 (M)

GAS FLOW INTO REACTION ZONE = .0051 KMOLE/S
CSA OF REACTION ZONE = .4560 M2
GAS FLOW INTO BYPASS ZONE = 0 KMOLE/S
CSA OF BYPASS ZONE = 0 M2

THE RESULTS FOR THE PLUG FLOW SECTION

LENGTH	TEMPERATURE	CONVERSION	M F O2	M F CO2	M F N2
0	794.3945	.3924	.1703	.0397	.7900
.1195	891.7975	.4670	.1628	.0472	.7900
.2395	1147.4868	.6787	.1414	.0686	.7900
.3595	1239.8575	.7627	.1329	.0771	.7900
.4795	1291.0842	.8111	.1280	.0820	.7900
.5995	1271.5159	.8486	.1299	.0801	.7900
.7195	1300.9971	.8787	.1271	.0829	.7900
1.2495	1365.1695	.9457	.1208	.0892	.7900
2.5535	1246.0061	.9995	.1314	.0786	.7900
4.0075	1237.4208	1.0000	.1314	.0786	.7900
5.5075	1228.4290	1.0000	.1314	.0786	.7900

Table J.5. Computer results for Test Run P3 using the direct method to calculate the solids flowrate.

THE RESULTS FOR THE SIMULATED COMBUSTION MODEL TEST RUN P3

THE INLET CONDITIONS FOR AIR AND WOODCHAR

FLOWRATE OF SOLIDS = .6055E-02 KG/S
TEMPERATURE OF SOLIDS= 285.0 K
COMBUSTIBLE CONTENT = .8233
MOISTURE CONTENT = .0507
INORGANIC CONTENT = .1260

MAIN AIR FLOWRATE = .4871E-02 KMOLE/S
TEMPERATURE OF AIR = 299.6 K
AIR FOR VIEW PORT 1 = .2217E-03 KMOLE/S
AIR FOR VIEW PORT 2 = .2217E-03 KMOLE/S
AIR FOR VIEW PORT 3+4= .4435E-03 KMOLE/S

THE INLET SIZE DISTRIBUTION FOR THE SOLIDS FEED

MEAN DIAMETER (M)	.2250E-04	.5400E-04	.9400E-04	.1880E-03	.3750E-03	.7500E-03	.1500E-02	.2665E-02	.4013E-02
SPHERICAL DIAMETER (M)	.1350E-04	.3240E-04	.5640E-04	.1128E-03	.2250E-03	.4500E-03	.9000E-03	.1599E-02	.2408E-02
WEIGHT FRACTION	.0210	.0410	.0367	.0411	.1272	.2942	.3410	.0921	.0057

THE TEMPERATURE OF THE REACTANTS LEAVING THE INITIAL MIXING ZONE IS 703.6 (K)

THE SIZE DISTRIBUTION LEAVING THE INITIAL MIXING ZONE

MEAN DIAMETER (M)	.1350E-04	.3240E-04	.5640E-04	.1128E-03	.2250E-03	.4500E-03	.4758E-03	.1599E-02	.2408E-02
WEIGHT FRACTION	.0336	.0657	.0588	.0658	.2037	.4712	.1012	0.0000	0.0000

THE CALCULATED SURFACE AVERAGE PARTICLE DIAMETER IS .1553E-03 (M)

GAS FLOW INTO REACTION ZONE = .0049 KMOLE/S
CSA OF REACTION ZONE = .4560 M2
GAS FLOW INTO BYPASS ZONE = 0 KMOLE/S
CSA OF BYPASS ZONE = 0 M2

THE RESULTS FOR THE PLUG FLOW SECTION

LENGTH	TEMPERATURE	CONVERSION	M F O2	M F CO2	M F N2
0	703.5742	.3756	.1780	.0320	.7900
.1197	747.8420	.3847	.1772	.0328	.7900
.2397	792.5817	.4078	.1752	.0348	.7900
.3597	874.1145	.4752	.1695	.0405	.7900
.4797	1085.6305	.6771	.1523	.0577	.7900
.5997	1149.2683	.7797	.1464	.0636	.7900
.7197	1199.0921	.8340	.1420	.0680	.7900
.8397	1236.4133	.8753	.1386	.0714	.7900
.9597	1264.3470	.9067	.1360	.0740	.7900
2.7237	1233.8309	1.0000	.1379	.0721	.7900
5.1237	1218.6524	1.0000	.1379	.0721	.7900

Table J.6. Computer results for Test Run P3 using the indirect method to calculate the solids flowrate.

THE RESULTS FOR THE SIMULATED COMBUSTION MODEL TEST RUN P3

THE INLET CONDITIONS FOR AIR AND WOODCHAR

FLOWRATE OF SOLIDS = .7724E-02 KG/S
TEMPERATURE OF SOLIDS= 285.0 K
COMBUSTIBLE CONTENT = .8233
MOISTURE CONTENT = .0507
INORGANIC CONTENT = .1260

MAIN AIR FLOWRATE = .4871E-02 KMOLE/S
TEMPERATURE OF AIR = 299.6 K
AIR FOR VIEW PORT 1 = .2217E-03 KMOLE/S
AIR FOR VIEW PORT 2 = .2217E-03 KMOLE/S
AIR FOR VIEW PORT 3+4= .4434E-03 KMOLE/S

THE INLET SIZE DISTRIBUTION FOR THE SOLIDS FEED

MEAN DIAMETER (M)	.2250E-04	.5400E-04	.9400E-04	.1880E-03	.3750E-03	.7500E-03	.1500E-02	.2665E-02	.4013E-02
SPHERICAL DIAMETER (M)	.1350E-04	.3240E-04	.5640E-04	.1128E-03	.2250E-03	.4500E-03	.9000E-03	.1599E-02	.2408E-02
WEIGHT FRACTION	.0210	.0410	.0367	.0411	.1272	.2942	.3410	.0921	.0057

THE TEMPERATURE OF THE REACTANTS LEAVING THE INITIAL MIXING ZONE IS 780.7 (K)

THE SIZE DISTRIBUTION LEAVING THE INITIAL MIXING ZONE

MEAN DIAMETER (M)	.1350E-04	.3240E-04	.5640E-04	.1128E-03	.2250E-03	.4500E-03	.9280E-03	.1599E-02	.2408E-02
WEIGHT FRACTION	.0325	.0635	.0569	.0637	.1971	.4559	.1304	0.0000	0.0000

THE CALCULATED SURFACE AVERAGE PARTICLE DIAMETER IS .1605E-03 (M)

GAS FLOW INTO REACTION ZONE = .0049 KMOLE/S
CSA OF REACTION ZONE = .4560 M2
GAS FLOW INTO BYPASS ZONE = 0 KMOLE/S
CSA OF BYPASS ZONE = 0 M2

THE RESULTS FOR THE PLUG FLOW SECTION

LENGTH	TEMPERATURE	CONVERSION	M F O2	M F CO2	M F N2
0	780.7227	.3547	.1714	.0386	.7900
.2117	1052.1068	.5620	.1489	.0611	.7900
.3317	1237.5318	.7127	.1325	.0775	.7900
.4517	1309.2676	.7743	.1258	.0842	.7900
.5717	1319.3924	.8188	.1248	.0852	.7900
.6917	1357.7997	.8544	.1211	.0889	.7900
.8117	1387.6894	.8828	.1181	.0919	.7900
1.2817	1447.7004	.9418	.1120	.0980	.7900
2.5417	1376.0092	1.0000	.1180	.0920	.7900
4.0417	1360.7554	1.0000	.1180	.0920	.7900
5.5417	1346.0828	1.0000	.1180	.0920	.7900

Table J.7. Computer results for Test Run P4 using the direct method to calculate the solids flowrate.

THE RESULTS FOR THE SIMULATED COMBUSTION MODEL TEST RUN P4

THE INLET CONDITIONS FOR AIR AND WOODCHAR

FLOWRATE OF SOLIDS = .7935E-02 KG/S
TEMPERATURE OF SOLIDS= 285.0 K
COMBUSTIBLE CONTENT = .7323
MOISTURE CONTENT = .0507
INORGANIC CONTENT = .2170

MAIN AIR FLOWRATE = .7400E-02 KMOLE/S
TEMPERATURE OF AIR = 305.2 K
AIR FOR VIEW PORT 1 = .1837E-03 KMOLE/S
AIR FOR VIEW PORT 2 = .1837E-03 KMOLE/S
AIR FOR VIEW PORT 3+4= .3675E-03 KMOLE/S

THE INLET SIZE DISTRIBUTION FOR THE SOLIDS FEED

MEAN DIAMETER (M)	.2250E-04	.5400E-04	.9400E-04	.1880E-03	.3750E-03	.7500E-03	.1500E-02	.2665E-02	.4013E-02
SPHERICAL DIAMETER (M)	.1350E-04	.3240E-04	.5640E-04	.1128E-03	.2250E-03	.4500E-03	.9000E-03	.1599E-02	.2408E-02
WEIGHT FRACTION	.0200	.0400	.0364	.0333	.1011	.1931	.3573	.1830	.0358

THE TEMPERATURE OF THE REACTANTS LEAVING THE INITIAL MIXING ZONE IS 698.7 (K)

THE SIZE DISTRIBUTION LEAVING THE INITIAL MIXING ZONE

MEAN DIAMETER (M)	.1350E-04	.3240E-04	.5640E-04	.1128E-03	.2250E-03	.4500E-03	.5373E-03	.1599E-02	.2408E-02
WEIGHT FRACTION	.0384	.0767	.0698	.0639	.1939	.3703	.1871	0.0000	0.0000

THE CALCULATED SURFACE AVERAGE PARTICLE DIAMETER IS .1450E-03 (M)

GAS FLOW INTO REACTION ZONE = .0074 KMOLE/S
CSA OF REACTION ZONE = .4560 M2
GAS FLOW INTO BYPASS ZONE = 0 KMOLE/S
CSA OF BYPASS ZONE = 0 M2

THE RESULTS FOR THE PLUG FLOW SECTION

LENGTH	TEMPERATURE	CONVERSION	M F O2	M F CO2	M F N2
0	698.6914	.4786	.1787	.0313	.7900
1.2837	933.6895	.6544	.1682	.0418	.7900
1.4037	1006.2987	.7694	.1609	.0491	.7900
1.5237	1043.2263	.8417	.1575	.0525	.7900
2.0397	1118.9018	.9387	.1515	.0585	.7900
4.2797	1122.4935	1.0000	.1505	.0595	.7900
6.6797	1113.8719	1.0000	.1505	.0595	.7900
9.0797	1105.8568	1.0000	.1505	.0595	.7900
11.4797	1098.4056	1.0000	.1505	.0595	.7900
13.8797	1091.4786	1.0000	.1505	.0595	.7900
16.2797	1085.0390	1.0000	.1505	.0595	.7900

Table J.8. Computer results for Test Run P4 using the indirect method to calculate the solids flowrate.

THE RESULTS FOR THE SIMULATED COMBUSTION MODEL TEST RUN P4

THE INLET CONDITIONS FOR AIR AND WOODCHAR

FLOWRATE OF SOLIDS = .1276E-01 KG/S
TEMPERATURE OF SOLIDS= 285.0 K
COMBUSTIBLE CONTENT = .7323
MOISTURE CONTENT = .0507
INORGANIC CONTENT = .2170

MAIN AIR FLOWRATE = .7400E-02 KMOLE/S
TEMPERATURE OF AIR = 305.2 K
AIR FOR VIEW PORT 1 = .1837E-03 KMOLE/S
AIR FOR VIEW PORT 2 = .1837E-03 KMOLE/S
AIR FOR VIEW PORT 3+4= .3675E-03 KMOLE/S

THE INLET SIZE DISTRIBUTION FOR THE SOLIDS FEED

MEAN DIAMETER (M)	.2250E-04	.5400E-04	.9400E-04	.1880E-03	.3750E-03	.7500E-03	.1500E-02	.2665E-02	.4013E-02
SPHERICAL DIAMETER (M)	.1350E-04	.3240E-04	.5640E-04	.1128E-03	.2250E-03	.4500E-03	.9000E-03	.1599E-02	.2408E-02
WEIGHT FRACTION	.0200	.0400	.0364	.0333	.1011	.1931	.3573	.1830	.0358

THE TEMPERATURE OF THE REACTANTS LEAVING THE INITIAL MIXING ZONE IS 743.6 (K)

THE SIZE DISTRIBUTION LEAVING THE INITIAL MIXING ZONE

MEAN DIAMETER (M)	.1350E-04	.3240E-04	.5640E-04	.1128E-03	.2250E-03	.4500E-03	.7484E-03	.1599E-02	.2408E-02
WEIGHT FRACTION	.0300	.0601	.0547	.0500	.1519	.2901	.3631	0.0000	0.0000

THE CALCULATED SURFACE AVERAGE PARTICLE DIAMETER IS .1885E-03 (M)

GAS FLOW INTO REACTION ZONE = .0074 KMOLE/S
CSA OF REACTION ZONE = .4560 M2
GAS FLOW INTO BYPASS ZONE = 0 KMOLE/S
CSA OF BYPASS ZONE = 0 M2

THE RESULTS FOR THE PLUG FLOW SECTION

LENGTH	TEMPERATURE	CONVERSION	M F O2	M F CO2	M F N2
0	743.6133	.3344	.1748	.0352	.7900
.2277	868.3226	.4081	.1670	.0430	.7900
.3657	1027.5314	.5364	.1535	.0565	.7900
.5457	1171.5359	.6700	.1412	.0688	.7900
.8097	1254.5893	.7467	.1333	.0767	.7900
1.4397	1361.4258	.8474	.1230	.0870	.7900
3.3997	1391.2211	.9649	.1176	.0924	.7900
5.7997	1394.9195	.9973	.1145	.0955	.7900
8.1997	1370.8694	1.0000	.1142	.0958	.7900
10.5997	1345.6369	1.0000	.1142	.0958	.7900
12.9997	1322.0373	1.0000	.1142	.0958	.7900

Table J.9. Computer results for Test Run CP1 using the direct method to calculate the solids flowrate.

THE RESULTS FOR THE SIMULATED COMBUSTION MODEL TEST RUN CP1

THE INLET CONDITIONS FOR AIR AND WOODCHAR

FLOWRATE OF SOLIDS = .5115E-02 KG/S
TEMPERATURE OF SOLIDS= 285.0 K
COMBUSTIBLE CONTENT = .8122
MOISTURE CONTENT = .0488
INORGANIC CONTENT = .1390

MAIN AIR FLOWRATE = .3735E-02 KMOLE/S
TEMPERATURE OF AIR = 313.6 K
AIR FOR VIEW PORT 1 = .3318E-03 KMOLE/S
AIR FOR VIEW PORT 2 = .3318E-03 KMOLE/S
AIR FOR VIEW PORT 3+4= .6636E-03 KMOLE/S

THE INLET SIZE DISTRIBUTION FOR THE SOLIDS FEED

MEAN DIAMETER (M)	.2250E-04	.5400E-04	.9400E-04	.1880E-03	.3750E-03	.7500E-03	.1500E-02	.2665E-02	.4013E-02
SPHERICAL DIAMETER (M)	.1350E-04	.3240E-04	.5640E-04	.1128E-03	.2250E-03	.4500E-03	.9000E-03	.1599E-02	.2408E-02
WEIGHT FRACTION	.0379	.0569	.0605	.0704	.1630	.2935	.2810	.0368	.0000

THE TEMPERATURE OF THE REACTANTS LEAVING THE INITIAL MIXING ZONE IS 737.8 (K)

THE SIZE DISTRIBUTION LEAVING THE INITIAL MIXING ZONE

MEAN DIAMETER (M)	.1350E-04	.3240E-04	.5640E-04	.1128E-03	.2250E-03	.4017E-03	.9000E-03	.1599E-02	.2408E-02
WEIGHT FRACTION	.0597	.0896	.0953	.1109	.2568	.3877	0.0000	0.0000	0.0000

THE CALCULATED SURFACE AVERAGE PARTICLE DIAMETER IS .1056E-03 (M)

GAS FLOW INTO REACTION ZONE = .0037 KMOLE/S
CSA OF REACTION ZONE = .4560 M2
GAS FLOW INTO BYPASS ZONE = 0 KMOLE/S
CSA OF BYPASS ZONE = 0 M2

THE RESULTS FOR THE PLUG FLOW SECTION

LENGTH	TEMPERATURE	CONVERSION	M F O2	M F CO2	M F N2
0	737.7539	.3652	.1761	.0339	.7900
.1557	912.4536	.4789	.1656	.0444	.7900
.2757	1266.8975	.7889	.1369	.0731	.7900
.4917	1387.9453	.9058	.1260	.0840	.7900
1.3037	1397.7759	.9975	.1251	.0849	.7900
3.7037	1192.1136	1.0000	.1416	.0684	.7900
6.1037	1181.1847	1.0000	.1416	.0684	.7900
8.5037	1170.8637	1.0000	.1416	.0684	.7900
10.9037	1161.1194	1.0000	.1416	.0684	.7900
13.3037	1151.9216	1.0000	.1416	.0684	.7900
15.7037	1143.2414	1.0000	.1416	.0684	.7900

Table J.10. Computer results for Test Run CP1 using the indirect method to calculate the solids flowrate.

THE RESULTS FOR THE SIMULATED COMBUSTION MODEL TEST RUN CP1

THE INLET CONDITIONS FOR AIR AND WOODCHAR

FLOWRATE OF SOLIDS = .6525E-02 KG/S
TEMPERATURE OF SOLIDS= 285.0 K
COMBUSTIBLE CONTENT = .8122
MOISTURE CONTENT = .0488
INORGANIC CONTENT = .1390

MAIN AIR FLOWRATE = .3735E-02 KMOLE/S
TEMPERATURE OF AIR = 313.6 K
AIR FOR VIEW PORT 1 = .3319E-03 KMOLE/S
AIR FOR VIEW PORT 2 = .3318E-03 KMOLE/S
AIR FOR VIEW PORT 3+4= .6636E-03 KMOLE/S

THE INLET SIZE DISTRIBUTION FOR THE SOLIDS FEED

MEAN DIAMETER (M)	.2250E-04	.5400E-04	.9400E-04	.1880E-03	.3750E-03	.7500E-03	.1500E-02	.2665E-02	.4013E-02
SPHERICAL DIAMETER (M)	.1350E-04	.3240E-04	.5640E-04	.1128E-03	.2250E-03	.4500E-03	.9000E-03	.1599E-02	.2408E-02
WEIGHT FRACTION	.0379	.0569	.0605	.0704	.1630	.2935	.2810	.0368	.0000

THE TEMPERATURE OF THE REACTANTS LEAVING THE INITIAL MIXING ZONE IS 785.6 (K)

THE SIZE DISTRIBUTION LEAVING THE INITIAL MIXING ZONE

MEAN DIAMETER (M)	.1350E-04	.3240E-04	.5640E-04	.1128E-03	.2250E-03	.4263E-03	.9000E-03	.1599E-02	.2408E-02
WEIGHT FRACTION	.0558	.0838	.0891	.1037	.2401	.4274	0.0000	0.0000	0.0000

THE CALCULATED SURFACE AVERAGE PARTICLE DIAMETER IS .1132E-03 (M)

GAS FLOW INTO REACTION ZONE = .0037 KMOLE/S
CSA OF REACTION ZONE = .4560 M2
GAS FLOW INTO BYPASS ZONE = 0 KMOLE/S
CSA OF BYPASS ZONE = 0 M2

THE RESULTS FOR THE PLUG FLOW SECTION

LENGTH	TEMPERATURE	CONVERSION	M F O2	M F CO2	M F N2
0	785.6055	.3212	.1720	.0380	.7900
.1197	1322.5778	.6744	.1303	.0797	.7900
.2397	1456.9475	.7838	.1173	.0927	.7900
.3597	1520.9443	.8404	.1106	.0994	.7900
.4797	1567.6384	.8833	.1056	.1044	.7900
.5997	1512.0499	.9159	.1105	.0995	.7900
1.0817	1567.3300	.9714	.1045	.1055	.7900
2.4457	1499.3212	1.0000	.1096	.1004	.7900
3.8997	1349.1607	1.0000	.1228	.0872	.7900
5.3997	1337.0243	1.0000	.1228	.0872	.7900
6.8997	1325.2668	1.0000	.1228	.0872	.7900

Table J.11. Computer results for Test Run CP2 using the direct method to calculate the solids flowrate.

THE RESULTS FOR THE SIMULATED COMBUSTION MODEL TEST RUN CP2

THE INLET CONDITIONS FOR AIR AND WOODCHAR

FLOWRATE OF SOLIDS = .6055E-02 KG/S
TEMPERATURE OF SOLIDS= 285.0 K
COMBUSTIBLE CONTENT = .8442
MOISTURE CONTENT = .0488
INORGANIC CONTENT = .1070

MAIN AIR FLOWRATE = .5311E-02 KMOLE/S
TEMPERATURE OF AIR = 308.0 K
AIR FOR VIEW PORT 1 = .3254E-03 KMOLE/S
AIR FOR VIEW PORT 2 = .3254E-03 KMOLE/S
AIR FOR VIEW PORT 3+4= .6508E-03 KMOLE/S

THE INLET SIZE DISTRIBUTION FOR THE SOLIDS FEED

MEAN DIAMETER (M)	.2250E-04	.5400E-04	.9400E-04	.1880E-03	.3750E-03	.7500E-03	.1500E-02	.2565E-02	.4013E-02
SPHERICAL DIAMETER (M)	.1350E-04	.3240E-04	.5640E-04	.1128E-03	.2250E-03	.4500E-03	.9000E-03	.1599E-02	.2408E-02
WEIGHT FRACTION	.0271	.0442	.0399	.0541	.1623	.2580	.3288	.0802	.0054

THE TEMPERATURE OF THE REACTANTS LEAVING THE INITIAL MIXING ZONE IS 664.5 (K)

THE SIZE DISTRIBUTION LEAVING THE INITIAL MIXING ZONE

MEAN DIAMETER (M)	.1350E-04	.3240E-04	.5640E-04	.1128E-03	.2250E-03	.4500E-03	.4846E-03	.1599E-02	.2408E-02
WEIGHT FRACTION	.0417	.0681	.0614	.0833	.2499	.3973	.0982	0.0000	0.0000

THE CALCULATED SURFACE AVERAGE PARTICLE DIAMETER IS .1399E-03 (M)

GAS FLOW INTO REACTION ZONE = .0053 KMOLE/S
CSA OF REACTION ZONE = .4560 M2
GAS FLOW INTO BYPASS ZONE = 0 KMOLE/S
CSA OF BYPASS ZONE = 0 M2

THE RESULTS FOR THE PLUG FLOW SECTION

LENGTH	TEMPERATURE	CONVERSION	M F O2	M F CO2	M F N2
0	664.5117	.3507	.1819	.0281	.7900
.4157	774.6954	.3698	.1803	.0297	.7900
.6917	828.2797	.4283	.1776	.0324	.7900
.8717	980.1830	.5869	.1656	.0444	.7900
1.0337	1154.2219	.7772	.1513	.0587	.7900
1.2977	1241.3123	.8803	.1435	.0665	.7900
2.5317	1199.6516	.9947	.1459	.0641	.7900
4.9317	1191.0987	1.0000	.1456	.0644	.7900
7.3317	1179.1768	1.0000	.1456	.0644	.7900
9.7317	1167.9907	1.0000	.1456	.0644	.7900
12.1317	1157.4965	1.0000	.1456	.0644	.7900

Table J.12. Computer results for Test Run CP2 using the indirect method to calculate the solids flowrate.

THE RESULTS FOR THE SIMULATED COMBUSTION MODEL TEST RUN CP2

THE INLET CONDITIONS FOR AIR AND WOODCHAR

FLOWRATE OF SOLIDS = .7724E-02 KG/S
TEMPERATURE OF SOLIDS= 285.0 K
COMBUSTIBLE CONTENT = .8442
MOISTURE CONTENT = .0488
INORGANIC CONTENT = .1070

MAIN AIR FLOWRATE = .5311E-02 KMOLE/S
TEMPERATURE OF AIR = 308.0 K
AIR FOR VIEW PORT 1 = .3254E-03 KMOLE/S
AIR FOR VIEW PORT 2 = .3254E-03 KMOLE/S
AIR FOR VIEW PORT 3+4= .6508E-03 KMOLE/S

THE INLET SIZE DISTRIBUTION FOR THE SOLIDS FEED

MEAN DIAMETER (M)	.2250E-04	.5400E-04	.9400E-04	.1880E-03	.3750E-03	.7500E-03	.1500E-02	.2665E-02	.4013E-02
SPHERICAL DIAMETER (M)	.1350E-04	.3240E-04	.5640E-04	.1128E-03	.2250E-03	.4500E-03	.9000E-03	.1599E-02	.2408E-02
WEIGHT FRACTION	.0271	.0442	.0399	.0541	.1623	.2580	.3288	.0802	.0054

THE TEMPERATURE OF THE REACTANTS LEAVING THE INITIAL MIXING ZONE IS 732.9 (K)

THE SIZE DISTRIBUTION LEAVING THE INITIAL MIXING ZONE

MEAN DIAMETER (M)	.1350E-04	.3240E-04	.5640E-04	.1128E-03	.2250E-03	.4500E-03	.5344E-03	.1599E-02	.2408E-02
WEIGHT FRACTION	.0405	.0661	.0596	.0809	.2426	.3856	.1247	0.0000	0.0000

THE CALCULATED SURFACE AVERAGE PARTICLE DIAMETER IS .1443E-03 (M)

GAS FLOW INTO REACTION ZONE = .0053 KMOLE/S
CSA OF REACTION ZONE = .4560 M2
GAS FLOW INTO BYPASS ZONE = 0 KMOLE/S
CSA OF BYPASS ZONE = 0 M2

THE RESULTS FOR THE PLUG FLOW SECTION

LENGTH	TEMPERATURE	CONVERSION	M F O2	M F CO2	M F N2
0	732.8711	.3310	.1761	.0339	.7900
.1185	774.7224	.3469	.1745	.0355	.7900
.2385	841.5548	.3882	.1703	.0397	.7900
.3585	1073.3032	.5677	.1519	.0581	.7900
.4785	1240.8436	.7126	.1371	.0729	.7900
.5985	1257.6548	.7739	.1354	.0746	.7900
.7185	1303.5060	.8181	.1311	.0789	.7900
.8385	1340.0026	.8538	.1277	.0823	.7900
.9585	1368.5644	.8824	.1249	.0851	.7900
1.6585	1385.6151	.9549	.1230	.0870	.7900
2.9925	1320.3021	.9999	.1278	.0822	.7900

Table J.13. Computer results for Test Run CP3 using the direct method to calculate the solids flowrate.

THE RESULTS FOR THE SIMULATED COMBUSTION MODEL TEST RUN CP3

THE INLET CONDITIONS FOR AIR AND WOODCHAR

FLOWRATE OF SOLIDS = .6995E-02 KG/S
TEMPERATURE OF SOLIDS= 285.0 K
COMBUSTIBLE CONTENT = .8397
MOISTURE CONTENT = .0488
INORGANIC CONTENT = .1115

MAIN AIR FLOWRATE = .6432E-02 KMOLE/S
TEMPERATURE OF AIR = 310.8 K
AIR FOR VIEW PORT 1 = .2777E-03 KMOLE/S
AIR FOR VIEW PORT 2 = .2777E-03 KMOLE/S
AIR FOR VIEW PORT 3+4= .5553E-03 KMOLE/S

THE INLET SIZE DISTRIBUTION FOR THE SOLIDS FEED

MEAN DIAMETER (M)	.2250E-04	.5400E-04	.9400E-04	.1880E-03	.3750E-03	.7500E-03	.1500E-02	.2665E-02	.4013E-02
SPHERICAL DIAMETER (M)	.1350E-04	.3240E-04	.5640E-04	.1128E-03	.2250E-03	.4500E-03	.9000E-03	.1599E-02	.2408E-02
WEIGHT FRACTION	.0214	.0438	.0431	.0445	.0973	.1681	.3493	.2200	.0125

THE TEMPERATURE OF THE REACTANTS LEAVING THE INITIAL MIXING ZONE IS 724.1 (K)

THE SIZE DISTRIBUTION LEAVING THE INITIAL MIXING ZONE

MEAN DIAMETER (M)	.1350E-04	.3240E-04	.5640E-04	.1128E-03	.2250E-03	.4500E-03	.6321E-03	.1599E-02	.2408E-02
WEIGHT FRACTION	.0376	.0769	.0756	.0781	.1707	.2950	.2662	0.0000	0.0000

THE CALCULATED SURFACE AVERAGE PARTICLE DIAMETER IS .1478E-03 (M)

GAS FLOW INTO REACTION ZONE = .0064 KMOLE/S
CSA OF REACTION ZONE = .4560 M2
GAS FLOW INTO BYPASS ZONE = 0 KMOLE/S
CSA OF BYPASS ZONE = 0 M2

THE RESULTS FOR THE PLUG FLOW SECTION

LENGTH	TEMPERATURE	CONVERSION	M F O2	M F CO2	M F N2
0	724.0820	.4301	.1773	.0327	.7900
.2755	791.5800	.4644	.1747	.0353	.7900
.5335	861.2426	.5481	.1700	.0400	.7900
.7435	1003.5807	.7063	.1585	.0515	.7900
.9595	1115.3792	.8328	.1492	.0608	.7900
2.0995	1195.8075	.9663	.1423	.0677	.7900
4.4595	1150.7631	1.0000	.1451	.0649	.7900
6.8595	1140.7819	1.0000	.1451	.0649	.7900
9.2595	1131.4576	1.0000	.1451	.0649	.7900
11.6595	1122.7478	1.0000	.1451	.0649	.7900
14.0595	1114.6126	1.0000	.1451	.0649	.7900

Table J.14. Computer results for Test Run CP3 using the indirect method to calculate the solids flowrate.

THE RESULTS FOR THE SIMULATED COMBUSTION MODEL TEST RUN CP3

THE INLET CONDITIONS FOR AIR AND WOODCHAR

FLOWRATE OF SOLIDS = .8923E-02 KG/S
TEMPERATURE OF SOLIDS= 285.0 K
COMBUSTIBLE CONTENT = .8397
MOISTURE CONTENT = .0488
INORGANIC CONTENT = .1115

MAIN AIR FLOWRATE = .6432E-02 KMOLE/S
TEMPERATURE OF AIR = 310.8 K
AIR FOR VIEW PORT 1 = .2777E-03 KMOLE/S
AIR FOR VIEW PORT 2 = .2777E-03 KMOLE/S
AIR FOR VIEW PORT 3+4= .5553E-03 KMOLE/S

THE INLET SIZE DISTRIBUTION FOR THE SOLIDS FEED

MEAN DIAMETER (M)	.2250E-04	.5400E-04	.9400E-04	.1880E-03	.3750E-03	.7500E-03	.1500E-02	.2665E-02	.4013E-02
SPHERICAL DIAMETER (M)	.1350E-04	.3240E-04	.5640E-04	.1128E-03	.2250E-03	.4500E-03	.9000E-03	.1599E-02	.2408E-02
WEIGHT FRACTION	.0214	.0438	.0431	.0445	.0973	.1681	.3493	.2200	.0125

THE TEMPERATURE OF THE REACTANTS LEAVING THE INITIAL MIXING ZONE IS 785.6 (K)

THE SIZE DISTRIBUTION LEAVING THE INITIAL MIXING ZONE

MEAN DIAMETER (M)	.1350E-04	.3240E-04	.5640E-04	.1128E-03	.2250E-03	.4500E-03	.6861E-03	.1599E-02	.2408E-02
WEIGHT FRACTION	.0352	.0720	.0709	.0732	.1600	.2765	.3121	0.0000	0.0000

THE CALCULATED SURFACE AVERAGE PARTICLE DIAMETER IS .1589E-03 (M)

GAS FLOW INTO REACTION ZONE = .0064 KMOLE/S
CSA OF REACTION ZONE = .4560 M2
GAS FLOW INTO BYPASS ZONE = 0 KMOLE/S
CSA OF BYPASS ZONE = 0 M2

THE RESULTS FOR THE PLUG FLOW SECTION

LENGTH	TEMPERATURE	CONVERSION	M F O2	M F CO2	M F N2
0	785.6055	.3921	.1719	.0381	.7900
.1197	877.4238	.4645	.1649	.0451	.7900
.2397	1053.9685	.6124	.1506	.0594	.7900
.3597	1172.8987	.7198	.1401	.0699	.7900
.4797	1222.0468	.7656	.1357	.0743	.7900
.5997	1221.7314	.7978	.1358	.0742	.7900
.7197	1249.1440	.8253	.1332	.0768	.7900
1.7197	1318.8771	.9320	.1267	.0833	.7900
3.9997	1293.0118	.9979	.1274	.0826	.7900
6.3997	1275.7422	1.0000	.1272	.0828	.7900
8.7997	1257.6391	1.0000	.1272	.0828	.7900

Table J.15. Computer results for Test Run CP4 using the direct method to calculate the solids flowrate.

THE RESULTS FOR THE SIMULATED COMBUSTION MODEL TEST RUN CP4

THE INLET CONDITIONS FOR AIR AND WOODCHAR

FLOWRATE OF SOLIDS = .7935E-02 KG/S
TEMPERATURE OF SOLIDS= 285.0 K
COMBUSTIBLE CONTENT = .7752
MOISTURE CONTENT = .0488
INORGANIC CONTENT = .1760

MAIN AIR FLOWRATE = .6805E-02 KMOLE/S
TEMPERATURE OF AIR = 302.4 K
AIR FOR VIEW PORT 1 = .2777E-03 KMOLE/S
AIR FOR VIEW PORT 2 = .2777E-03 KMOLE/S
AIR FOR VIEW PORT 3+4= .5553E-03 KMOLE/S

THE INLET SIZE DISTRIBUTION FOR THE SOLIDS FEED

MEAN DIAMETER (M)	.2250E-04	.5400E-04	.9400E-04	.1880E-03	.3750E-03	.7500E-03	.1500E-02	.2665E-02	.4013E-02
SPHERICAL DIAMETER (M)	.1350E-04	.3240E-04	.5640E-04	.1128E-03	.2250E-03	.4500E-03	.9000E-03	.1599E-02	.2408E-02
WEIGHT FRACTION	.0310	.0650	.0657	.0612	.1357	.2926	.2855	.0567	.0060

THE TEMPERATURE OF THE REACTANTS LEAVING THE INITIAL MIXING ZONE IS 572.7 (K)

THE SIZE DISTRIBUTION LEAVING THE INITIAL MIXING ZONE

MEAN DIAMETER (M)	.1350E-04	.3240E-04	.5640E-04	.1128E-03	.2250E-03	.4500E-03	.9244E-03	.1599E-02	.2408E-02
WEIGHT FRACTION	.0431	.0903	.0913	.0850	.1885	.4064	.0947	0.0000	0.0000

THE CALCULATED SURFACE AVERAGE PARTICLE DIAMETER IS .1262E-03 (M)

GAS FLOW INTO REACTION ZONE = .0068 KMOLE/S
CSA OF REACTION ZONE = .4560 M2
GAS FLOW INTO BYPASS ZONE = 0 KMOLE/S
CSA OF BYPASS ZONE = 0 M2

THE RESULTS FOR THE PLUG FLOW SECTION

LENGTH	TEMPERATURE	CONVERSION	M F O2	M F CO2	M F N2
0	572.7148	.2801	.1889	.0211	.7900
1.2937	774.9858	.2944	.1887	.0213	.7900
1.8097	906.6774	.4310	.1800	.0300	.7900
1.9417	1074.8192	.6331	.1659	.0441	.7900
2.1517	1184.8317	.7677	.1565	.0535	.7900
2.6557	1216.8278	.8844	.1527	.0573	.7900
4.6957	1287.7786	.9987	.1453	.0647	.7900
7.0957	1269.4814	.9994	.1453	.0647	.7900
9.4957	1251.8267	.9994	.1453	.0647	.7900
11.8957	1235.2882	.9994	.1453	.0647	.7900
14.2957	1219.8036	.9994	.1453	.0647	.7900

Table J.16. Computer results for Test Run CP4 using the indirect method to calculate the solids flowrate.

THE RESULTS FOR THE SIMULATED COMBUSTION MODEL TEST RUN CP4

THE INLET CONDITIONS FOR AIR AND WOODCHAR

FLOWRATE OF SOLIDS = .1012E-01 KG/S
TEMPERATURE OF SOLIDS= 285.0 K
COMBUSTIBLE CONTENT = .7752
MOISTURE CONTENT = .0488
INORGANIC CONTENT = .1760

MAIN AIR FLOWRATE = .6805E-02 KMOLE/S
TEMPERATURE OF AIR = 302.4 K
AIR FOR VIEW PORT 1 = .3276E-03 KMOLE/S
AIR FOR VIEW PORT 2 = .3276E-03 KMOLE/S
AIR FOR VIEW PORT 3+4= .6553E-03 KMOLE/S

THE INLET SIZE DISTRIBUTION FOR THE SOLIDS FEED

MEAN DIAMETER (M)	.2250E-04	.5400E-04	.9400E-04	.1880E-03	.3750E-03	.7500E-03	.1500E-02	.2665E-02	.4013E-02
SPHERICAL DIAMETER (M)	.1350E-04	.3240E-04	.5640E-04	.1128E-03	.2250E-03	.4500E-03	.9000E-03	.1599E-02	.2408E-02
WEIGHT FRACTION	.0310	.0650	.0657	.0612	.1357	.2926	.2855	.0567	.0060

THE TEMPERATURE OF THE REACTANTS LEAVING THE INITIAL MIXING ZONE IS 621.5 (K)

THE SIZE DISTRIBUTION LEAVING THE INITIAL MIXING ZONE

MEAN DIAMETER (M)	.1350E-04	.3240E-04	.5640E-04	.1128E-03	.2250E-03	.4500E-03	.5705E-03	.1599E-02	.2408E-02
WEIGHT FRACTION	.0420	.0881	.0891	.0830	.1839	.3966	.1165	0.0000	0.0000

THE CALCULATED SURFACE AVERAGE PARTICLE DIAMETER IS .1297E-03 (M)

GAS FLOW INTO REACTION ZONE = .0068 KMOLE/S
CSA OF REACTION ZONE = .4560 M2
GAS FLOW INTO BYPASS ZONE = 0 KMOLE/S
CSA OF BYPASS ZONE = 0 M2

THE RESULTS FOR THE PLUG FLOW SECTION

LENGTH	TEMPERATURE	CONVERSION	M F O2	M F CO2	M F N2
0	621.5430	.2623	.1848	.0252	.7900
1.1477	923.8780	.3880	.1744	.0356	.7900
1.2677	1177.3176	.6180	.1533	.0567	.7900
1.3877	1251.3473	.6914	.1466	.0634	.7900
1.5077	1258.5793	.7374	.1454	.0646	.7900
1.6277	1291.4747	.7729	.1423	.0677	.7900
1.7477	1319.5002	.8035	.1396	.0704	.7900
2.4117	1407.6471	.8988	.1312	.0788	.7900
4.5357	1395.0318	.9965	.1297	.0803	.7900
6.9357	1372.8703	.9994	.1295	.0805	.7900
9.3357	1349.4656	.9994	.1295	.0805	.7900

Table J.17. Computer results for Test Run C9 using the direct method to calculate the solids flowrate

THE RESULTS FOR THE SIMULATED COMBUSTION MODEL TEST RUN C9

THE INLET CONDITIONS FOR AIR AND WOODCHAR

FLOWRATE OF SOLIDS = .9816E-02 KG/S
TEMPERATURE OF SOLIDS= 285.0 K
COMBUSTIBLE CONTENT = .7143
MOISTURE CONTENT = .0477
INORGANIC CONTENT = .2380

MAIN AIR FLOWRATE = .6701E-02 KMOLE/S
TEMPERATURE OF AIR = 302.4 K
AIR FOR VIEW PORT 1 = .3819E-03 KMOLE/S
AIR FOR VIEW PORT 2 = .3819E-03 KMOLE/S
AIR FOR VIEW PORT 3+4= .7638E-03 KMOLE/S

THE INLET SIZE DISTRIBUTION FOR THE SOLIDS FEED

MEAN DIAMETER (M)	.2250E-04	.5400E-04	.9400E-04	.1880E-03	.3750E-03	.7500E-03	.1500E-02	.2665E-02	.4013E-02
SPHERICAL DIAMETER (M)	.1350E-04	.3240E-04	.5640E-04	.1128E-03	.2250E-03	.4500E-03	.9000E-03	.1599E-02	.2408E-02
WEIGHT FRACTION	.0237	.0432	.0424	.0428	.1184	.2220	.2558	.1953	.0564

THE TEMPERATURE OF THE REACTANTS LEAVING THE INITIAL MIXING ZONE IS 718.2 (K)

THE SIZE DISTRIBUTION LEAVING THE INITIAL MIXING ZONE

MEAN DIAMETER (M)	.1350E-04	.3240E-04	.5640E-04	.1128E-03	.2250E-03	.4500E-03	.6527E-03	.1599E-02	.2408E-02
WEIGHT FRACTION	.0383	.0699	.0686	.0692	.1915	.3591	.2034	0.0000	0.0000

THE CALCULATED SURFACE AVERAGE PARTICLE DIAMETER IS .1512E-03 (M)

GAS FLOW INTO REACTION ZONE = .0067 KMOLE/S
CSA OF REACTION ZONE = .4560 M2
GAS FLOW INTO BYPASS ZONE = 0 KMOLE/S
CSA OF BYPASS ZONE = 0 M2

THE RESULTS FOR THE PLUG FLOW SECTION

LENGTH	TEMPERATURE	CONVERSION	M F O2	M F CO2	M F N2
0	718.2227	.3818	.1767	.0333	.7900
.3937	806.2837	.4195	.1734	.0366	.7900
.6577	872.6757	.4957	.1691	.0409	.7900
.8317	1015.7110	.6394	.1573	.0527	.7900
1.0057	1140.7700	.7675	.1467	.0633	.7900
1.3537	1223.4921	.8529	.1396	.0704	.7900
3.0177	1204.6339	.9843	.1401	.0699	.7900
5.4177	1204.0231	1.0000	.1390	.0710	.7900
7.8177	1191.2081	1.0000	.1390	.0710	.7900
10.2177	1179.1935	1.0000	.1390	.0710	.7900
12.6177	1167.9303	1.0000	.1390	.0710	.7900

Table J.18. Computer results for Test Run C9 using the indirect method to calculate the solids flowrate.

THE RESULTS FOR THE SIMULATED COMBUSTION MODEL TEST RUN C9

THE INLET CONDITIONS FOR AIR AND WOODCHAR

FLOWRATE OF SOLIDS = .1124E-01 KG/S
TEMPERATURE OF SOLIDS= 285.0 K
COMBUSTIBLE CONTENT = .7143
MOISTURE CONTENT = .0477
INORGANIC CONTENT = .2380

MAIN AIR FLOWRATE = .6701E-02 KMOLE/S
TEMPERATURE OF AIR = 302.4 K
AIR FOR VIEW PORT 1 = .3819E-03 KMOLE/S
AIR FOR VIEW PORT 2 = .3819E-03 KMOLE/S
AIR FOR VIEW PORT 3+4= .7638E-03 KMOLE/S

THE INLET SIZE DISTRIBUTION FOR THE SOLIDS FEED

MEAN DIAMETER (M)	.2250E-04	.5400E-04	.9400E-04	.1880E-03	.3750E-03	.7500E-03	.1500E-02	.2665E-02	.4013E-02
SPHERICAL DIAMETER (M)	.1350E-04	.3240E-04	.5640E-04	.1128E-03	.2250E-03	.4500E-03	.9000E-03	.1599E-02	.2408E-02
WEIGHT FRACTION	.0237	.0432	.0424	.0428	.1184	.2220	.2558	.1953	.0564

THE TEMPERATURE OF THE REACTANTS LEAVING THE INITIAL MIXING ZONE IS 753.4 (K)

THE SIZE DISTRIBUTION LEAVING THE INITIAL MIXING ZONE

MEAN DIAMETER (M)	.1350E-04	.3240E-04	.5640E-04	.1128E-03	.2250E-03	.4500E-03	.6854E-03	.1599E-02	.2408E-02
WEIGHT FRACTION	.0373	.0679	.0666	.0673	.1861	.3489	.2259	0.0000	0.0000

THE CALCULATED SURFACE AVERAGE PARTICLE DIAMETER IS .1562E-03 (M)

GAS FLOW INTO REACTION ZONE = .0067 KMOLE/S
CSA OF REACTION ZONE = .4560 M2
GAS FLOW INTO BYPASS ZONE = 0 KMOLE/S
CSA OF BYPASS ZONE = 0 M2

THE RESULTS FOR THE PLUG FLOW SECTION

LENGTH	TEMPERATURE	CONVERSION	M F O2	M F CO2	M F N2
0	753.3789	.3638	.1737	.0363	.7900
.2275	848.0062	.4224	.1678	.0422	.7900
.3835	1013.7718	.5567	.1544	.0556	.7900
.5395	1145.7674	.7065	.1433	.0667	.7900
.8035	1233.3502	.7925	.1352	.0748	.7900
1.4335	1334.8702	.8933	.1256	.0844	.7900
3.5235	1281.3885	.9923	.1293	.0807	.7900
5.9235	1270.7859	1.0000	.1287	.0813	.7900
8.3235	1254.2082	1.0000	.1287	.0813	.7900
10.7235	1238.6038	1.0000	.1287	.0813	.7900
13.1235	1223.9221	1.0000	.1287	.0813	.7900

Table J.19. Computer results for Test Run C10 using the direct method to calculate the solids flowrate.

THE RESULTS FOR THE SIMULATED COMBUSTION MODEL TEST RUN C10

THE INLET CONDITIONS FOR AIR AND WOODCHAR

FLOWRATE OF SOLIDS = .7935E-02 KG/S
TEMPERATURE OF SOLIDS= 285.0 K
COMBUSTIBLE CONTENT = .7573
MOISTURE CONTENT = .0477
INORGANIC CONTENT = .1950

MAIN AIR FLOWRATE = .5835E-02 KMOLE/S
TEMPERATURE OF AIR = 305.2 K
AIR FOR VIEW PORT 1 = .3071E-03 KMOLE/S
AIR FOR VIEW PORT 2 = .3071E-03 KMOLE/S
AIR FOR VIEW PORT 3+4= .6142E-03 KMOLE/S

THE INLET SIZE DISTRIBUTION FOR THE SOLIDS FEED

MEAN DIAMETER (M)	.2250E-04	.5400E-04	.9400E-04	.1880E-03	.3750E-03	.7500E-03	.1500E-02	.2665E-02	.4013E-02
SPHERICAL DIAMETER (M)	.1350E-04	.3240E-04	.5640E-04	.1128E-03	.2250E-03	.4500E-03	.9000E-03	.1599E-02	.2408E-02
WEIGHT FRACTION	.0329	.0576	.0629	.0539	.1233	.2510	.2554	.1289	.0341

THE TEMPERATURE OF THE REACTANTS LEAVING THE INITIAL MIXING ZONE IS 600.1 (K)

THE SIZE DISTRIBUTION LEAVING THE INITIAL MIXING ZONE

MEAN DIAMETER (M)	.1350E-04	.3240E-04	.5640E-04	.1128E-03	.2250E-03	.4500E-03	.5398E-03	.1599E-02	.2406E-02
WEIGHT FRACTION	.0504	.0883	.0964	.0826	.1890	.3848	.1083	0.0000	0.0000

THE CALCULATED SURFACE AVERAGE PARTICLE DIAMETER IS .1210E-03 (M)

GAS FLOW INTO REACTION ZONE = .0058 KMOLE/S
CSA OF REACTION ZONE = .4560 M2
GAS FLOW INTO BYPASS ZONE = 0 KMOLE/S
CSA OF BYPASS ZONE = 0 M2

THE RESULTS FOR THE PLUG FLOW SECTION

LENGTH	TEMPERATURE	CONVERSION	M F O2	M F CO2	M F N2
0	680.1367	.3477	.1802	.0298	.7900
.2567	744.4387	.3536	.1796	.0304	.7900
.5327	792.3981	.3882	.1783	.0317	.7900
.7847	905.3168	.4840	.1705	.0395	.7900
.9107	1118.8329	.6988	.1530	.0570	.7900
1.1327	1226.8244	.8137	.1437	.0663	.7900
1.6427	1279.0107	.9174	.1388	.0712	.7900
3.7627	1255.6850	1.0000	.1391	.0709	.7900
6.1627	1239.3465	1.0000	.1391	.0709	.7900
8.5627	1224.0443	1.0000	.1391	.0709	.7900
10.9627	1209.7143	1.0000	.1391	.0709	.7900

Table J.20. Computer results for Test Run C10 using the indirect method to calculate the solids flowrate.

THE RESULTS FOR THE SIMULATED COMBUSTION MODEL TEST RUN C10

THE INLET CONDITIONS FOR AIR AND WOODCHAR

FLOWRATE OF SOLIDS = .1012E-01 KG/S
TEMPERATURE OF SOLIDS= 285.0 K
COMBUSTIBLE CONTENT = .7573
MOISTURE CONTENT = .0477
INORGANIC CONTENT = .1950

MAIN AIR FLOWRATE = .5835E-02 KMOLE/S
TEMPERATURE OF AIR = 305.2 K
AIR FOR VIEW PORT 1 = .3071E-03 KMOLE/S
AIR FOR VIEW PORT 2 = .3071E-03 KMOLE/S
AIR FOR VIEW PORT 3+4= .6142E-03 KMOLE/S

THE INLET SIZE DISTRIBUTION FOR THE SOLIDS FEED

MEAN DIAMETER (M)	.2250E-04	.5400E-04	.9400E-04	.1880E-03	.3750E-03	.7500E-03	.1500E-02	.2665E-02	.4013E-02
SPHERICAL DIAMETER (M)	.1350E-04	.3240E-04	.5640E-04	.1128E-03	.2250E-03	.4500E-03	.9000E-03	.1599E-02	.2408E-02
WEIGHT FRACTION	.0329	.0576	.0629	.0539	.1233	.2510	.2554	.1289	.0341

THE TEMPERATURE OF THE REACTANTS LEAVING THE INITIAL MIXING ZONE IS 748.5 (K)

THE SIZE DISTRIBUTION LEAVING THE INITIAL MIXING ZONE

MEAN DIAMETER (M)	.1350E-04	.3240E-04	.5640E-04	.1128E-03	.2250E-03	.4500E-03	.5946E-03	.1599E-02	.2408E-02
WEIGHT FRACTION	.0488	.0855	.0934	.0800	.1830	.3725	.1368	0.0000	0.0000

THE CALCULATED SURFACE AVERAGE PARTICLE DIAMETER IS .1256E-03 (M)

GAS FLOW INTO REACTION ZONE = .0058 KMOLE/S
CSA OF REACTION ZONE = .4560 M2
GAS FLOW INTO BYPASS ZONE = 0 KMOLE/S
CSA OF BYPASS ZONE = 0 M2

THE RESULTS FOR THE PLUG FLOW SECTION

LENGTH	TEMPERATURE	CONVERSION	M F O2	M F CO2	M F N2
0	748.4961	.3263	.1743	.0357	.7900
.3397	899.4329	.4231	.1638	.0462	.7900
.4597	1215.0797	.6605	.1377	.0723	.7900
.5797	1255.8936	.7320	.1339	.0761	.7900
.6997	1303.7429	.7757	.1293	.0807	.7900
.8197	1339.5991	.8095	.1258	.0842	.7900
.9397	1369.3996	.8382	.1228	.0872	.7900
1.3477	1436.0823	.8989	.1165	.0935	.7900
3.2757	1380.3303	.9970	.1198	.0902	.7900
5.6757	1359.4464	1.0000	.1196	.0904	.7900
8.0757	1336.8677	1.0000	.1196	.0904	.7900

Table J.21. Computer results for Test Run P3 using the direct method to calulate the solids flowrate and a terminal velocity 1.2 times greater than the original correlation by Becker (20).

THE RESULTS FOR THE SIMULATED COMBUSTION MODEL TEST RUN P3

THE INLET CONDITIONS FOR AIR AND WOODCHAR

FLOWRATE OF SOLIDS = .6055E-02 KG/S
TEMPERATURE OF SOLIDS= 285.0 K
COMBUSTIBLE CONTENT = .8233
MOISTURE CONTENT = .0507
INORGANIC CONTENT = .1260

MAIN AIR FLOWRATE = .4871E-02 KMOLE/S
TEMPERATURE OF AIR = 299.6 K
AIR FOR VIEW PORT 1 = .2217E-03 KMOLE/S
AIR FOR VIEW PORT 2 = .2217E-03 KMOLE/S
AIR FOR VIEW PORT 3+4= .4434E-03 KMOLE/S

THE INLET SIZE DISTRIBUTION FOR THE SOLIDS FEED

MEAN DIAMETER (M)	.2250E-04	.5400E-04	.9400E-04	.1880E-03	.3750E-03	.7500E-03	.1500E-02	.2665E-02	.4013E-02
SPHERICAL DIAMETER (M)	.1350E-04	.3240E-04	.5640E-04	.1128E-03	.2250E-03	.4500E-03	.9000E-03	.1599E-02	.2408E-02
WEIGHT FRACTION	.0210	.0410	.0367	.0411	.1272	.2942	.3410	.0921	.0057

THE TEMPERATURE OF THE REACTANTS LEAVING THE INITIAL MIXING ZONE IS 805.1 (K)

THE SIZE DISTRIBUTION LEAVING THE INITIAL MIXING ZONE

MEAN DIAMETER (M)	.1350E-04	.3240E-04	.5640E-04	.1128E-03	.2250E-03	.4036E-03	.9000E-03	.1599E-02	.2408E-02
WEIGHT FRACTION	.0400	.0781	.0699	.0783	.2423	.4914	0.0000	0.0000	0.0000

THE CALCULATED SURFACE AVERAGE PARTICLE DIAMETER IS .1317E-03 (M)

GAS FLOW INTO REACTION ZONE = .0049 KMOLE/S
CSA OF REACTION ZONE = .4560 M2
GAS FLOW INTO BYPASS ZONE = 0 KMOLE/S
CSA OF BYPASS ZONE = 0 M2

THE RESULTS FOR THE PLUG FLOW SECTION

LENGTH	TEMPERATURE	CONVERSION	M F O2	M F CO2	M F N2
0	805.1367	.4751	.1695	.0405	.7900
.1197	1025.1578	.6768	.1523	.0577	.7900
.2877	1204.8254	.8548	.1371	.0729	.7900
.5277	1243.5519	.9376	.1335	.0765	.7900
2.2877	1257.9545	1.0000	.1318	.0782	.7900
4.6877	1178.4726	1.0000	.1379	.0721	.7900
7.0877	1166.7261	1.0000	.1379	.0721	.7900
9.4877	1155.7510	1.0000	.1379	.0721	.7900
11.8877	1145.4970	1.0000	.1379	.0721	.7900
14.2877	1135.9170	1.0000	.1379	.0721	.7900
16.6877	1126.9670	1.0000	.1379	.0721	.7900

Table J.22. Computer results for Test Run P3 using the indirect method to calculate the solids flowrate and a terminal velocity 0.8 times greater than the original correlation by Becker (20).

THE RESULTS FOR THE SIMULATED COMBUSTION MODEL TEST RUN P3

THE INLET CONDITIONS FOR AIR AND WOODCHAR

FLOWRATE OF SOLIDS = .7724E-02 KG/S
TEMPERATURE OF SOLIDS= 285.0 K
COMBUSTIBLE CONTENT = .8233
MOISTURE CONTENT = .0507
INORGANIC CONTENT = .1260

MAIN AIR FLOWRATE = .4871E-02 KMOLE/S
TEMPERATURE OF AIR = 299.6 K
AIR FOR VIEW PORT 1 = .2217E-03 KMOLE/S
AIR FOR VIEW PORT 2 = .2217E-03 KMOLE/S
AIR FOR VIEW PORT 3+4= .4435E-03 KMOLE/S

THE INLET SIZE DISTRIBUTION FOR THE SOLIDS FEED

MEAN DIAMETER (M)	.2250E-04	.5400E-04	.9400E-04	.1880E-03	.3750E-03	.7500E-03	.1500E-02	.2665E-02	.4013E-02
SPHERICAL DIAMETER (M)	.1350E-04	.3240E-04	.5640E-04	.1128E-03	.2250E-03	.4500E-03	.9000E-03	.1599E-02	.2408E-02
WEIGHT FRACTION	.0210	.0410	.0367	.0411	.1272	.2942	.3410	.0921	.0057

THE TEMPERATURE OF THE REACTANTS LEAVING THE INITIAL MIXING ZONE IS 701.6 (K)

THE SIZE DISTRIBUTION LEAVING THE INITIAL MIXING ZONE

MEAN DIAMETER (M)	.1350E-04	.3240E-04	.5640E-04	.1128E-03	.2250E-03	.4500E-03	.6448E-03	.1599E-02	.2408E-02
WEIGHT FRACTION	.0297	.0580	.0519	.0581	.1800	.4162	.2060	0.0000	0.0000

THE CALCULATED SURFACE AVERAGE PARTICLE DIAMETER IS .1763E-03 (M)

GAS FLOW INTO REACTION ZONE = .0049 KMOLE/S
CSA OF REACTION ZONE = .4560 M2
GAS FLOW INTO BYPASS ZONE = 0 KMOLE/S
CSA OF BYPASS ZONE = 0 M2

THE RESULTS FOR THE PLUG FLOW SECTION

LENGTH	TEMPERATURE	CONVERSION	M F O2	M F CO2	M F N2
0	701.6211	.2932	.1781	.0319	.7900
.3397	825.4709	.3404	.1730	.0370	.7900
.4597	1005.3745	.4707	.1588	.0512	.7900
.5797	1178.3343	.6368	.1437	.0663	.7900
.6997	1251.9469	.7017	.1370	.0730	.7900
.8197	1304.6602	.7497	.1320	.0780	.7900
.9397	1346.8819	.7890	.1279	.0821	.7900
1.0597	1380.2674	.8210	.1246	.0854	.7900
1.5757	1415.9255	.8954	.1207	.0893	.7900
3.4957	1416.8471	.9954	.1184	.0916	.7900
5.8957	1395.3849	1.0000	.1180	.0920	.7900

Table J.23. Computer results for Test Run P3 using the indirect method to calculate the solids flowrate and a terminal velocity 1.2 times greater than the original correlation by Becker (20).

THE RESULTS FOR THE SIMULATED COMBUSTION MODEL TEST RUN P3 TVC 1.2 corr

THE INLET CONDITIONS FOR AIR AND WOODCHAR

FLOWRATE OF SOLIDS = .7724E-02 KG/S
TEMPERATURE OF SOLIDS= 285.0 K
COMBUSTIBLE CONTENT = .8233
MOISTURE CONTENT = .0507
INORGANIC CONTENT = .1260

MAIN AIR FLOWRATE = .4871E-02 KMOLE/S
TEMPERATURE OF AIR = 299.6 K
AIR FOR VIEW PORT 1 = .2217E-03 KMOLE/S
AIR FOR VIEW PORT 2 = .2217E-03 KMOLE/S
AIR FOR VIEW PORT 3+4= .4435E-03 KMOLE/S

THE INLET SIZE DISTRIBUTION FOR THE SOLIDS FEED

MEAN DIAMETER (M)	.2250E-04	.5400E-04	.9400E-04	.1880E-03	.3750E-03	.7500E-03	.1500E-02	.2665E-02	.4013E-02
SPHERICAL DIAMETER (M)	.1350E-04	.3240E-04	.5640E-04	.1128E-03	.2250E-03	.4500E-03	.9000E-03	.1599E-02	.2408E-02
WEIGHT FRACTION	.0210	.0410	.0367	.0411	.1272	.2942	.3410	.0921	.0057

THE TEMPERATURE OF THE REACTANTS LEAVING THE INITIAL MIXING ZONE IS 838.3 (K)

THE SIZE DISTRIBUTION LEAVING THE INITIAL MIXING ZONE

MEAN DIAMETER (M)	.1350E-04	.3240E-04	.5640E-04	.1128E-03	.2250E-03	.4427E-03	.9000E-03	.1599E-02	.2408E-02
WEIGHT FRACTION	.0350	.0683	.0612	.0685	.2120	.5550	0.0000	0.0000	0.0000

THE CALCULATED SURFACE AVERAGE PARTICLE DIAMETER IS .1496E-03 (M)

GAS FLOW INTO REACTION ZONE = .0049 KMOLE/S
CSA OF REACTION ZONE = .4560 M2
GAS FLOW INTO BYPASS ZONE = 0 KMOLE/S
CSA OF BYPASS ZONE = 0 M2

THE RESULTS FOR THE PLUG FLOW SECTION

LENGTH	TEMPERATURE	CONVERSION	M F O2	M F CO2	M F N2
0	838.3398	.4001	.1665	.0435	.7900
.1197	1225.8333	.6918	.1347	.0753	.7900
.2397	1325.1747	.7765	.1255	.0845	.7900
.3597	1383.0680	.8280	.1199	.0901	.7900
.4797	1426.1518	.8674	.1156	.0944	.7900
.5997	1415.9032	.8986	.1165	.0935	.7900
1.0477	1479.6418	.9565	.1105	.0995	.7900
3.2877	1378.1119	1.0000	.1180	.0920	.7900
5.6877	1353.4349	1.0000	.1180	.0920	.7900
8.0877	1330.3389	1.0000	.1180	.0920	.7900
10.4877	1308.7301	1.0000	.1180	.0920	.7900

Table J.24. Computer results for Test Run P4 using the direct method to calculate the solids flowrate and a terminal velocity 2.0 times greater than the original correlation by Becker (20).

THE RESULTS FOR THE SIMULATED COMBUSTION MODEL TEST RUN P4

THE INLET CONDITIONS FOR AIR AND WOODCHAR

FLOWRATE OF SOLIDS = .7935E-02 KG/S
TEMPERATURE OF SOLIDS= 285.0 K
COMBUSTIBLE CONTENT = .7323
MOISTURE CONTENT = .0507
INORGANIC CONTENT = .2170

$V = 2.0$

MAIN AIR FLOWRATE = .7400E-02 KMOLE/S
TEMPERATURE OF AIR = 305.2 K
AIR FOR VIEW PORT 1 = .1837E-03 KMOLE/S
AIR FOR VIEW PORT 2 = .1837E-03 KMOLE/S
AIR FOR VIEW PORT 3+4= .3675E-03 KMOLE/S

THE INLET SIZE DISTRIBUTION FOR THE SOLIDS FEED

MEAN DIAMETER (M)	.2250E-04	.5400E-04	.9400E-04	.1880E-03	.3750E-03	.7500E-03	.1500E-02	.2665E-02	.4013E-02
SPHERICAL DIAMETER (M)	.1350E-04	.3240E-04	.5640E-04	.1128E-03	.2250E-03	.4500E-03	.9000E-03	.1599E-02	.2408E-02
WEIGHT FRACTION	.0200	.0400	.0364	.0333	.1011	.1931	.3573	.1830	.0356

THE TEMPERATURE OF THE REACTANTS LEAVING THE INITIAL MIXING ZONE IS 846.2 (K)

THE SIZE DISTRIBUTION LEAVING THE INITIAL MIXING ZONE

MEAN DIAMETER (M)	.1350E-04	.3240E-04	.5640E-04	.1128E-03	.2250E-03	.3218E-03	.9000E-03	.1599E-02	.2408E-02
WEIGHT FRACTION	.0605	.1209	.1100	.1007	.3056	.3022	0.0000	0.0000	0.0000

THE CALCULATED SURFACE AVERAGE PARTICLE DIAMETER IS .9145E-04 (M)

GAS FLOW INTO REACTION ZONE = .0074 KMOLE/S
CSA OF REACTION ZONE = .4560 M2
GAS FLOW INTO BYPASS ZONE = 0 KMOLE/S
CSA OF BYPASS ZONE = 0 M2

THE RESULTS FOR THE PLUG FLOW SECTION

LENGTH	TEMPERATURE	CONVERSION	M F O2	M F CO2	M F N2
0	846.1523	.6692	.1662	.0438	.7900
.1357	923.0472	.7587	.1603	.0497	.7900
.2677	1011.2841	.8681	.1532	.0568	.7900
.4157	1073.9207	.9505	.1478	.0622	.7900
1.1837	1096.2278	1.0000	.1461	.0639	.7900
1.9837	1077.8306	1.0000	.1477	.0623	.7900
2.7517	1043.8310	1.0000	.1505	.0595	.7900
3.5517	1042.7778	1.0000	.1505	.0595	.7900
4.3517	1041.7499	1.0000	.1505	.0595	.7900
5.1517	1040.7468	1.0000	.1505	.0595	.7900
5.9517	1039.7677	1.0000	.1505	.0595	.7900

Table J.25. Computer results for Test Run P1 using the direct method to calculate the solids flowrate and a terminal velocity 1.5 times greater than the original correlation by Becker (20).

THE RESULTS FOR THE SIMULATED COMBUSTION MODEL TEST RUN P1

THE INLET CONDITIONS FOR AIR AND WOODCHAR

FLOWRATE OF SOLIDS = .5115E-02 KG/S
TEMPERATURE OF SOLIDS= 285.0 K
COMBUSTIBLE CONTENT = .7373
MOISTURE CONTENT = .0507
INORGANIC CONTENT = .2120

MAIN AIR FLOWRATE = .4033E-02 KMOLE/S
TEMPERATURE OF AIR = 313.6 K
AIR FOR VIEW PORT 1 = .1538E-03 KMOLE/S
AIR FOR VIEW PORT 2 = .1538E-03 KMOLE/S
AIR FOR VIEW PORT 3+4= .3076E-03 KMOLE/S

THE INLET SIZE DISTRIBUTION FOR THE SOLIDS FEED

MEAN DIAMETER (M)	.2250E-04	.5400E-04	.9400E-04	.1880E-03	.3750E-03	.7500E-03	.1500E-02	.2665E-02	.4013E-02
SPHERICAL DIAMETER (M)	.1350E-04	.3240E-04	.5640E-04	.1128E-03	.2250E-03	.4500E-03	.9000E-03	.1599E-02	.2408E-02
WEIGHT FRACTION	.0235	.0450	.0432	.0568	.1529	.2787	.3532	.0367	.0100

THE TEMPERATURE OF THE REACTANTS LEAVING THE INITIAL MIXING ZONE IS 863.7 (K)

THE SIZE DISTRIBUTION LEAVING THE INITIAL MIXING ZONE

MEAN DIAMETER (M)	.1350E-04	.3240E-04	.5640E-04	.1128E-03	.2250E-03	.2957E-03	.9000E-03	.1599E-02	.2408E-02
WEIGHT FRACTION	.0552	.1058	.1015	.1335	.3594	.2446	0.0000	0.0000	0.0000

THE CALCULATED SURFACE AVERAGE PARTICLE DIAMETER IS .9407E-04 (M)

GAS FLOW INTO REACTION ZONE = .0040 KMOLE/S
CSA OF REACTION ZONE = .4560 M2
GAS FLOW INTO BYPASS ZONE = 0 KMOLE/S
CSA OF BYPASS ZONE = 0 M2

THE RESULTS FOR THE PLUG FLOW SECTION

LENGTH	TEMPERATURE	CONVERSION	M F O2	M F CO2	M F N2
0	863.7305	.5746	.1652	.0448	.7900
.0837	1063.3305	.7761	.1495	.0605	.7900
.1797	1187.0517	.9113	.1390	.0710	.7900
.3357	1241.5890	.9740	.1341	.0759	.7900
1.0077	1235.3122	1.0000	.1349	.0751	.7900
1.7757	1200.3239	1.0000	.1376	.0724	.7900
2.5757	1142.9702	1.0000	.1424	.0676	.7900
3.3397	1139.8472	1.0000	.1424	.0676	.7900
4.1397	1136.6499	1.0000	.1424	.0676	.7900
4.9397	1133.5255	1.0000	.1424	.0676	.7900
5.7397	1130.4723	1.0000	.1424	.0676	.7900

Table J.26. Computer results for Test Run P2 using the direct method to calculate the solids flowrate and a terminal velocity 1.5 times greater than the original correlation by Becker (20).

THE RESULTS FOR THE SIMULATED COMBUSTION MODEL TEST RUN P2

THE INLET CONDITIONS FOR AIR AND WOODCHAR

FLOWRATE OF SOLIDS = .6607E-02 KG/S
TEMPERATURE OF SOLIDS= 285.0 K
COMBUSTIBLE CONTENT = .7093
MOISTURE CONTENT = .0507
INORGANIC CONTENT = .2400

MAIN AIR FLOWRATE = .5077E-02 KMOLE/S
TEMPERATURE OF AIR = 305.2 K
AIR FOR VIEW PORT 1 = .3625E-03 KMOLE/S
AIR FOR VIEW PORT 2 = .3625E-03 KMOLE/S
AIR FOR VIEW PORT 3+4= .7250E-03 KMOLE/S

THE INLET SIZE DISTRIBUTION FOR THE SOLIDS FEED

MEAN DIAMETER (M)	.2250E-04	.5400E-04	.9400E-04	.1880E-03	.3750E-03	.7500E-03	.1500E-02	.2665E-02	.4013E-02
SPHERICAL DIAMETER (M)	.1350E-04	.3240E-04	.5640E-04	.1128E-03	.2250E-03	.4500E-03	.9000E-03	.1599E-02	.2408E-02
WEIGHT FRACTION	.0215	.0403	.0420	.0476	.1254	.2370	.3171	.1293	.0398

THE TEMPERATURE OF THE REACTANTS LEAVING THE INITIAL MIXING ZONE IS 864.7 (K)

THE SIZE DISTRIBUTION LEAVING THE INITIAL MIXING ZONE

MEAN DIAMETER (M)	.1350E-04	.3240E-04	.5640E-04	.1128E-03	.2250E-03	.3529E-03	.9000E-03	.1599E-02	.2408E-02
WEIGHT FRACTION	.0507	.0949	.0990	.1121	.2954	.3478	0.0000	0.0000	0.0000

THE CALCULATED SURFACE AVERAGE PARTICLE DIAMETER IS .1048E-03 (M)

GAS FLOW INTO REACTION ZONE = .0051 KMOLE/S
CSA OF REACTION ZONE = .4560 M2
GAS FLOW INTO BYPASS ZONE = 0 KMOLE/S
CSA OF BYPASS ZONE = 0 M2

THE RESULTS FOR THE PLUG FLOW SECTION

LENGTH	TEMPERATURE	CONVERSION	M F O2	M F CO2	M F N2
0	864.7070	.5756	.1644	.0456	.7900
.0837	1021.9316	.7332	.1519	.0581	.7900
.1757	1148.2322	.8671	.1413	.0687	.7900
.3317	1209.9549	.9368	.1357	.0743	.7900
.7797	1208.9362	.9958	.1363	.0737	.7900
1.5797	1157.2318	1.0000	.1406	.0694	.7900
2.3437	1153.7725	1.0000	.1406	.0694	.7900
3.1437	1066.6589	1.0000	.1483	.0617	.7900
3.9437	1065.2893	1.0000	.1483	.0617	.7900
4.7437	1063.9477	1.0000	.1483	.0617	.7900
5.5437	1062.6338	1.0000	.1483	.0617	.7900

Table J.27. Computer results for Test Run P3 using the direct method to calculate the solids flowrate and a terminal velocity 1.5 times greater than the original correlation by Becker (20).

THE RESULTS FOR THE SIMULATED COMBUSTION MODEL TEST RUN P3

THE INLET CONDITIONS FOR AIR AND WOODCHAR

FLOWRATE OF SOLIDS = .6055E-02 KG/S
TEMPERATURE OF SOLIDS= 285.0 K
COMBUSTIBLE CONTENT = .8233
MOISTURE CONTENT = .0507
INORGANIC CONTENT = .1260

MAIN AIR FLOWRATE = .4871E-02 KMOLE/S
TEMPERATURE OF AIR = 299.6 K
AIR FOR VIEW PORT 1 = .2217E-03 KMOLE/S
AIR FOR VIEW PORT 2 = .2217E-03 KMOLE/S
AIR FOR VIEW PORT 3+4= .4434E-03 KMOLE/S

THE INLET SIZE DISTRIBUTION FOR THE SOLIDS FEED

MEAN DIAMETER (M)	.2250E-04	.5400E-04	.9400E-04	.1880E-03	.3750E-03	.7500E-03	.1500E-02	.2665E-02	.4013E-02
SPHERICAL DIAMETER (M)	.1350E-04	.3240E-04	.5640E-04	.1128E-03	.2250E-03	.4500E-03	.9000E-03	.1599E-02	.2408E-02
WEIGHT FRACTION	.0210	.0410	.0367	.0411	.1272	.2942	.3410	.0921	.0057

THE TEMPERATURE OF THE REACTANTS LEAVING THE INITIAL MIXING ZONE IS 888.1 (K)

THE SIZE DISTRIBUTION LEAVING THE INITIAL MIXING ZONE

MEAN DIAMETER (M)	.1350E-04	.3240E-04	.5640E-04	.1128E-03	.2250E-03	.3504E-03	.9000E-03	.1599E-02	.2408E-02
WEIGHT FRACTION	.0476	.0929	.0832	.0931	.2882	.3950	0.0000	0.0000	0.0000

THE CALCULATED SURFACE AVERAGE PARTICLE DIAMETER IS .1114E-03 (M)

GAS FLOW INTO REACTION ZONE = .0049 KMOLE/S
CSA OF REACTION ZONE = .4560 M2
GAS FLOW INTO BYPASS ZONE = 0 KMOLE/S
CSA OF BYPASS ZONE = 0 M2

THE RESULTS FOR THE PLUG FLOW SECTION

LENGTH	TEMPERATURE	CONVERSION	M F O2	M F CO2	M F N2
0	888.1445	.5587	.1624	.0476	.7900
.1257	1181.3423	.8338	.1389	.0711	.7900
.3717	1288.0318	.9422	.1296	.0804	.7900
1.7617	1261.3730	1.0000	.1318	.0782	.7900
4.0157	1181.2973	1.0000	.1379	.0721	.7900
6.4157	1169.4354	1.0000	.1379	.0721	.7900
8.8157	1158.3414	1.0000	.1379	.0721	.7900
11.2157	1147.9673	1.0000	.1379	.0721	.7900
13.6157	1138.2679	1.0000	.1379	.0721	.7900
16.0157	1129.2002	1.0000	.1379	.0721	.7900
18.4157	1120.7240	1.0000	.1379	.0721	.7900

Table J.28. Computer results for Test Run P4 using the direct method to calculate the solids flowrate and a terminal velocity 1.5 times greater than the original correlation by Becker (20).

THE RESULTS FOR THE SIMULATED COMBUSTION MODEL TEST RUN P4

THE INLET CONDITIONS FOR AIR AND WOODCHAR

FLOWRATE OF SOLIDS = .7935E-02 KG/S
TEMPERATURE OF SOLIDS= 285.0 K
COMBUSTIBLE CONTENT = .7323
MOISTURE CONTENT = .0507
INORGANIC CONTENT = .2170

$V = 1.5$

MAIN AIR FLOWRATE = .7400E-02 KMOLE/S
TEMPERATURE OF AIR = 305.2 K
AIR FOR VIEW PORT 1 = .1837E-03 KMOLE/S
AIR FOR VIEW PORT 2 = .1837E-03 KMOLE/S
AIR FOR VIEW PORT 3+4= .3675E-03 KMOLE/S

THE INLET SIZE DISTRIBUTION FOR THE SOLIDS FEED

MEAN DIAMETER (M)	.2250E-04	.5400E-04	.9400E-04	.1880E-03	.3750E-03	.7500E-03	.1500E-02	.2665E-02	.4013E-02
SPHERICAL DIAMETER (M)	.1350E-04	.3240E-04	.5640E-04	.1128E-03	.2250E-03	.4500E-03	.9000E-03	.1599E-02	.2408E-02
WEIGHT FRACTION	.0200	.0400	.0364	.0333	.1011	.1931	.3573	.1830	.0358

THE TEMPERATURE OF THE REACTANTS LEAVING THE INITIAL MIXING ZONE IS 757.3 (K)

THE SIZE DISTRIBUTION LEAVING THE INITIAL MIXING ZONE

MEAN DIAMETER (M)	.1350E-04	.3240E-04	.5640E-04	.1128E-03	.2250E-03	.4259E-03	.9000E-03	.1599E-02	.2408E-02
WEIGHT FRACTION	.0446	.0393	.0812	.0743	.2256	.4849	0.0000	0.0000	0.0000

THE CALCULATED SURFACE AVERAGE PARTICLE DIAMETER IS .1244E-03 (M)

GAS FLOW INTO REACTION ZONE = .0074 KMOLE/S
CSA OF REACTION ZONE = .4560 M2
GAS FLOW INTO BYPASS ZONE = 0 KMOLE/S
CSA OF BYPASS ZONE = 0 M2

THE RESULTS FOR THE PLUG FLOW SECTION

LENGTH	TEMPERATURE	CONVERSION	M F O2	M F CO2	M F N2
0	757.2852	.5519	.1739	.0361	.7900
.1817	818.3642	.5998	.1707	.0393	.7900
.3817	882.0592	.6692	.1662	.0438	.7900
.5697	961.3484	.7840	.1599	.0501	.7900
.7517	1049.1002	.8990	.1526	.0574	.7900
1.5017	1104.4794	.9893	.1483	.0617	.7900
3.1017	1075.1896	1.0000	.1505	.0595	.7900
4.7017	1071.6197	1.0000	.1505	.0595	.7900
6.3017	1068.2191	1.0000	.1505	.0595	.7900
7.9017	1064.9800	1.0000	.1505	.0595	.7900
9.5017	1061.8947	1.0000	.1505	.0595	.7900

Table J.29. Computer results for Test Run CP1 using the direct method to calculate the solids flowrate and a terminal velocity 1.5 times greater than the original correlation by Becker (20).

THE RESULTS FOR THE SIMULATED COMBUSTION MODEL TEST RUN CP1

THE INLET CONDITIONS FOR AIR AND WOODCHAR

FLOWRATE OF SOLIDS = .5115E-02 KG/S
TEMPERATURE OF SOLIDS= 285.0 K
COMBUSTIBLE CONTENT = .8122
MOISTURE CONTENT = .0488
INORGANIC CONTENT = .1390

MAIN AIR FLOWRATE = .3735E-02 KMOLE/S
TEMPERATURE OF AIR = 313.6 K
AIR FOR VIEW PORT 1 = .3318E-03 KMOLE/S
AIR FOR VIEW PORT 2 = .3318E-03 KMOLE/S
AIR FOR VIEW PORT 3+4= .6636E-03 KMOLE/S

THE INLET SIZE DISTRIBUTION FOR THE SOLIDS FEED

MEAN DIAMETER (M)	.2250E-04	.5400E-04	.9400E-04	.1880E-03	.3750E-03	.7500E-03	.1500E-02	.2665E-02	.4013E-02
SPHERICAL DIAMETER (M)	.1350E-04	.3240E-04	.5640E-04	.1128E-03	.2250E-03	.4500E-03	.9000E-03	.1599E-02	.2408E-02
WEIGHT FRACTION	.0379	.0569	.0605	.0704	.1630	.2935	.2810	.0268	.0000

THE TEMPERATURE OF THE REACTANTS LEAVING THE INITIAL MIXING ZONE IS 896.0 (K)

THE SIZE DISTRIBUTION LEAVING THE INITIAL MIXING ZONE

MEAN DIAMETER (M)	.1350E-04	.3240E-04	.5640E-04	.1128E-03	.2250E-03	.2899E-03	.9000E-03	.1599E-02	.2408E-02
WEIGHT FRACTION	.0776	.1165	.1239	.1442	.3338	.2040	0.0000	0.0000	0.0000

THE CALCULATED SURFACE AVERAGE PARTICLE DIAMETER IS .8027E-04 (M)

GAS FLOW INTO REACTION ZONE = .0037 KMOLE/S
CSA OF REACTION ZONE = .4560 M2
GAS FLOW INTO BYPASS ZONE = 0 KMOLE/S
CSA OF BYPASS ZONE = 0 M2

THE RESULTS FOR THE PLUG FLOW SECTION

LENGTH	TEMPERATURE	CONVERSION	M F O2	M F CO2	M F N2
0	895.9570	.5117	.1626	.0474	.7900
.0797	1271.3281	.8238	.1336	.0764	.7900
.1797	1364.2794	.9113	.1255	.0845	.7900
.3317	1420.0684	.9679	.1203	.0897	.7900
.8437	1372.3693	1.0000	.1249	.0851	.7900
1.6077	1293.4045	1.0000	.1313	.0787	.7900
2.4077	1286.9297	1.0000	.1313	.0787	.7900
3.1717	1168.3862	1.0000	.1416	.0684	.7900
3.9717	1165.1034	1.0000	.1416	.0684	.7900
4.7717	1161.8839	1.0000	.1416	.0684	.7900
5.5717	1158.7267	1.0000	.1416	.0684	.7900

Table J.30. Computer results for Test Run CP2 using the direct method to calculate the solids flowrate and a terminal velocity 1.5 times greater than the original correlation by Becker (20).

THE RESULTS FOR THE SIMULATED COMBUSTION MODEL TEST RUN CP2

THE INLET CONDITIONS FOR AIR AND WOODCHAR

FLOWRATE OF SOLIDS = .6055E-02 KG/S
TEMPERATURE OF SOLIDS= 285.0 K
COMBUSTIBLE CONTENT = .6442
MOISTURE CONTENT = .0489
INORGANIC CONTENT = .1070

MAIN AIR FLOWRATE = .5311E-02 KMOLE/S
TEMPERATURE OF AIR = 308.0 K
AIR FOR VIEW PORT 1 = .3254E-03 KMOLE/S
AIR FOR VIEW PORT 2 = .3254E-03 KMOLE/S
AIR FOR VIEW PORT 3+4= .6508E-03 KMOLE/S

THE INLET SIZE DISTRIBUTION FOR THE SOLIDS FEED

MEAN DIAMETER (M)	.2250E-04	.5400E-04	.9400E-04	.1880E-03	.3750E-03	.7500E-03	.1500E-02	.2665E-02	.4013E-02
SPHERICAL DIAMETER (M)	.1350E-04	.3240E-04	.5640E-04	.1128E-03	.2250E-03	.4500E-03	.9000E-03	.1599E-02	.2408E-02
WEIGHT FRACTION	.0271	.0442	.0399	.0541	.1623	.2580	.3286	.0802	.0054

THE TEMPERATURE OF THE REACTANTS LEAVING THE INITIAL MIXING ZONE IS 825.6 (K)

THE SIZE DISTRIBUTION LEAVING THE INITIAL MIXING ZONE

MEAN DIAMETER (M)	.1350E-04	.3240E-04	.5640E-04	.1128E-03	.2250E-03	.3498E-03	.9000E-03	.1599E-02	.2408E-02
WEIGHT FRACTION	.0562	.0917	.0828	.1122	.3367	.3204	0.0000	0.0000	0.0000

THE CALCULATED SURFACE AVERAGE PARTICLE DIAMETER IS .1039E-03 (M)

GAS FLOW INTO REACTION ZONE = .0053 KMOLE/S
CSA OF REACTION ZONE = .4560 M2
GAS FLOW INTO BYPASS ZONE = 0 KMOLE/S
CSA OF BYPASS ZONE = 0 M2

THE RESULTS FOR THE PLUG FLOW SECTION

LENGTH	TEMPERATURE	CONVERSION	M F O2	M F CO2	M F N2
0	825.6445	.5180	.1685	.0415	.7900
.0877	944.0449	.6332	.1592	.0508	.7900
.1677	1113.1276	.8060	.1454	.0646	.7900
.2837	1194.6347	.8939	.1383	.0717	.7900
.4437	1244.5156	.9473	.1340	.0760	.7900
1.0197	1243.7663	.9993	.1345	.0755	.7900
1.7837	1192.5982	1.0000	.1386	.0714	.7900
2.5837	1110.0428	1.0000	.1456	.0644	.7900
3.3837	1107.6992	1.0000	.1456	.0644	.7900
4.1837	1105.4052	1.0000	.1456	.0644	.7900
4.9837	1103.1600	1.0000	.1456	.0644	.7900

Table J.31. Computer results for Test Run CP3 using the direct method to calculate the solids flowrate and a terminal velocity 1.5 times greater than the original correlation by Becker (20).

THE RESULTS FOR THE SIMULATED COMBUSTION MODEL TEST RUN CP3

THE INLET CONDITIONS FOR AIR AND WOODCHAR

FLOWRATE OF SOLIDS = .6995E-02 KG/S
TEMPERATURE OF SOLIDS= 285.0 K
COMBUSTIBLE CONTENT = .8397
MOISTURE CONTENT = .0488
INORGANIC CONTENT = .1115

MAIN AIR FLOWRATE = .6432E-02 KMOLE/S
TEMPERATURE OF AIR = 310.8 K
AIR FOR VIEW PORT 1 = .2777E-03 KMOLE/S
AIR FOR VIEW PORT 2 = .2777E-03 KMOLE/S
AIR FOR VIEW PORT 3+4= .5553E-03 KMOLE/S

THE INLET SIZE DISTRIBUTION FOR THE SOLIDS FEED

MEAN DIAMETER (M)	.2250E-04	.5400E-04	.9400E-04	.1880E-03	.3750E-03	.7500E-03	.1500E-02	.2665E-02	.4013E-02
SPHERICAL DIAMETER (M)	.1350E-04	.3240E-04	.5640E-04	.1128E-03	.2250E-03	.4500E-03	.9000E-03	.1599E-02	.2408E-02
WEIGHT FRACTION	.0214	.0438	.0431	.0445	.0973	.1681	.3493	.3200	.0125

THE TEMPERATURE OF THE REACTANTS LEAVING THE INITIAL MIXING ZONE IS 843.2 (K)

THE SIZE DISTRIBUTION LEAVING THE INITIAL MIXING ZONE

MEAN DIAMETER (M)	.1350E-04	.3240E-04	.5640E-04	.1128E-03	.2250E-03	.4182E-03	.9000E-03	.1599E-02	.2408E-02
WEIGHT FRACTION	.0491	.1004	.0988	.1020	.2231	.4265	0.0000	0.0000	0.0000

THE CALCULATED SURFACE AVERAGE PARTICLE DIAMETER IS .1111E-03 (M)

GAS FLOW INTO REACTION ZONE = .0064 KMOLE/S
CSA OF REACTION ZONE = .4560 M2
GAS FLOW INTO BYPASS ZONE = 0 KMOLE/S
CSA OF BYPASS ZONE = 0 M2

THE RESULTS FOR THE PLUG FLOW SECTION

LENGTH	TEMPERATURE	CONVERSION	M F O2	M F CO2	M F N2
0	843.2227	.5639	.1671	.0429	.7900
.0877	958.1988	.6824	.1581	.0519	.7900
.1677	1074.6788	.8086	.1485	.0615	.7900
.2997	1147.3393	.8886	.1424	.0676	.7900
.6837	1181.5549	.9624	.1398	.0702	.7900
1.4837	1207.9231	.9995	.1371	.0729	.7900
2.2517	1171.7738	1.0000	.1399	.0701	.7900
3.0157	1110.8313	1.0000	.1451	.0649	.7900
3.8157	1108.3187	1.0000	.1451	.0649	.7900
4.6157	1105.8631	1.0000	.1451	.0649	.7900
5.4157	1103.4630	1.0000	.1451	.0649	.7900

Table J.32. Computer results for Test Run CP4 using the direct method to calculate the solids flowrate and a terminal velocity 1.5 times greater than the original correlation by Becker (20).

THE RESULTS FOR THE SIMULATED COMBUSTION MODEL TEST RUN CP3

THE INLET CONDITIONS FOR AIR AND WOODCHAR

FLOWRATE OF SOLIDS = .7935E-02 KG/S
TEMPERATURE OF SOLIDS= 285.0 K
COMBUSTIBLE CONTENT = .7752
MOISTURE CONTENT = .0488
INORGANIC CONTENT = .1760

MAIN AIR FLOWRATE = .6805E-02 KMOLE/S
TEMPERATURE OF AIR = 302.4 K
AIR FOR VIEW PORT 1 = .3276E-03 KMOLE/S
AIR FOR VIEW PORT 2 = .3276E-03 KMOLE/S
AIR FOR VIEW PORT 3+4= .6553E-03 KMOLE/S

THE INLET SIZE DISTRIBUTION FOR THE SOLIDS FEED

MEAN DIAMETER (M)	.2250E-04	.5400E-04	.9400E-04	.1880E-03	.3750E-03	.7500E-03	.1500E-02	.2665E-02	.4013E-02
SPHERICAL DIAMETER (M)	.1350E-04	.3240E-04	.5640E-04	.1128E-03	.2250E-03	.4500E-03	.9000E-03	.1599E-02	.2406E-02
WEIGHT FRACTION	.0310	.0650	.0657	.0612	.1357	.2926	.2855	.0567	.0060

THE TEMPERATURE OF THE REACTANTS LEAVING THE INITIAL MIXING ZONE IS 717.2 (K)

THE SIZE DISTRIBUTION LEAVING THE INITIAL MIXING ZONE

MEAN DIAMETER (M)	.1350E-04	.3240E-04	.5640E-04	.1128E-03	.2250E-03	.3746E-03	.9000E-03	.1599E-02	.2406E-02
WEIGHT FRACTION	.0552	.1157	.1169	.1089	.2415	.3608	0.0000	0.0000	0.0000

THE CALCULATED SURFACE AVERAGE PARTICLE DIAMETER IS .9731E-04 (M)

GAS FLOW INTO REACTION ZONE = .0068 KMOLE/S
CSA OF REACTION ZONE = .4560 M2
GAS FLOW INTO BYPASS ZONE = 0 KMOLE/S
CSA OF BYPASS ZONE = 0 M2

THE RESULTS FOR THE PLUG FLOW SECTION

LENGTH	TEMPERATURE	CONVERSION	M F O2	M F CO2	M F N2
0	717.2461	.4381	.1770	.0330	.7900
.1517	770.9718	.4538	.1758	.0342	.7900
.3117	814.4413	.4819	.1737	.0363	.7900
.4637	884.7585	.5466	.1688	.0412	.7900
.5757	957.2677	.6575	.1627	.0473	.7900
.6557	1075.5532	.7923	.1531	.0569	.7900
.7757	1150.3966	.8800	.1468	.0632	.7900
1.0957	1213.5899	.9511	.1416	.0684	.7900
1.8637	1210.0042	.9987	.1414	.0686	.7900
2.6637	1139.6873	.9994	.1469	.0631	.7900
3.4637	1136.5874	.9994	.1469	.0631	.7900

Table J.33. Computer results for Test Run C9 using the direct method to calculate the solids flowrate and a terminal velocity 1.5 times greater than the original correlation by Becker (20).

THE RESULTS FOR THE SIMULATED COMBUSTION MODEL TEST RUN C9

THE INLET CONDITIONS FOR AIR AND WOODCHAR

FLOWRATE OF SOLIDS = .9816E-02 KG/S
TEMPERATURE OF SOLIDS= 285.0 K
COMBUSTIBLE CONTENT = .7143
MOISTURE CONTENT = .0477
INORGANIC CONTENT = .2380

MAIN AIR FLOWRATE = .6701E-02 KMOLE/S
TEMPERATURE OF AIR = 302.4 K
AIR FOR VIEW PORT 1 = .3819E-03 KMOLE/S
AIR FOR VIEW PORT 2 = .3819E-03 KMOLE/S
AIR FOR VIEW PORT 3+4= .7638E-03 KMOLE/S

THE INLET SIZE DISTRIBUTION FOR THE SOLIDS FEED

MEAN DIAMETER (M)	.2250E-04	.5400E-04	.9400E-04	.1880E-03	.3750E-03	.7500E-03	.1500E-02	.2665E-02	.4013E-02
SPHERICAL DIAMETER (M)	.1350E-04	.3240E-04	.5640E-04	.1128E-03	.2250E-03	.4500E-03	.9000E-03	.1599E-02	.2408E-02
WEIGHT FRACTION	.0237	.0432	.0424	.0428	.1184	.2220	.2558	.1993	.0564

THE TEMPERATURE OF THE REACTANTS LEAVING THE INITIAL MIXING ZONE IS 834.4 (K)

THE SIZE DISTRIBUTION LEAVING THE INITIAL MIXING ZONE

MEAN DIAMETER (M)	.1350E-04	.3240E-04	.5640E-04	.1128E-03	.2250E-03	.4386E-03	.9000E-03	.1599E-02	.2408E-02
WEIGHT FRACTION	.0470	.0857	.0841	.0849	.2348	.4635	0.0000	0.0000	0.0000

THE CALCULATED SURFACE AVERAGE PARTICLE DIAMETER IS .1219E-03 (M)

GAS FLOW INTO REACTION ZONE = .0067 KMOLE/S
CSA OF REACTION ZONE = .4560 M2
GAS FLOW INTO BYPASS ZONE = 0 KMOLE/S
CSA OF BYPASS ZONE = 0 M2

THE RESULTS FOR THE PLUG FLOW SECTION

LENGTH	TEMPERATURE	CONVERSION	M F O2	M F CO2	M F N2
0	834.4336	.4958	.1668	.0432	.7900
.0797	960.2293	.6106	.1568	.0532	.7900
.1597	1107.3703	.7521	.1444	.0656	.7900
.2797	1190.2728	.8345	.1372	.0728	.7900
.4397	1242.1146	.8890	.1325	.0775	.7900
.8877	1266.4596	.9612	.1307	.0793	.7900
1.6877	1247.6023	.9974	.1319	.0781	.7900
2.4877	1244.1907	1.0000	.1317	.0783	.7900
3.2517	1162.5341	1.0000	.1390	.0710	.7900
4.0517	1159.0527	1.0000	.1390	.0710	.7900
4.8517	1155.6457	1.0000	.1390	.0710	.7900

Table J.34. Computer results for Test Run C10 using the direct method to calculate the solids flowrate and a terminal velocity 1.5 times greater than the original correlation by Becker (20).

THE RESULTS FOR THE SIMULATED COMBUSTION MODEL TEST RUN C10

THE INLET CONDITIONS FOR AIR AND WOODCHAR

FLOWRATE OF SOLIDS = .7935E-02 KG/S
TEMPERATURE OF SOLIDS= 285.0 K
COMBUSTIBLE CONTENT = .7573
MOISTURE CONTENT = .0477
INORGANIC CONTENT = .1950

MAIN AIR FLOWRATE = .5835E-02 KMOLE/S
TEMPERATURE OF AIR = 305.2 K
AIR FOR VIEW PORT 1 = .3071E-03 KMOLE/S
AIR FOR VIEW PORT 2 = .3071E-03 KMOLE/S
AIR FOR VIEW PORT 3+4= .6142E-03 KMOLE/S

TV = 1.5

THE INLET SIZE DISTRIBUTION FOR THE SOLIDS FEED

MEAN DIAMETER (M)	.2250E-04	.5400E-04	.9400E-04	.1880E-03	.3750E-03	.7500E-03	.1500E-02	.2665E-02	.4013E-02
SPHERICAL DIAMETER (M)	.1350E-04	.3240E-04	.5640E-04	.1128E-03	.2250E-03	.4500E-03	.9000E-03	.1599E-02	.2408E-02
WEIGHT FRACTION	.0329	.0576	.0629	.0539	.1233	.2510	.2554	.1289	.0351

THE TEMPERATURE OF THE REACTANTS LEAVING THE INITIAL MIXING ZONE IS 824.7 (K)

THE SIZE DISTRIBUTION LEAVING THE INITIAL MIXING ZONE

MEAN DIAMETER (M)	.1350E-04	.3240E-04	.5640E-04	.1126E-03	.2250E-03	.3768E-03	.9000E-03	.1599E-02	.2408E-02
WEIGHT FRACTION	.0644	.1128	.1232	.1056	.2415	.3524	0.0000	0.0000	0.0000

THE CALCULATED SURFACE AVERAGE PARTICLE DIAMETER IS .9316E-04 (M)

GAS FLOW INTO REACTION ZONE = .0058 KMOLE/S
CSA OF REACTION ZONE = .4560 M2
GAS FLOW INTO BYPASS ZONE = 0 KMOLE/S
CSA OF BYPASS ZONE = 0 M2

THE RESULTS FOR THE PLUG FLOW SECTION

LENGTH	TEMPERATURE	CONVERSION	M F O2	M F CO2	M F N2
0	824.6680	.4895	.1680	.0420	.7900
.0877	948.9897	.6024	.1583	.0517	.7900
.1677	1152.1079	.7963	.1417	.0683	.7900
.2677	1231.8458	.8765	.1348	.0752	.7900
.4477	1278.8944	.9268	.1305	.0795	.7900
.9917	1296.1370	.9904	.1292	.0808	.7900
1.7557	1256.7144	1.0000	.1323	.0777	.7900
2.5557	1177.8090	1.0000	.1391	.0709	.7900
3.3197	1174.1201	1.0000	.1391	.0709	.7900
4.1197	1170.3385	1.0000	.1391	.0709	.7900
4.9197	1166.6383	1.0000	.1391	.0709	.7900

Figure J.35. Computer results for Test Run CP1 using the direct method to calculate the solids flowrate. The value of the gas split parameter was 0.8 The value of the reactor split parameter was 0.9

```
THE RESULTS FOR THE SIMULATED COMBUSTION MODEL TEST RUN CP1

THE INLET CONDITIONS FOR AIR AND WOODCHAR

FLOWRATE OF SOLIDS =    .5115E-02 KG/S
TEMPERATURE OF SOLIDS= 285.0 K
COMBUSTIBLE CONTENT =  .8122
MOISTURE CONTENT    =  .0488
INORGANIC CONTENT   =  .1390

MAIN AIR FLOWRATE   =    .3735E-02 KMOLE/S
TEMPERATURE OF AIR  =   313.6 K
AIR FOR VIEW PORT 1 =   .3318E-03 KMOLE/S
AIR FOR VIEW PORT 2 =   .3318E-03 KMOLE/S
AIR FOR VIEW PORT 3+4=  .6636E-03 KMOLE/S


THE INLET SIZE DISTRIBUTION FOR THE SOLIDS FEED

MEAN DIAMETER (M)        .2250E-04  .5400E-04  .9400E-04  .1880E-03  .3750E-03  .7500E-03  .1500E-02  .2665E-02  .4013E-02
SPHERICAL DIAMETER (M)   .1350E-04  .3240E-04  .5640E-04  .1128E-03  .2250E-03  .4500E-03  .9000E-03  .1599E-02  .2408E-02
WEIGHT FRACTION          .0379      .0569      .0605      .0704      .1630      .2935      .2810      .0368      .0000

THE TEMPERATURE OF THE REACTANTS LEAVING THE INITIAL MIXING ZONE IS  771.0 (K)

THE SIZE DISTRIBUTION LEAVING THE INITIAL MIXING ZONE

MEAN DIAMETER (M)     .1350E-04   .3240E-04   .5640E-04   .1128E-03   .2250E-03   .3829E-03   .9000E-03   .1599E-02   .2408E-02
WEIGHT FRACTION          .0627       .0942       .1001       .1165       .2697       .3568      0.0000      0.0000      0.0000
```

THE CALLULATED SURFACE AVERAGE PARTICLE DIAMETER IS .1003E-03 (M)

GAS FLOW INTO REACTION ZONE = .0030 KMOLE/S
CSA OF REACTION ZONE = .4104 M2
GAS FLOW INTO BYPASS ZONE = .0007 KMOLE/S
CSA OF BYPASS ZONE = .0456 M2

THE RESULTS FOR THE PLUG FLOW SECTION

LENGTH	TEMPERATURE	CONVERSION	M F O2	M F CO2	M F N2
0	770.9570	.3957	.1733	.0367	.7900
.0797	937.4134	.4946	.1527	.0573	.7900
.1597	1325.6309	.7614	.1218	.0882	.7900
.2517	1422.2488	.8373	.1130	.0970	.7900
.3997	1496.4187	.9025	.1054	.1046	.7900
.5517	1438.9664	.9467	.1113	.0987	.7900
1.1277	1490.7146	.9955	.1062	.1038	.7900
1.9277	1392.1117	1.0000	.1152	.0948	.7900
2.6917	1172.2578	1.0000	.1416	.0684	.7900
3.4917	1169.2550	1.0000	.1416	.0684	.7900
4.2917	1166.3044	1.0000	.1416	.0684	.7900

Table J.36. Computer results for Test Run CP1 using the direct method to calculate the solids flowrate. The value of the gas split parameter was 0.9 The value of the reactor split parameter was 0.9

THE RESULTS FOR THE SIMULATED COMBUSTION MODEL TEST RUN CP1

THE INLET CONDITIONS FOR AIR AND WOODCHAR [illegible].

FLOWRATE OF SOLIDS = .5115E-02 KG/S
TEMPERATURE OF SOLIDS= 285.0 K
COMBUSTIBLE CONTENT = .8122
MOISTURE CONTENT = .0488
INORGANIC CONTENT = .1390

MAIN AIR FLOWRATE = .3735E-02 KMOLE/S
TEMPERATURE OF AIR = 313.6 K
AIR FOR VIEW PORT 1 = .3318E-03 KMOLE/S
AIR FOR VIEW PORT 2 = .3318E-03 KMOLE/S
AIR FOR VIEW PORT 3+4= .6636E-03 KMOLE/S

THE INLET SIZE DISTRIBUTION FOR THE SOLIDS FEED

MEAN DIAMETER (M)	.2250E-04	.5400E-04	.9400E-04	.1880E-03	.3750E-03	.7500E-03	.1500E-02	.2665E-02	.4013E-02
SPHERICAL DIAMETER (M)	.1350E-04	.3240E-04	.5640E-04	.1128E-03	.2250E-03	.4500E-03	.9000E-03	.1599E-02	.2408E-02
WEIGHT FRACTION	.0379	.0569	.0605	.0704	.1630	.2935	.2810	.0368	.0000

THE TEMPERATURE OF THE REACTANTS LEAVING THE INITIAL MIXING ZONE IS 737.8 (K)

THE SIZE DISTRIBUTION LEAVING THE INITIAL MIXING ZONE

MEAN DIAMETER (M)	.1350E-04	.3240E-04	.5640E-04	.1128E-03	.2250E-03	.4017E-03	.9000E-03	.1599E-02	.2408E-02
WEIGHT FRACTION	.0597	.0896	.0953	.1109	.2568	.3877	0.0000	0.0000	0.0000

THE CALCULATED SURFACE AVERAGE PARTICLE DIAMETER IS .1056E-03 (M)

GAS FLOW INTO REACTION ZONE = .0034 KMOLE/S
CSA OF REACTION ZONE = .4104 M2
GAS FLOW INTO BYPASS ZONE = .0004 KMOLE/S
CSA OF BYPASS ZONE = .0456 M2

THE RESULTS FOR THE PLUG FLOW SECTION

LENGTH	TEMPERATURE	CONVERSION	M F O2	M F CO2	M F N2
0	737.7539	.3652	.1761	.0339	.7900
.1037	844.6288	.4185	.1669	.0431	.7900
.1837	1138.4268	.6314	.1450	.0650	.7900
.2637	1308.6444	.7797	.1297	.0803	.7900
.3837	1393.2666	.8560	.1218	.0882	.7900
.5357	1364.5619	.9127	.1244	.0856	.7900
.7917	1416.4942	.9604	.1200	.0900	.7900
1.5917	1362.7784	1.0000	.1240	.0860	.7900
2.3917	1354.2846	1.0000	.1240	.0860	.7900
3.1557	1186.0322	1.0000	.1416	.0684	.7900
3.9557	1182.4231	1.0000	.1416	.0684	.7900

Table J.37. Computer results for Test Run CP2 using the direct method to calculate the solids flowrate. The value of the gas split parameter was 0.8 The value of the reactor split parameter was 0.9

THE RESULTS FOR THE SIMULATED COMBUSTION MODEL TEST RUN CP2

THE INLET CONDITIONS FOR AIR AND WOODCHAR

FLOWRATE OF SOLIDS = .6055E-02 KG/S
TEMPERATURE OF SOLIDS= 285.0 K
COMBUSTIBLE CONTENT = .8442
MOISTURE CONTENT = .0488
INORGANIC CONTENT = .1070

MAIN AIR FLOWRATE = .5311E-02 KMOLE/S
TEMPERATURE OF AIR = 308.0 K
AIR FOR VIEW PORT 1 = .3254E-03 KMOLE/S
AIR FOR VIEW PORT 2 = .3254E-03 KMOLE/S
AIR FOR VIEW PORT 3+4= .6508E-03 KMOLE/S

THE INLET SIZE DISTRIBUTION FOR THE SOLIDS FEED

MEAN DIAMETER (M)	.2250E-04	.5400E-04	.9400E-04	.1880E-03	.3750E-03	.7500E-03	.1500E-02	.2665E-02	.4013E-02
SPHERICAL DIAMETER (M)	.1350E-04	.3240E-04	.5640E-04	.1128E-03	.2250E-03	.4500E-03	.9000E-03	.1599E-02	.2408E-02
WEIGHT FRACTION	.0271	.0442	.0399	.0541	.1623	.2580	.3288	.0802	.0054

THE TEMPERATURE OF THE REACTANTS LEAVING THE INITIAL MIXING ZONE IS 680.1 (K)

THE SIZE DISTRIBUTION LEAVING THE INITIAL MIXING ZONE

MEAN DIAMETER (M)	.1350E-04	.3240E-04	.5640E-04	.1128E-03	.2250E-03	.4478E-03	.9000E-03	.1599E-02	.2408E-02
WEIGHT FRACTION	.0428	.0698	.0630	.0854	.2562	.4828	0.0000	0.0000	0.0000

THE CALCULATED SURFACE AVERAGE PARTICLE DIAMETER IS .1365E-03 (M)

GAS FLOW INTO REACTION ZONE = .0042 KMOLE/S
CSA OF REACTION ZONE = .4104 M2
GAS FLOW INTO BYPASS ZONE = .0011 KMOLE/S
CSA OF BYPASS ZONE = .0456 M2

THE RESULTS FOR THE PLUG FLOW SECTION

LENGTH	TEMPERATURE	CONVERSION	M F O2	M F CO2	M F N2
0	680.1367	.3666	.1806	.0294	.7900
.1317	755.3378	.3762	.1723	.0377	.7900
.2797	834.4211	.4181	.1681	.0419	.7900
.3637	958.2830	.5158	.1583	.0517	.7900
.4437	1175.1696	.6958	.1402	.0698	.7900
.5597	1210.5246	.7792	.1374	.0726	.7900
.7157	1277.7555	.8452	.1313	.0787	.7900
.8757	1325.8977	.8935	.1268	.0832	.7900
1.3237	1386.8912	.9531	.1212	.0888	.7900
2.0877	1355.5351	.9963	.1234	.0866	.7900
2.8517	1158.9404	1.0000	.1456	.0644	.7900

Table J.38. Computer results for Test Run CP3 using the direct method to calculate the solids flowrate. The value of the gas split parameter was 0.8 The value of the reactor split parameter was 0.9

THE RESULTS FOR THE SIMULATED COMBUSTION MODEL TEST RUN CP3

THE INLET CONDITIONS FOR AIR AND WOODCHAR

FLOWRATE OF SOLIDS = .6995E-02 KG/S
TEMPERATURE OF SOLIDS= 285.0 K
COMBUSTIBLE CONTENT = .8397
MOISTURE CONTENT = .0488
INORGANIC CONTENT = .1115

MAIN AIR FLOWRATE = .6432E-02 KMOLE/S
TEMPERATURE OF AIR = 310.8 K
AIR FOR VIEW PORT 1 = .2777E-03 KMOLE/S
AIR FOR VIEW PORT 2 = .2777E-03 KMOLE/S
AIR FOR VIEW PORT 3+4= .5553E-03 KMOLE/S

THE INLET SIZE DISTRIBUTION FOR THE SOLIDS FEED

MEAN DIAMETER (M)	.2250E-04	.5400E-04	.9400E-04	.1880E-03	.3750E-03	.7500E-03	.1500E-02	.2665E-02	.4013E-02
SPHERICAL DIAMETER (M)	.1350E-04	.3240E-04	.5640E-04	.1128E-03	.2250E-03	.4500E-03	.9000E-03	.1599E-02	.2408E-02
WEIGHT FRACTION	.0214	.0438	.0431	.0445	.0973	.1681	.3493	.2200	.0123

THE TEMPERATURE OF THE REACTANTS LEAVING THE INITIAL MIXING ZONE IS 749.5 (K)

THE SIZE DISTRIBUTION LEAVING THE INITIAL MIXING ZONE

MEAN DIAMETER (M)	.1350E-04	.3240E-04	.5640E-04	.1128E-03	.2250E-03	.4500E-03	.5850E-03	.1599E-02	.2408E-02
WEIGHT FRACTION	.0396	.0810	.0797	.0823	.1799	.3108	.2267	0.0000	0.0000

THE CALCULATED SURFACE AVERAGE PARTICLE DIAMETER IS .1395E-03 (M)

GAS FLOW INTO REACTION ZONE = .0051 KMOLE/S
CSA OF REACTION ZONE = .4104 M2
GAS FLOW INTO BYPASS ZONE = .0013 KMOLE/S
CSA OF BYPASS ZONE = .0456 M2

THE RESULTS FOR THE PLUG FLOW SECTION

LENGTH	TEMPERATURE	CONVERSION	M F O2	M F CO2	M F N2
0	749.4727	.4592	.1751	.0349	.7900
.1515	805.8356	.4902	.1634	.0466	.7900
.2955	888.7616	.5519	.1575	.0525	.7900
.3835	1002.3411	.6505	.1481	.0619	.7900
.4715	1130.2633	.7618	.1375	.0725	.7900
.6155	1154.5401	.8227	.1358	.0742	.7900
.7755	1195.2131	.8634	.1321	.0779	.7900
1.2875	1268.9561	.9342	.1257	.0843	.7900
2.0875	1265.7416	.9822	.1257	.0843	.7900
2.8515	1126.9980	.9984	.1452	.0648	.7900
3.6515	1125.6280	1.0000	.1451	.0649	.7900

Table J.39. Computer results for Test Run CP4 using the direct method to calculate the solids flowrate. The value of the gas split parameter was 0.7 The value of the reactor split parameter was 0.9

THE RESULTS FOR THE SIMULATED COMBUSTION MODEL TEST RUN CP4

THE INLET CONDITIONS FOR AIR AND WOODCHAR

FLOWRATE OF SOLIDS = .7935E-02 KG/S
TEMPERATURE OF SOLIDS= 285.0 K
COMBUSTIBLE CONTENT = .7752
MOISTURE CONTENT = .0488
INORGANIC CONTENT = .1760

MAIN AIR FLOWRATE = .6805E-02 KMOLE/S
TEMPERATURE OF AIR = 302.4 K
AIR FOR VIEW PORT 1 = .3276E-03 KMOLE/S
AIR FOR VIEW PORT 2 = .3276E-03 KMOLE/S
AIR FOR VIEW PORT 3+4= .6553E-03 KMOLE/S

THE INLET SIZE DISTRIBUTION FOR THE SOLIDS FEED

MEAN DIAMETER (M)	.2250E-04	.5400E-04	.9400E-04	.1880E-03	.3750E-03	.7500E-03	.1500E-02	.2665E-02	.4013E-02
SPHERICAL DIAMETER (M)	.1350E-04	.3240E-04	.5640E-04	.1128E-03	.2250E-03	.4500E-03	.9000E-03	.1599E-02	.2408E-02
WEIGHT FRACTION	.0310	.0650	.0657	.0612	.1357	.2926	.2855	.0567	.0060

THE TEMPERATURE OF THE REACTANTS LEAVING THE INITIAL MIXING ZONE IS 586.4 (K)

THE SIZE DISTRIBUTION LEAVING THE INITIAL MIXING ZONE

MEAN DIAMETER (M)	.1350E-04	.3240E-04	.5640E-04	.1128E-03	.2250E-03	.4500E-03	.4804E-03	.1599E-02	.2408E-02
WEIGHT FRACTION	.0440	.0922	.0931	.0868	.1924	.4148	.0759	0.0000	0.0000

THE CALCULATED SURFACE AVERAGE PARTICLE DIAMETER IS .1234E-03 (M)

GAS FLOW INTO REACTION ZONE = .0054 KMOLE/S
CSA OF REACTION ZONE = .4104 M2
GAS FLOW INTO BYPASS ZONE = .0014 KMOLE/S
CSA OF BYPASS ZONE = .0456 M2

THE RESULTS FOR THE PLUG FLOW SECTION

LENGTH	TEMPERATURE	CONVERSION	M F O2	M F CO2	M F N2
0	586.3867	.2947	.1878	.0222	.7900
.2117	662.3502	.2948	.1822	.0278	.7900
.4517	717.7434	.2964	.1821	.0279	.7900
1.0037	803.0160	.3238	.1812	.0288	.7900
1.1877	907.5021	.4094	.1736	.0364	.7900
1.3077	1163.5449	.6468	.1526	.0574	.7900
1.4877	1269.1021	.7521	.1432	.0668	.7900
1.7197	1287.4295	.8240	.1407	.0693	.7900
2.5037	1181.4227	.9345	.1472	.0628	.7900
3.7037	1219.0446	.9947	.1472	.0628	.7900
4.9037	1216.0996	.9994	.1469	.0631	.7900

Table J.40. Computer results for Test Run CP4 using the direct method to calculate the solids flowrate. The value of the gas split parameter was 0.8 The value of the reactor split parameter was 0.9

THE RESULTS FOR THE SIMULATED COMBUSTION MODEL TEST RUN CP4

THE INLET CONDITIONS FOR AIR AND WOODCHAR

FLOWRATE OF SOLIDS = .7935E-02 KG/S
TEMPERATURE OF SOLIDS= 285.0 K
COMBUSTIBLE CONTENT = .7752
MOISTURE CONTENT = .0488
INORGANIC CONTENT = .1760

MAIN AIR FLOWRATE = .6805E-02 KMOLE/S
TEMPERATURE OF AIR = 302.4 K
AIR FOR VIEW PORT 1 = .3276E-03 KMOLE/S
AIR FOR VIEW PORT 2 = .3276E-03 KMOLE/S
AIR FOR VIEW PORT 3+4= .6553E-03 KMOLE/S

THE INLET SIZE DISTRIBUTION FOR THE SOLIDS FEED

MEAN DIAMETER (M)	.2250E-04	.5400E-04	.9400E-04	.1880E-03	.3750E-03	.7500E-03	.1500E-02	.2665E-02	.4013E-02
SPHERICAL DIAMETER (M)	.1350E-04	.3240E-04	.5640E-04	.1128E-03	.2250E-03	.4500E-03	.9000E-03	.1599E-02	.2408E-02
WEIGHT FRACTION	.0310	.0650	.0657	.0612	.1357	.2926	.2855	.0567	.0060

THE TEMPERATURE OF THE REACTANTS LEAVING THE INITIAL MIXING ZONE IS 608.8 (K)

THE SIZE DISTRIBUTION LEAVING THE INITIAL MIXING ZONE

MEAN DIAMETER (M)	.1350E-04	.3240E-04	.5640E-04	.1128E-03	.2250E-03	.4435E-03	.9000E-03	.1599E-02	.2408E-02
WEIGHT FRACTION	.0454	.0951	.0962	.0896	.1986	.4742	0.0000	0.0000	0.0000

THE CALCULATED SURFACE AVERAGE PARTICLE DIAMETER IS .1194E-03 (M)

GAS FLOW INTO REACTION ZONE = .0048 KMOLE/S
CSA OF REACTION ZONE = .4104 M2
GAS FLOW INTO BYPASS ZONE = .0020 KMOLE/S
CSA OF BYPASS ZONE = .0456 M2

THE RESULTS FOR THE PLUG FLOW SECTION

LENGTH	TEMPERATURE	CONVERSION	M F O2	M F CO2	M F N2
0	608.8477	.3169	.1861	.0239	.7900
.1797	707.6796	.3179	.1758	.0342	.7900
.4117	780.6537	.3312	.1744	.0356	.7900
.6077	846.2324	.3867	.1711	.0389	.7900
.7397	1100.6616	.5865	.1509	.0591	.7900
.8917	1265.2675	.7478	.1347	.0753	.7900
1.0997	1364.2419	.8237	.1271	.0829	.7900
1.4037	1434.2412	.8880	.1206	.0894	.7900
2.5677	1174.0297	.9866	.1477	.0623	.7900
3.7317	1180.0321	.9994	.1469	.0631	.7900
4.9317	1175.4072	.9994	.1469	.0631	.7900

Table J.41. Computer results for Test Run C9 using the direct method to calculate the solids flowrate. The value of the gas split parameter was 0.8 The value of the reactor split parameter was 0.9

THE RESULTS FOR THE SIMULATED COMBUSTION MODEL TEST RUN C9

THE INLET CONDITIONS FOR AIR AND WOODCHAR

FLOWRATE OF SOLIDS = .9816E-02 KG/S
TEMPERATURE OF SOLIDS= 285.0 K
COMBUSTIBLE CONTENT = .7143
MOISTURE CONTENT = .0477
INORGANIC CONTENT = .2380

MAIN AIR FLOWRATE = .6701E-02 KMOLE/S
TEMPERATURE OF AIR = 302.4 K
AIR FOR VIEW PORT 1 = .3819E-03 KMOLE/S
AIR FOR VIEW PORT 2 = .3819E-03 KMOLE/S
AIR FOR VIEW PORT 3+4= .7638E-03 KMOLE/S

THE INLET SIZE DISTRIBUTION FOR THE SOLIDS FEED

MEAN DIAMETER (M)	.2250E-04	.5400E-04	.9400E-04	.1880E-03	.3750E-03	.7500E-03	.1500E-02	.2665E-02	.4013E-02
SPHERICAL DIAMETER (M)	.1350E-04	.3240E-04	.5640E-04	.1128E-03	.2250E-03	.4500E-03	.9000E-03	.1599E-02	.2408E-02
WEIGHT FRACTION	.0237	.0432	.0424	.0428	.1184	.2220	.2558	.1953	.0564

THE TEMPERATURE OF THE REACTANTS LEAVING THE INITIAL MIXING ZONE IS 743.6 (K)

THE SIZE DISTRIBUTION LEAVING THE INITIAL MIXING ZONE

MEAN DIAMETER (M)	.1350E-04	.3240E-04	.5640E-04	.1128E-03	.2250E-03	.4500E-03	.6031E-03	.1599E-02	.2408E-02
WEIGHT FRACTION	.0399	.0728	.0714	.0721	.1994	.3739	.1705	0.0000	0.0000

THE CALCULATED SURFACE AVERAGE PARTICLE DIAMETER IS .1446E-03 (M)

GAS FLOW INTO REACTION ZONE = .0054 KMOLE/S
CSA OF REACTION ZONE = .4104 M2
GAS FLOW INTO BYPASS ZONE = .0013 KMOLE/S
CSA OF BYPASS ZONE = .0456 M2

THE RESULTS FOR THE PLUG FLOW SECTION

LENGTH	TEMPERATURE	CONVERSION	M F O2	M F CO2	M F N2
0	743.6133	.4063	.1746	.0354	.7900
.2517	826.4306	.4461	.1614	.0486	.7900
.3717	921.3437	.5139	.1540	.0560	.7900
.4517	1076.0407	.6311	.1412	.0688	.7900
.5517	1141.4767	.7249	.1363	.0737	.7900
.6997	1207.2102	.7842	.1302	.0798	.7900
.8597	1253.0727	.8270	.1259	.0841	.7900
1.0197	1288.9219	.8612	.1224	.0876	.7900
1.7517	1312.1442	.9386	.1205	.0895	.7900
2.5517	1168.1269	.9807	.1404	.0696	.7900
3.3157	1178.4520	.9971	.1392	.0708	.7900

Table J.42. Computer results for Test Run C10 using the direct method to calculate the solids flowrate. The value of the gas split parameter was 0.8 The value of the reactor split parameter was 0.9

THE RESULTS FOR THE SIMULATED COMBUSTION MODEL TEST RUN C10

THE INLET CONDITIONS FOR AIR AND WOODCHAR

FLOWRATE OF SOLIDS = .7935E-02 KG/S
TEMPERATURE OF SOLIDS= 285.0 K
COMBUSTIBLE CONTENT = .7573
MOISTURE CONTENT = .0477
INORGANIC CONTENT = .1950

MAIN AIR FLOWRATE = .5835E-02 KMOLE/S
TEMPERATURE OF AIR = 305.2 K
AIR FOR VIEW PORT 1 = .3071E-03 KMOLE/S
AIR FOR VIEW PORT 2 = .3071E-03 KMOLE/S
AIR FOR VIEW PORT 3+4= .6142E-03 KMOLE/S

THE INLET SIZE DISTRIBUTION FOR THE SOLIDS FEED

MEAN DIAMETER (M)	.2250E-04	.5400E-04	.9400E-04	.1880E-03	.3750E-03	.7500E-03	.1500E-02	.2665E-02	.4013E-02
SPHERICAL DIAMETER (M)	.1350E-04	.3240E-04	.5640E-04	.1128E-03	.2250E-03	.4500E-03	.9000E-03	.1599E-02	.2408E-02
WEIGHT FRACTION	.0329	.0576	.0629	.0539	.1233	.2510	.2554	.1289	.0341

THE TEMPERATURE OF THE REACTANTS LEAVING THE INITIAL MIXING ZONE IS 695.8 (K)

THE SIZE DISTRIBUTION LEAVING THE INITIAL MIXING ZONE

MEAN DIAMETER (M)	.1350E-04	.3240E-04	.5640E-04	.1128E-03	.2250E-03	.4500E-03	.4966E-03	.1599E-02	.2408E-02
WEIGHT FRACTION	.0516	.0903	.0986	.0845	.1933	.3935	.0882	0.0000	0.0000

THE CALCULATED SURFACE AVERAGE PARTICLE DIAMETER IS .1181E-03 (M)

GAS FLOW INTO REACTION ZONE = .0047 KMOLE/S
CSA OF REACTION ZONE = .4104 M2
GAS FLOW INTO BYPASS ZONE = .0012 KMOLE/S
CSA OF BYPASS ZONE = .0456 M2

THE RESULTS FOR THE PLUG FLOW SECTION

LENGTH	TEMPERATURE	CONVERSION	M F O2	M F CO2	M F N2
0	695.7617	.3621	.1789	.0311	.7900
.1517	749.5878	.3678	.1705	.0395	.7900
.3117	815.2080	.3932	.1678	.0422	.7900
.4157	918.0884	.4653	.1601	.0499	.7900
.4957	1182.8909	.6657	.1386	.0714	.7900
.6077	1233.2034	.7512	.1344	.0756	.7900
.7597	1297.8633	.8117	.1283	.0817	.7900
.9197	1343.7254	.8562	.1238	.0862	.7900
1.2397	1403.5153	.9105	.1183	.0917	.7900
2.0037	1399.7455	.9725	.1178	.0922	.7900
2.7677	1221.4010	.9986	.1392	.0708	.7900

Table J.43. Computer results for CP4 using the direct method to calculate the solids flowrate and a reactor wall temperature of 1100 K

THE RESULTS FOR THE SIMULATED COMBUSTION MODEL TEST RUN CP4

THE INLET CONDITIONS FOR AIR AND WOODCHAR

FLOWRATE OF SOLIDS = .7935E-02 KG/S
TEMPERATURE OF SOLIDS= 285.0 K
COMBUSTIBLE CONTENT = .7752
MOISTURE CONTENT = .0488
INORGANIC CONTENT = .1760

MAIN AIR FLOWRATE = .6805E-02 KMOLE/S
TEMPERATURE OF AIR = 302.4 K
AIR FOR VIEW PORT 1 = .3276E-03 KMOLE/S
AIR FOR VIEW PORT 2 = .3276E-03 KMOLE/S
AIR FOR VIEW PORT 3+4= .6553E-03 KMOLE/S

THE INLET SIZE DISTRIBUTION FOR THE SOLIDS FEED

MEAN DIAMETER (M)	.2250E-04	.5400E-04	.9400E-04	.1880E-03	.3750E-03	.7500E-03	.1500E-02	.2665E-02	.4013E-02
SPHERICAL DIAMETER (M)	.1350E-04	.3240E-04	.5640E-04	.1128E-03	.2250E-03	.4500E-03	.9000E-03	.1599E-02	.2408E-02
WEIGHT FRACTION	.0310	.0650	.0657	.0612	.1357	.2926	.2855	.0567	.0060

THE TEMPERATURE OF THE REACTANTS LEAVING THE INITIAL MIXING ZONE IS 572.7 (K)

THE SIZE DISTRIBUTION LEAVING THE INITIAL MIXING ZONE

MEAN DIAMETER (M)	.1350E-04	.3240E-04	.5640E-04	.1128E-03	.2250E-03	.4500E-03	.5244E-03	.1599E-02	.2408E-02
WEIGHT FRACTION	.0431	.0903	.0913	.0850	.1885	.4064	.0947	0.0000	0.0000

THE CALCULATED SURFACE AVERAGE PARTICLE DIAMETER IS .1262E-03 (M)

GAS FLOW INTO REACTION ZONE = .0068 KMOLE/S
CSA OF REACTION ZONE = .4560 M2
GAS FLOW INTO BYPASS ZONE = 0 KMOLE/S
CSA OF BYPASS ZONE = 0 M2

THE RESULTS FOR THE PLUG FLOW SECTION

LENGTH	TEMPERATURE	CONVERSION	M F O2	M F CO2	M F N2
0	572.7148	.2801	.1889	.0211	.7900
.2517	634.2742	.2801	.1889	.0211	.7900
.9557	723.2341	.2823	.1897	.0203	.7900
1.7557	829.5380	.3449	.1863	.0237	.7900
1.9697	935.7810	.4666	.1779	.0321	.7900
2.0917	1100.4003	.6640	.1644	.0456	.7900
2.2457	1172.9929	.7560	.1581	.0519	.7900
2.4057	1212.1367	.8075	.1545	.0555	.7900
2.9817	1220.5629	.9082	.1526	.0574	.7900
3.7817	1260.1794	.9713	.1486	.0614	.7900
4.5817	1273.5863	.9978	.1470	.0630	.7900

Table J.44. Computer results for Test Run CP4 using the direct method to calculate the solids flowrate and half the step length for integration.

THE RESULTS FOR THE SIMULATED COMBUSTION MODEL TEST RUN CP4

THE INLET CONDITIONS FOR AIR AND WOODCHAR

FLOWRATE OF SOLIDS = .7935E-02 KG/S
TEMPERATURE OF SOLIDS= 285.0 K
COMBUSTIBLE CONTENT = .7752
MOISTURE CONTENT = .0488
INORGANIC CONTENT = .1760

MAIN AIR FLOWRATE = .6805E-02 KMOLE/S
TEMPERATURE OF AIR = 302.4 K
AIR FOR VIEW PORT 1 = .3276E-03 KMOLE/S
AIR FOR VIEW PORT 2 = .3276E-03 KMOLE/S
AIR FOR VIEW PORT 3+4= .6553E-03 KMOLE/S

THE INLET SIZE DISTRIBUTION FOR THE SOLIDS FEED

MEAN DIAMETER (M)	.2250E-04	.5400E-04	.9400E-04	.1880E-03	.3750E-03	.7500E-03	.1500E-02	.2665E-02	.4013E-02
SPHERICAL DIAMETER (M)	.1350E-04	.3240E-04	.5640E-04	.1128E-03	.2250E-03	.4500E-03	.9000E-03	.1599E-02	.2408E-02
WEIGHT FRACTION	.0310	.0650	.0657	.0612	.1357	.2926	.2855	.0567	.0060

THE TEMPERATURE OF THE REACTANTS LEAVING THE INITIAL MIXING ZONE IS 572.7 (K)

THE SIZE DISTRIBUTION LEAVING THE INITIAL MIXING ZONE

MEAN DIAMETER (M)	.1350E-04	.3240E-04	.5640E-04	.1128E-03	.2250E-03	.4500E-03	.5244E-03	.1599E-02	.2408E-02
WEIGHT FRACTION	.0431	.0903	.0913	.0850	.1885	.4064	.0947	0.0000	0.0000

THE CALCULATED SURFACE AVERAGE PARTICLE DIAMETER IS .1262E-03 (M)

GAS FLOW INTO REACTION ZONE = .0068 KMOLE/S
CSA OF REACTION ZONE = .4560 M2
GAS FLOW INTO BYPASS ZONE = 0 KMOLE/S
CSA OF BYPASS ZONE = 0 M2

THE RESULTS FOR THE PLUG FLOW SECTION

LENGTH	TEMPERATURE	CONVERSION	M F O2	M F CO2	M F N2
0	572.7148	.2801	.1889	.0211	.7900
.1997	625.4591	.2801	.1889	.0211	.7900
.6637	687.2007	.2808	.1898	.0202	.7900
1.3997	783.5676	.3007	.1884	.0216	.7900
1.7597	836.4510	.3615	.1852	.0248	.7900
1.8817	889.0989	.4205	.1811	.0289	.7900
1.9777	974.5622	.5224	.1741	.0359	.7900
2.0577	1088.3022	.6622	.1645	.0455	.7900
2.1697	1148.4963	.7373	.1593	.0507	.7900
2.3037	1186.8452	.7872	.1559	.0541	.7900
2.5417	1166.9628	.8512	.1562	.0538	.7900

Table J.45. Computer results for Test Run P3 using the direct method to calculate the solids flowrate and including an Ash Resistance term.

THE RESULTS FOR THE SIMULATED COMBUSTION MODEL TEST RUN P3

THE INLET CONDITIONS FOR AIR AND WOODCHAR ASH RESIST

FLOWRATE OF SOLIDS = .6055E-02 KG/S
TEMPERATURE OF SOLIDS= 285.0 K
COMBUSTIBLE CONTENT = .8233
MOISTURE CONTENT = .0507
INORGANIC CONTENT = .1260

MAIN AIR FLOWRATE = .4871E-02 KMOLE/S
TEMPERATURE OF AIR = 299.6 K
AIR FOR VIEW PORT 1 = .2217E-03 KMOLE/S
AIR FOR VIEW PORT 2 = .2217E-03 KMOLE/S
AIR FOR VIEW PORT 3+4= .4434E-03 KMOLE/S

THE INLET SIZE DISTRIBUTION FOR THE SOLIDS FEED

MEAN DIAMETER (M)	.2250E-04	.5400E-04	.9400E-04	.1880E-03	.3750E-03	.7500E-03	.1500E-02	.2665E-02	.4013E-02
SPHERICAL DIAMETER (M)	.1350E-04	.3240E-04	.5640E-04	.1128E-03	.2250E-03	.4500E-03	.9000E-03	.1599E-02	.2408E-02
WEIGHT FRACTION	.0210	.0410	.0367	.0411	.1272	.2942	.3410	.0921	.0057

THE TEMPERATURE OF THE REACTANTS LEAVING THE INITIAL MIXING ZONE IS 703.6 (K)

THE SIZE DISTRIBUTION LEAVING THE INITIAL MIXING ZONE

MEAN DIAMETER (M)	.1350E-04	.3240E-04	.5640E-04	.1128E-03	.2250E-03	.4500E-03	.4758E-03	.1599E-02	.2408E-02
WEIGHT FRACTION	.0336	.0657	.0588	.0658	.2037	.4712	.1012	0.0000	0.0000

THE CALCULATED SURFACE AVERAGE PARTICLE DIAMETER IS .1553E-03 (M)

GAS FLOW INTO REACTION ZONE = .0049 KMOLE/S
CSA OF REACTION ZONE = .4560 M2
GAS FLOW INTO BYPASS ZONE = 0 KMOLE/S
CSA OF BYPASS ZONE = 0 M2

THE RESULTS FOR THE PLUG FLOW SECTION

LENGTH	TEMPERATURE	CONVERSION	M F O2	M F CO2	M F N2
0	703.5742	.3756	.1780	.0320	.7900
.1357	775.0367	.3891	.1768	.0332	.7900
.2717	857.9446	.4405	.1724	.0376	.7900
.3917	951.1052	.5197	.1657	.0443	.7900
.5237	995.9035	.5910	.1618	.0482	.7900
.6837	1038.2275	.6305	.1586	.0514	.7900
1.4517	1119.3153	.7101	.1521	.0579	.7900
2.2517	1123.1784	.7505	.1513	.0587	.7900
3.0157	1087.9878	.7763	.1540	.0560	.7900
3.8157	1105.4530	.7966	.1525	.0575	.7900
4.6157	1117.8778	.8125	.1514	.0586	.7900

Table J.46. Computer results for Test Run P3 using the direct method to calculate the solids flowrate and the original Size Distribution for the Wood Char

THE RESULTS FOR THE SIMULATED COMBUSTION MODEL TEST RUN P3

THE INLET CONDITIONS FOR AIR AND WOODCHAR

FLOWRATE OF SOLIDS = .6055E-02 KG/S
TEMPERATURE OF SOLIDS= 285.0 K
COMBUSTIBLE CONTENT = .8233
MOISTURE CONTENT = .0507
INORGANIC CONTENT = .1260

MAIN AIR FLOWRATE = .4871E-02 KMOLE/S
TEMPERATURE OF AIR = 299.6 K
AIR FOR VIEW PORT 1 = .2217E-03 KMOLE/S
AIR FOR VIEW PORT 2 = .2217E-03 KMOLE/S
AIR FOR VIEW PORT 3+4= .4434E-03 KMOLE/S

THE INLET SIZE DISTRIBUTION FOR THE SOLIDS FEED

MEAN DIAMETER (M)	.2250E-04	.5400E-04	.9400E-04	.1880E-03	.3750E-03	.7500E-03	.1500E-02	.2665E-02	.4013E-02
SPHERICAL DIAMETER (M)	.1350E-04	.3240E-04	.5640E-04	.1128E-03	.2250E-03	.4500E-03	.9000E-03	.1599E-02	.2408E-02
WEIGHT FRACTION	.0010	.0010	.0067	.0111	.0372	.2342	.4810	.2021	.0257

THE TEMPERATURE OF THE REACTANTS LEAVING THE INITIAL MIXING ZONE IS 872.5 (K)

THE SIZE DISTRIBUTION LEAVING THE INITIAL MIXING ZONE

MEAN DIAMETER (M)	.1350E-04	.3240E-04	.5640E-04	.1128E-03	.2250E-03	.4500E-03	.5892E-03	.1599E-02	.2408E-02
WEIGHT FRACTION	.0022	.0022	.0147	.0243	.0814	.5126	.3626	0.0000	0.0000

THE CALCULATED SURFACE AVERAGE PARTICLE DIAMETER IS .3891E-03 (M)

GAS FLOW INTO REACTION ZONE = .0049 KMOLE/S
CSA OF REACTION ZONE = .4560 M2
GAS FLOW INTO BYPASS ZONE = 0 KMOLE/S
CSA OF BYPASS ZONE = 0 M2

THE RESULTS FOR THE PLUG FLOW SECTION

LENGTH	TEMPERATURE	CONVERSION	M F O2	M F CO2	M F N2
0	872.5195	.5431	.1637	.0463	.7900
.0917	985.5094	.6530	.1543	.0557	.7900
.2157	1077.9154	.7440	.1466	.0634	.7900
.3717	1144.8667	.8137	.1406	.0694	.7900
.5237	1153.6124	.8617	.1397	.0703	.7900
.6037	1171.2109	.8811	.1381	.0719	.7900
1.2957	1254.0819	.9694	.1309	.0791	.7900
2.0957	1239.2076	.9997	.1319	.0781	.7900
2.8597	1169.7447	1.0000	.1379	.0721	.7900
3.6597	1165.9341	1.0000	.1379	.0721	.7900
4.4597	1162.2090	1.0000	.1379	.0721	.7900